Applications and Industry®

September 1959

Transactions Papers

NUMBER 44

Published Bimonthly by

AMERICAN INSTITUTE OF ELECTRICAL ENGINEERS

(See inside back cover)

Note to Librarians. The six bimonthly issues of "Applications and Industry," March 1959–January 1960, will also be available in a single volume (no. 78) entitled "AIEE Transactions—Part II. Applications and Industry," which includes all technical papers on that subject presented during 1959. Bibliographic references to Applications and Industry and to Part II of the Transactions are therefore equivalent.

Applications and Industry. Published bimonthly by the American Institute of Electrical Engineers, from 20th and Northampton Streets, Easton, Pa. AIEE Headquarters: 33 West 39th Street, New York 18, N. Y. Address changes must be received at AIEE Headquarters by the first of the month to be effective with the succeeding issue. Copies undelivered because of incorrect address cannot be replaced without charge. Editorial and Advertising offices: 33 West 39th Street, New York 18, N. Y. Nonmember subscription $8.00 per year (plus 50 cents extra for foreign postage payable in advance in New York exchange). Member subscriptions: one subscription at $2.50 per year (balance of $5.00 subscription price to be paid by application of annual dues) to any one of three divisional publications: Communication and Electronics, Applications and Industry, or Power Apparatus and Systems: additional annual subscriptions $5.00 each. Single copies when available $1.50 each. Second-class mail privileges authorized at Easton, Pa. This publication is authorized to be mailed at the special rates of postage prescribed by Section 132.122.

Printed in United States of America

Number of copies of this issue 6,000

valuation of Transient System Response

F. P. DE MELLO
MEMBER AIEE

REQUENCY-RESPONSE techniques are among the most powerful tools in hands of the feedback control systems gineer. Perhaps of greatest use today the attenuation and phase-angle plot hniques developed by Bode. These hniques are particularly effective in alysis and synthesis of stable systems in ablishing the relative stability of a sys-n.[1] Although it is possible to estimate transient response of a system whose en-loop frequency response is known, accurate prediction of this transient ponse by analytical means involves taining the roots of the characteristic uation for the closed-loop system. owing the system's closed-loop factored nsfer function, the transient response the system may then be obtained ana-lically by means of Laplace transform thods. Thus, if

$$) = \frac{C(s)}{R(s)}$$

the system's closed-loop transfer func-n, then the Laplace transform of the tput $C(s)$ for a reference step of magni-ie $A(R(s)=A/s)$ would be $C(s)=$ $/s)S(s)$.

The only difficulty with the application Laplace transform methods lies in the t that, in order to obtain the inverse ne solution, the roots of the denominator the closed-loop transfer function

$$\frac{G(s)}{1+G(s)H(s)}$$

ust be determined. Although the func-n $G(s)H(s)$ is generally known in terms its poles and zeros, the expression $1+$ $s)H(s)$ usually turns out to be a high-ler polynomial in s whose roots are t easily extracted.

This paper illustrates a straightforward thod of obtaining the closed-loop sys-n transfer function in terms of an £ nsform expression whose inverse may readily obtained. This method is sed in part on some ideas which re presented in a discussion by A. Leonhard.[2] It is a logical extension of attenuation and phase-angle plot techniques using damped frequencies. It is considerably easier than Root Locus methods[3] and has much appeal to the engineer who is trained in Bode's attenuation and phase-angle techniques.

The application of the method developed in this paper is illustrated with examples.

In the analysis and synthesis of systems it often is necessary to represent into factored transfer function form inner loops, or sections which may be known as a summation of transfer functions. The method of obtaining roots outlined in this paper permits expressing any part of a system, made up of components in feedback or in summation, into factored transfer function form.

The Problem

The general problem can be stated as one of expressing the transfer function of a closed loop in terms of a factored numerator and denominator.

Thus, if $G(s)H(s)$ is the open-loop transfer known in terms of its poles and zeros

$G(s)$ the forward function

$$=\frac{(s+a_1)(s+a_2)(s+a_3)\dots}{(s+b_1)(s+b_2)(s+b_3)\dots} \quad (1)$$

$H(s)$ the feedback function

$$=\frac{(s+c_1)(s+c_2)(s+c_3)\dots}{(s+d_1)(s+d_2)(s+d_3)\dots} \quad (2)$$

The closed-loop transfer function is

$$\frac{G(s)}{1+G(s)H(s)} = \frac{(s+a_1)(s+a_2)\dots(s+d_1)(s+d_2)\dots}{(s+a_1)(s+a_2)\dots(s+c_1)(s+c_2)\dots} \quad (3)$$
$$(s+b_1)(s+b_2)\dots(s+d_1)(s+d_2)\dots$$

The numerator of the expression contains the same factors as appear in the numerator of the forward function $G(s)$ multiplied by those in the denominator of the feedback function $H(s)$.

The factors in the denominator are the roots of $(1+GH)$ and can be expressed as

$(s+r_1)(s+r_2)(s+r_3)\dots$ where $r_1, r_2, r_3\dots$

are real or complex roots of $1+GH=0$, i.e., values of s for which $G(s)H(s)=-1$.

The determination of these roots is all that is required to obtain the transient response of a system in terms of a Laplace transform expression whose inverse or time solution can be easily extracted.

As a corollary, if the summation of two functions $G_1(s)+G_2(s)$ has to be represented into an over-all factored function $G_3(s)$, and if

$$G_1(s)=\frac{(s+e_1)(s+e_2)(s+e_3)}{(s+f_1)(s+f_2)(s+f_3)} \quad (4)$$

and

$$G_2(s)=\frac{(s+g_1)(s+g_2)(s+g_3)}{(s+h_1)(s+h_2)(s+h_3)} \quad (5)$$

Then

$$G_3(s)=\frac{K[(s+i_1)(s+i_2)(s+i_3)\dots]}{(s+f_1)(s+f_2)(s+f_3)(s+h_1)\times (s+h_2)(s+h_3)} \quad (6)$$

where K is a constant which may be readily determined.

The roots of the following expression are i_1, i_2, i_3, etc.

$$1+\frac{G_1(s)}{G_2(s)}=0$$

i.e., values of s which make

$$\frac{G_1(s)}{G_2(s)}=-1$$

Determination of Roots

A polynomial in s will have real roots and/or pairs of conjugate complex roots. For a polynomial in s describing the characteristic equation of a stable system, the real roots or real parts of the complex roots will always be negative.

Thus the roots of a stable system can only be of the two forms

$$s_0=-\alpha_0 \quad (7)$$

and

$$s_{1,2}=-\alpha\pm j\omega \quad (8)$$

A polynomial having such roots could be expressed, in factored form, as

$$(s+\alpha_0)[(s+\alpha)^2+\omega^2] \quad (9)$$

The techniques of attenuation and phase-angle plots versus frequency, so effectively and widely used for system synthesis and analysis, can be adapted for use with complex frequencies. The procedure of locating the roots can then be stated as the search for the real or complex frequencies for which the magnitude of the function $G(s)H(s)$ is equal to 1 and its phase angle is 180 deg (degrees) or odd multiples of 180 deg.

Real Roots of Closed Loop

Examine the function

$$F(s)=\frac{1}{(1+sT)} \quad (10)$$

per 59-255, recommended by the AIEE Feedback Control Systems Committee and approved the AIEE Technical Operations Department presentation at the AIEE Winter General eting, New York, N. Y., February 1-6, 1959. anuscript submitted August 29, 1958; made ilable for printing December 3, 1958.

P. DE MELLO is with the General Electric mpany, Schenectady, N. Y.

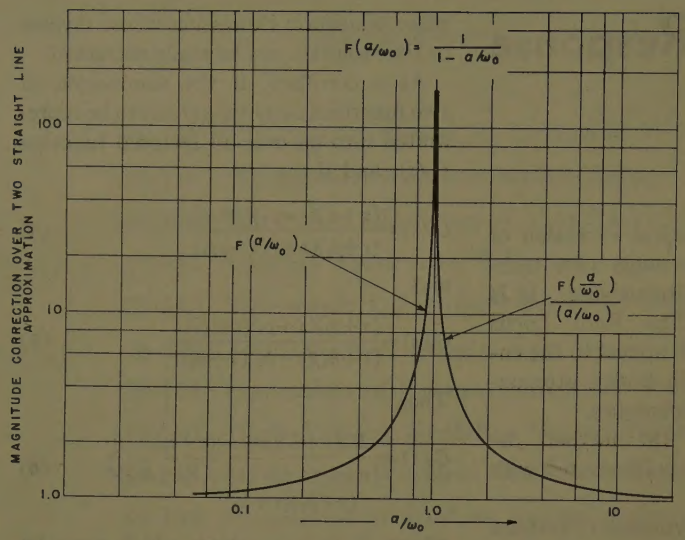

Fig. 1. Magnitude corrections over two straight-line Bode approximation for function F(S), with $s=-\alpha$ plotted as function of α/ω_0

$$F(s)=\frac{1}{1+\frac{s}{\omega_0}}$$

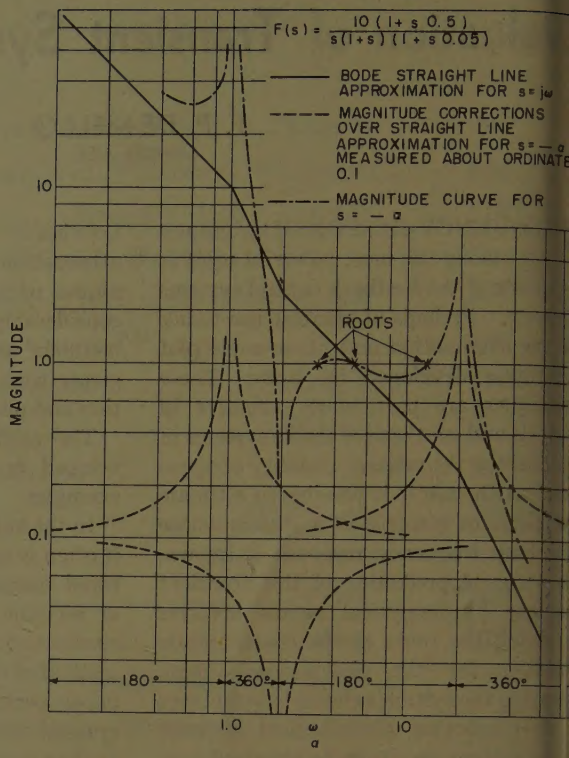

Fig. 2 (right). Bode plot of open-loop function given in curve

for $s=-\alpha$,

$$F(-\alpha)=\frac{1}{1-\alpha T} \tag{11}$$

$$=\frac{1}{\left[1-\frac{\alpha}{\omega_0}\right]} \tag{12}$$

where $\omega_0=1/T$ is known as the break frequency in Bode plot language.

The magnitude plot of $F(-\alpha)$ has asymptotic values of

$$|F(-\alpha)|=1 \text{ for } \frac{\alpha}{\omega_0}<<1 \text{ and } |F(-\alpha)| = \frac{1}{\frac{\alpha}{\omega_0}} \text{ for } \frac{\alpha}{\omega_0}>>1$$

As α/ω_0 approaches 1.0, the magnitude of the function increases rapidly and becomes infinite at $\alpha/\omega_0=1.0$. It decays rapidly from infinity as α/ω_0 becomes greater than 1.0.

The phase angle of the function $F(-\alpha)$ is 0 deg from $0<\alpha/\omega_0<1$ and is 180 deg for $\alpha/\omega_0>1.0$.

One easy way of finding the real roots of a closed-loop system from a Bode plot of its open-loop function is to prepare a template for the function $F(-\alpha/\omega_0)$ giving the magnitude correction over the two straight-line asymptotic approximation for real frequencies, as shown in Fig. 1.

Fig. 2 illustrates an example of solution for the real roots of a system whose forward function is $1/s(1+s)$ and feedback function is $10(1+s0.5)/(1+s0.05)$. The over-all open-loop function is $10(1+s0.5)/s(1+s)(1+s0.05)$.

The break frequencies for the denominator are $\omega_1=1.0$, $\omega_2=20$.

The numerator has a lead factor with a break frequency of $\omega_1'=2.0$.

On the log-magnitude versus log-frequency plot of the function's straight-line approximation, we have also drawn in the magnitude corrections for real frequencies. This was done with the aid of the real frequency template which was placed with its $\alpha/\omega_0=1.0$ marker opposite each break frequency. Note that the corrections for a lead factor in the numerator are a mirror image of the corrections for a lag factor in the denominator. For convenience, these component corrections were drawn about the ordinate 0.1. A negative correction is measured as the distance of the component curve below the ordinate 0.1. A positive correction would be the distance of component curve above the ordinate 0.1. The total magnitude correction to be applied to the straight-line approximation would be obtained by summing all component corrections which can be conveniently done with a pair of dividers.

It is also a simple matter to establish the regions where the function has a phase angle of 0 deg or even multiples of 180 deg and those regions where the function has a phase angle of 180 deg and/or odd multiples of 180 deg. Wherever the Bode straight-line approximation has slope of one or odd multiples, the phase angle for real frequencies 180 deg or odd multiples of 180 deg Crossovers of the magnitude $GH(-\alpha$ with the ordinate 1 represent real roots $GH+1=0$.

From Fig. 2, the roots of $1+GH$ are

$s_1=-3.10$
$s_2=-5.0$
$s_3=-12.9$

The transfer function of the closed loo can be written as

$$F(s)=\frac{\left(1+\frac{s}{20}\right)}{10\left(1+\frac{s}{3.10}\right)\left(1+\frac{s}{5.0}\right)\left(1+\frac{s}{12.9}\right)}$$

or in the form more readily adaptable fc the inverse transformation

$$F(s)=\frac{3.10(5.0)(12.9)(s+20)}{10[20(s+3.1)(s+5.0)(s+12.9)]}$$

The response for a unit step input woul be $C(s)=F(s)/s$

$$=\frac{3.10(5.0)(12.9)(s+20)}{10[20s(s+3.1)(s+5.0)(s+12.9)]}$$

The time response would then be

$$C(t)=K+K_1\epsilon^{-3.10t}+K_2\epsilon^{-5.0t}+K_3\epsilon^{-12.9t}$$

where

$$K=\frac{3.10(5.0)(12.9)(20)}{10(20)(3.10)(5.0)(12.9)}=0.10$$

$$K_1=\frac{3.10(5.0)(12.9)(20-3.10)}{10(20)(-3.10)(5.0-3.10)(12.9-3.10)}$$
$$=-0.293$$

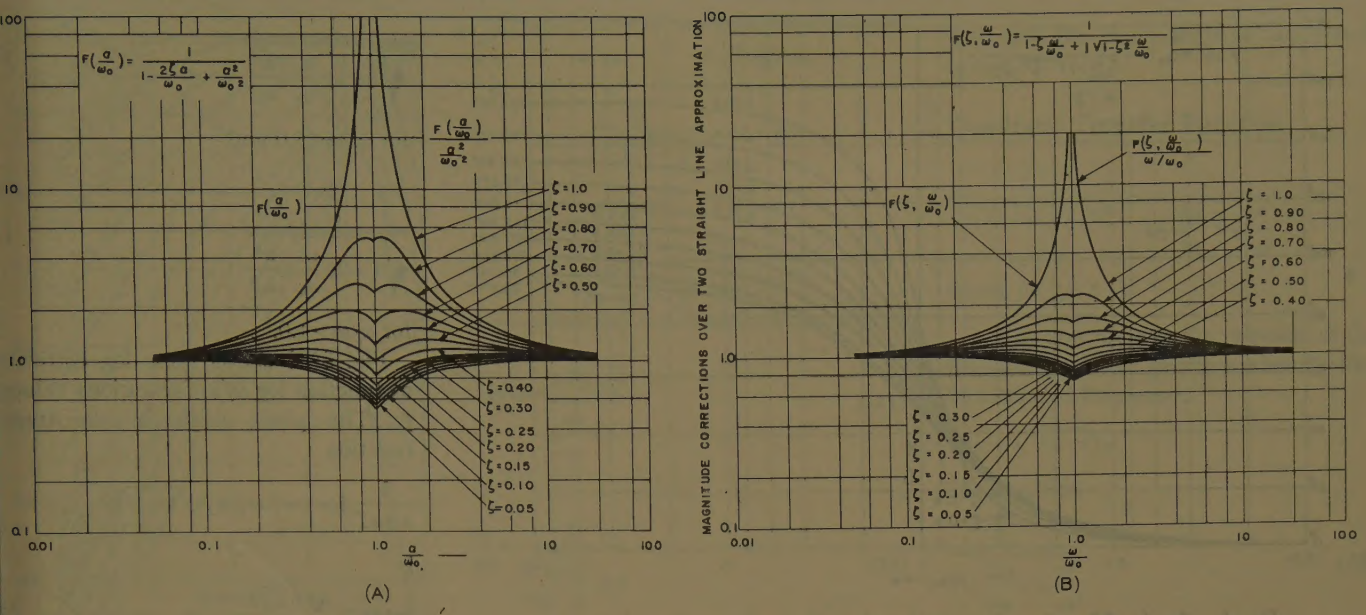

Fig. 3. Magnitude corrections over two straight-line Bode approximation for function F(S)

A—$s=-\alpha$ plotted as function of α/ω_0

$$F(s)=\frac{1}{1+\frac{2\zeta s}{\omega_0}+\frac{s^2}{\omega_0^2}}$$

B—Plotted as function of ω/ω_0 for various values of ζ

$$F(s)=\frac{1}{1+\frac{s}{\omega_0}} \text{ with } s=(-\zeta+j\sqrt{1-\zeta^2})\omega$$

$$=\frac{3.10(5.0)(12.9)(20-5.0)}{20(-5.0)(3.10-5.0)(12.9-5.0)}$$

$$=0.200$$

$$=\frac{3.10(5.0)(12.9)(20-12.9)}{20(-12.9)(3.10-12.9)(5.0-12.9)}$$

$$=0.0071$$

$$(t)=0.10-0.293\epsilon^{-3.10t}+0.200\epsilon^{-5.0t}-0.007\epsilon^{-12.9t}$$

A factor in the open-loop function containing complex roots is usually expressed the form

$$(s)=\frac{1}{1+\frac{2\zeta}{\omega_0}s+\frac{s^2}{\omega_0^2}} \tag{13}$$

here the roots are

$$_2=(-\zeta\pm j\sqrt{1-\zeta^2})\omega_0$$

$<\zeta<1$

or $s=-\alpha$

$$(-\alpha)=\frac{1}{\left[1+\frac{\alpha^2}{\omega_0^2}-\frac{2\zeta}{\omega_0}\alpha\right]} \tag{14}$$

nce $0<\zeta<1.0$, this function is always positive (phase angle=0 deg) and its agnitude is asymptotic to 1 at $\alpha/\omega_0<<1$ nd asymptotic to

$$\text{at } \frac{\alpha}{\omega_0}>>1$$

ith a resonant peak at

$\frac{\alpha}{\omega_0}=\zeta$ equal to $\frac{1}{1-\zeta^2}$

Curves of the magnitude of log $F(-\alpha)$ minus log of the two straight-line approximation versus α/ω_0 are shown on Fig. 3(A).

Since such complex root factors do not contribute any phase shift, their effect on real roots is merely by changing the magnitude curve and thereby possibly changing the point of crossover.

Complex Roots of Closed Loop

Pairs of conjugate complex roots

$$(-\zeta\pm j\sqrt{1-\zeta^2})\omega$$

are the other possibility. It suffices to test for one of the conjugates, say

$$(-\zeta+j\sqrt{1-\zeta^2})\omega$$

and find the complex frequency in terms of the parameters ζ and ω for which the magnitude of the function $GH(\zeta,\omega)=1.0$ and its phase angle is equal to 180 deg or odd multiples of 180 deg.

The magnitude and phase-angle behavior of the common transfer functions when excited by damped frequencies will be discussed in the following. A transfer function

$$F(s)=\frac{1}{1+sT} \tag{15}$$

for $s=[-\zeta+j\sqrt{1-\zeta^2}]\,\omega$ becomes

$$\frac{1}{1-\zeta\frac{\omega}{\omega_0}+j\sqrt{1-\zeta^2}\frac{\omega}{\omega_0}} \tag{16}$$

where $\omega_0=1/T$ is ordinarily known as break frequency in Bode asymptotic techniques.

Since the magnitude of the complex frequency

$$|(-\zeta+j\sqrt{1-\zeta^2})\omega|=\omega$$

it is evident that a plot of the log of the magnitude of the function

$$F[(-\zeta+j\sqrt{1-\zeta^2})\omega]$$

versus the log of the magnitude of complex frequency ω will be asymptotic to log 1 at $\omega/\omega_0<<1.0$ and asymptotic to log

$$\frac{1}{\omega/\omega_0} \text{ at } \frac{\omega}{\omega_0}>>1.0$$

and therefore the complex break frequency which is the intersection of the two asymptotes will again occur at ω_0. The actual magnitude is

$$\frac{1}{\sqrt{1-2\zeta\frac{\omega}{\omega_0}+\frac{\omega^2}{\omega_0^2}}} \tag{17}$$

It is interesting that this expression is equal to the square root of the magnitude of a quadratic transfer function when excited by a real frequency α, equation 14. The ratio between the actual magnitude and the two straight-line approximation is

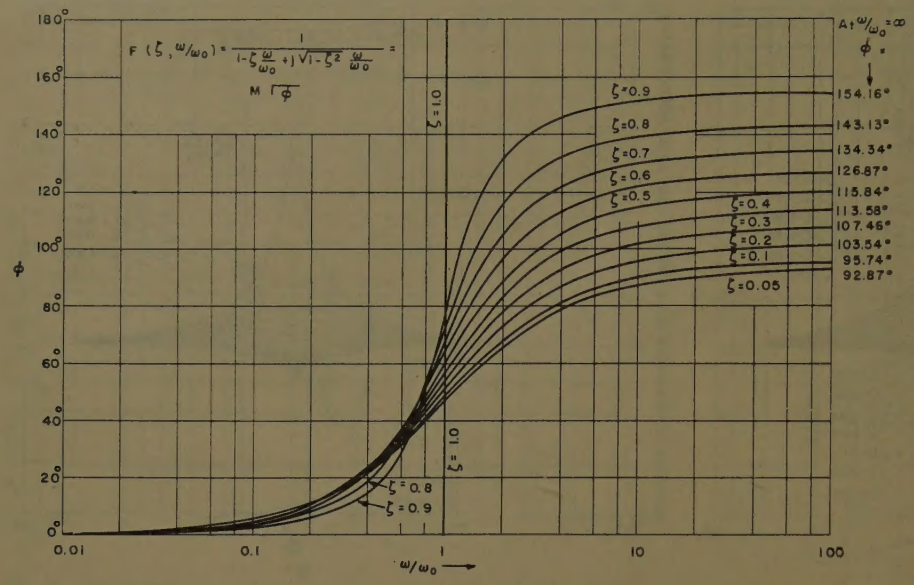

Fig. 4. Angle of function plotted as function of ω/ω_0 for various values of ζ

$$F(s)=\frac{1}{1+\frac{s}{\omega_0}} \text{ for } s=(\zeta+j\sqrt{1-\zeta^2})\omega$$

$$\frac{1}{\sqrt{1-2\zeta\frac{\omega}{\omega_0}+\frac{\omega^2}{\omega_0^2}}} \quad (1$$

for $\omega/\omega_0<1.0$ and

$$\frac{\frac{\omega_0}{\omega}}{\sqrt{1-2\zeta\frac{\omega}{\omega_0}+\frac{\omega^2}{\omega_0^2}}} \quad (1$$

for $\omega/\omega_0>1.0$.

Fig. 3(B) shows these log correctio as function log ω/ω_0 for various values ζ. The phase angle of the transf function

$$\frac{1}{1+sT} \text{ for } s=[-\zeta+j\sqrt{1-\zeta^2}]\omega$$

is

$$-\tan^{-1}\frac{\sqrt{1-\zeta^2}}{\frac{\omega_0}{\omega}-\zeta} \quad (2$$

From this expression the following rel tions are apparent.

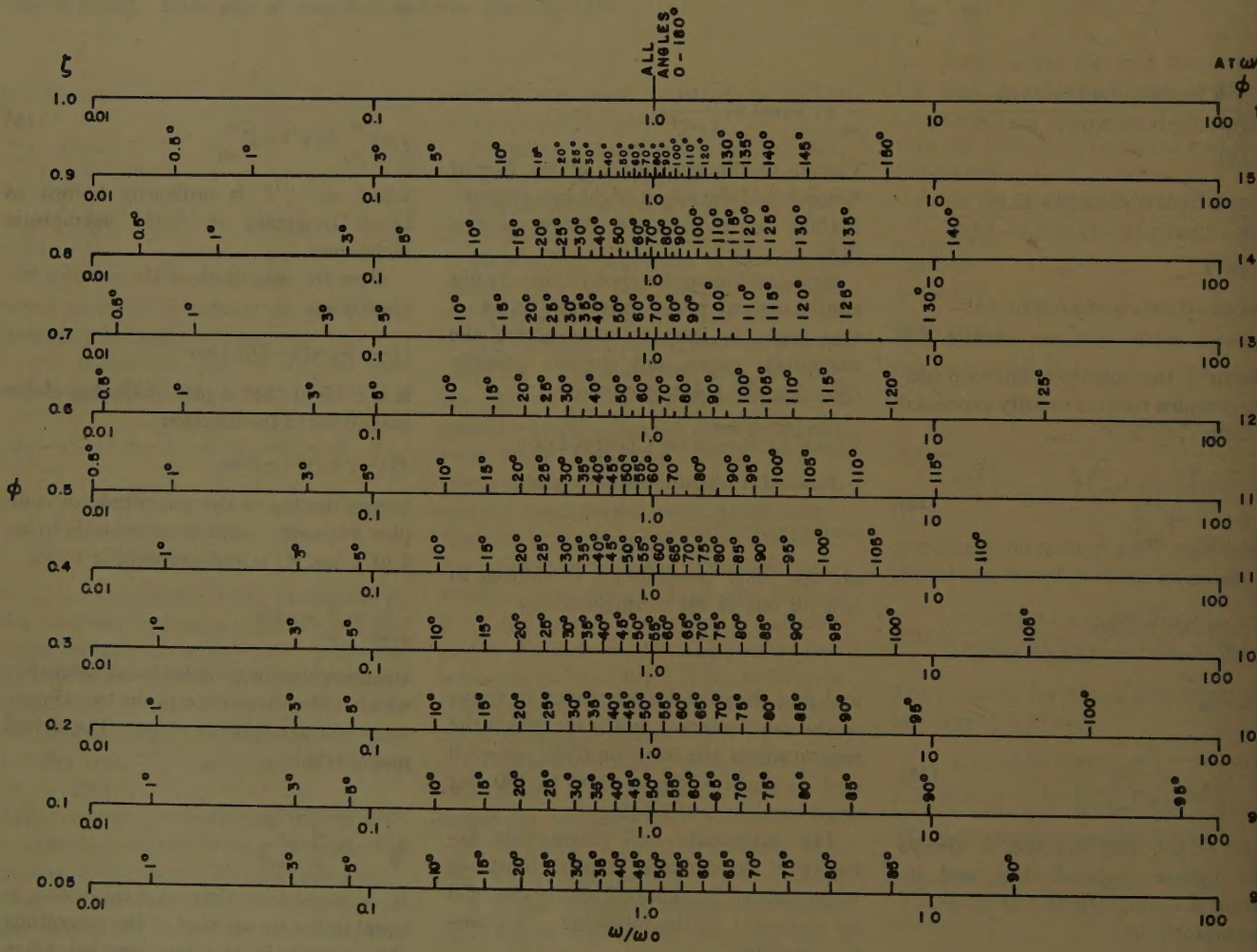

Fig. 5. Phase-angle rulers giving angle of F(S) as function of ω/ω_0 for various values of ζ

$$F(s)=\frac{1}{1+\frac{s}{\omega_0}} \text{ for } s=(-\zeta+j\sqrt{1-\zeta^2})\omega$$

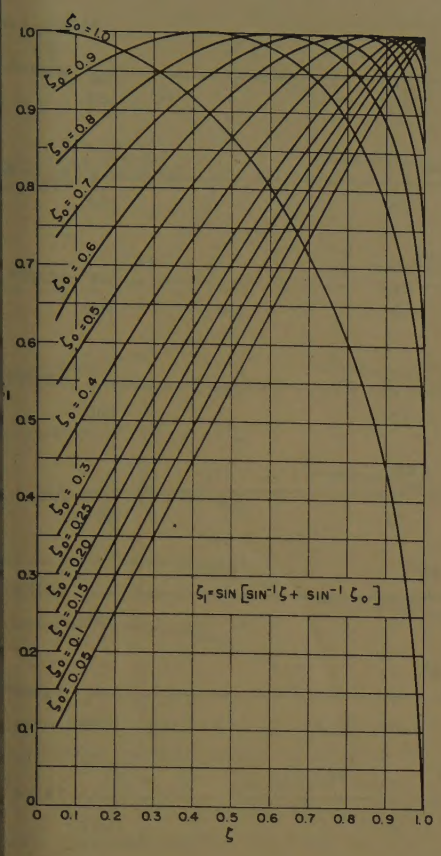

ig. 6. Plots of ζ_1 as function of ζ for various values of ζ_0

ω/ω_0	ϕ, Degrees
$\frac{1}{\zeta+\sqrt{1-\zeta^2}}$	-45
$\frac{1}{\zeta}$	-90
$\frac{1}{\zeta-\sqrt{1-\zeta^2}}$	-135

$$\tan\phi = \frac{\sqrt{1-\zeta^2}}{\frac{\omega_0}{\omega}-\zeta} \qquad (21)$$

or

$$\frac{\omega}{\omega_0} = \frac{1}{\frac{\sqrt{1-\zeta^2}}{\tan\phi}+\zeta} \qquad (22)$$

for $\omega/\omega_0 = 1.0$

$$\phi = \tan^{-1}\frac{\sqrt{1+\zeta}}{\sqrt{1-\zeta}} \qquad (23)$$

Fig. 4 shows values of angle as function of ω/ω_0 for various values of ζ. Phase-angle rules for various values of ζ can be conveniently made up as shown on Fig. 5 to give the phase angle as function of ω/ω_0.

Quadratic Transfer Function

$$\frac{1}{1+2\zeta_0 T_0 s+T_0^2 s^2} \text{ or } \frac{1}{1+\frac{2\zeta_0}{\omega_0}s+\frac{s^2}{\omega_0^2}}$$

where $0<\zeta_0<1$

Let us now observe the response of the resonant quadratic function when excited by a damped frequency.

$(-\zeta+\sqrt{1-\zeta^2})\omega$

The function

$$\frac{1}{1+\frac{2\zeta_0}{\omega_0}s+\frac{s^2}{\omega_0^2}} \qquad (24)$$

can be written as

$$F(s) = \frac{1}{\left[1+\frac{s}{(\zeta_0+j\sqrt{1-\zeta_0^2})\omega_0}\right]\times\left[1+\frac{s}{(\zeta_0-j\sqrt{1-\zeta_0^2})\omega_0}\right]} \qquad (25)$$

With $s=[-\zeta+\sqrt{1-\zeta^2}]\omega$

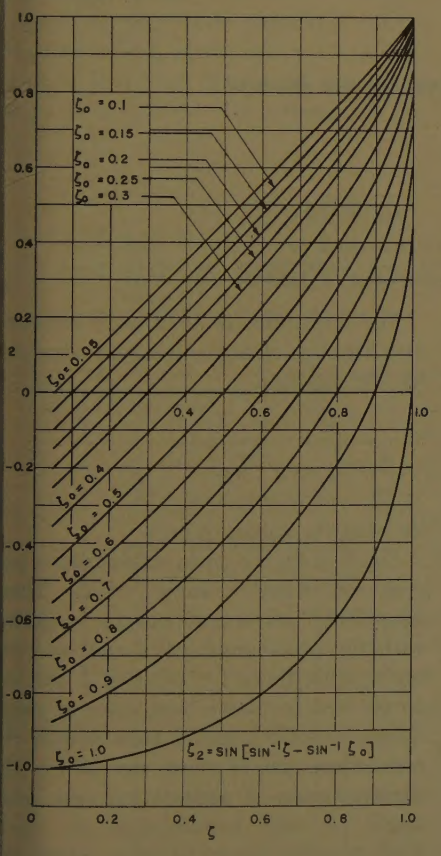

ig. 7. Plots of ζ_2 as function of ζ for various values of ζ_0

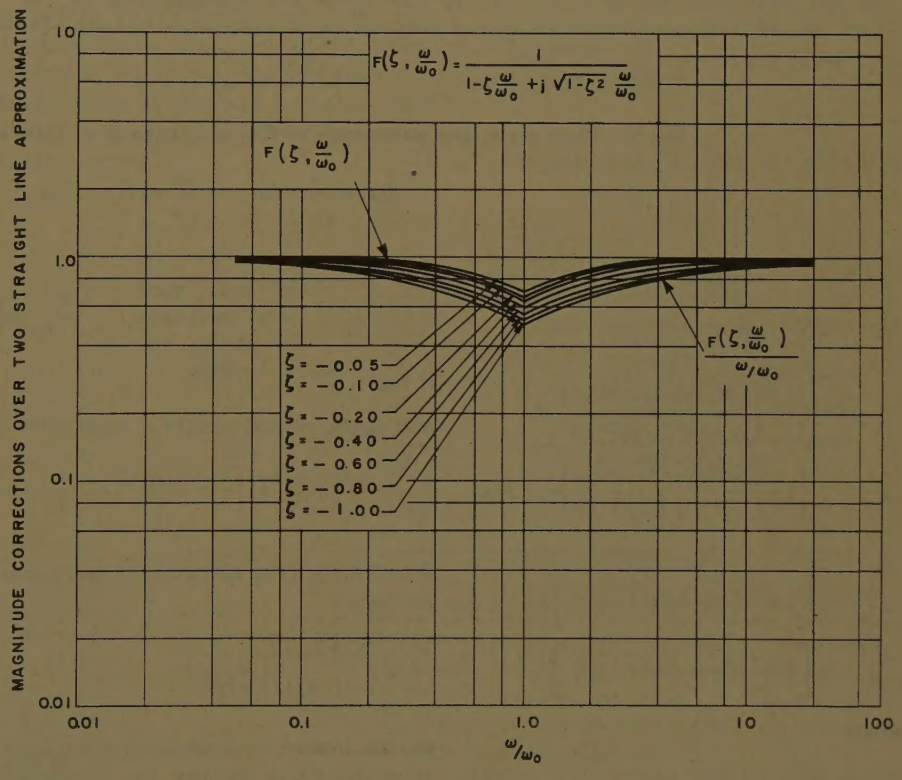

Fig. 8. Magnitude corrections over two straight-line approximation for the function F(S), and negative values of ζ

$$F(s) = \frac{1}{1+\frac{s}{\omega_0}} \text{ with } s=(-\zeta+j\sqrt{1-\zeta^2})\omega$$

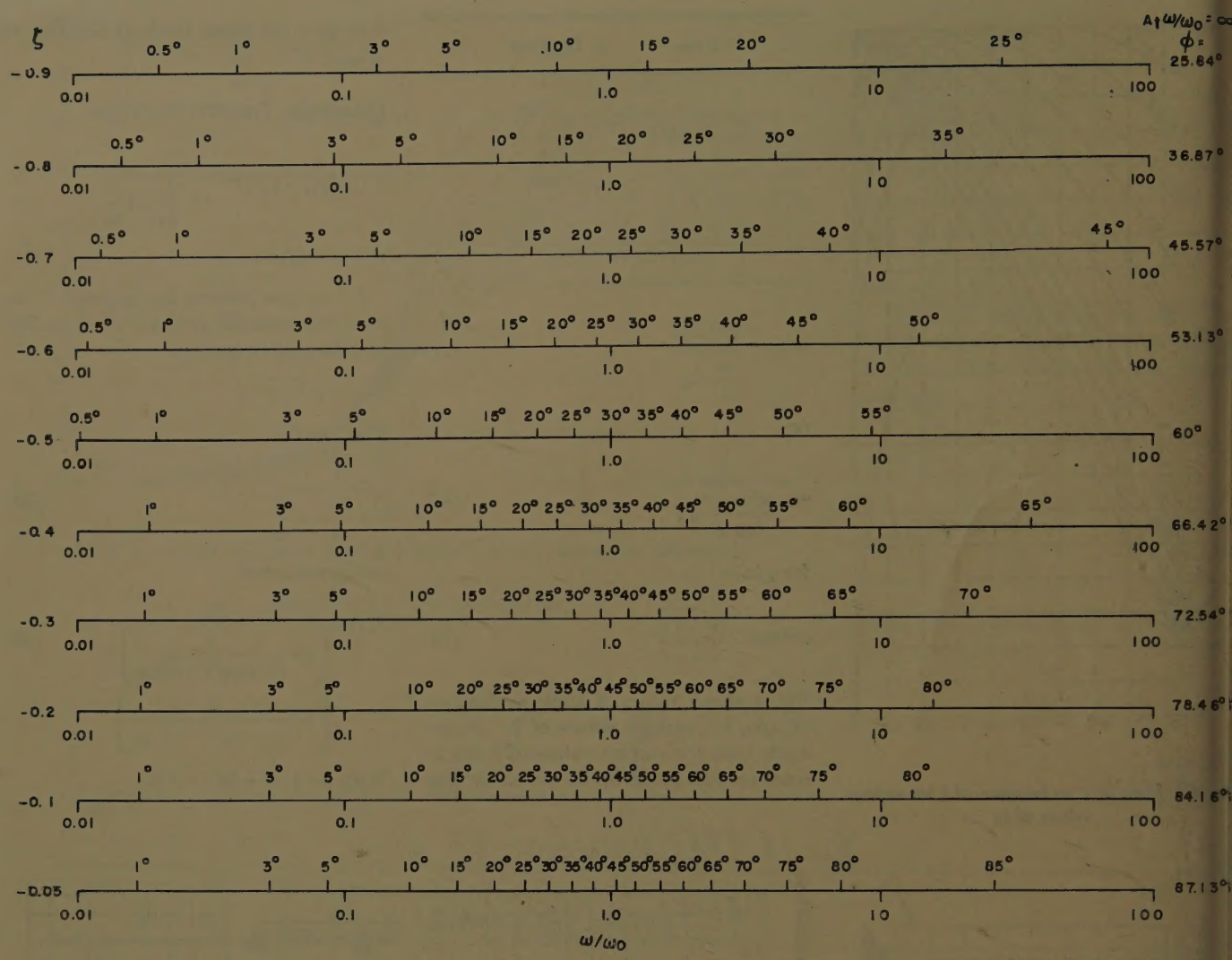

Fig. 9. Phase angle rules giving angle of F(S) as function of ω/ω_0 for various negative values of ζ

$$F(s)=\frac{1}{1+\frac{s}{\omega_0}} \quad \text{for } s=(-\zeta+j\sqrt{1-\zeta^2})\omega$$

$$F(-\zeta+j\sqrt{1-\zeta^2})\omega$$

$$=\frac{1}{\left\{1+\left[\frac{-\zeta+j\sqrt{1-\zeta^2}}{\zeta_0+j\sqrt{1-\zeta_0^2}}\right]\frac{\omega}{\omega_0}\right\}\times \left\{1+\left[\frac{-\zeta+j\sqrt{1-\zeta^2}}{\zeta_0-j\sqrt{1-\zeta_0^2}}\right]\frac{\omega}{\omega_0}\right\}} \qquad (26)$$

$$=\frac{1}{\left[1+\frac{\omega}{\omega_0}(-\zeta_1+j\sqrt{1-\zeta_2^2})\right]\times \left[1+\frac{\omega}{\omega_0}(-\zeta_2+\sqrt{1-\zeta_2^2})\right]}$$

where

$$\zeta_1=\sin\left[\sin^{-1}\zeta+\sin^{-1}\zeta_0\right] \qquad (27)$$

$$\zeta_2=\sin\left[\sin^{-1}\zeta-\sin^{-1}\zeta_0\right] \qquad (28)$$

Figs. 6 and 7 are plots of ζ_1 and ζ_2 as function of ζ for various values of ζ_0. ζ_1 is always positive for values of ζ and ζ_0 from 0 to 1.0, and the factor

$$\frac{1}{1+\frac{\omega}{\omega_0}(-\zeta_1+j\sqrt{1-\zeta_2^2})}$$

and can be treated exactly as a factor

$$\frac{1}{1+\frac{s}{\omega_0}} \text{ with } s=-\zeta_1+j\sqrt{1-\zeta_1^2}\omega$$

When $\zeta>\zeta_0$, ζ_2 is also positive and again the factor

$$\frac{1}{1+\frac{\omega}{\omega_0}(-\zeta_2+j\sqrt{1-\zeta_2^2})}$$

can be treated as a single time constant term $1/1+s/\omega_0$ excited by a damped frequency

$$(-\zeta_2+j\sqrt{1-\zeta_2^2})$$

when $\zeta<\zeta_0$, ζ_2 is negative, which is equivalent to having the function $1/1+s/\omega_0$ excited by

$$s=(\zeta_2+j\sqrt{1-\zeta^2})\omega$$

Fig. 8 contains plots of log correction over the two straight-line approximation for the function

$$\frac{1}{1+\frac{\omega}{\omega_0}(-\zeta+j\sqrt{1-\zeta_2^2})}$$

for negative values of ζ.

Fig. 9 gives the phase-angle rule versus ω/ω_0 for negative values of ζ. These magnitude correction curves, together with the phase-angle rules, can be combined with those for positive ζ and incorporated in plastic templates or rules. These templates would then permit the convenient use of these curves for the determination of attenuation and phase angle of any combination of open loop transfer functions from which the closed-loop roots can be easily extracted.

The essential magnitude correction

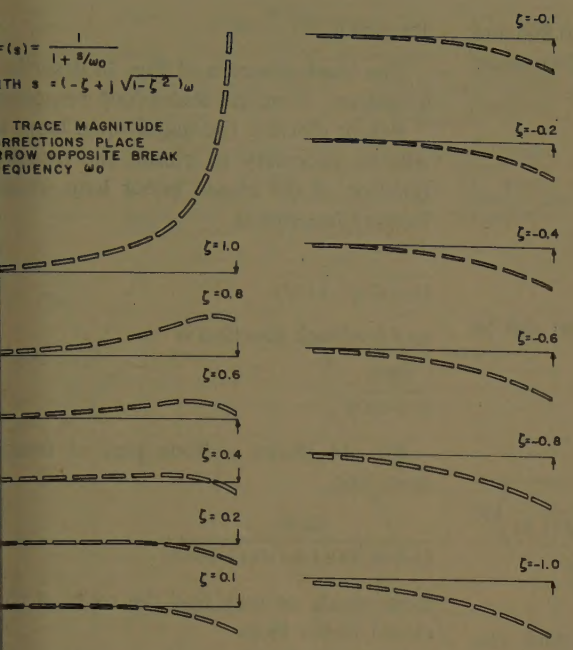

Fig. 10. Model of template for magnitude corrections for different damping ratios ζ

rves can be presented in templates or ansparent plastic rulers as shown on g. 10. Here the magnitude correc- on curves are stamped through the astic template so that they can be con- niently drawn onto a log-log plot by iding a sharp pencil through the narrow p along the curve. The phase-angle les shown on Figs. 5 and 9 can also presented in transparent plastic rulers r convenient use.

Since the magnitude correction curves e symmetrical, about $\omega/\omega_0=1.0$ on log- g plots, it suffices to plot the correction rves for $\omega/\omega_0<1.0$. By turning over the template, the same curve would apply for $\omega/\omega_0>1.0$.

The magnitude corrections for a complex quadratic factor of damping ratio ζ excited by real frequencies is equal to twice the magnitude correction of a normal time constant factor excited by a damped frequency with same damping ratio ζ. It is therefore unnecessary to include in a template the magnitude corrections for a complex quadratic factor excited by real frequencies since these corrections can be obtained by using twice the corrections given by the damped frequency curves.

On another template could also be included the curves of Figs. 6 and 7 relating ζ_1 and ζ_2 to ζ and ζ_0. These are of use in dealing with quadratic complex factors as explained in the text.

These templates, together with the phase-angle rules of Figs. 5 and 9, would be all that is needed for determination of roots of any system made up of components whose factored transfer functions are known.

EXAMPLE

Take the system whose forward function is given by the expression

$$\frac{0.10}{s(1+0.5s)}$$

and the feedback function by the expression

$$\frac{(1+s20)}{(1+s3.33)}$$

The plot of the open-loop function GH is shown on Fig. 11. The closed-loop response function would evidently be

$$\frac{(1+s3.33)}{(\quad)(\quad)(\quad)}$$

where the factors of the denominator are the roots of $GH+1$, to be determined from the magnitude and phase-angle plot of

$$\frac{0.1(1+20s)}{s(1+0.5s)(1+3.33s)} \text{ for } s=-\alpha \text{ and } s=(-\zeta+j\sqrt{1-\zeta^2})\omega$$

The gain of the function is 1 since it is

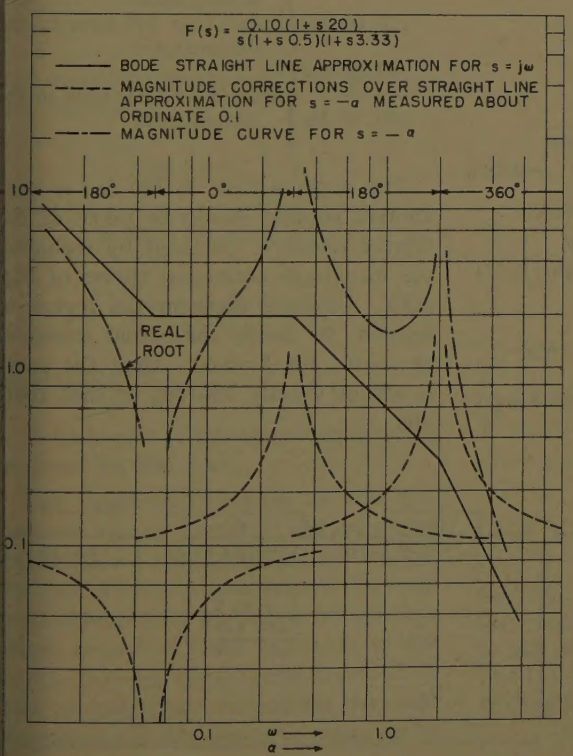

Fig. 11 (left). Bode plots of open-loop function given in curve

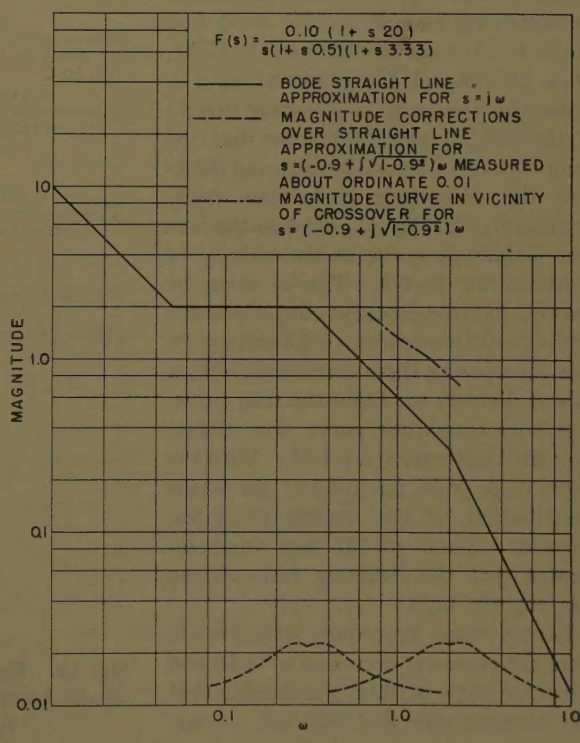

Fig. 12 (right). Bode plot of open-loop function given in curve

an integrating system and the numerator contains the denominator of H as a clearing of fractions operation of the function

$$\frac{G}{1+GH}$$

will indicate.

Scanning for Real Roots

Using the real-root template, the magnitude curve of $GH(s)$ can be drawn for $s=-\alpha$ as function of α. Fig. 11 shows this curve as composed from the corrections corresponding to each break which can be added with a pair of dividers to give the total correction. By inspection it is evident that the single slope regions, whether upward or downward, are the regions of 180-deg phase shift. (Odd multiples of such slopes are also regions of 180-deg phase shift.) Crossovers of the magnitude of $GH(-\alpha)$ with the ordinate 1 do give real roots only in these regions. The small portions of the magnitude curves of interest are quickly spotted and these regions can be drawn in with accuracy to obtain the roots.

On Fig. 11 it is seen that in the first section of 180-deg phase shift there is a crossover at 0.035 radian indicating a negative real root $=-0.035$. The next crossovers occur in regions of 0-deg phase shift and therefore there are no further real roots.

Complex Roots

Using the phase-angle rule for damped frequencies of Fig. 5 and the magnitude correction curves of Figs. 3(B) or 10, find the value of ζ for which the angle of $GH(\zeta, \omega)$ is 180 deg at the crossover with 1. From the relatively large phase margin of the $GH(j\omega)$ plot, it follows that the damping ratio ζ should be high and therefore the magnitude corrections fairly significant. In Fig. 12, draw in the correct magnitude curve in the vicinity of crossover for $\zeta=0.9$. This is done by drawing in the component corrections due to the break frequencies $\omega=0.3$ and $\omega=2.0$ and superposing these corrections with a pair of dividers to obtain the true curve. The true magnitude curve now crosses over the 1 ordinate at $\omega=1.55$. With the phase-angle rule for $\zeta=0.9$, the angle contribution by the various break frequencies amount to 187 deg which indicates that the damping ratio chosen was slightly high.

Repeat same procedure with $\zeta=0.8$. Here the crossover occurs at $\omega=1.10$ and the phase angle is 160 deg indicating that this damping ratio is a little low. Interpolation will yield a value of $\zeta=0.866$ and $\omega=1.31$ as the correct complex frequency for which

$$GH[-\zeta+j\sqrt{1-\zeta^2}]\omega=-1$$

i.e., the required complex root.

The roots then are

$$s=-0.035$$
$$s=(0.866\pm j0.50)\ 1.31$$

The closed-loop transfer function can be written as

$$\frac{(G)s}{1+G(s)H(s)} = \frac{(1+s3.33)}{\left(1+\frac{s}{0.035}\right)\left(1+\frac{s}{(0.866+j0.50)1.31}\right)\times \left(1+\frac{s}{(0.866-j0.50)1.31}\right)}$$

Expressed into a form from which the inverse Laplace transform can be readily extracted

$$\frac{G(s)}{1+G(s)H(s)} = \frac{0.035[1.31]^2 s(1+3.33s)}{(s+0.035)[(s+1.138)^2+(0.65)^2]}$$

The Laplace transform expression for the response to a unit step input would then be

$$C(s)=\frac{0.060(1+3.33s)}{s(s+0.035)[(s+1.138)^2+(0.65)^2]}$$

and its inverse time response would be

$$C(t)=K+K_1\epsilon^{-0.035t}+K_2\epsilon^{-1.138t}\times \sin(0.65t+\psi)$$

where

$$K=\frac{0.060}{0.035(1.138^2+0.65^2)}=1.0$$

$$K_1=\frac{0.060[(1-3.33)(0.035s)]}{-0.035(1.138-0.035)^2+(0.065)}=0.920$$

$$K_2=\frac{0.060(1+3.33)(-1.138+j0.65)}{0.65[-1.138+0.035+j0.65]\times[-1.138+j0.65]}$$

$$\psi=158.5 \text{ deg}$$

$$C(t)=1.0-0.920\epsilon^{-0.035t}+0.190\epsilon^{-1.138t}\times \sin\left(\frac{0.65\pi}{180}t-158.5 \text{ deg}\right)$$

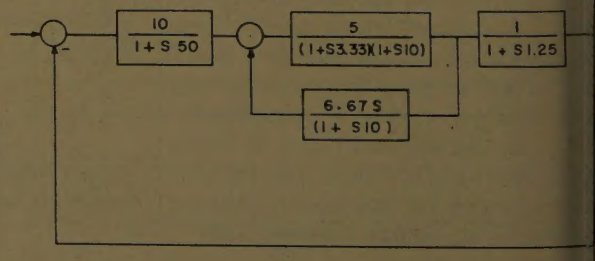

Fig. 13. Block diagram with transfer functions of a control system

EXAMPLE

The block diagram of Fig. 13 describes a system. Find its closed-loop response.

Before plotting the major open loop, it will be necessary to obtain the transfer function of the closed minor loop whose forward function is

$$\frac{5}{(1+s3)(1+s10)}$$

and feedback function is

$$\frac{6.67s}{(1+s10)}$$

Fig. 14 shows a Bode plot of minor open loop

$$\frac{33.3s}{(1+s3.33)(1+s10)(1+s10)}$$

from which we may find the roots of the closed minor loop.

By inspection it can be seen that the only region that will give real root is the upward slope from $\alpha=0$ to $\alpha=0.1$. A plot of the magnitude curve in this region obtained by adding the corrections because the two breaks at $\alpha=0.1$ and the break at $\alpha=0.3$, quickly locates this root as $\alpha=0.0186$.

The other crossover of interest is in the vicinity of 0.4 radian where complex roots will occur. The magnitude straight line approximation has a crossover at $\omega=0.32$ radian. At this point, for $\zeta=0.60$, the lagging phase angle is found with the help of phase angle rules of Fig. 5 to add to 160.1 deg as follows

−126.87 deg	from s term in the numerator
110.00 deg	from $(1+s\ 10)$ term in the denominator
110.00 deg	from $(1+s\ 10)$ term in the denominator
67.00 deg	from $(1+s\ 3.33)$ term in the denominator
160.13 deg	

This angle is close to 180 deg so that another reading should be taken at the correct crossover obtained by including the magnitude correction curves of Fig. 3(B). Drawing these in the region of interest, we locate the actual crossover at $\omega=0.4$ for $\zeta=0.60$. Here the angle is almost exactly 180 deg so that roots are

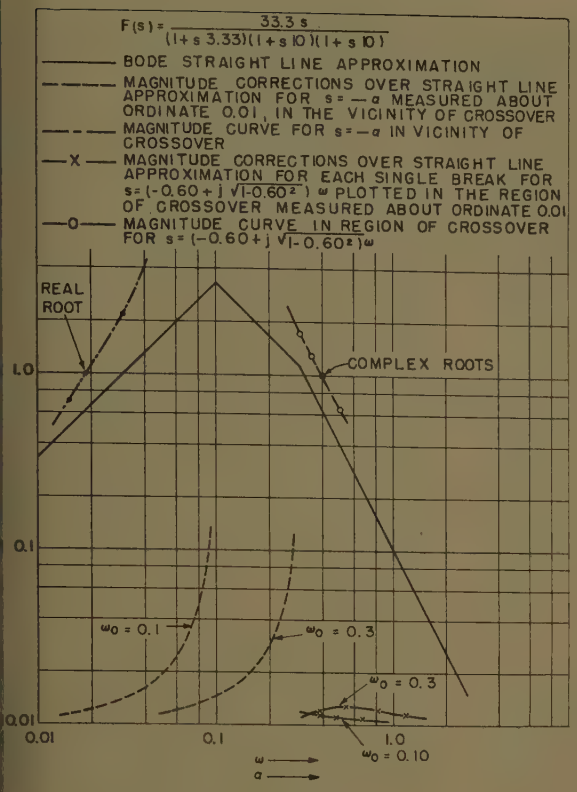

Fig. 14 (left). Bode plot of minor open loop function given in curve

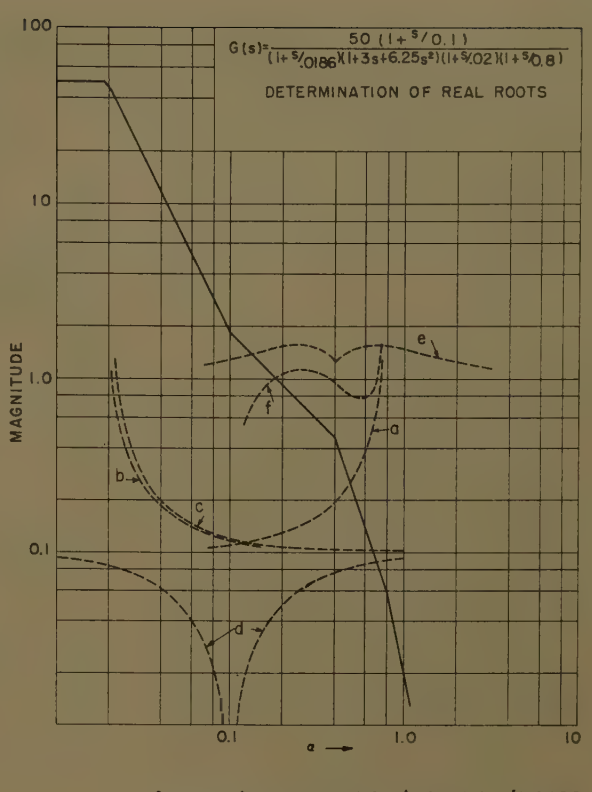

Fig. 15 (right). Bode plot of open-loop function G(s) for s = jω with auxiliary plot for s = −α for location of real roots

$-0.60 \pm j\sqrt{1-0.60^2})0.40$

The transfer function describing the closed-loop response for the minor loop is then found as

$$\frac{5(1+s10)}{\left(1+\frac{s}{0.0186}\right)\left(1+\frac{2(0.60)}{0.40}s+\frac{s^2}{(0.40)^2}\right)}$$

i.e.,

$=0.0186$
$=0.60$
$=0.40$

The expression for the over-all major loop will then be

$$G(s)=\frac{50\left(1+\frac{s}{0.1}\right)}{\left(1+\frac{s}{0.0186}\right)(1+3s+6.25s^2)\times\left(1+\frac{s}{0.02}\right)\left(1+\frac{s}{0.8}\right)}$$

Real Roots

A Bode plot of this open-loop function is shown on Fig. 15.

The closed-loop response of this system can now be found by first obtaining the roots of the equation $1+G(s)=0$. An inspection of possibilities for real roots reveals that the region of 180 deg, where crossovers may occur, is in the region between $\alpha=0.1$ and $\alpha=0.8$. A plot of magnitude corrections for real frequencies in this region is made up of contributions from each single time constant factor as well as from the quadratic factor for which the correction curve of Fig. 3(B) applies, with $\zeta=0.60$.

These individual corrections in the region of interest are drawn as dashed curves for convenience about the ordinate 0.1 for the single time constant terms, and about the ordinate 1.0 for the quadratic factor. Curves *a*, *b*, *c* are correction factors for terms $1+s/0.8$, $1+s/0.0186$ and $1+s/0.1$ in the denominator. Curves *d* are correction factors for the term $1+s/0.1$ in the numerator, and curves *e* are correction curves for the quadratic factor $(1+3s+6.25s^2)$. Curves *a*, *b*, *c*, and *d* are to be measured with respect to the ordinate 0.1. The difference between curve *e* and the ordinate 1 gives the corrections for the quadratic factor.

The addition of all of the contributing correction factors can be conveniently

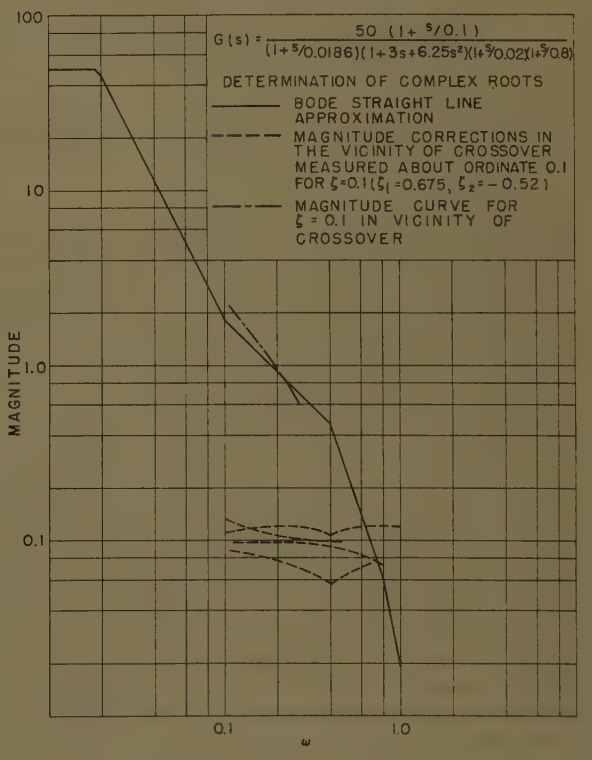

Fig. 16. Bode plot of open-loop function G(s) for s = jω with auxiliary lot for s = $(-\zeta+j\sqrt{1-\zeta^2})\omega$ for location of complex roots. Trial value of ζ is s = 0.1

done by means of a pair of dividers. The total correction when applied to the straight line approximation in the region of interest yields curve f which crosses over the ordinate 1 at $\alpha=0.186$, $\alpha=0.385$, and $\alpha=0.680$.

The real roots of the over-all closed loop are then:

$s=-0.186$
$s=-0.385$
$s=-0.680$

Complex Roots

The search for the value of ζ and ω for which the magnitude of G is 1 and its phase angle is 180 deg is again undertaken as indicated in previous examples.

Here, however, the contribution from the complex factor $\zeta_0=0.6$, $\omega_0=0.1$ is obtained as follows. For any trial value of ζ, say $\zeta=0.1$, values of ζ_1 and ζ_2 are obtained from Figs. 6 and 7, by entering in $\zeta=0.1$ and $\zeta_0=0.60$. From these figures, these values are $\zeta_1=0.675$, $\zeta_2=-0.52$. Treat the quadratic factor as two ordinary breaks at $\omega_0=0.40$ but use $\zeta=0.675$ on one and $\zeta=-0.52$ on the other instead of $\zeta=0.1$. As ζ_2 is negative, the magnitude curves of Fig. 8 apply as well as the phase values of Fig. 9.

In Fig. 16, entering in the magnitude correction curves for $\zeta=0.1$ ($\zeta_1=0.675$ and $\zeta_2=-0.52$ for the quadratic factor) the crossover is found at $\omega=0.2$ where the total angle is 175 deg, made up as follows:

90	deg from the break frequency 0.0186
90.5	deg from the break frequency 0.02
−68	deg from the break frequency 0.10
14.5	deg from the break frequency 0.80
29.5	deg from quadratic factor $\zeta_1=0.675$
18.5	deg from quadratic factor $\zeta_2=-0.52$
175	

Next try for $\zeta=0.20$. (For the quadratic factor, $\zeta_1=0.75$ and $\zeta_2=-0.43$.) Here the magnitude correction curves when applied indicate a crossover of 0.24 radian where the angle is 191 deg. Interpolation will yield a root at approximately $\omega=0.22$ and $\zeta=0.14$.

Conclusions

This paper presents a simple and effective technique of determining the roots of a closed-loop system or the roots of the summation of factored transfer functions. Determination of such roots is valuable in synthesis of systems made up of minor loops or components in summation. The combinations of such components often have to be described in factored transfer-function form in order to permit a frequency response analysis of the over-all major loop.

Determining the roots of such system also permits the evaluation of the transient response of the system by use of inverse Laplace transform methods.

The magnitude correction curves and phase angle rules which are the essential tools for this technique are shown on Figs. 5–10. They can be conveniently incorporated in plastic templates or rules which would be of great use to the control systems engineer. The method described in this paper is considerably easier to apply than the root locus methods which have recently been gaining much acceptance.

References

1. Servomechanisms and Regulating System Design (book), H. Chestnut, R. W. Mayer. John Wiley & Sons, Inc., New York, N. Y., vol. I, 195

2. Discussion by A. Leonhard of Frequency Response Data Presentation Standards and Design Criteria, Rufus Oldenburger. *Transactions*, American Society of Mechanical Engineers, New York, N. Y., vol. 76, no. 8, Nov. 1954, pp. 1155–76.

3. Automatic Feedback Control System Synthesis (book), J. G. Truxal. McGraw-Hill Book Company, Inc., New York, N. Y., 1955.

Improved D-C High-Potential Testing of Insulation Systems in Low- and Medium-Voltage D-C Equipment

A. M. ODOK
ASSOCIATE MEMBER AIEE

T. M. SOELAIMAN
ASSOCIATE MEMBER AIEE

Synopsis: Elimination of unexpected breakdowns in d-c high-potential testing is made possible by observing the electrical noise caused by ionization. (The terms ionization and ionization discharges are used as common terminology to refer to charge redistributions as a result of gaseous breakdowns in the insulation systems; see Appendix I. However, it will be more appropriate for the purposes of this paper to include in this term the charge redistributions taking place whenever a minute conducting path on the insulation surface is broken down.) The relative severity of ionization discharges is easily detected by picking up a voltage drop proportional to the current in the test circuit. The high-frequency discharges can then be observed on an oscilloscope screen or measured by other means. It is found that:

1. Direct-current high-potential tests are nondestructive if they are stopped at the voltage value at which any appreciable amount of ionization is observed, because breakdown is always preceded by ionization discharges in the insulation system.
2. The noise pattern on the oscilloscope screen is different for different conditions of insulation. This, in conjunction with the leakage- and absorption-current characteristics, enables one to tell whether the insulation is dry or wet, clean or dirty.

Tests have been made on small laboratory samples of insulation; on components of railroad equipment, such as armatures and field windings; and on entire locomotive power circuits. A great number of tests were carried out without any unanticipated breakdowns occurring.

TWO METHODS are at present widely used for evaluation of insulation systems in machines and equipment: the low direct-voltage resistance measurement (so-called megohmmeter tests); and the a-c high-voltage tests with prescribed overvoltages and measurement of the loss angle.

Both of these methods are subject to criticism, and much research and development work is still being done to find a satisfactory substitute. The main reasons for dissatisfaction with the test methods include the fact that the megohmmeter readings are not conclusive for comprehensive evaluation of insulation. Machine insulations with a very low insulation resistance, as measured with an ohmmeter, are very often known to give satisfactory service. An example of this is the electric equipment of diesel-electric locomotives in very humid atmospheres. If the low megohmmeter reading were to be taken as a measure, many of the locomotives would be taken out of service.

Paper 59-247, recommended by the AIEE Land Transportation Committee and approved by the AIEE Technical Operations Department for presentation at the AIEE Winter General Meeting, New York, N. Y., February 1–6, 1959. Manuscript submitted November 28, 1958; made available for printing January 28, 1959.

A. M. Odok is with the General Electric Company, Erie, Pa., and T. M. Soelaiman is with Universitas Indonesia, Djakarta, Indonesia.

However, experience shows that most of these locomotives operate satisfactorily. Alternating high-potential tests, on the other hand, which include loss-angle measurements, are complicated and require bulky equipment because of the large reactive power needed to charge the machine capacitances. Apart from this drawback, the tests are mostly of the go-or-no-go type and are based on fixed overstress determined by experience.

Mainly for the afore-mentioned reasons, various scientists and engineers have devoted much time to investigating the merits of high-potential direct current for evaluation of insulation systems.[1–16] The main issue in the previous work has been the validity and methods of interpretation of the d-c high-potential test results for high-voltage a-c motors and generators.

Since d-c high-potential testing is inherently better suited for d-c machines and equipment than for a-c machines, some of the controversies arising in its use on a-c machines are of less significance here. However, the d-c high-potential test procedure proposed and discussed in various publications to date is still not directly useful even for d-c equipment because of certain oversimplifications in interpreting the test results, particularly those concerning the physical picture of insulation behavior.

In this paper it will be shown that the d-c high-potential tests, when supplemented by observation of ionization discharges during test and when properly interpreted, can provide information about the insulation condition. Further, a test procedure will be described, and results obtained on specimens as well as on d-c machine components will be discussed. Finally, some results of testing the insulation of entire power circuits of locomotives will be presented.

Discussion

Aim of D-C High-Potential Testing

In the most general terms, the aim of an insulation-system test is to predict whether the system will withstand, for a prescribed period of time, the dielectric stresses imposed by its mode of operation. Therefore, the normal operating stresses and the nature of the breakdown must be considered when designing an insulation test method and interpreting experimental results.

The dielectric strength of insulation is affected by one or more of several conditions: mechanical damage; chemical deterioration; and the presence of dirt, dust, and moisture. The mechanism of breakdown varies with the insulation condition; basically it can be either intrinsic or result from discharges and thermal instability (see Appendix I).

Since this study is restricted to low- and medium-voltage d-c equipment, the expected operating stresses and mechanism of breakdown may be defined as follows:

1. Stresses. By low and medium voltage is meant those operating voltages for which test voltages do not exceed 8 kv. The operating stresses are supposed to be constant. (This is actually true of the field windings. The armature, however, is subjected to stresses which vary from zero to a maximum. These correspond to superposition of d-c on a-c stresses.)

2. Breakdown mechanism. Ionization discharges and resulting thermal instability are the most probable mechanisms involved in the breakdown of insulation systems considered here.

On the basis of these definitions and assumptions, it follows that the test method should be designed to satisfy the following conditions:

1. Insulation system under test should be stressed by direct voltage.

2. Any discharges which may induce the breakdown of the insulation should be detected before reaching any dangerous extent.

3. The cause for a low ionization starting voltage should be detected reliably.

In other words, the purpose of the test method is to determine the highest voltage level at which the given insulation will be free of damaging ionization; which, presumably, is the first stage in the breakdown of insulation systems under consideration here. Moreover, the results should show whether discharges are attributable to moisture, dirt, or conducting paths on creepage surfaces.

Shortcomings of Present Techniques

The present d-c high-potential test procedure and methods of interpreting its results have been described in numerous papers.[1–16] This discussion of their limitations is with a view toward improving the method of interpretation. It avoids a controversial part of the previous work, namely, whether information gained under d-c stresses can be of any use for a-c applications and, specifically, whether the connection between the breakdown voltages under the two kinds of stresses can be expressed as a single number, such as the 1.6 d-c–a-c ratio adopted by some investigators.

The present technique of d-c high-potential testing consists of measuring the following two quantities:

1. The steady-state leakage current is measured as a function of voltage applied between conductors and ground (leakage-current characteristic).

2. The leakage current is measured as a function of time with voltage held constant (absorption- or polarization-current characteristic).

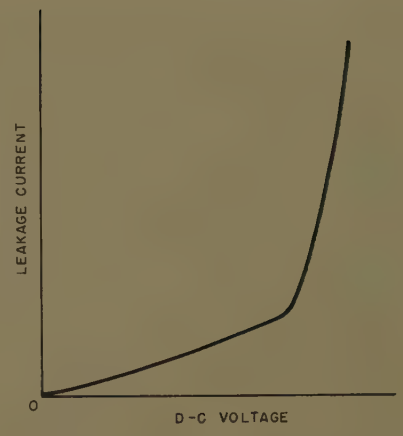

Fig. 1. Typical leakage-current characteristic for insulation in poor condition

In all previous work the evaluation of insulation has been based on these quantities, with a few exceptions where ionization probes have been used to detect electric discharges at certain locations of the winding.[6] Foust and Bhimani have used the additional tool of detecting the over-all electrical noise.[11] As a consequence of the limited information gained in this way, the publications on the subject differ mainly in the interpretation of these two measured quantities and so a brief discussion of the proposed ways of interpreting the leakage-current characteristic is appropriate.

The curve $i=f(v)$ has been used in different ways for predicting the breakdown voltages: In all cases where polar materials, such as water and certain types of contaminants, are present or a "deteriorated" insulation is being tested, the leakage-current characteristic will have a more or less pronounced knee after which the current increases more rapidly with increase in voltage (Fig. 1). This led to the hope that an asymptote may be found to indicate the value of voltage at which the current would increase to infinity. This voltage would then be looked upon as a breakdown level. The arbitrariness in this procedure can be demonstrated by changing the scale for the current ordinate. Evidently the geometrical shape of the leakage-current curve and the location of the visual asymptote are dependent on the scale chosen. Moreover, if this method is used with a good, dry insulation, it will lead to breakdown during test because no knee will be observed to indicate the approaching failure. With

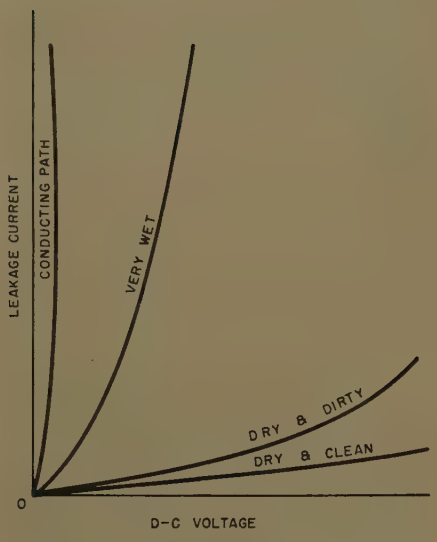

Fig. 2. Typical leakage-current characteristics for various conditions of insulation

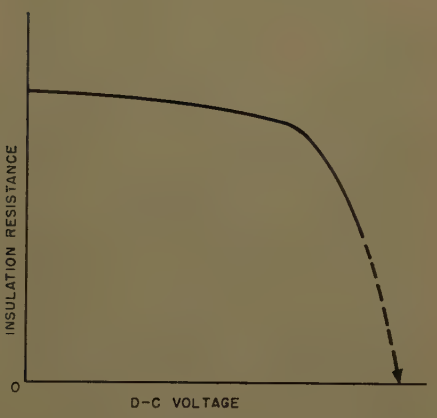

Fig. 3. Typical insulation resistance characteristic

changing amounts of humidity almost any shape of curve can be obtained, ranging from a very rapid increase of current with very wet insulations to the low-current straight-line characteristic of good, dry insulation (Fig. 2).

Another version of the foregoing method of prediction has been proposed in which the resistance characteristic $R=f(V)$ is extrapolated to $R=0$. The voltage at which the resistance approaches zero is taken to be the breakdown voltage (Fig. 3).

The leakage-current characteristic alone cannot tell anything about the presence of polar materials, such as moisture or contamination, because rapid increase of current is a relative condition which is difficult to recognize unless the characteristic of the clean, dry insulation for the machine under investigation is available. In the absence of this information, the absorption-current characteristic must be used to determine whether the insulation is contaminated or moist.

Fig. 4 (right). Simple circuit for ionization detection

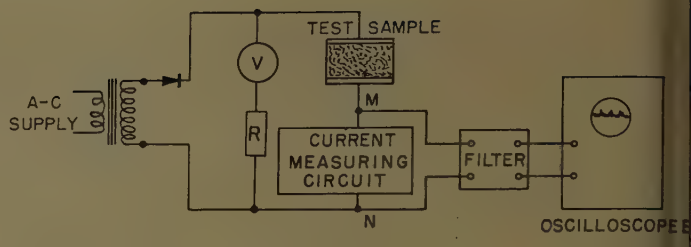

Fig. 5 (right). Ionization detection circuit with insulating transformer

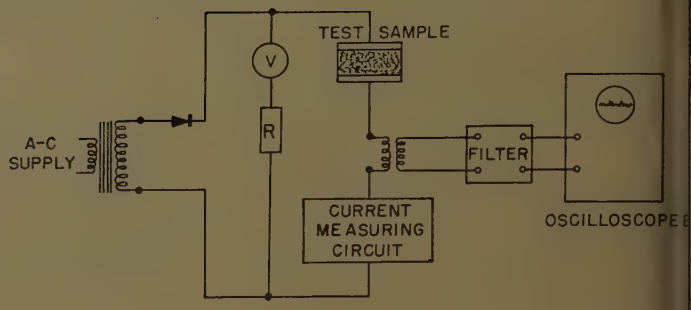

Improved Test Method

An observation made by the authors, and substantiated by careful study of the previously published work, can be made the basis of a nondestructive test method.

None of the insulation systems investigated broke down without discharges starting at a lower voltage level than the ultimate breakdown value. The discharges were external, internal, or on the surface, but usually two or all three kinds occurred simultaneously. (See Appendix I for explanation of terms.) Consequently, an ionization detection method which would cover all three kinds of discharges in the insulation system under test would indicate any approaching breakdown. Figs. 4 and 5 show two possible arrangements for this purpose. Essentially, this circuit consists of a means for picking up the voltage drop across the current-measuring circuit or an inductor coil, preferably through an insulation transformer, and an oscilloscope for observation of this voltage. Filters may be used to eliminate external noise resulting from industry frequency and other possible sources. The simple *R-C* high-pass filter has been found quite satisfactory. If it were desired to detect only the start of a certain ionization level some type of warning device could be used instead of the oscilloscope. However, the discharge pattern on the oscilloscope supplies additional valuable information (see Fig. 6).

Discharges start in a moist, contaminated insulation system at a much lower voltage level than the actual breakdown voltage. The test therefore usually will be stopped long before a breakdown can be anticipated. This may result in overcautiousness so that the anticipation of breakdown will be too far on the safe side. This circumstance, which can to a great extent be corrected by experience and skill in testing, is no drawback be-

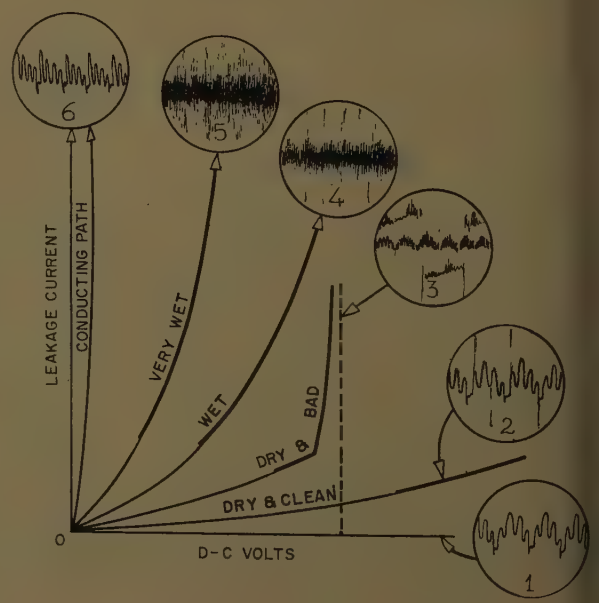

Fig. 6. Typical oscilloscope patterns for various conditions of insulation

1—No discharges
2—Occasional discharges
3—Broken down
4—Frequent discharges
5—Hazy picture due to very high frequency of discharges
6—Conduction only, no discharges

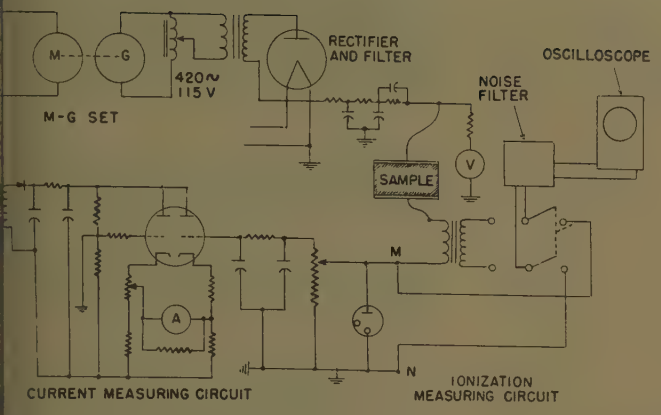

Fig. 7. Schematic of main circuits

ıse moist and contaminated insulations
l usually be treated in some way to
ıove polar materials before being put
o service and subjected to normal
erating stresses.

The cleaner and drier the insulation,
more closely the discharge starting
tage approaches the actual breakdown
ue. Therefore, the prediction of the
akdown voltage in clean and dry in-
ation without conducting paths on the
face is rather accurate. With the
rt of discharges of any appreciable
gnitude and frequency the test must be
pped because the breakdown follows
se discharges closely.

When the observation of discharges is
d together with absorption-current ver-
time and leakage-current versus
tage characteristics, it will reliably
icate:

The presence of polar materials and
ıducting paths (moisture, dust, dirt,
bon tracks) and gross insulation defects.

The maximum direct voltage which can
impressed on the insulation system with-
damaging it.

The breakdown voltage under d-c
esses for a clean and dry insulation. This
ue contains a certain safety margin be-
ıse breakdown occurs at a higher voltage
ın that at which discharges start.

Certain insulation weaknesses, such as
n-to-turn faults, mechanical damage, and delamination, cannot be reliably detected by a d-c high-potential test unless they have become sources of ionization previous to the time of tests. However, since no other single high-voltage test method will reveal all of these inherent weaknesses, this circumstance cannot be looked upon as a drawback to the proposed technique.

It should be noted that the observation of electrical noise need not necessarily be restricted to d-c stresses, but may perhaps be used with a-c stresses as well. This would make a-c high-potential tests nondestructive also. It is conceivable that discharge detectors could be built into the three phases of a generator, making it possible to follow the insulation quality closely under operating conditions.[9]

Equipment and Test Procedure

Before presenting results obtained by this technique of d-c high-potential testing, the test equipment and procedure will be explained in some detail.

Equipment and Circuitry

The principal circuit of a d-c high-potential test set is shown in Fig. 7. If the equipment to be tested is grounded, point M instead of N can be put on ground potential.

Additional equipment needed for observing the ionization discharges consists of an insulation transformer with a broad frequency band, a cathode-ray oscilloscope, and, in case of strong interference from other equipment, a filter. All three elements are readily built into the basic circuit, as shown in Fig. 7.

Discharge frequencies range from about 1,000 cycles per second to a few hundred kilocycles. However, there is no need to cover the whole range, so the frequency response of the series circuit transformer-filter-oscilloscope need be more or less flat only in the region from 1 to approximately 50 kc.

Test Procedure

The d-c high-potential test procedure involving only the absorption-current versus time and the leakage-current versus voltage measurements has been repeatedly described and discussed.[1–16] Although this paper is principally concerned with the technique and advantages of studying ionization discharges, certain observed peculiarities of absorption and leakage current characteristics will also be considered.

Absorption-Current Characteristics

When a constant direct voltage is suddenly applied to an insulation system, a rather high current inrush is observed. After a certain time the current settles to a lower steady value called the leakage current (Fig. 8). This time-dependent absorption current contains several components with different time constants. The longest time constant is due to a physical process called interfacial or space-charge polarization. The high sensitivity of this component to the presence of water or other polar material makes the ratio i_1/i_{10} (the absorption coefficient) meaningful for insulation evaluation. Here i_1 is the current 1 minute and i_{10} the current 10 minutes after application of the test voltage (Appendix II).

The presence of polar molecules causes

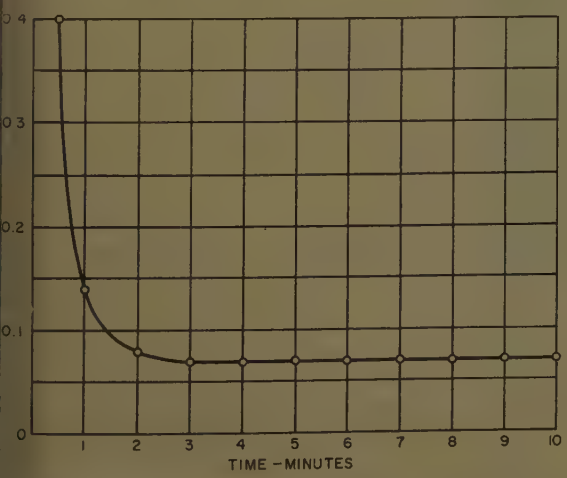

Fig. 8 (left). Typical dielectric - absorption characteristic of dry insulation in good condition

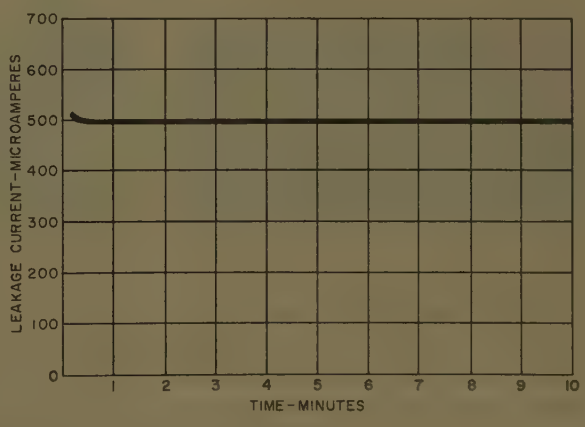

Fig. 9 (right). Typical dielectric - absorption characteristic of wet insulation in poor condition

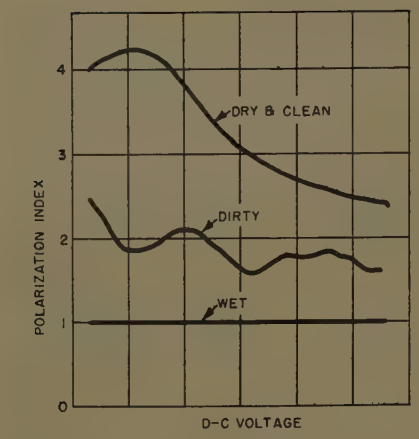

Fig. 10 (left). Typical polarization indexes for various conditions of insulation

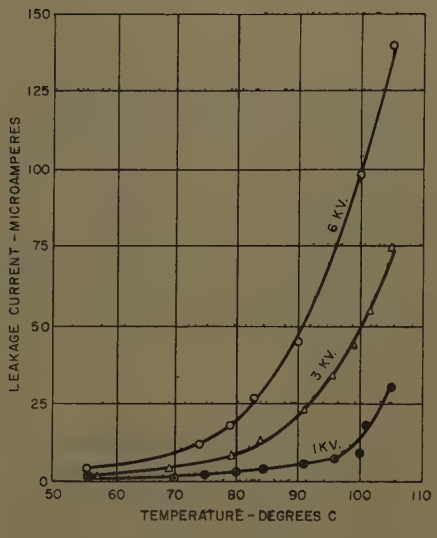

Fig. 11 (lower left). Effect of temperature on leakage-current characteristics

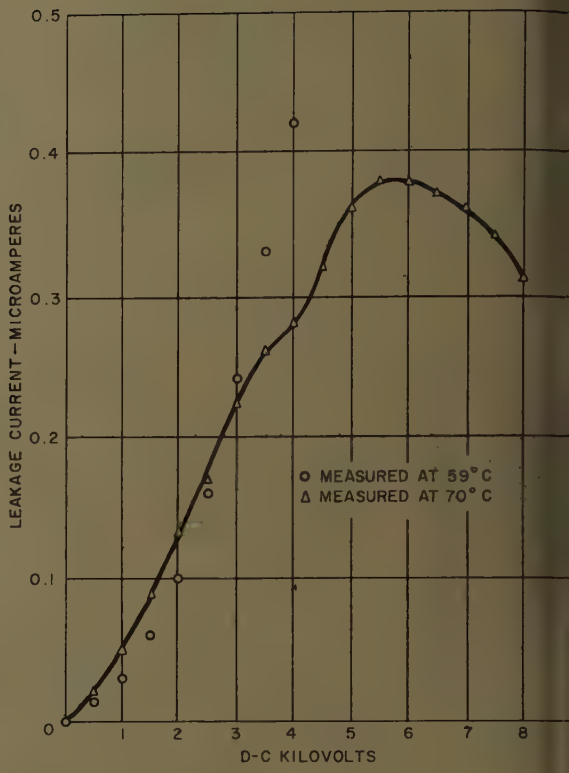

Fig. 12 (right). Effect of humidity on leakage-current characteristic

insulation to behave more like a pure ohmic resistance. This is characterized by a very short time constant for the establishment of the current (Fig. 9).

In choosing the voltage level for the absorption test the following two facts must be considered:

1. The polarization index depends on the voltage at which the absorption-current characteristic is being measured (Fig. 10).

2. For humid or heavily contaminated insulation, a low test voltage must be chosen for the absorption-current characteristic since discharges start very early and can be damaging to insulations under these conditions (Fig. 6).

Leakage-Current Characteristic

As already pointed out, the leakage-current characteristic in itself supplies practically no information about the insulation condition. Its shape is only indirectly related to discharge severity and its geometrical slope is as much a function of the chosen scale of co-ordinates as it is of the physical condition of the insulation. The fact that the leakage current is considered under a separate heading does not imply that its use apart from the absorption-current test and discharge observation is recommended. When supplemented with these two, however, it serves a certain purpose.

For practical reasons, the applied voltage is increased in finite steps during the leakage-current test. Consequently, with each increase of voltage some time must be allowed to establish a steady-state current. For the kind and size of machines here considered and the voltage steps used (500 to 2,000 volts), experience shows that 1 minute at each voltage step is long enough for the current to settle at a practically constant value.

If the preceding absorption-current test has shown the insulation system to be moist or dirty, the initial voltage must be very low, small voltage steps must be used, and electric discharges must be observed closely.

Some peculiarities of the leakage-current characteristics found by experimental analysis:

1. Shape of the curve. If the same insulation is tested under different conditions and the leakage-current characteristics are plotted using the same scale for the co-ordinates, certain trends are observed depending on moisture and dirt content and the presence of conducting paths in the insulation system. A schematic representation of various curve shapes is given in Fig. 2.

2. Effect of temperature. Temperature has a bearing on the magnitude of the leakage current. Results of an experiment are shown in Fig. 11. From this it appears that tests at room temperature are best suited for purposes of comparison. At these temperatures the current for a given voltage is least affected by changes in temperature.

3. Effect of repeated tests. A repetiti of test usually gives a different leakag current characteristic. The current ten to decrease with repetition in the case clean dry insulations, and to increase if t insulation is moist. In this respect, dirt dry insulations usually behave like clean-d insulations and dirty-wet ones like moi insulations.

4. Effect of humidity. Under certain c cumstances humidity can give rise to characteristic such as shown in Fig. 12.

5. Effect of dirt and conducting patl Sometimes no increase in leakage curre with increasing voltage is observed until certain voltage level is reached. Above th the current starts to increase until it reach another steady value at a higher volta and so on. The leakage-current characte istic in this case looks as shown in Fig. 1 A possible explanation of this phenomen is given in Appendix III.

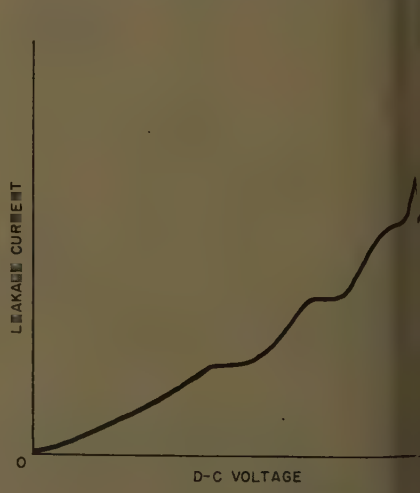

Fig. 13. Effect of dirt on leakage-curre characteristic

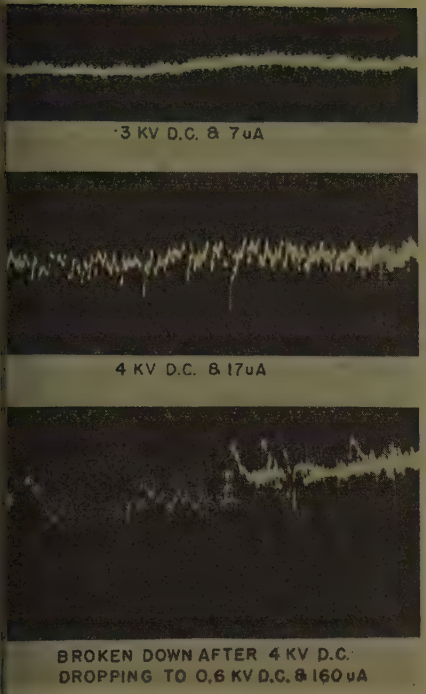

g. 14. Oscilloscope patterns for insulation mples (moistured mica mat, double sheets)

nization Discharge Characteristics

The oscilloscope screen must be ob-rved during the recording of the leakage rrent versus voltage to determine the scharge pattern, since discharges are a easure of the damaging effect of the test the insulation.

Occasionally discharges will occur at latively low voltages. Persistent and vere discharges are a sign that damage the insulation is starting. Tests must stopped at the first sight of these dis-arges, unless breakdown of the insula-n is intended.

Expected discharge patterns under rious conditions of the insulation are own in Fig. 6. These assume that the ual interference from industry fre-ency is not completely filtered out.

Following are some characteristics of e discharge patterns, depending on sulation condition:

Clean and dry insulation. Discharges art at a high voltage level close to the eakdown value. Occasional single dis-arges may occur before this level is ached.

Dry but slightly dirty insulation. Sim-r to item 1 but discharges are more fre-ent and easier to detect.

Wet and/or heavily contaminated insu-tion. Discharges start at very low volt-es and the pattern is hazy, a sign of higher equency discharges.

est Results

In the following section some ionization scharge characteristics obtained by using the methods described are discussed. Furthermore, tests on the insulation systems of two diesel-electric locomotives are described. Since the purpose was to demonstrate the usefulness of ionization discharge study, a thorough discussion of tests, including absorption- and leakage-current characteristics, seemed unnecessary.

Tests on a Small Sample of Insulation

The oscillograms in Fig. 14 show the increase of discharge frequency and magnitude with increasing voltage on a double-sheet sample of moistened mica insulation. Discharges started at approximately 3.5 kv and increased rapidly. The pattern at 4 kv indicated that the discharges had assumed a magnitude damaging for the insulation. The sample broke down as the voltage was being increased to the next step of 4.5 kv. Because of the high internal resistance of the test set, the voltage dropped to a low value after breakdown.

Tests on Machine Parts

Each of the oscillograms reproduced in Figs. 15(A) and 15(B) shows two curves corresponding to the two methods (Figs. 4 and 5) used for picking up the voltage drop proportional to the discharge current. The curve with high ripple content is obtained by using the arrangement shown in Fig. 4 and the smooth curve by using a transformer shown in Fig. 5. The transformer used attenuated the lower frequencies, thus eliminating the ripple on the d-c high voltage.

1. Test of a d-c motor field coil. Fig. 15(A) shows the discharge characteristics of a field coil which was dirty but dry. Discharges started at 9 kv, and the insulation broke down at the next voltage step.

2. Test of a d-c motor armature. The oscillograms of Fig. 15(B) were taken on a motor armature which was wet and dirty. The noise detected at lower voltages by the transformer pickup is external. The insulation broke down as 2 kv was exceeded. Note the hazy discharge pattern indicating the presence of moisture and dirt.

Tests on Locomotive Power Circuits

The insulation systems of two diesel-electric locomotives were tested. Although the ionization discharges were observed on the oscilloscope, no oscillograms were taken. Only a summary of observations made during the test will be given since these tests are yet in preliminary stage.

Tests followed the usual sequence of (1) a visual inspection of the insulation, (2) the dielectric absorption test, and (3) the

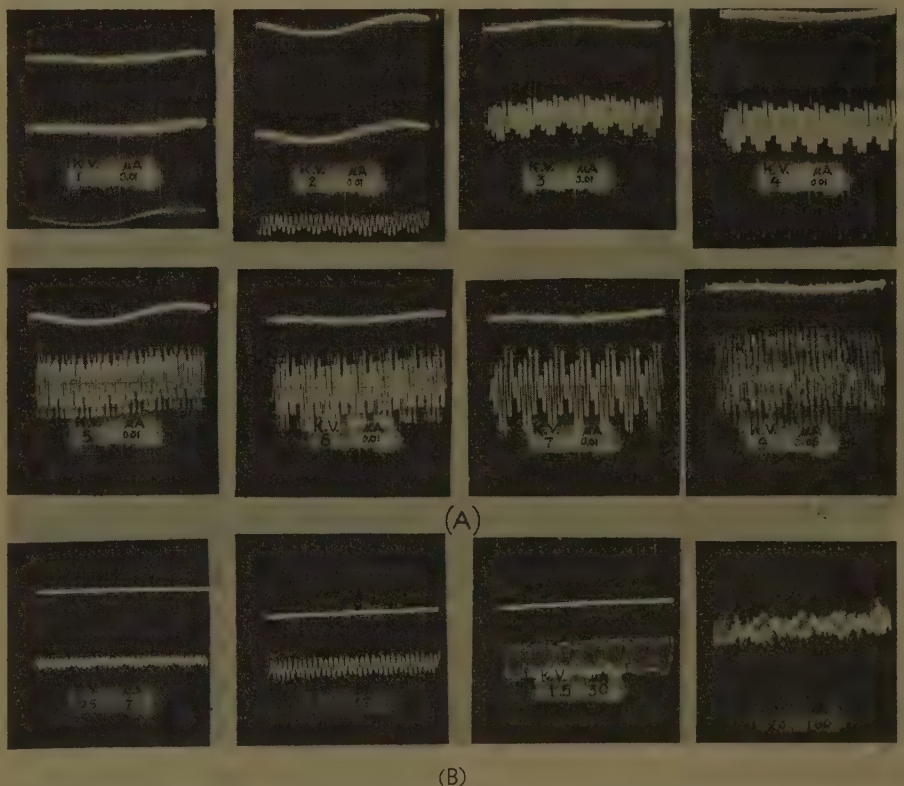

Fig. 15. Oscilloscope patterns obtained with test circuits shown in Figs. 4 and 5

A—D-c motor field coil
B—D-c motor armature

leakage-current test, together with the observation of ionization discharges.

In each case, the circuit under test consisted of one generator, two motors, and the power supply cable.

The inspection revealed that all components accessible to visual inspection were in a highly contaminated state.

The polarization index was practically unity, and the leakage current increased very rapidly, reaching the maximum output of the test set (2 milliamperes) at 350 volts. Discharges started at a low voltage and the discharge pattern was hazy.

A diagnosis, based on the electrical testing only, would have reliably detected what in this special case could be found by visual inspection. Further tests on individual components showed that the motors were free of ionization discharges up to 1,000 volts and had a low leakage current. The generators and cables were found to be the main source of high leakage and excessive discharge currents.

Conclusions

If, in addition to the usual measurement of absorption and leakage current, means of electric discharge detection are employed, d-c high-potential tests yield additional information and become nondestructive.

Observation of ionization discharges, in conjunction with the leakage- and absorption-current characteristics, indicates the condition of the insulation, i.e., whether it is dry or wet, clean or dirty.

When insulation is wet or dirty, the breakdown voltage can be predicted only with a large margin of uncertainty. With dry, clean insulation, however, a much closer prediction is possible.

A quantitative analysis of the ionization discharges with respect to magnitude, power, and frequency spectrum may supply valuable information about insulation condition. This aspect presents a promising field for further investigation.

It is suggested that a similar approach be investigated for use during a-c high-potential tests.

Appendix I. Theories of Breakdown

The following three kinds of breakdown of solids are known to occur either singly or in combination under dielectric stresses.[13-16]

Intrinsic Breakdown

This is best defined as the type of breakdown which occurs at very high voltages if the possibility of the two other kinds of breakdown is well excluded. Its mechanism is almost certain to be electronic (theories by von Hippel and Fröhlich). The intrinsic dielectric strength is a function of time, temperature, and sample thickness (for very thin samples), and its value is of the order of magnitude 10^6 to 10^7 volts per centimeter.

Thermal Breakdown

The heat generated in conducting paths and/or the dielectric losses with a-c stresses change with temperature as well as with voltage. Hence a thermal instability can occur in which the generated losses cannot be dissipated as rapidly as they are produced. Consequently, very high local temperatures can occur, leading to destruction of the insulation material.

This type of breakdown is usually the second stage in a breakdown caused by d-c stresses, the first phase being some kind of discharge impinging on the insulation surface.

Breakdown by Discharges

The test sample or machine consists of three elements: the two electrodes and a composite insulation. The latter is not of a homogeneous structure, and may have many more or less conducting cross paths inside and on the surface, and voids of different sizes. This system is best regarded as a random lattice network of capacitors and resistors. For a given potential difference between the electrodes there is a certain potential and current distribution in this lattice. If, however, the potential difference between any two points exceeds the ionization value for the gas between these points, the gas will be conducting and shifting of charges in the insulation system will take place. With the new distribution, or especially during the redistribution, some new gaps will be conducting. Therefore, random discharges will occur, although the voltage between the electrodes may be kept at a constant value.

Despite the fact that ionization of a gas adjacent to or trapped-in the insulation is the common feature for all types of discharge, it is useful for purposes of analysis to differentiate between the following types:

1. Internal discharges, which result from the breakdown of the gases in the voids inside the insulation.
2. External discharges, which result from the formation of an ionization path between the surface of the insulation and one electrode. Any discharges between the slot wall and wall insulation in a machine must be considered in this category. The spot where the discharge impinges on the insulation surface is usually the starting point of a breakdown caused by thermal instability.
3. Surface discharges, which is most likely to occur in machines, especially under d-c stresses. Surface discharges occur between conducting spots on the insulation where high enough stresses can build up if a large part of the insulation surface is covered by such conducting paths or substances as carbon tracks, water, and dirt. The discharge develops along the surface between the conducting spots. After each discharge a redistribution of potential on the surface takes place. This phenomenon keeps repeating, so that a rather-high-frequenc current component is observed in the e: ternal circuit.

Appendix II. Polarization and Absorption

Maxwell's Theory on Composite Dielectrics

Any insulation material used in practic contains a certain amount of more or le conducting components and is, as a whol nonhomogeneous with voids of differe sizes. A composite insulation has the add tional feature of consisting of layers materials differing in their dielectric as we as their conducting properties. Thus, ele trically speaking, a composite insulation ca be considered as representing a lattice ne work of randomly connected resistors an capacitors of various sizes.

The instant a constant direct voltage applied to the electrodes between which composite insulation is placed, the fre charges (and to a certain extent the boun charges) will start to move. Dielectr dipoles will orient themselves according the applied potential difference between th electrodes until a balance between th applied voltage and the back potential established. This back potential resul from the charge distribution and the voltag drop caused by the current across the con ducting paths. Because of this the initi current will contain a part attributable charge displacements and dipole orientatio in addition to a part flowing through th conducting paths. The final current will only the conduction current flowing throug paths which extend from one electrode to th other.

Polarization in Homogeneous Materials[14,15]

Three principal kinds of polarization ar possible in a homogeneous solid insulatio

1. Polarization caused by induced dipo moments. Electrons surrounding th atomic nuclei or unequally shared by atom of a molecule will tend to follow a distorte trajectory under the influence of an externa field, thus giving rise to an increase capacity. The so-called electronic an atomic polarizations are of this type.
2. Orientation polarization is attributab to the fact that an external field will tend t orient the dipoles already existing in th insulation in the absence of this field.
3. Space charge or interfacial polarizatio are caused by charges which can move in side of the dielectric until they becom trapped in the material or on interfaces.

Appendix III. Effect of Discharges on the Shape of the Leakage Current Characteristic

Experimental studies imply a defini relationship between the increasing slope

the leakage current characteristic and the frequency of electric discharges. The following hypothesis about the mechanism behind the shape of the leakage current characteristic may help to explain some of the peculiarities observed experimentally.

The picture of a random lattice network of resistances and capacitances underlying Maxwell's theory of composite insulations must be supplemented, in the case of actual insulation, by certain assumptions about the potential and current distribution on the surface of the insulation, e.g., on the surface of the end windings. This surface is far from being absolutely clean; in addition to water, it carries dust and certain other contaminants. Carbon deposits will also be found on this surface, especially in cases of machines with carbon brushes or organic insulation.

Aggregates of such conducting or polarized materials are at practically equal potential. Consequently, the total potential difference is distributed only on the small remaining area which is free of such foreign matter.

As explained in Appendix II for the interfaces and inside of the insulation, the potential distribution on the surface will be disturbed if the field strength at any point exceeds the ionization level of the adjacent air. The redistribution of charges on the surface leads to a new balance of potentials. A certain leakage current corresponds to the newly established conducting paths. With increasing voltage, rearrangement of potentials inside and on the surface of the insulation will occur. The more discharges occur at a given voltage, the higher the stress imposed on the remaining parts of the insulation so that with the beginning of any appreciable amount of discharges an exponential take-off of the current would be expected. In fact this is observed in all insulation systems where the surfaces are contaminated or moist.

With dry insulations, the leakage current characteristic more closely follows a straight line. The insulation behaves like an ohmic resistor and no shifting of charges takes place as voltage is increased. Of course, this is true only up to that voltage at which even the more uniformly distributed potential of the dry insulation will be enough to start ionization. A more sudden increase of ionization and insulation damage is to be expected in this case since, with the disturbed balance of potential distribution, other points already stressed to the very limit will be overstressed and break down.

The step-like leakage current characteristic often observed with dirty insulation (Fig. 13) can be explained on the basis of discharges on the surface. During the increase of voltage, a point in the potential distribution on the surface may be reached above which a further increase of voltage produces no new discharges. The current may then stay at a practically constant value until the voltage is increased to a value high enough to create new ionization channels.

References

1. Dielectric Strength Ratio Between Alternating and Direct Voltages, J. L. R. Hayden, W. N. Eddy. *General Electric Review*, Schenectady, N. Y., vol. 26, Sept. 1923, pp. 646–52.

2. Maintenance Over-Potential Tests for Armature Windings in Service, R. N. Wieseman. *Ibid.*, vol. 53, Aug. 1950, pp. 24–28.

3. Alternating and Direct Voltage Endurance Studies on Mica Insulation for Electric Machinery, G. L. Moses. *AIEE Transactions*, pt. I, vol. 70, 1951, pp. 763–69.

4. Nondestructive Testing of Generator Insulation, E. H. Povey, F. S. Oliver. *Electrical Engineering*, vol. 70, June 1951, p. 498.

5. A Maintenance Inspection Program for Large Rotating Machines, J. S. Johnson. *AIEE Transactions*, pt. I, vol. 70, 1951, pp. 749–55.

6. Diagnosis of A-C Generator Insulation Condition by Nondestructive Tests, A. W. W. Cameron. *Ibid.*, pt. III (*Power Apparatus and Systems*), vol. 71, Jan. 1952, pp. 263–74.

7. Techniques and Examples of High-Voltage D-C Testing of Rotating-Machine Windings, C. L. Sidway, B. R. Loxley. *Ibid.*, vol. 72, Dec. 1953, pp. 1121–29.

8. Leakage-Voltage Characteristics of Insulation Related to D-C Dielectric Strength, J. S. Johnson, J. W. Clokey. *Ibid.*, Aug. 1953, pp. 681–86.

9. Examination of High-Voltage D-C Testing Applied to Large Stator Windings, R. T. Rushall, J. S. Simons. *Proceedings*, Institution of Electrical Engineers, London, England, vol. 102, pt. A, Oct. 1955, pp. 565–80.

10. D-C High-Potential Maintenance Testing of Traction Motors and Generators, W. Schneider. *AIEE CP56-372* (available on request).

11. Predicting Insulation Failures with Direct Voltage, C. M. Foust, B. V. Bhimani. *AIEE Transactions*, pt. III, vol. 76, Dec. 1957, pp. 1120–39.

12. The Insulation of Electric Equipment (book), W. Jackson. John Wiley & Sons, Inc., New York, N. Y., 1954.

13. Dielectric Breakdown of Solids (book), S. Whitehead. Oxford Clarendon Press, New York, N. Y., 1951.

14. Dielectrics and Waves (book), A. V. Hippel. John Wiley & Sons, Inc., 1954.

15. Dielectric Materials and Applications (book), A. V. Hippel. John Wiley & Sons, Inc., 1954.

16. Some Recent Studies of Random Noise Between Metals and Dielectrics, S. I. Reynolds. *Journal of Applied Physics*, New York, N. Y., vol. 27, 1956, pp. 728–34.

Discussion

A. Wichmann (Siemens-Schuckert-Werke AG, Mülheim, Germany): The paper is a very useful contribution to the development of d-c insulation test methods and a better understanding and analysis of d-c ionization measurements. It would be of interest to know what method was used to distinguish between external, internal, and surface discharges, and possibly disturbances from outside. In our very similar investigations on high-voltage insulation for turbogenerators made some years ago in our laboratory it was difficult to avoid disturbances from outside of the test specimen. However, the test voltage needed for internal ionization was higher than the voltage used by the authors.

We tried to separate the internal ionization from discharges on surface and outside in a special way.[1] In this method the test bar insulation is charged with direct current for a certain period to obtain good polarization of the insulating material, and after ionization in the holes a nearly complete compensation of the charge on the hole by charges of other polarity on the surface of the holes as shown in Fig. 16(A). Removing direct voltage and connecting both electrodes, the polarization of the solid insulation is equalized in a time given by the absorption current equation.

$$i_a = Kt^{-n}$$

The surface charges in the holes are no longer compensated for and thus cause increasing voltage and, finally, a gas breakdown to equalize the positive and negative charges. These breakdowns may be seen as current pulses on an oscilloscope screen or be counted by an impulse recorder. The pulses are now of opposite polarity as during charging time. The number of pulses per second is decreasing with time and increasing with voltage. The slope of the curve given in Fig. 17 is very similar to the tan δ increase with voltage caused by a-c glow discharges in the holes of the insulation.

The ionization caused by direct or alternating current will not act as a signal of breakdown if the insulation contains mica flakes. High-voltage insulation for electric machines contains large mica splittings and, therefore, it is able to withstand glow discharges during service or test over a very long time without damage and failure. The insulation system tested by the authors seems to be made without mica, otherwise it would not be understood that d-c ionization is followed by breakdown. Ionization in generator insulation normally starts at

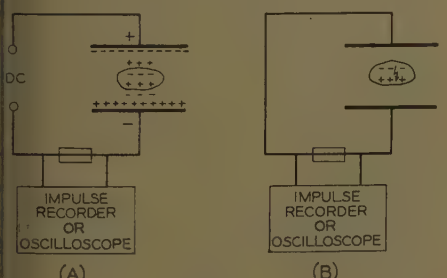

Fig. 16. Direct-current polarization and ionization during (A) charging and (B) discharging time

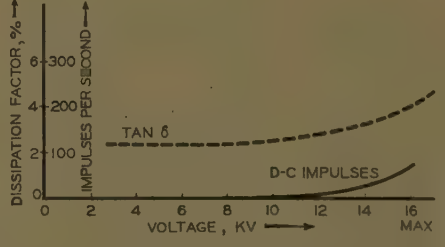

Fig. 17. Tan δ and d-c ionization pulses during first 5 seconds' discharging time on generator bar insulation

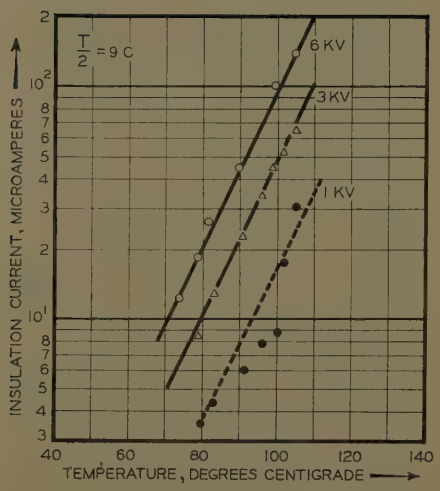

Fig. 18. Effect of temperature on leakage-current characteristic (based on Fig. 11)

rated voltage, sometimes lower, while breakdown occurs at ten times higher voltage, and very seldom at only two or three times higher voltage if the insulation is mechanically deteriorated. Therefore, the experience of the authors as to the indication of breakdown by ionization is limited to their special insulation system.

I also would like to comment on Fig. 11 of the paper which shows the effect of temperature on the leakage-current characteristic. If the points given in Fig. 11 are plotted versus voltage it may be seen the leakage current follows Ohm's law at any temperature between 55 and 105 degrees centigrade. In plotting leakage current versus temperature as shown in Fig. 18 we recognize the normal temperature dependency valid for all insulators and given by the formula

$$i(\zeta) = i(\zeta_0)e^{\alpha(\zeta-\zeta_0)}$$

Measurements at different temperatures may be reduced to the same temperature for comparison by a straight line on log paper without difficulty.[2] If we apply this knowledge to the measurements given in Fig. 12 we must conclude that the decreasing leakage current with increasing voltage may be caused by drying during test.

References

1. Maintenance Testing of High Voltage Insulation in Electrical Machines, A. Wichmann. *VDE Fachberichte*, Wuppertal-Elberfeld, Germany, vol. 19, 1956, pp. I/136–46.

2. Drying of Electrical Machines, A. Wichmann. *Elektrotechnische Zeitschrift*, Wuppertal-Elberfeld, Germany, vol. 76, 1955, pp. 340–47.

J. S. Simons (British Thomson-Houston Company, Ltd., London, England): The authors are to be congratulated on their useful contribution to a better understanding of the behavior of insulation under high d-c stress. The measurement of the presence and magnitude of discharges often provides very significant information when evidence of impending breakdown is being sought.

Unfortunately the larger the machine the more difficult is the interpretation of results, as the discharges observed may represent the summation of many separate sites each consisting of a cluster, and involving external, internal, and surface types of discharge.

When we recently carried out high-voltage d-c tests both on individual stator coils and on a complete stator winding, in many cases breakdown was preceded by visible and audible discharging. However, in some cases failure occurred suddenly and in such cases even ionization detection measurements would not prevent serious damage being done before the test could be stopped. In the majority of cases ionization measurements would assist substantially in the interpretation of results.

We favor a-c testing for large a-c machines and we have carried out a-c ionization measurements both on complete windings and on individual coils. Such measurements assist materially in assessing insulation quality. The use of discharge detection methods is to be encouraged and the authors have demonstrated the potentialities of such techniques.

B. V. Bhimani (General Electric Company, Schenectady, N. Y.): The authors' conclusive evaluation of direct-voltage tests, applied to composite insulation systems of rotating machines, is a significant contribution to the field of insulation testing. There is considerable information in their paper that attracts attention, and it is specifically based on tests performed on complete machine windings.

Their evaluation separates the reliable aspects of direct-voltage tests from limitations of such tests. Their recommendation of measuring ionization, along with leakage current and polarization index of insulation, seems to increase the reliability of interpretation of such data. Another important aspect of this recommendation is that it reduces the possibility of damage to insulation during direct voltage tests. These aspects of the authors' work are discussed in the following.

Evaluation of Direct-Voltage Tests

Reliable Aspects

The authors reaffirm that direct voltage tests are reliable indicators of the following:

1. Dirt, dust, and "moisture" content of insulation.
2. Presence of carbon tracks of conducting particles in or on an insulation tested.
3. Some gross insulation defects, e.g., short circuits from conductor to ground.

They also recommend the addition of ionization measurements, to those of leakage current and polarization index, for increasing the reliability of interpretation of direct voltage test data.

Limitations

Limitations of direct-voltage tests, as indicated by the authors, are

1. The effect, on insulation strength, of mechanical damage and chemical deterioration, cannot be reliably detected by such tests.
2. These tests cannot reliably detect turn-to-turn faults in a winding, and insulation delaminations, i.e., insulation that has satisfactorily withstood such tests may still have serious "weaknesses" that could affect its operating characteristics.
3. Results of such tests are affected by the temperature of the insulation tested.
4. Leakage current readings may vary from one direct-voltage test to another, on the same insulation, even when factors such as temperature, humidity, dirt content, and "condition" of insulation and the method of application of the test are controlled to be the same for all such tests.
5. It is not possible reliably to "predict" breakdown of insulation under such tests, from leakage-current characteristics.
6. Distribution of electric stresses under direct-voltage tests are different from those under alternating-voltage stresses. The results of direct-voltage tests, therefore, cannot reliably indicate whether an insulation has sufficient voltage strength for operating under alternating voltage stresses.

The authors' evaluation, that separates the reliable aspects of direct-voltage tests from limitations of such tests, based on results of tests on complete machine windings, complements a similar evaluation of these tests, based on results of tests on special sheet insulation samples (see reference 11 of the paper).

Measurement of Ionization During Direct-Voltage Tests

The additional measurement of ionization, during direct-voltage tests, as recommended by the authors, seems to increase the reliability of interpretation of such test data. It also reduces the possibility of damage to insulation under test, for reasons briefly discussed in the following and described in detail in reference 11 of the paper.

Under direct-voltage stresses, on special sheet insulation samples tested between circular brass electrodes, extensive regions of the samples had binder material degraded by "the current density-thermal-ionic mechanism." Such a degradation of the binder was caused by interlayer ionization activity inside the samples. Under alternating-voltage stresses, no such regions of degraded binder were observed. Surface ionization was very profuse and evenly distributed, under alternating-voltage stresses, while it was almost totally absent under direct-voltage stresses. Such differences in the nature of ionization, under the two types of stresses, resulted in degradation of insulation, under direct-voltage stresses, in regions where alternating voltage had little immediate effect.

The test data by Odok and Soelaiman indicate that some ionization preceded direct-voltage breakdown of insulation. While this does not conclusively prove that the insulation was being progressively degraded by the ionization activity, it does indicate that by stopping direct-voltage tests, when ionization is initiated, the possibility of damage to insulation, under such tests, may be reduced or eliminated.

Summary

1. The authors' recommendation of measuring ionization along with leakage current and polarization index, during direct-voltage tests, will increase the reliability of interpretation of such data, and it will reduce the possibility of damage to insulation under test.

Their evaluation separates the reliable spects of direct-voltage tests from limitations of such tests.

This paper is a very timely and significant ontribution to the field of insulation testing.

. W. W. Cameron (Hydro-Electric Power Commission of Ontario, Toronto, Ont., Canada): The authors should be congratulated on an interesting study, carefully eported. High-frequency discharge detection, as they have developed it, shows romise of being a useful adjunct to d-c igh-potential testing of some insulations. t is hoped that further study and experience vill show the areas in which it may most ffectively be applied.

One question I would like to ask is whether the authors have encountered, in heir experiments, pulses, resembling ionization pulses, which are associated with the bsorption current, and also with the orresponding discharge current. Apparntly some of the polarization processes roceed in discrete bursts. In 1950 I bserved these pulses by a circuit similar to ig. 4, and saw that they recurred very apidly after a stepwise increase in direct oltage, becoming progressively less frequent as the absorption component of curent decayed. Upon removing test supply, nd short-circuiting the specimen, pulses of imilar amplitude but opposite polarity ccompanied the discharge current in the ame manner, diminishing in repetition rate s the d-c microampere reading decreased. was able to puzzle my colleagues by showng them what seemed to be ionization ulses in insulation at zero voltage, although uch a process should not, of course, be alled ionization. This phenomenon has lso been reported by Dr. Wichmann (see eference 1 of his discussion).

It would seem that some care would be equired in discriminating between these bsorption pulses and the discharges which he authors wish to utilize.

Fig. 15(A) shows discharges from 5 kv pwards, suggesting some difficulty in udging when intensity is dangerous. On he other hand, a sixfold increase in direct urrent between 7 kv and 9 kv looks like a ather clear indication. Fig. 15(B) shows hat external interference may be a complication in assessing discharges; again, more han five times increase in current or four imes decrease in resistance between 1.5 kv nd 2.0 kv is hardly to be overlooked. I hink these current indications call for reconsideration of the statement that leakage urrent gives "practically no information."

The authors' findings refer to d-c machines, in which leakage is complicated, or even dominated, by commutators and other components offering surface leakage paths. The insulations investigated seem also to have had very little absorption compared with insulations usual in high-voltage tator windings. Therefore, I am wondering to what extent these findings will be pplicable to the higher-voltage machines.

Regarding Appendix II on absorption, I believe that the major absorption in high-oltage machine insulations, which may ake hours to diminish to insignificance, has sually been ascribed to interfacial polarizaions.

The statement that "high-voltage d-c testing is inherently better suited for d-c machines and equipment than for a-c machines" is one which I question. The armature coil of an operating d-c machine is subject to alternating voltage superimposed on a direct voltage. It is insulated generally in the same manner as an a-c machine coil. It is my belief that a testing voltage should be selected according only to the condition which it is required to detect, and that our commonly assumed relations between testing and operating voltages are liable to be illusory. I heartily echo the authors' warning against the use of magic single values of "d-c–a-c ratio."

Direct-voltage tests have been found suitable for detecting cracks, fissures, delaminated areas, and other conditions involving paths through high-voltage machine insulations. This paper indicates that d-c tests also detect adverse conditions in open creepage paths. I am rather surprised that some failures of traction machines are not ascribed to fissuring of insulation, and to tracking on creepage paths. Also, I would not have expected many faults in these lower-voltage machines to be caused by ionization. In my experience, d-c tests have not indicated thermal degradation, unless it was so far advanced that ionization or cracking presented a through path.

The fears which the authors express regarding d-c leakage-versus-voltage tests have not been justified in my 7 years' experience of their application to high-voltage a-c machines. These tests have been reliably nondestructive. If the authors' discharge detection method can confer any additional significance upon such tests, may I be the first to welcome it. Figs. 1, 2, 3, and 6 indicate experience consistent with my own. I cannot agree that a d-c test on "good dry insulation" involves any danger of breakdown, because if the insulation is good and intact it will very easily withstand a suitable maximum test voltage. If the insulation is wet, however, this should be detected by a simple megger test before a high-voltage test is attempted.

Appendix III appeals to me as giving a very good picture of a mechanism of d-c conduction across an insulating surface with increasing voltage. The point which I think has been missed here is that similar mechanisms would be expected to apply also to conduction along the surfaces of fissures through the insulation. Therefore, this may well be an explanation for high-voltage d-c tests detecting such fissures reliably and nondestructively.

The effect of moisture is obviously important in such surface and fissure conduction mechanisms. Fig. 12 does not specify humidity conditions, but the peculiar leakage-current behavior at the higher temperature may be due to drying up, by the current, of small amounts of moisture. In my experience, consistent and significant d-c nondestructive tests are obtained when windings are cooled to ambient temperature in air of normal humidities. Adverse reports seem to have been based upon tests made on warm or very dry windings.[1]

Regarding applications to a-c testing, I would say that my colleagues are using a discharge detector to determine ionization inception and extinction voltages in large rotating machines. A few minutes' running on open circuit, with varying excitation, is all that is required. This seems to give a good indication of void formation, and of the general loosening of the insulation structure which gives a predisposition to turn-to-turn faults.

Attention is invited to a paper by F. S. Oliver which contains interesting information on discharge measurements.[2]

In conclusion, I am interested in the possible benefits of quantitative analysis of discharges, and I hope the authors will be encouraged to continue these studies and to favor us with further reports. I thank them again for a wealth of valuable data and a thoughtful paper.

REFERENCES

1. EXPERIENCE AND DEVELOPMENT IN NONDESTRUCTIVE D-C TESTING FOR MAINTENANCE OF HIGH-VOLTAGE STATORS, **A. W. W. Cameron, A. M. Sinclair.** *AIEE Transactions*, pt. III (*Power Apparatus and Systems*), vol. 75, Apr. 1956, pp. 201–10.

2. MEDIUM-VOLTAGE A-C TESTING OF ROTATING MACHINERY INSULATION, **F. S. Oliver.** *AIEE CP 58-203* (available on request).

E. B. Curdts (James G. Biddle Company, Philadelphia, Pa.): I agree with the authors of this paper that tests on the insulation systems of low- and medium-voltage equipment which includes the detection of corona or gaseous ionization should be useful in evaluating the condition of such systems. Whether a supplementary ionization test can be economically justified as a maintenance procedure is open to question and should be further investigated. The skill required of repair-shop personnel in interpreting test results may present a problem of economics, and electrical noise causing unpredictable distortions of the cathode-ray oscilloscope pattern may point to the need of effective input filtering and specimen shielding which may add to this economical problem.

I believe that something can be learned by the ionization tests suggested by the authors and further investigation is certainly justified. However, there are several categorically made statements in this paper which should be questioned.

One of these concerns the megohmmeter test described in the opening section of the paper. The insulation-resistance test as made by such instruments is not necessarily a low-voltage test for equipment considered in this paper. Numerous motor repair shops and others use megohmmeters rated up to 5,000 volts with provisions for selecting several voltages below the maximum.

Second, regardless of statements made by the authors, insulation-resistance tests have been for years and are continuing to be used with a great deal of success in preventive maintenance activities. Several methods are in use, their choice depending somewhat on economics. The simplest of these, the 1-minute test at a voltage usually low compared to the rating of the specimen, very faithfully reveals the presence of dirt, moisture, and carbonized paths. Its usefulness is limited only because it cannot distinguish between relatively harmless generally distributed leakage conditions and localized incipient faults. Insulation-resistance tests made with several voltage steps ranging from below to somewhat above the rated voltage of the equipment under test can give more information than a single-voltage

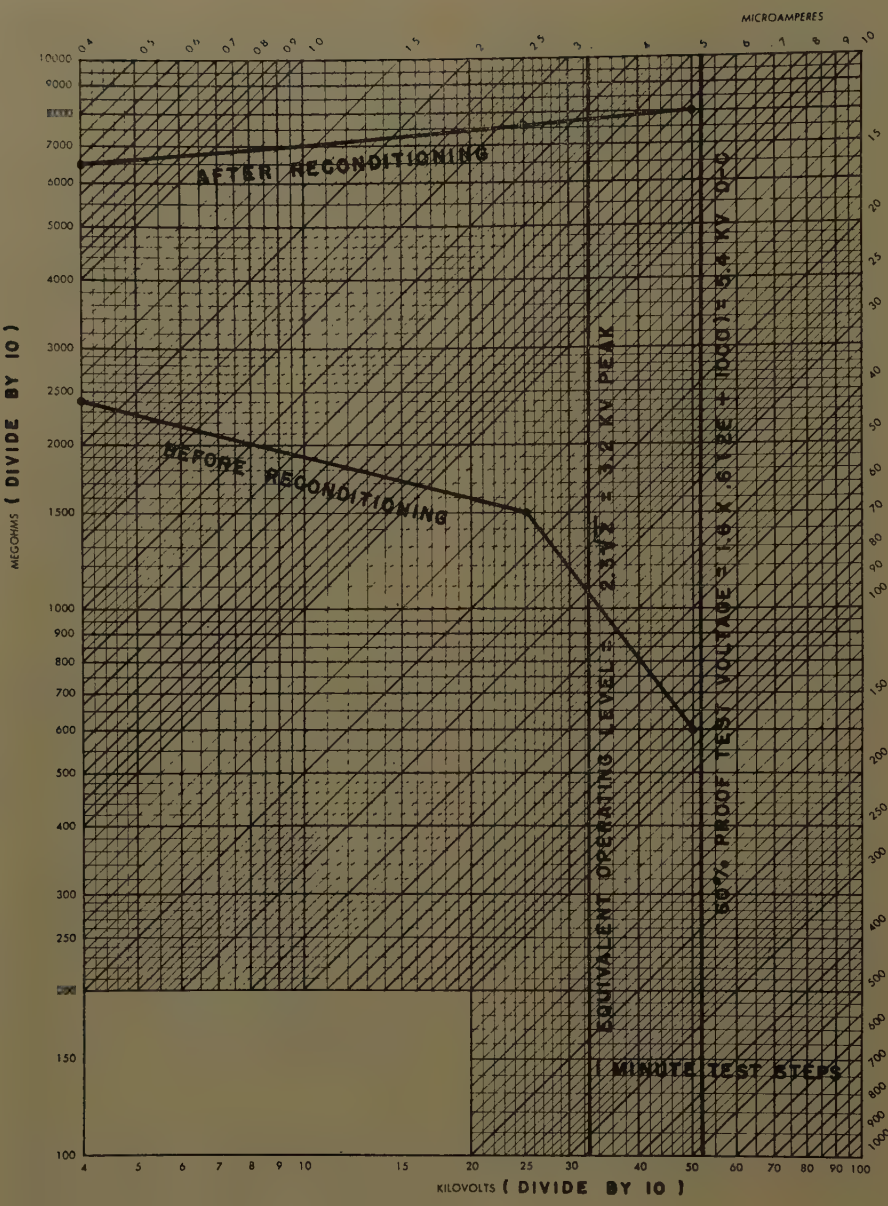

Fig. 19. A 350-horsepower 2,300-volt 3-phase motor armature before and after reconditioning

resistance measurement concerning the localized characteristics of abnormal leakage current.

The authors give an example of the unreliability of low insulation-resistance values on diesel-electric locomotive equipment resulting from tests made in very humid atmospheres. If such humid atmospheres are not representative of operating conditions because the insulation is operated at temperatures in excess of the dew point, then the test is not realistic in the first place. On the other hand, if the same conditions of humidity prevail in service as exist during tests, then the measurement tells us from experience what values can be tolerated in service when caused only by generally distributed leakages. However, for maximum reliability higher step-voltage insulation-resistance tests can also be made in an effort to reveal any incipient faults that may exist. I doubt very much if ionization tests, under the high-humidity conditions cited, can do more. In fact the authors make the following statement in their paper:

"Discharges start in a moist, contaminated insulation system at a much lower voltage level than the actual breakdown voltage. The test will therefore usually be stopped long before a breakdown can be anticipated. This may result in overcautiousness so that the anticipation of breakdown will be too far on the safe side. This circumstance, which can to a great extent be corrected by experience and skill in testing, is no drawback because moist and contaminated insulations will usually be treated in some way to remove polar materials before being put into service and subjected to normal operating stresses."

I am afraid that the authors, in their understandable enthusiasm for the ionization test, have become unduly critical of the voltage–current or voltage–resistance method of test. They say that it alone cannot tell anything about the presence of moisture or contamination, and supply practically no information about the insulation condition. Our experience definitely does not bear this out. We have found that excessive moisture and dirt, or what might be called "poor housekeeping," can be easily detected by the voltage–resistance or voltage–current method. Fig. 19 is a typical example of conditions as found and the results of reconditioning a 2,300-volt motor armature. I can find nothing in the data given in this paper to indicate that the ionization test would be a more convincing detector of dirt and moisture than the voltage–resistance or voltage–current test. The nonlinear behavior of the currents given in Fig. 15 of the paper certainly seem to be as informative as the corona patterns. Incidentally, the nonlinearity of the current given in these figures can be easily appreciated without resorting to curves with ill-chosen co-ordinates which is one of the objections raised by the authors to the analysis of leakage current. Furthermore, it is not necessary, in the analysis of leakage-current behavior, to apply each voltage step long enough to establish a "steady-state current." The rising characteristics of the insulation resistance of the curve shown in Fig. 19 after the armature was reconditioned is caused by the remanent, superimposed absorption currents at the end of each 1-minute step. Understanding the reason for this rising behavior makes it unnecessary to eliminate it by increasing the time for each voltage step.

The authors state that repeated voltage–resistance or voltage–current tests are not usually reproducible. We have found the contrary to be usually true, particularly in the case of clean dry windings. Very dirty or wet windings will sometimes change their leakage-current behavior from one test to another. This being so, and in view of the authors statements to the effect that the corona inception voltage may be very close to the actual breakdown value for clean dry windings, I do not agree that it is necessarily true that the corona test is less destructive. I do not believe that either test is destructive if conducted properly, even on insulation systems involving localized areas which are in a marginal condition.

In connection with the authors' statements concerning absorption tests, I would like to make a few brief comments. First, the absorption or time-resistance test as usually made in maintenance practices is not done to determine the absorption characteristics of the insulation, but rather to determine the relative magnitude of the leakage current. In other words, the polarization index provides an indication of the relative dryness and cleanliness of the insulation, again a measure of "good housekeeping." If the test voltage is raised to levels that cause leakage-current nonlinearities then the ratio of absorption to leakage current changes which in turn changes the polarization index. The perfectly flat curve for wet insulation given in Fig. 10 to me seems odd indeed, and I question its validity.

In closing this discussion I would like to raise an academic question concerning the authors' repeated reference to "polar materials such as dirt and moisture," and that "the presence of polar molecules causes the insulation to behave more like a pure ohmic resistance." I do not question the fact that the high dielectric constant of pure water is largely due to dipole polarization, but I do not see the point of dwelling on this since the high conductivity of contaminated

ater, which we would expect to find in sulation that has seen service, may out-igh its significance. I have found no idence of a predominate reversable energy dirty and wet insulation after having been bjected to a direct voltage. I would preciate the authors' further comments on is phase of the subject.

The authors also make several contradic-ry references to interfacial polarization hich leaves me somewhat confused. In e place they attribute the capacitance of a achine winding wholely to interfacial polar-ation when measured at power frequencies, d in another they say the interfacial larization contribution to the d-c dielec-c constant is complete in less than a nute. In a third place they say that terfacial polarization plays only an in-nificant part in current behavior from the ndpoint of the time constant with which e steady-state current is established. Un-s I have misunderstood the meaning of ese statements I must disagree with all of em. For example, the 60-cycle capaci-nce of the usual machine winding is made largely of contributions from the so-lled infinite-frequency polarizations as ell as dipole and possibly some interfacial sorption. Since the time constant of the terfacial type of absorption is often found be longer than 1/120 second its contribu-n to the 60-cycle capacitance may not cessarily be significant. The infinite-quency polarizations, such as the elec-onic and atomic types, have very short ne constants in themselves and, unless the sistance of the test circuit is quite high, ould be complete within a minute. It is avoid the measurement of these polariza-ns that one minute has been chosen as the st time interval for polarization index easurements. The interfacial absorption n be observed for hours.

Klein (Israel Institute of Technology, ifa, Israel): This paper presents ob-vations and testing proposals of basic portance and it is of great interest to certain their range of validity at higher ltages and for other equipment and ma-ials. It is a merit of this paper that thors clearly differentiate between the ormation obtainable from the leakage rrent, absorption current, and discharge eption tests respectively.

The essential point appears to be the commendation to introduce discharge in-otion measurements on d-c tests. This d of test is customary with a-c apparatus. the case of alternating current however, servations show completely different be-vior, as frequent discharges start at com-ratively low voltages, when breakdown lows only after a long time, or not at all. the other hand, in the case of direct rrent the authors' observations indicate t frequent discharges start at much her voltages than with alternating cur-t and with dry insulations breakdown lows soon.

It will be important to investigate the sons for these differences in behavior and ne comments will be made here in this nnection. The breakdown tracks ob-ved by the authors developed along ex-nal surfaces and across the insulation. t us consider the part across the insula-n and the consequences of discharges in cavities occurring in the insulation. According to a simple model, it is often assumed that when the voltage is increased to V_i and a discharge occurs in the cavity, positive and negative charges become attached to opposite surfaces of the cavity and the electric field vanishes in the cavity owing to these charges. On increasing the voltage to $2V_i$ discharges occur again, the charges are added at the cavity surfaces to the charges of the previous discharge, and the field in the cavity vanishes again. This process is repeated on further voltage increase and it is expected that infrequent discharges will be observed on the oscilloscope at about equal time intervals.

The authors observed however a sudden increase in the repetition rate of the discharges at a voltage which is a multiple of V_i. In the light of the model of discharge sequence described it would appear then that the charges attached to opposite cavity surfaces diminished and it could be assumed that they were neutralized, or conducted away. In the case of damp insulations the first assumption seems likely. In the case of dry insulations, however, neutralization of negative charges does not seem to be plausible and the question arises: "How are the observations connected with an increase in the conductivity of the insulation?" Consider the electrons of the discharge. These impinge upon the cavity surface with energies up to 100 electron volts and to a great part penetrate into the solid, where they ultimately become attached to trapping sites. On repeated discharges trapping sites increasingly closer to the electrodes become filled. When with increased voltage the discharge frequency suddenly increases, it is suggested that several processes can take place in the solid. Possibly the trapping centers are filled to such an extent that electrons from further discharges move to the electrodes without being trapped. Possibly electrons are liberated owing to the high electric field by various mechanisms, e.g., from traps. Processes connected with positive ions at the cavity surface are even less clear and neutralization by electrons from the solid might be instrumental. In any case a sudden increase in the conductivity of the solid adjacent to the cavity seems to be connected with the increase in the frequency of discharges and consequent breakdown and experiments will have to show whether the afore-mentioned or other processes cause the conductivity increase.

Such a mechanism of d-c breakdown appears to be different from those known and also to a certain extent from the mechanisms of a-c breakdowns, caused by discharges in cavities. It would be important to ascertain to what extent the development of breakdown on external surfaces is influenced by trapping centers. It seems from these observations, and mainly from such with alternating current, that the trapping sites, which constitute a very small fraction of the insulating materials, can influence the breakdown strength. The question arises then as to whether a control of the trapping centers could not help in the improvement of insulating materials.

The authors consider that the use of discharge detection for a-c conditions on alternating current is more involved and it is not clear what value information obtained on d-c discharge inception tests can have for estimating insulation quality on a-c operation.

It is stated in the paper that practically no information can be obtained about the insulation condition by the leakage-current characteristic in itself. This is most probably true with regard to the imminence of breakdown, for which discharge inception and absorption current tests, as recommended by the authors, can give the information. On the other hand, leakage-current tests instruct about the conducting properties; e.g., the leakage current versus temperature measurements recorded in Fig. 11. When plotting the logarithm of the leakage current against the reciprocal absolute temperature, it is interesting to note that for various voltages parallel straight lines can be drawn through the experimental points with quite good accuracy.

It would appear that the authors have made an important contribution to the subject of testing insulating materials and are to be congratulated. It is hoped that this work will be continued experimentally on apparatus and on samples of insulating materials under carefully controlled conditions.

E. W. Bultman and **C. W. Martin** (Baltimore and Ohio Railroad Company, Baltimore, Md.): We feel that this paper is very interesting and informative. It is another link in the continuing investigations that are being made in d-c testing of insulation systems in low-voltage d-c equipment.

We are engaged in the maintenance and repair of diesel-electric locomotive equipment. For several years we have been conducting an intensive investigation from all sources available to us on the subject of insulation testing and the evaluation of these tests. Present uses of d-c testing, while considerably improved over former methods of testing insulation, still are not fully informative.

The concept presented raises the hopes for improving test programs on the railroads, but it also raises some questions. The data presented in this and previous papers are always concerned with the insulation resistance levels that we as operators never see or attempt to achieve as they are not economically feasible. In our own motor shops equipment is released for service with several microamperes leakage current and the equipment operates successfully. Also, we have received, repaired, and rewound traction motors and main generators from leading manufacturers which, when received, meggered 5 megohms with a 500-volt megohmmeter yet they carry a new motor warranty. If we used an ionization-detection method to test this equipment would we be able to release it for service?

What will be the ionization pattern for a traction motor's insulation system which is very dry and clean but which has a puncture? This type of fault on a d-c test usually has a gradual smooth straight curve to a given impressed voltage and then breakdown comes without warning. No knee occurs in the curve for this type of failure.

Investigations and discussions with other railroad personnel indicate that locomotives are being operated with power circuits having insulation resistance in the order of 5

milliamperes at 1,500 volts d-c. Have any tests been made at this level of insulation resistance? If so, what were the results?

What voltage test level and leakage-current values do the authors recommend for testing complete locomotive power circuits, individual traction motors, and main generators on the locomotive, and the same equipment in a rewind shop?

It seems the most practical use of the ionization theory is in predicting the breakdown voltage and stopping the test prior to reaching this point. Do the authors agree?

We would appreciate a discussion of the availability and costs of the component parts of the test equipment used by the authors and if such a test set is or might become available commercially.

G. L. Moses and **J. S. Johnson** (Westinghouse Electric Corporation, East Pittsburgh, Pa.): The authors should be congratulated on the preparation of a very thorough and well-documented paper on the subject of d-c high-potential testing of insulation systems for low- and medium-voltage d-c equipment. The authors make a very strong case for the use of ionization measurements to determine the condition of the insulation with respect to dirt and moisture contamination, and the probable level of insulation strength on clean and dry insulation, for the types of insulation systems which they have investigated. In connection with the development of applicable test methods for insulation evaluation, caution should be exercised in assuming general applicability of a test method which has shown a great deal of promise when used for limited types of equipment. While we have seen some evidence that ionization phenomena precedes breakdown on higher voltage equipment, the correlation has not been as marked as the authors have experienced in connection with the insulation systems which they have studied. This is probably due to the difference in the insulation system, the thickness of insulation used, and probably to a large extent, the conditions of use. The components of railroad equipment are subject to much more adverse treatment from the standpoint of exposure to contaminating influences than are the large turbine generators, which operate in a clean and dry atmosphere. It therefore must not be assumed that the same measure of success would be experienced in making similar tests on this type of equipment.

It is probably true, however, that more emphasis should be placed on the detection of ionization pulses and their relative frequency with increasing test voltages even for this type of equipment. Studies along these lines were reported as early as 1941 when the Edison Electric Institute Subject Committee on field testing the generator insulation reported results of destructive tests on 106 large generators which were about to be rewound. Among these a series of ionization studies were reported for eight generators, with the conclusion that the ionization measurements made did not appear to be effective in indicating the existence of isolated points of weakness in the windings tested. There is certainly room for further investigation, however, of this general field.

The authors very correctly point out that the shape of leakage-voltage characteristics may be greatly distorted by the arbitrary selection of scales used in plotting these characteristics. We have found that in interpreting leakage-voltage characteristics of machines, the basis of comparison should be the leakages which are normally expected for machines of the type being tested. If the absolute magnitude of the leakages or the rate of increase are high, when compared to those which would normally be expected, this is investigated and the possible causes determined. Also, care is exercised in the selection of scales so that unusual leakages will be readily indicated. Here, again, it should be pointed out that in the testing of high-voltage insulations, moisture contamination is relatively unimportant as compared with the equipment which the authors have studied.

While there may be some question as to the general applicability of this method the authors have made a very constructive contribution to the problem of anticipating electric failure at least for the equipment which they have studied.

Direct-voltage testing has been used quite successfully for some time as an over-voltage proof test to demonstrate the adequacy of a winding to withstand a certain direct-voltage level. There have been many attempts made to use leakage current versus direct voltage to provide a forecast of impending failure but with somewhat mixed success. The authors' proposal to observe the ionization discharges while applying a direct-voltage test certainly warrants further study and trial.

The method proposed by the authors should be employed by several investigators on a variety of electric equipment with different kinds of insulation. It is recommended that the authors make statistical studies on a large number of laboratory-prepared specimens and report their data at a subsequent meeting of the Institute. If this method proves to be as useful as the authors' preliminary study indicates, it would truly be a significant contribution to the art of testing.

A. M. Odok and **T. M. Soelaiman:** We wish to thank all who contributed discussions for the very gratifying interest shown in this paper. So wide a response, it seems, is an indication of dissatisfaction with the present status of insulation-evaluation methods and of open-mindedness toward new approaches in this field.

Before considering the discussion in detail, it seems appropriate to stress some facts concerning the general aspects of the method described in this paper:

1. Contrary to first impression, the use of this method involves no more skill than does the step-voltage d-c test. In fact, it has been found unnecessary to plot the leakage-current characteristic during the test since a good picture of the insulation condition can be obtained without checking the slope of this curve. The oscilloscope need not be an elaborate universal type, but can be simplified as single-purpose instrument, thus reducing weight, size, and complexity.
2. Since the noise current is picked up by a series resistor or choke no tuning circuit is used parallel to the test sample. Also, the method proposed in this paper differs from ionization-detection methods usin probes.
3. Field-testing experience on a prototyp equipment with built-in oscilloscope indi cates that radio noise causes no particula difficulty with this type of noise-curren pickup, except under highly adverse condi tions, such as closeness of arcing device etc.

In response to Dr. Wichman's very thor ough discussion, it may be pointed out tha disturbances by radiated or line-transmitte noise have not been a particularly difficul problem in these investigations. If noise i displayed on a Lissajous figure where th horizontal deflection is, for example, th ripple voltage of the rectified direct voltag the line pickup and interference are avoide since such noise then shows up in a radia direction on the Lissajous ellipse, whereas the discharge noise appears as vertica pulses on the screen.

The insulation system tested was class *I* However, we would like to point out tha we have not tested any high-voltage appa ratus such as that to which Dr. Wichma refers.

Mr. Simons' experiences with high-voltag d-c tests seem partially to support the work ing hypothesis that d-c breakdown always preceded by noise current. It would b interesting to know what ionization-dete tion method was used in the tests he me tions. In the absence of this information it may be assumed that probes external t the test circuit have been used, so that onl local discharges were picked up.

It is interesting that Mr. Simons repor success with a-c ionization detection simila to that reported in this paper for d-c tests.

Mr. Bhimani, in his discussion, attemp to itemize the conclusions reached in th paper. We would like to thank him f this contribution to a further clarification o our stand, but feel obliged to comment o some points which might be misunderstoo

The first two "limitations" which he lis seem to imply that some other single te exists which will supply all this informatio conclusively. Since the purpose of the te is to detect weaknesses of the insulation t electrical stresses, the method need not b sensitive to every kind of abnormity in th system unless it represents an inherent d electric weakness.

Although the temperature is significa for the absolute level of leakage current, does not affect the application of the d scribed method, as long as it is constant an within reasonable limits.

Comment should also be made on item under "Limitations" where the difference distribution of stresses under direct an alternating voltages is brought out. Wh we agree with the principle stated therei we wish to point out that no attempt wa made to correlate or compare the value an effects of the two types of stresses, and t two types of tests.

Mr. Cameron's question regarding ioniz tion pulses occurring during discharging the insulation system seems to have found plausible explanation in Dr. Wichman discussion. We have observed this ph nomenon without attempting to use it differentiate between void discharges an other types of discharges as reported Dr. Wichman.

Mr. Cameron and Mr. Curdts point

ne increase of leakage current in Fig. 15 and sk whether this is not as good a measure of pproaching breakdown as the noise current. nfortunately these two examples are not ypical of all possible conditions of the in-ulation. Experience indicates that there some connection between increasing leak-ge current and intensive noise current. he curve in Fig. 17 of Dr. Wichman's dis-ussion also points out the parallel between ne dissipation factor and the frequency of -c pulses. Combining this with, on one and, Dr. Klein's attempt to explain the ature of pulses, and, on the other hand, the xperience of Mr. Cameron and the authors ith pulses during charging and discharging, ne is led to speculate that the space-charge nization takes place in discrete bursts. n other words, the noise observed consists Barkhausen pulses similar to the domain rientation phenomena in magnetics.

Mr. Cameron questions the statement at "high-voltage d-c testing is inherently etter suited for d-c machines and equip-ent than for a-c machines." Despite the ct that d-c machine armatures are sub-cted to a combined stress composed of an ternating voltage superimposed on a direct oltage, we think the statement holds for ne following reasons:

There are parts in a d-c machine which e exposed only to direct-voltage stresses.

No information is yet available as to the fect of a pulsating unipolar voltage on sulation. However, this type of stress nd a constant-voltage stress have at least ne point in common: the polarity does ot change, therefore the ionization mecha-sm is different from that under alternat-g-voltage stresses.

Mr. Bultman and Mr. Martin report ex-eriences with resistance testing which are perfect conformity with those of the uthors. The answer to the question as to hether the proposed method would help ward a more definite screening of traction motors than is possible by resistance measurement is indicated by our field experience. Even though the proposed method is still being evaluated in service shop use, experience thus far shows that the additional information obtained is of considerable help in determining the cause of low resistance and deciding whether or not it represented a weakness of permanent nature which would lead to breakdown under service conditions. Of course, more field data are needed to answer the specific questions these discussers have asked. Generally speaking, neither a low nor a very high resistance, as measured with a low voltage, is useful unless its cause is known. Undoubtedly, both leakage- and absorption-current measurements supply useful information. Our experience indicates that the proposed test method is quicker and supplies as much or more information than leakage-current and absorption tests.

Comments on some other questions asked by Mr. Bultman and Mr. Martin are:

1. A puncture will be detected if it is at a point so highly stressed as to give rise to ionization of the surrounding air or if its surface is sufficiently contaminated to cause surface tracking.
2. Resistances as low as the 300,000 ohms mentioned have been encountered. Most often this occurred with moist insulation and the diagnosis of humidity usually helped to classify the insulation as not permanently weakened.
3. The authors are not in a position to recommend general rules as to voltage and current levels in traction equipment, since these depend on nominal voltage, size of equipment and many other factors. These values are not highly significant in nondestructive testing since the real voltage limit is found by observing the conditions which will start damaging the insulation.
4. Certainly the most practical use of the noise-current detection is to give a more dependable prediction of breakdown than could be obtained with other methods. Other useful features might, however, prove even more important in service shop applications as described in the paper; these concern mainly the condition of the insulation system.

We are grateful to Mr. Curdts for having called our attention to various inconsistencies which have since been corrected in the text.

Dr. Klein's attempt to explain the mechanism of discharges observed under constant direct voltages has much appeal and we agree with the necessity of carefully controlled experiments to check his hypothesis. We also hope that other workers will gain more experience with the method described in order to prove the extent to which it will be of practical value to the field engineer.

We wholeheartedly agree with Mr. Moses and Mr. Johnson that too early a generalization of the presented method to high-voltage equipment should be avoided. This caution was implied in the title of the paper and the specific reference to the types of machines tested. It is to be hoped that other investigators will supply information regarding the usefulness of this method in other types of equipment.

The leakage-current characteristics would be more informative and easier to interpret if normal leakage-current curves were available for each piece of equipment to be tested. While this might be economically justifiable for large machines, it is doubtful whether a user of a large number of small machines would be willing to keep accurate records of their individual insulation resistance. Furthermore, tests would have to be made under more carefully controlled conditions than those usually associated with periodic inspection testing of such machines. It should here be pointed out that, as reported by Mr. Bultman and Mr. Martin, a change in leakage resistance has not been found to be a good measure of the operability of traction motors.

A Recommended Program for Resistance-Welding Instrumentation

A. DIXON
MEMBER AIEE

In a study of the characteristics of known basic variables in resistance welding, a preliminary conclusion indicated that the magnitude of variation in each function in the order of the severity of their variance is: weld current, most variable; weld force, less variable; and weld time, least variable. Consideration of these conditions indicated the desirability of a continuous system for monitoring of current and force, with periodic checking of the weld-time function.

Upon evaluation of existing methods, the following mediums were considered of acceptable reliability for instrumenta-

THE PROBLEM of developing a practical method of instrumentation r production use at the Westinghouse lectric Corporation has been advanced y the combined interest and efforts of search, development, and manufactur-g people within the company. The use instrumentation for resistance welding volves wide economic considerations in roduct quality and production costs and as thereby greatly stimulated this in-rest.

In the process of this work many mediums of instrumentation were compared and evaluated in the manufacturing laboratory and production departments. The standard for comparison was the very accurate magnetic oscillograph. The outcome of this effort was the adaptation of instrumentation methods having simplicity as a keynote, to enable the effective use of such procedures at the resistance-welding operator level and at a minimum cost per unit machine.

Paper 58-210, recommended by the AIEE Electric Welding Committee, and approved by the AIEE Technical Operations Department for presentation at the AIEE Winter General Meeting, New York, N. Y., February 2–7, 1958. Manuscript submitted October 16, 1957; made available for printing January 7, 1959.

A. Dixon is with the Westinghouse Electric Corporation, East Pittsburgh, Pa.

tion of variables on single-phase equipment:

1. *Weld current.* A back-stop current ammeter and a primary current transformer for weld-current amplitude setting of machine and monitoring. This is supplemented by the brush amplifier and oscillograph where modulated current waveforms are used (current rise and taper characteristic). Relative current amplitudes are thus observed and recorded. Certain Military Standard resistance-welding work includes this as an inspection and quality control requirement.

2. *Weld force.* A pressure gage and pneumatic pressure regulator, which is standard equipment on most resistance-welding machines, is used for setup and monitoring. Where schedules require the use of dual force systems, a strain gage and amplifier are used in conjunction with the brush oscillograph. The specific purpose in this case is to determine correct timing for the forge-pressure delay function.

3. *Weld time.* This variable is predetermined by an initial calibration test, and is recorded on standard calibration and schedule charts. Periodic maintenance checks are the maximum requirement. However, when using brush instrumentation for current measurement, a monitor and permanent record are also provided for the weld-time variable.

In considering the over-all problem, other factors such as condensed welding schedules and recommended resistance-welding electrode combinations were determined. Maintenance programs have also improved considerably with established calibration procedures and recorded machine calibration charts of instrumented variables.

The simplicity of the program as outlined in the following has established economic advantages, and presents a practical manufacturing engineering approach to instrumentation of and improved resistance-welding operations at Westinghouse.

Background

Resistance-welding operations within the company are in many diverse forms, which impose varying degrees of instrumentation requirements, many of which have been standardized and recommended welding schedules applied. These methods, which will be described in the following section, may be categorically classified as follows:

1. Machine preparation, or equipping the resistance-welding machine for instrumentation.
2. Making machine calibration records.
3. Preparing welding schedule charts.
4. Resistance-welding instrumentation for aluminum work.
5. Miscellaneous applications.
6. Effective use and application of instrumentation.

A preliminary survey of the basic variables which can be readily instrumented indicates a maximum need for the instrumentation of weld current, since this quantity is readily affected by factors which are not within the scope of simple control. Such factors include line-voltage changes, the addition of weld material in the throat of the machine, and physical changes on the secondary electric circuit of the welder transformer due to operator changes in welding setup of electrodes or fixturing.

Although the variable of weld force does not have the severity of change characteristic of weld current, the facility for continuous monitoring of this variable is provided as standard equipment on most resistance-welder machines. This consists of a pneumatic-pressure regulator and a pressure gage which indicates the air pressure to the air cylinder of the machine. An occasional reference to actual air-gage readings by the operator and the posted calibration or schedul chart, detects any change due to in consistencies in pneumatic systems an supplies.

The weld-time variable is the mos consistent factor and therefore, for mos work, does not require the continuous us of a monitor-type instrument by th operator. An exception to this is wher an oscillographic record is required in th certification of work schedules as an in spection or quality-control requirement This is frequently the case where a modu lated current wave is used in the weldin schedule.

A system of providing machine calibra tion records and charts offers the followin advantages:

1. It enables better scheduling of wor within welder machine capacities, thu obtaining good consistency machine b machine.

2. It enables the use of a process specifica tion, which includes the recommende welding schedules and can be specified o engineering design drawings.

3. It reduces machine setup time an places the initial responsibility for corre welding procedures within visual super visory control.

4. It encourages standardization and th use of recommended practices in resistance welding production operations, reflectin considerable savings in labor and materia and reduced waste in defective work.

5. Machine calibration record charts en able the detection of failure and the rapi localizing of machine defects. A knowledg of normal machine performance in th adjustable variables of time, force, an current offers a convenient standard fo

Fig. 1 (left). Current transformer

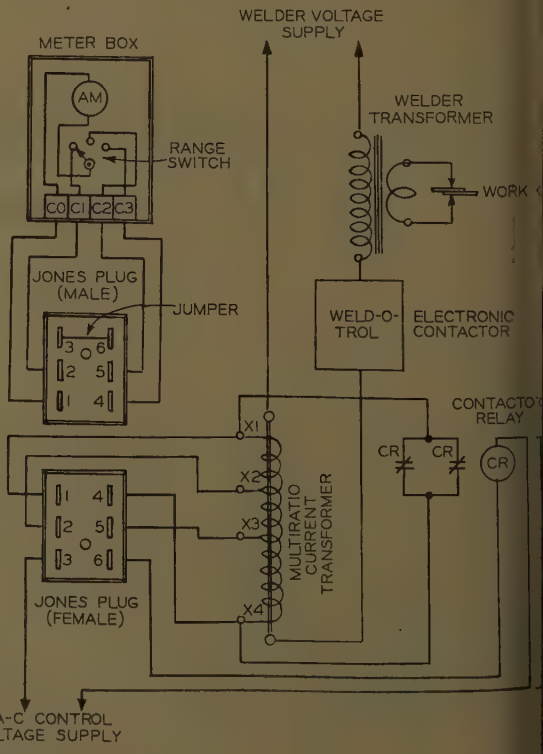

Fig. 2 (right). Weld current meter diagram of connections with automatic current transformer short-circuiting relay

Weld current (amperes) = ammeter reading × welder transformer ratio × current transformer ratio

mparison at the time of failure or sus-
cted failure.

alibration and Welding Procedures

ACHINE PREPARATION

The first step in preparing a specific sistance-welding machine for instrumen-tion is in the selection and installation the primary current transformer. Two andard styles of current transformers ovide the required range of primary rrent coverage. The first style has tios of 200, 400, and 600 to 5, and the cond style has ratios of 1,200, 600, and 0 to 5. A typical current transformer this purpose is shown in Fig. 1. A rmanent installation is preferred be-use of convenience and low cost. To termine the correct size of current trans-rmer required, a reasonable approxima-n of the maximum value of primary ad amperes can be made from the name-ate output rating of the resistance-lding machine in secondary amperes vided by the welder transformer ratio. The second step is in the selection and ounting of a back-stop current ammeter. hen possible, a permanent installation also desirable. However, if a portable eter arrangement is desired, a "Jones"-pe disconnect plug can be used, as ustrated in Fig. 2. This system will able the portable use of one ammeter

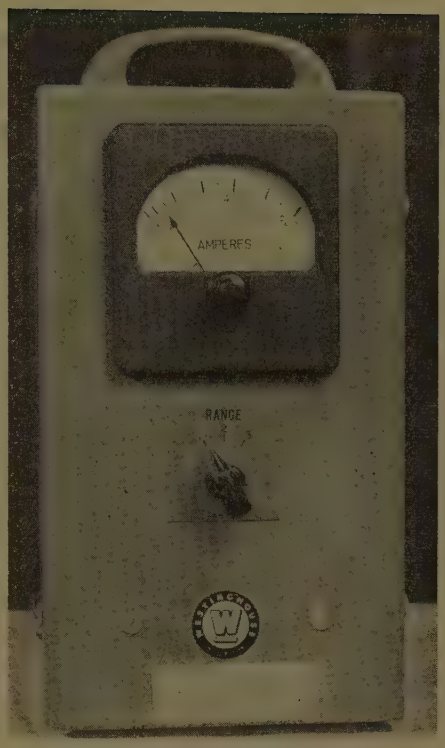

Fig. 3. Weld current meter

on N number of machines. The system incorporates an automatic short-circuiting feature for the current transformer secondary, which is done by an electric contactor relay when the plug is disengaged. The most widely used back-stop current ammeter, shown in Fig. 3,

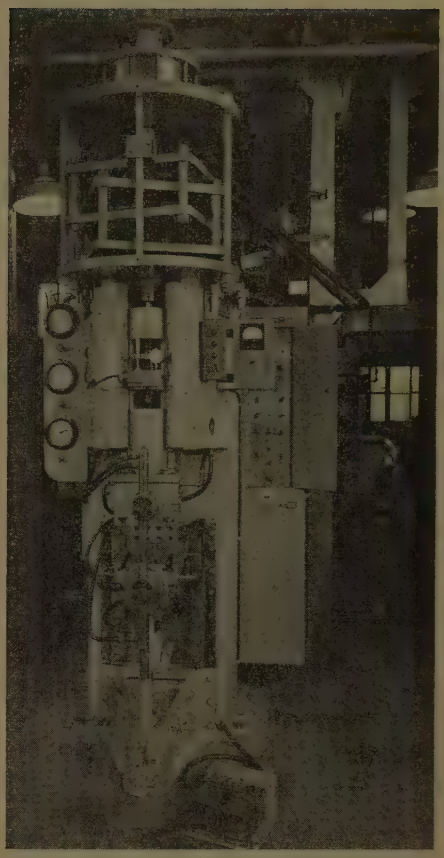

Federal Machine and Welder Company

Fig. 4. Spot-projection welder with correct meter installation

Table I. Welder and Meter Data for Precision Rocker Arm 250-Kva Spot Welder

Welder Transformer Data			Weld Current Meter Data	
mary Tap	Secondary Volts	Welder Transformer Ratio	Range Switch Position*	Meter Multiplier
Lo-1	7.3	60.25 to 1	1	0.5
Lo-2	7.9	56.7 to 1	(Use up to 300 amperes primary current)	
Lo-3	8.5	51.8 to 1	2	1
Lo-4	9.2	47.8 to 1	(Use up to 600 amperes primary current)	
Hi-1	10.5	41.9 to 1	3	2
Hi-2	11.6	37.9 to 1	(Use up to 1,200 amperes primary current)	
Hi-3	13.0	33.84 to 1		
Hi-4	14.7	29.9 to 1		

mary volts = 440

T. Ratio = $\frac{\text{Primary Volts}}{\text{Secondary Volts}}$

ample: Ratio of tap Lo-4 = $\frac{440}{9.2}$ = 47.8

set current meter for required secondary current:

Meter reading = $\frac{\text{Required secondary amperes}}{\text{Meter multiplier} \times \text{welder transformer ratio}}$

ample: To set weld current meter for 26,100 amperes

$\frac{26,100}{29.9\dagger}$ = 874 amperes, primary current

Use range switch on no. 3 position

Meter reading = $\frac{26,100}{(2 \times 29.9\dagger)}$ = 437 amperes

Set pointer stop for 437

Determine primary current by dividing secondary current by the welder transformer ratio for primary used.

Hi-4 primary tap setting on welder.

Table II. Short-Circuit Weld Current Calibration for Precision 250-Kva Rocker-Arm Spot Welder

Primary Tap	% Current Dial	Primary Amperes	Secondary Amperes
Hi-4	20	264	7,900
	30	372	11,130
	40	540	16,150
	50	684	20,450
	60	888	26,600
	70	1,057	31,600
	80	1,249	37,350
	90	1,512	45,200
	100	1,583	47,300
Hi-3	20	216	7,320
	50	540	18,300
	100	1,249	42,250
Hi-2	20	168	6,370
	50	444	16,820
	100	1,080	35,100
Hi-1	20	132	5,530
	50	360	15,100
	100	888	37,250
Lo-4	20	108	5,170
	50	276	13,200
	100	660	31,550
Lo-3	20	96	4,975
	50	252	13,070
	100	570	29,550
Lo-2	20	84	4,760
	50	210	11,900
	100	516	29,250
Lo-1	20	72	4,340
	50	180	10,850
	100	438	26,400

Calibrated with 1 1/2-inch-diameter copper bar.
Throat dimensions: opening, 8 inches; depth, 24 inches.
No-load volts, 446.
Full-load volts, 440.

Fig. 5. Portable weld-time meter

has a 5-ampere movement and a dial calibration of 0 to 600 amperes, full scale. In some cases, it is desirable to use a meter movement of other than the 5-ampere range, depending on the maximum kilovolt-ampere rating of the machine and power supply voltage. For example, it has been preferable in some installations to use a 2.5-, 10-, or even a 20-ampere range meter. This selection is determined from the maximum welder transformer primary current divided by the current transformer ratio. The recommended location for mounting of the meter is on the side frame of the machine near the front and above the welder throat or work area. Fig. 4 shows one example of installation. This location provides convenience of accessibility by machine operators.

The third step in preparing the machine is in obtaining the turns ratio characteristic of the welder transformer for the various primary taps. These data in most cases are immediately available from the manufacturer's instruction book. Where the data are not available, the turns ratios are determined by measuring the voltage ratio. The primary voltage divided by the open-circuit secondary voltages for the various primary tap settings is indicative of the welder transformer ratios. To do this, a jumper is placed across the ignitron contactor tube terminals, and voltage applied by a manual breaker or switch. A typical machine data sheet is illustrated in Table I. This is a standard form, which is suitably framed and posted on or near the machine. In practice, turns ratio = voltage ratio.

Making Machine Calibration Records

The machine calibration records of current, time, and weld force are made in the following order:

1. The short-circuit current calibration is made basically as outlined by the Resistance Welders Manufacturers Association (RWMA) Equipment Standards.[1] This means that the secondary short-circuit path is adjusted to a recommended throat opening and depth, and short-circuiting bars used as specified. Normally this work requires solid copper bars of the same diameter as the electrode holder. In the case of a projection-press welder, a short-circuiting bar of recommended length and diameter is placed between the faces of the platens and full head pressure is applied. In this case, the calibration is used for projection work. Where the machine is to be used for spot welding, a calibration is made with the short-circuiting bar solidly clamped in the welder horns, extended to the RWMA recommended throat depth and opening for the size of machine involved. In the making of spot-welder current calibrations where the short-circuiting bar is solidly clamped between the welder horns, the pneumatic pressure should be removed from the machine. Where a machine is used for both spot and projection work, two sets of current calibrations are made for the respective work applications. The mathematics of calculating short-circuit secondary currents from ammeter readings is quite simple:

Secondary current = ammeter reading × current transformer ratio × welder transformer ratio

Table I gives an example of how to set the meter for a required welding or short-circuit current. Current readings are usually taken on every ten points of the heat-control dial setting for the highest primary tap. On the other low and intermediate primary tap settings, readings are taken at three points only; for example, at 40%, 70%, and 100% heat. Full-load and no-load primary supply voltage readings are also observed and recorded on the current calibration chart and throat dimensions are also recorded. Table II shows a typical form used for this purpose.

2. The calibration of the weld-time function is then made before the short-circuiting bar is removed. The primary tap or heat-control setting is reduced to some intermediate or low value for this work. A number of standard cycle-counter instruments may be adapted as a standard for calibration, but the one found most practical is the Westinghouse style *1501174* weld-time meter, which is conveniently connected to the ignitron circuit by means of large, rubber-insulated clip leads. An important reason for this preference is that the instrument may be connected for maintenance testing without interrupting operation of the machine and production. This instrument is shown in Fig. 5. The operation of all timing switches and/or major

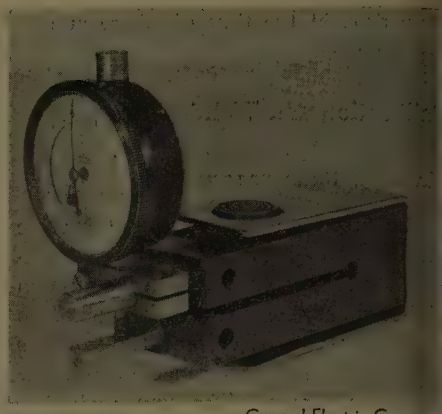

General Electric Company

Fig. 6. Weld-forge gage

points of all timing potentiometers is checked. If the error in cycles exceeds the control manufacturer's accuracy tolerance guarantee, the *RC* timing circuit is adjusted or repaired according to requirements. On some control units, a manual adjustment is provided. The weld timer calibration is recorded as shown in Table III.

3. The short-circuiting bar is then removed and the pressure calibration is made. The weld–no-weld switch should be turned to the "no-weld" position for this work. A force gage is inserted between the electrodes of the machine and head pressure applied. Major points on the pressure gage are checked by adjusting the air regulator and recording force-gage reading in pounds. A preferred type of portable, low-cost gage for this work is the General Electric spring-type force gage, catalog no. *6987801G1*, as shown in Fig. 6. A machine weld-force calibration chart is illustrated in Table III.

Preparing Welding Schedule Charts

A considerable amount of work has been done in the manufacturing laboratory to develop optimum resistance-welding schedules for commercial welding to both mild steel and aluminum. One phase of endeavor in this work has been to keep the machine setting of variables to a minimum for a maximum range of

Table III. Weld Force and Time Calibration for Precision 250-Kva Rocker Arm Spot Welder

Weld-Pressure Calibration		Welder Timer Calibration	
Pressure Gage	Weld Pressure, Pounds	Timing Range Switch	Cycles, ±
10	370	1–30	0
20	980	31–60	1
30	1,490	61–90	3
40	2,050	91–120	5
50	2,630	121–150	7
60	3,180	151–180	9
70	3,720	181–210	16
		211–240	20

To make correction when selecting weld time: Subtract correction in time cycles as indicated from required weld time. Set timer switches to this value.

Table IV. Resistance Spot-Welding Schedules for "Mild Steel" (0.18 Carbon Maximum)

WELDING DATA							INSPECTION & ENGINEERING DATA						
THK COMB. NOTE 1 (IN.)	ELECTRODE DIA & SHAPE COMB. SEE BELOW 	WELDING FORCE LB NOTE 2	WELD TIME CYCLES	WELDING CUR AMP NOTE 3	SHORT CKT CUR THRU COPPER NOTE 4	HOLD TIME CYCLES NOTE 5	DIA OF WELD NUGGET OF MULTI-WELDS INCHES NOTE 6 	MIN. SPACING IN. 	MIN. MULTI-WELD SHEAR STR LB BASED ON STL OF ULT STR OF 45,000 P.S.I.	SINGLE WELD SHEAR STR LB NOTE 7	MIN. EDGE DISTANCE IN. 	MIN. OVERLAP DISTANCE 	THK COMB. NOTE 1 (IN.)
.015-.015	1 or 2	250	3	7000	8200	10	3/32	1/4	150	150	1/8	1/4	.015-.015
-.036	1 or 2	250	9	7000	8200	10	5/32	1/4	150	200	5/32	5/16	.036
.050	1 or 2	250	9	7000	8200	10	5/32	1/4	150	200	5/32	5/16	.050
.064	1 or 2	250	9	7000	8200	10	5/32	1/4	200	200	5/32	5/16	.064
.036-.036	1 or 2	250	9	7000	8200	10	3/32	1/4	350	500	5/32	5/16	.036-.036
.050	1 or 2	400	14	8400	9900	20	13/64	3/8	550	700	5/32	1/2	.050
.064	1 or 2	400	14	8400	9900	20	13/64	3/8	550	700	1/4	1/2	.064
.078	1 or 2	600	21	9200	10800	20	3/16	1/2	700	1000	1/4	1/2	.078
.094	1 or 2	600	21	9200	10800	20	3/16	1/2	700	1050	1/4	1/2	.094
.109	2	800	28	11400	13400	30	9/32	5/8	900	1250	5/16	5/8	.109
.125	2	800	28	11400	13400	30	1/4	5/8	900	1300	5/16	5/8	.125
.050-.050	1 or 2	400	14	8400	9900	20	3/16	3/8	725	1000	1/4	1/2	.050-.050
.064	1 or 2	600	21	9200	10800	20	1/4	1/2	1000	1500	1/4	1/2	.064
.078	1 or 2	600	21	9200	10800	20	1/4	1/2	1000	1500	1/4	1/2	.078
.094	2	800	28	11400	13400	30	1/4	5/8	1100	1700	5/16	5/8	.094
.109	2	800	28	11400	13400	30	17/64	5/8	1100	1700	5/16	5/8	.109
.125	2 or 3	1050	37	11400	13400	30	17/64	7/8	1700	2200	3/8	3/4	.125
.156	2 or 3	1300	47	14600	17200	30	5/16	7/8	1800	2400	3/8	3/4	.156
.064-.064	1 or 2	600	21	9200	10800	20	9/32	1/2	1100	1800	1/4	1/2	.064-.064
.078	2	800	28	11400	13400	30	1/4	5/8	1600	2200	5/16	5/8	.078
.094	2	800	28	11400	13400	30	15/64	5/8	1700	2200	5/16	5/8	.094
.109	2 or 3	1050	37	11400	13400	30	9/32	7/8	2100	2700	3/8	3/4	.109
.125	2 or 3	1050	37	11400	13400	30	1/4	7/8	2100	2700	3/8	3/4	.125
.156	2 or 3	1500	59	14600	17200	30	5/16	1	2400	3100	7/16	7/8	.156
.188	2 or 3	1500	59	14600	17200	30	1/4	1	2400	3300	7/16	7/8	.188
.250	3	2200	93	19200	22600	45	9/32	1	2900	4100	1/2	1	.250
.078-.078	2	800	28	11400	13400	30	9/32	5/8	1900	3400	5/16	5/8	.078-.078
.094	2 or 3	1050	37	11400	13400	30	17/64	7/8	2800	3700	3/8	3/4	.094
.109	2 or 3	1050	37	11400	13400	30	9/32	7/8	2900	3900	3/8	3/4	.109
.125	2 or 3	1300	47	14600	17200	30	11/32	7/8	2900	3900	3/8	3/4	.125
.156	2 or 3	1500	59	14600	17200	30	5/16	1	2900	3900	7/16	7/8	.156
.188	2 or 3	1500	59	14600	17200	30	11/32	1	3000	3900	7/16	7/8	.188
.250	3	2200	93	19200	22600	45	11/32	1	3000	4500	1/2	1	.250
.094-.094	2 or 3	1050	37	11400	13400	30	9/32	7/8	2700	3600	3/8	3/4	.094-.094
.109	2 or 3	1300	47	14600	17200	30	5/16	7/8	3000	4800	3/8	3/4	.109
.125	2 or 3	1300	47	14600	17200	30	5/16	1	3900	5000	3/8	3/4	.125
.156	2 or 3	1500	59	14600	17200	30	11/32	1	4300	5500	7/16	7/8	.156
.188	3	2200	93	19200	22600	45	3/8	1	4400	6500	1/2	1	.188
.250	3 or 4	2700	130	22200	26100	45	3/8	1-1/8	5000	7900	5/8	1-1/4	.250
.109-.109	2 or 3	1300	47	14600	17200	30	5/16	7/8	2900	4000	3/8	3/4	.109-.109
.125	2 or 3	1500	59	14600	17200	30	3/8	1	3500	5900	7/16	7/8	.125
.156	2 or 3	2200	93	19200	22600	30	7/16	1	4600	6600	7/16	7/8	.156
.188	3	2200	93	19200	22600	45	7/16	1	4600	7400	1/2	1	.188
.250	3 or 4	2700	130	22200	26100	45	15/32	1-1/8	5100	8200	5/8	1-1/4	.250
.125-.125	2 or 3	1500	59	14600	17200	30	5/16	1	4000	4800	7/16	7/8	.125-.125
.156	3	2200	93	19200	22600	45	15/32	1	5000	7300	1/2	1	.156
.188	3	2200	93	19200	22600	45	7/16	1	5100	7900	1/2	1	.188
.250	3 or 4	2700	130	22200	26100	45	5/8	1-1/8	6200	9300	5/8	1-1/4	.250
.156-.156	3	2200	93	19200	22600	45	1/2	1	6400	9400	1/2	1	.156-.156
.188	3 or 4	2700	130	22200	26100	45	19/32	1-1/8	7200	10500	5/8	1-1/4	.188
.250	3 or 4	2700	130	22200	26100	45	19/32	1-1/8	7400	11800	5/8	1-1/4	.250
.188-.188	3 or 4	2700	130	22200	26100	45	1/2	1-1/8	8000	13600	5/8	1-1/4	.188-.188
.250	4	3700	230	28000	33000	90	5/8	1-3/8	11700	14000	3/4	1-1/2	.250
.250-.250	4	3700	153	28000	33000	90	3/4	4	15000	15000	3/4	1-1/2	.250 .250
.250-.250	4	3700	230	28000	33000	90	5/8	1-3/8	13500	15000	3/4	1-1/2	.250-.250

COMBINATION 1: .482 D-2 IN. SPHERICAL RADIUS FACE
.482 D-FLAT

COMBINATION 2: 5/8 D-2 IN. SPHERICAL RADIUS FACE
5/8 D-FLAT

COMBINATION 3: 7/8 D-6 IN. SPHERICAL RADIUS FACE
7/8 D-FLAT

COMBINATION 4: 1-1/2 D-6 IN. SPHERICAL RADIUS FACE
1-1/2 D-FLAT

Explanatory Notes Pertaining to Chart on Spotwelding Schedules

Note 1: On dissimilar thickness combinations, the average thickness determines the weld schedules. These average thicknesses are established to the nearest similar thickness combination. Example, average thickness of 0.050 to 0.094 is 0.072. Average thickness is taken as 0.078. For similar thicknesses not listed, use nearest thickness combination.

Note 2: Welding Force is the net electrode force measured in pounds exerted on the work.

Note 3: Welding Current is the secondary current during the actual welding cycle. It is not the same as Short-Circuit Current. Welding Current variation during welding should be held to ±5%.

Note 4: Short-Circuit Current through copper is used as an aid in setting the welding machine to the schedules. If this value is obtained while firing the machine through copper, it will give approximately the correct welding current. Final adjustments should be made on the work.

Note 5: Hold time is the time required to solidify the weld under pressure after the welding current has been terminated. This time is set on the welder control.

Note 6: The diameter of the weld nugget is the basis for determining the weld strength. The weld diameter should not be confused with the imprint of the electrodes on the work.

Note 7: Shear strengths are obtained by pulling the overlapped weld joints to destruction in a standard testing machine with the specimens unconfined. These are generally known as Tension-Shear tests. These particular shear strengths are obtained with widths equal to 4 times the minimum edge distance.

Table V. Mild Steel Schedule Chart, Precision Rocker-Arm 250-Kva Spot Welder

Two Thicknesses of	Welding Current, Amperes	Meter Reading for Welding Current	Short-Circuit Current Through Copper, Amperes	Meter Reading Through Copper	Meter Range Switch	Heat Control Dial, Per Cent Approximate	Tap Setting	Welding Force, Pounds	Gage Pressure, Pounds	Weld Time, Cycles	Hold Time, Cycles	Electrode Diameter and Shape Combination*
0.036	7,000	230	8,200	270	1	35	Lo-1	250	5	9	10	A or B
0.050	8,400	280	9,900	330	1	40	Lo-1	400	8	14	20	A or B
0.064	9,200	310	10,800	360	1	45	Lo-1	600	12	21	20	A or B
0.078	11,400	380	13,400	450	1	50	Lo-1	800	16	28	30	A or B
0.094	11,400	380	13,400	450	2	30	Hi-4	1,050	20	37	30	C
0.109	14,600	490	17,200	575	2	35	Hi-4	1,300	25	47	30	C
0.125	14,600	490	17,200	575	2	35	Hi-4	1,500	30	59	30	C
0.156	19,200	330	22,600	380	3	40	Hi-4	2,200	42	93	45	C
0.188	22,200	370	26,100	435	3	47	Hi-4	2,700	52	130	45	C or D
0.250	28,000	470	33,000	550	3	55	Hi-4	3,700	70	153	90	D, 2 single welds only
0.250	28,000	470	33,000	550	3	55	Hi-4	3,700	70	230	90	Same as above. Use 230-cycle timing on second or more weld

Notes on Welding Schedule:

1. Short-Circuit Current Through Copper or Meter Reading Through Copper.
   These columns are to aid in setting up the machine for the required welding current. If this value is obtained while firing the machine through copper, it will give approximately the correct welding current. Meter readings should be established with one division deflection of the pointer. If there is no pointer deflection, increase the heat per cent until recommended reading is obtained.
2. Welding Current or Meter Reading for Welding Current.
   These are the values that the machine must be set for when the welds are actually being made. If more than one weld is made, the machine must be set to obtain these values for the spot weld which has the most metal in the throat of the machine. Spitting or expulsion of metal should not be tolerated. If this occurs, decrease Heat Control dial setting by one or two points, until spitting or expulsion stops.
3. Approximate Heat Dial Per Cent.
   These values are only approximate and are figured with the throat opening and throat depth of the machine set where they are most likely to be used. They are given to aid in setting up the machine. If the throat opening or throat depth of the machine is increased, the Heat Dial per cent will have to be increased to obtain the correct current during welding. Also, if metal is placed in the throat of the machine during the welding cycle, the Heat Dial per cent will have to be increased to obtain correct current during welding.
4. Electrodes.
   Use the electrodes given in the chart above for the various thicknesses of material. Do no file the electrodes in the machine. If the electrodes become worn replace them with new or refaced electrodes.
5. Thickness Combinations.
   When two unequal thicknesses are to be welded, use the machine settings for the average thickness. For example, in welding one thickness of 0.125 inch to one thickness of 0.188 inch the average thickness is 0.156 inch, and settings for this thickness are used. See Weld Schedule Chart for other dissimilar thickness combinations.
6. Hold Time.
   The hold time shown for each thickness should be rigidly maintained. Insufficient hold time results in greatly weakened welds.

   If something goes wrong with the machine or welding schedule settings cannot be maintained, notify the supervisor at once.

* Electrode diameter and shape combinations:
A—1/2-inch-diameter 2-inch-radius face and 1/2-inch-diameter flat
B—5/8-inch-diameter 2-inch-radius face and 5/8-inch-diameter flat
C—One 7/8-inch-diameter flat and one 7/8-inch-diameter 6-inch-radius face
D—One $1^1/_8$-inch-diameter flat and one $1^1/_8$-inch-diameter 6-inch-radius face

work. In the case of mild steel schedules, a company-wide process specification has been issued and the schedule is included as an integral part. Thus, the requirements for the variables are determined. Typical data, as developed and accepted for the company-wide resistance welding of mild steel, are given in Table IV.

The first step in the preparation of a schedule chart is to compare the machine output in terms of maximum force, time, and current with these requirements for the widest range of work possible at these maximum values. To illustrate how this is done, assume that a schedule chart for mild steel is desired. Also for illustration, assume that the machine under consideration is a 250-kva Rocker-arm type, whose calibration of variables is as given in Tables II and III. The maximum short-circuit current output of the machine is 47,300 amperes, which is well above the requirement of welding two pieces of 0.250-inch mild steel (33,000 amperes per Table IV). It is also noted from the schedule that a weld force of 3,700 pounds is required for welding two pieces of 0.250-inch mild steel. The force system on this particular machine is then adequate for this range of work. The next reference is made to the weld-time requirements for the 0.250-inch combination thickness material and is noted to be 230 cycles. A check with the weld-time function on the calibration chart shows that this requirement can be met. Thus, the machine is capable of welding a range of work up to two thicknesses of 0.250-inch material.

A typical mild steel schedule chart is shown in Table V. All machine settings

Table VI. Resistance Welding Schedules

Variable	Schedule	
	Single-Force	Dual-Force
Current, amperes		
Weld	33,000	33,000
Starting	10,000	10,000
Final	20,000	10,000
Time, cycles		
Rise	5	5
Taper	16	8
Total	32	25
Cycles of weld before taper	16	16
Force, pounds		
Weld	750	750
Forge		1,500
Forge time delay, cycles		14

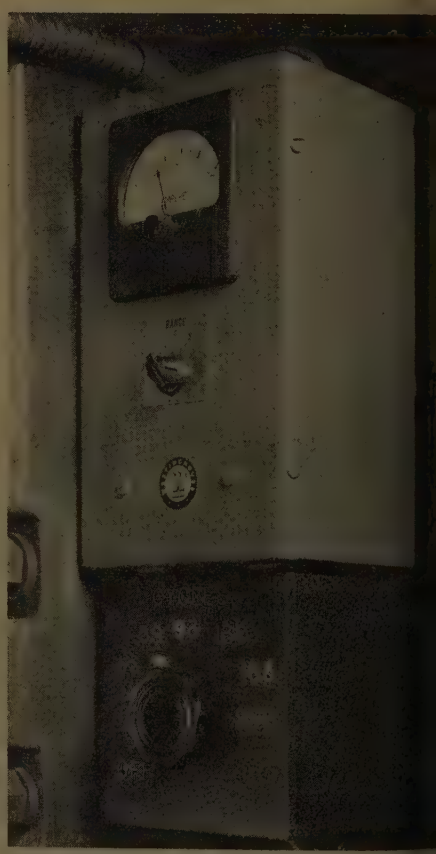

Fig. 7. Rapid time selector box and current meter

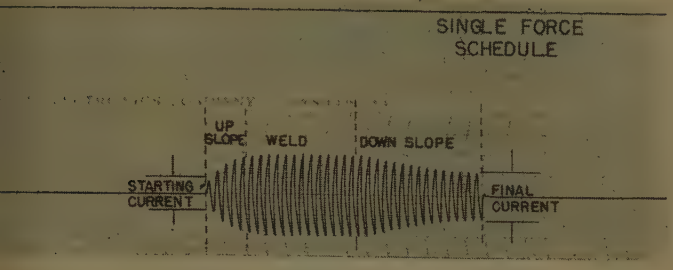

Fig. 8. Single-force schedule

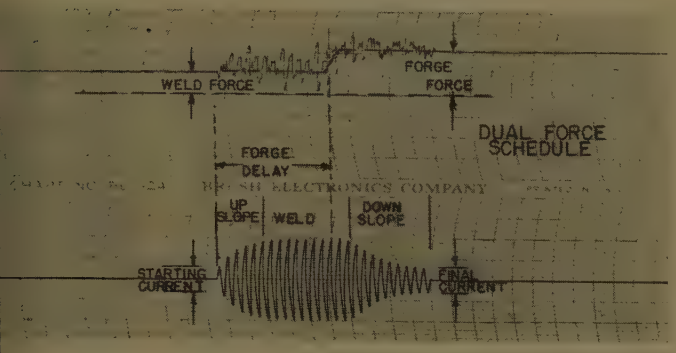

Fig. 9. Dual-force schedule

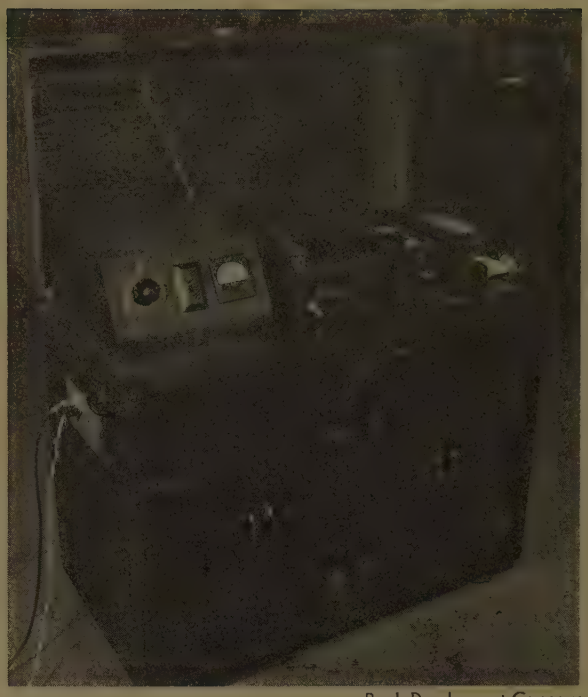

Brush Development Company

Fig. 10. Portable recording equipment

were derived from the welding variable requirements as outlined in the process specification schedule. Specifically, the current ammeter settings for "short circuit" and for "welding current" are calculated as outlined in Table I.

It should be noted that the purpose of including meter readings for short circuit or "through copper" is to enable the welding operator to adjust the machine heat-control setting to a close value for welding current without actually firing the welder through steel parts. For setup purposes, the operator merely places a piece of 1/8-inch-thick copper between the welding electrodes and adjusts the heat control until he obtains the current meter deflection as indicated on the chart for copper." This value automatically drops to the "meter reading for welding current" value, when welding current is passed through the actual steel work. The only operator requirement, then, is to lower the back-stop on the ammeter to the setting for "welding current" and observe the meter deflection. No further adjustment of heat control is ordinarily required.

It is also noted that a meter range switch is a desirable feature for selecting the required primary current transformer ratio. This feature permits the selection of the most desirable or uppermost scale deflection.

In making up the schedule chart, the remaining machine settings for weld force, weld time, and recommended electrode combinations are determined from the schedule requirements, Table IV, and the corresponding machine settings from the calibration charts, Table III.

A convenient time-selector switch is frequently used for the rapid selection of specific weld-time machine settings. The switch is calibrated to select and impose predetermined values of resistance R in the welding control RC timing circuit. Fig. 7 shows a mounting of the time selector directly below the weld current meter. In using this time selector, the convenience and rapid setup affords an obvious advantage in time saving over the regular setting of control time dials and/or switches.

Resistance-Welding Instrumentation for Aluminum Work

All procedures for machine preparation and calibration as outlined for mild steel spot welding are identical for the single-phase spot welding of aluminum. Other recommended resistance-welding schedules in use for this work involve additional requirements for the following supplementary instrumentation:

1. *Weld current measurement.* In the in-

C. B. Smith Company

Fig. 11 (left). Strain-gage installation

C. B. Smith Company

Fig. 12 (right). Surface resistance analyzer

Table VII. Recommended Single-Phase Resistance-Spot-Welding Schedules for Simil

Thickness Combination, Inches	Electrode Combination	Welding Force, Pounds (Note 1)	Up-Slope Time, Cycles (Note 2)	Up-Slope Preheat Current, Amperes (30% of Weld Current) (Note 3)	Weld Heat Time, Cycles (Note 4)	Weld Current, Amperes (Note 5)	Cycles of Weld Before Down-Slope Time (Up Slope plus Weld Time) (Note 6)	Down-Slope Postheat Time, Cycles (Note 7)	Final Down-Slope Current, Amperes (60% of Weld Current) (Note 8)	52SH34 to 52SH34	52SH34 to 61ST6	52SH34 to 24ST3	52SH34 to 3SH14
0.032–0.032	A	500	4	7,500	8	25,000	12	10	15,000	400	400	450	320
0.032–0.064	A	600	4	8,500	10	28,000	14	12	17,000	650	675	650	550
0.032–0.091	C or F	750	4	10,000	12	33,000	16	16	20,000	1,050	925	950	600
0.032–0.125	F	1,000	4	11,500	12	38,000	16	16	23,000	1,450	1,150	1,300	1,050
0.064–0.032	A	600	4	8,500	10	28,000	14	12	17,000	650	675	650	550
0.064–0.064	A or D	750	4	10,000	12	33,000	16	16	20,000	1,125	1,050	1,175	1,000 (NM)
0.064–0.091	F	1,000	4	11,500	12	38,000	16	16	23,000	1,450 (D)	1,450 (D)	1,650 (E)	1,400 (F)
0.064–0.125	F	1,200	4	12,000	12	40,000	16	18	24,000	1,850	1,650	1,750 (E)	1,700
0.091–0.032	B or E	750	4	10,000	12	33,000	16	16	20,000	1,050	925	950	600
0.091–0.064	E	1,000	4	11,500	12	38,000	16	16	23,000	1,450	1,700	1,650	1,250 (F)
0.091–0.091	D	1,200	4	12,000	12	40,000	16	18	24,000	1,800	2,000	1,800 (E)	1,490 (F)
0.091–0.125	F	1,600	4	13,500	14	45,000	18	18	27,000	2,000	2,150	2,700	1,770
0.125–0.032	E	1,000	4	11,500	12	38,000	16	16	23,000	1,450	1,150	1,300	1,050
0.125–0.064	E	1,200	4	12,000	12	40,000	16	18	24,000	1,850	1,850	1,750	1,350 (F)
0.125–0.091	E	1,600	4	13,500	14	45,000	18	18	27,000	2,000	2,400	2,200 (NM)	1,445 (F)
0.125–0.125	D	2,000	4	15,000	15	50,000	19	20	30,000	2,250	1,900	3,500	2,000 (NM)
0.125 24ST3–0.125 24ST3	D	3,000	4	16,500	15	55,000	19	20	33,000				

Note 1. Welding force is the net electrode force measured in pounds exerted on the materials being welded.
Note 2. Up-slope time is the total time for the up-slope current to rise from 30% of the weld current to full value of the weld current. This is 4 cycles for all thickness combinations between 0.032 and 0.125 as shown.
Note 3. Up-slope current is the impulse of current which flows from the end of squeeze time to the beginning of weld time.
Note 4. Weld heat time is the time during which welding current flows through the materials being welded.
Note 5. Welding current is the secondary current during the actual welding cycle.
Note 6. "Cycles of weld before down slope" is the dial setting calibrated in cycles and is the sum of the up-slope time plus the weld heat time cycles.
Note 7. Down-slope time is the total time during which postheat or taper current flows.
Note 8. Down-slope current is the impulse of current which flows from the end of the weld time cycle tapering down to 60% of the weld current.
Note 9. Tensile shear strengths are obtained by pulling the overlapped spot-weld joints to destruction in a standard testing machine with the specimens unconfined. These particular shear strengths are obtained with specimen widths equal to recommended spot spacings. The above strengths are the average of 100 multispot welds. The letter in parentheses adjacent to strength values indicates the electrode combination required. For example, the combination of 0.064 *61ST6* to 0.091 *24ST3* shows a tensile shear designation of 1,550(E). By this is meant that this combination has a tensile shear strength of 1,550 pounds. Also, referring to the electrode combination reference for (E), it can be said that a 7/8-inch-diameter, 8-inch-spherical-radius-face electrode is used against the 0.064 thickness of *61ST6* and a 7/8-inch-diameter flat electrode is used against the 0.091 *24ST3* material. Similarly, with 0.064 *52SH34* welded to 0.091 *3SH14* material, the electrode combination is (F). Thus, a 7/8-inch-diameter flat electrode is used against the 0.064 *52S* material and a 7/8-inch-diameter, 8-inch-spherical-radius-face electrode is used against the 0.091 *3S* material. The designation (NM) adjacent to strength values indicates that this particular combination is not a military quality combination; i.e., the minimum weld nugget penetration required in Military Specification *6860* cannot be met with these schedules.
General Note. Minimum squeeze and hold time should be 15 cycles.

strumentation of weld current where a modulated current waveform is used (i.e., where the current is initially applied at some low value, increases to a nominal or welding value, and then tapers off to a final amplitude), a medium of measurement is required which will register the relative current amplitude values in a chronological manner. A brush amplifier and oscillograph has proved to be a practical instrument for this application.

For setup purposes, the weld current meter provides the necessary medium for machine setting to the nominal or maximum weld current. This measurement is initially made with a constant-amplitude current waveform (no up-slope or down-slope) using a minimum 15-cycle timing.

In this setup of the weld current meter to the required aluminum schedule current, it is noted that only one current setting is necessary. The weld current for aluminum has been found to be virtually the same as that of the short-circuit current values; i.e., when the welder is fired through a piece of copper strap between the welding electrodes for setup purposes, this same meter reading is usually obtained when the welder is fired through the actual aluminum work. Thus the machine schedule chart has but one current setting for the material thickness involved.

The brush oscillograph is then adjusted for an average pen deflection of 10 millimeters, or divisions on each side of center-zero. This adjustment is arbitrarily made for the scheduled weld current, or as determined in using the weld current meter reading.

The up-slope and down-slope current amplitude is then adjusted on the machine control and the waveform observed on the oscillograph. The amplitudes of starting and final current are read as a per cent of the maximum, or 10-millimeter pen deflection. A typical brush recording of a modulated current waveform is shown in Fig. 8. This record represents current readings for the spot welding of 0.064-inch aluminum type *52SH34*, using a single-weld-force system.

2. *Instrumentation of weld force* (*S*). In the spot welding of aluminum using weld schedules which are developed for single-force systems, the same medium of measurement is adequate as that for mild steel spot welding. This involves the setting of an air gage on the machine to render the desired schedule weld force.

Where aluminum work is done with dual-force schedules, a medium for measuring the actual "forge time delay" is required. This is true because in the use of dual force or forge pressure, the advantage of maximum grain refinement in the weld will only be obtained when the forge pressure is applied in the exact chronological sequence on the welding cycle. Specifically, a desirable combination of current waveform modula-

Inspection and Engineering Data

Average Tensile Shear Strengths								(Note 9)				Recommended Minimum			Thickness Combination, Inches
61ST6 to				3SH14 to				24ST3 to				Edge Distance†	Overlap‡	Spot Spacing§	
1ST6	24ST3	3SH14	52SH34	3SH14	52SH34	61ST6	24ST3	24ST3	3SH14	52SH34	61ST6				
400....	400....	310....	400....	300.....	320.....	310....	300....	400....	300....	450....	400....	1/4	1/2...	3/4..	0.032–0.032
650....	650....	525....	675....	550.....	550.....	525....	625....	700....	625....	650....	650....	1/4	1/2...	3/4..	0.032–0.063
							(NM)		(NM)						
,050....	900....	*600....	925....	850.....	600.....	575....	675....	1,150....	675....	700....	700....	5/16....	5/8...	1	0.032–0.091
							(NM)		(NM)						
,450....	1,100....	800....	1,150....	1,085.....	1,050.....	800....	725....	1,600....	725....	725....	725....	5/16....	5/8...	1	0.032–0.125
650....	650....	525....	675....	550.....	550.....	525....	625....	700....	625....	650....	650....	1/4	1/2...	3/4..	0.063–0.032
							(NM)		(NM)						
,050....	1,100....	900....	1,050....	750.....	1,050.....	900....	850....	1,150....	870....	1,175....	1,100....	5/16....	5/8...	1	0.063–0.063
				(NM)			(NM)		(NM)						
,450....	1,550....	1,450....	1,700....	1,085.....	1,250.....	1,900....	1,150....	1,600....	1,350....	1,650....	1,550....	3/8	3/4...	1	0.063–0.091
(D)	(E)				(E)	(E)	(NM)		(NM)						
,850....	1,675....	1,550....	1,850....	1,200.....	1,350.....	1,300....	1,200....	1,950....	1,450....	1,750....	1,800....	3/8	3/4...	1	0.063–0.125
		(NM)			(E)(NM)	(E)	(NM)								
,050....	900....	600....	925....	850.....	600.....	575....	675....	1,150....	675....	700....	700....	5/16....	5/8...	1	0.091–0.032
									(NM)						
,450....	1,550....	1,100....	1,700....	1,050.....	1,400.....	1,400....	1,350....	1,600....	1,150....	1,650....	1,550....	3/8	3/4...	1	0.091–0.064
		(F)							(NM)	(F)	(F)				
,650....	1,825....	1,550....	2,050....	1,100.....	1,500.....	1,550....	1,300....	2,000....	1,290....	1,800....	1,825....	1/2	1	1	0.091–0.091
	(E)	(F)			(E)	(E)			(NM)	(F)	(F)				
,700....	2,400....	1,650....	2,400....	1,250.....	1,450.....	1,425....	1,650....	2,250....	1,450....	2,190....	2,090....	1/2	1	1	0.091–0.125
		(F)			(E)	(E)	(NM)		(NM)	(NM)	(E)				
,450....	1,100....	800....	1,150....	1,050.....	1,050.....	800....	725....	1,600....	725 ..	725....	725....	5/16....	5/8...	1	0.125–0.032
,650....	1,800....	1,275....	1,650....	1,200.....	1,700.....	1,550....	1,450....	1,950....	1,200....	1,750....	1,675....	5/16....	5/8...	1	0.125–0.064
		(F)							(NM)	(F)	(F)				
,700....	2,100....	1,425....	2,150....	1,250.....	1,750.....	1,650....	1,500....	2,250....	1,635....	2,750....	2,400....	1/2	1	1	0.125–0.091
(F)	(F)	(F)		(F)	(F)	(F)	(NM)		(NM)						
,250....	2,600....	1,600....	1,900....	1,500.....	2,000.....	1,600....	1,800.....		1,800....	3,550....	2,600....	5/8	1¼....	1½...	0.125–0.125
		(F)			(NM)	(E)	(NM)		(NM)						
.....								3,000				5/8	1¼....	1½...	0.01254 ST3
															0.01254 ST3

Electrode combinations (see diagram, Table IV, column 2):
A—Two 5/8-inch-diameter, 3-inch-spherical-radius face
B—One 5/8-inch-diameter, 3-inch-spherical-radius face and one 5/8-inch-diameter flat
C—One 5/8-inch-diameter flat and one 5/8-inch-diameter, 3-inch-spherical-radius face
D—Two 7/8-inch-diameter, 8-inch-spherical-radius face
E—One 7/8-inch-diameter, 8-inch-spherical-radius face and one 7/8-inch-diameter flat
F—One 7/8-inch-diameter flat and one 7/8-inch-diameter, 8-inch-spherical-radius face
Electrode material is Resistance Welder Manufacturers Association class *I*.
ee diagram, Table IV, column 12.
ee diagram, Table IV, column 13.
ee diagram, Table IV, column 9.

n and forge pressure requires the control justment of forge delay time (after start the current flow) to render the application forge pressure just prior to the tapering down-slope of weld current. The exact ne for the forge pressure application is ermined to be just 2 cycles (based on 60- le per-second timing) before the start of rent tapering.

On modern resistance-welding control tems, the setting of forge time delay action does not afford sufficient accuracy render the foregoing requirement. This particularly true when considering the tification of welding schedules for mili- y work. The combination of strain ge, brush amplifier, and oscillograph is an eptable medium for this measurement. . 9 shows an oscillogram of a modulated rent wave, and the application of forge ce at the correct point in the chronological uence of the weld cycle. The welding edule for this particular oscillogram is 0.064–0.064, type *52SH34* aluminum. 2-channel oscillograph is used for this rpose. Fig. 10 shows a practical instru- ntation console, which combines all com- nents in a portable unit, as required this work. A strain-gage assembly, mounted on a resistance-welding holder is shown in Fig. 11. This item is commercially available. The specific aluminum schedules which are instrumented in the oscillograms, Figs. 8 and 9, are shown for comparison in Table VI.

3. *Other instrumentation requirements.* The brush oscillograph method of instrumenting the current waveform also gives a check of weld timing. In a production setup, however, the work schedule certification usually does not require the continuous monitoring of the variables just described, and in most cases periodical checks will suffice. However, in the brush equipment as shown in Fig. 10, a provision for remote-control operation of the oscillograph chart is provided whereby each weld can be recorded if desired.

In the spot welding of aluminum, good weld quality depends directly on the degree of cleanliness of the material. Since considerations of dirt and oxide contribute toward an appreciable increase in surface resistance, it has been found necessary in some cases to equip production departments with a facility for measurement to determine acceptable resistance values on the material to be welded. In general, a surface resistance of less than 50 microhms on material to be welded is acceptable. A portable instrument which meets the requirements for this work is the surface resistance analyzer, model *VT11A*, commercially available from the same company which supplies the strain gage pickup device. This instrument is direct reading and has a pneumatic clamp for holding the material during test. The electric probe or contact points for measurement are included as a built-in feature, which eliminates the need for external electric probes. Fig. 12 shows this device.

4. *Aluminum spot-welding schedules and machine schedule charts.* Typical data developed for company-wide use in aluminum work are shown in Table VII. These data represent the schedule requirements when a single-weld-force system is used. The data can be used in conjunction with dual-force operation by reducing the current taper time and final current by 50%. To illustrate, assume a taper time of 16 cycles and a final current of 20,000 amperes as used on single-force machines. For dual-force application, the taper time then would be reduced to 8 cycles and the final current to 10,000 amperes.

Table VIII. Aluminum Spot-Welding Schedule, 250-Kva Taylor-Winfield

Alloy	Thickness Combination Two of	Welding Current, Amperes	Meter Reading for Welding Current	Meter Range Switch	Per Cent Heat Dial, Approximate	Primary Tap Setting	Starting Current, Amperes (Note 1)	Final Current, Amperes (Note 2)	Start Current Dial, Approximate (Note 1)	Final Current Dial, Approximate (Note 2)	Current Rise Time, Cycles	Current Taper Time, Cycles	Total Weld Time, Cycles	Cycles of Weld Before Taper	Weld Force, Pounds (Note 3)	Pressure Gage at Note 3	Forge Time Delay	Electrode Combination*
3SH14	0.064	33,000	3.95	3	85%	Hi-2	9,900	9,900	20	30	4	8	24	16	750	13	16	A or B
52SH34	0.064	33,000	3.95	3	85%	Hi-2	9,900	9,900	20	30	4	8	24	16	1,500	38	16	A or B
61ST6	0.064	33,000	3.95	3	85%	Hi-2	9,900	9,900	20	30	4	8	24	16	1,000	22	16	B
24ST3	0.091	40,000	7.0	3	85%	Hi-8	12,000	12,000	20	30	4	9	25	16	1,000	22	16	B
3SH14	0.091	40,000	7.0	3	85%	Hi-8	12,000	12,000	20	30	4	9	25	16	2,200	60	16	B
52SH34	0.091	40,000	7.0	3	85%	Hi-8	12,000	12,000	20	30	4	9	25	16	2,200	60	16	B
61ST6	0.125	50,000	8.75	3	95%	Hi-8	15,000	15,000	25	35	4	10	29	19	2,200	60	19	B

Note 1. Starting currents are adjusted and readings taken on the brush. Oscillogram should indicate the "Start" point of the current trace as 30% of maximum deflection as that obtained for weld current. Dial settings for starting current are approximate.

Note 2. Final currents are adjusted and readings taken on the brush. Oscillogram should indicate the "Final" point of the current trace as 30% of maximum deflection as that obtained for weld current. Dial settings for final current adjustment are approximate.

Note 3. Set the retired stroke gage at 60 and the down-stroke gage at 100.

* Recommended electrode combinations:
A—5/8-inch diameter, top and bottom, 3-inch radius, PDS 9438-1 material (average hold time, 60 cycles).
B—7/8-inch diameter, top and bottom, 8-inch radius, PDS 9438-1 material.

Table VIII shows a sample machine schedule chart for spot welding of aluminum. This chart covers the range of work within the confines of machine capacity and production materials. With the exception of current wave-modulation measurement, the steps in preparation of aluminum schedule charts are virtually the same as those in making charts for spot welding of mild steel.

Miscellaneous Applications

Seam Welding

The use of instrumentation for seam welding presents more potential advantage than with other forms of resistance welding because of relatively higher duty cycle, and any variation can be quickly detected. Basic techniques used are virtually the same. The requirements for seam welding are similar to those for spot welding except for weld current considerations. The duty-cycle pattern of current (i.e., on-time and off-time×number of pulses) usually dictates the need for a weld current meter with a movement with a greater dampening characteristic. The standard thermal-type radio-frequency ammeter has proved satisfactory for shop use. The meter movement is encased in the same metal enclosure as the one used for mild steel and aluminum (Fig. 3) and is equipped with the standard pointer back-stop for adjustment.

Higher Speed Welds (Less Than 10 Cycles)

Where applications require short weld time, which is insufficient for normal deflection of the current meter, the following sequence is used:

1. The proper machine settings to render acceptable work quality are determined by empirical, or other, means.

2. For the purpose of job records, the true current is then measured with the primary meter, using an extended weld time (15 cycles minimum). Short-circuit values with "current-through-copper" should be used as the recorded schedule machine setting.

3. The weld time is then reduced to the required value for welding and meter reading noted. If meter deflection is not the same as with the 15-cycle timing, the meter is adjusted for the lower or indicated value. Thus, the weld current meter serves as a monitor in this case and the indicated values of current do not represent true amplitude.

Effective Use and Application of Instrumentation

A broad responsibility for the effective use of instrumentation and recommended procedures starts with product engineering designs. This is particularly true since manufacturing people can only use and standardize methods within the limitations of actual work requirements. Some important items which engineering designers should consider are

The proper selection and specification material and favorable combinations, re possible.

The consideration of joint designs which themselves more favorably to the use standard spot-welding electrodes and ple fixturing.

Provision in product designs for ade- te overlap of material to maintain the ssary edge distance for location of the spot. This is important to obtain mum weld strengths.

preliminary consideration of these ors will greatly enable standardization methods and materially reduce shop blems which would ordinarily arise if basic requirements of the resistance- ding process are not considered in duct designs.

ther responsibilities for an effective rumentation program as herein out- d are

Assignment of optimum welding sched- which permit an acceptable quality k with the minimum equipment and r requirements.

Standardization of manufacturing and rumentation procedures.

3. The posting and maintenance of welding machine calibration and schedule charts for convenient use by the operator or setup man.

4. Organization of a competent machine maintenance program.

5. The assistance of qualified and competent setup people for this work. Operator training programs help considerably.

Conclusions

1. In general, with the objectives of maximum simplicity of operation, low cost, and acceptable accuracy, the pointer back-stop primary meter is preferred for measurement of basic weld-current values.

2. Where modulated current waveform is used, the Brush-type recorder is recommended.

3. In the use of welding schedules with dual-force systems, a strain-gage measurement and recording brush oscillograph has practical value.

4. Wide economic benefits of major significance in labor and material savings can be realized by the use of instrumentation on the production line.

5. Further economic benefits in manufacturing costs are obtained with standardization of equipment and procedures, which is aided considerably by instrumentation.

6. The machine records of instrumented variables determine equipment performance and serve as a tangible aid in maintenance work. This greatly reduces production downtime in the localizing of machine defects.

7. Standard calibrating and instrumentation procedures which are used in accordance with RWMA standards are valuable in checking performance when a new resistance-welding machine is purchased.

8. Improved product designs with uniform consistency are possible at a lower cost where an effective instrumentation program is used.

References

1. Equipment Standards. *Bulletin no. 16*, Resistance Welders Manufacturers Association, June 1952.

2. A Practical Method for Obtaining Consistent Resistance Welds, **J. W. Kehoe.** *The Welding Journal*, New York, N. Y., Oct. 1950.

3. Spot Welding Aluminum with Single Phase Equipment, **J. W. Kehoe, D. R. McCutcheon.** *Ibid.*, Oct. 1954.

4. Recommended Practices for Spot Welding Aluminum and Aluminum Alloys. American Welding Society, New York, N. Y., Oct. 1954.

Electrical Features of the Four Corners Pipe Line

J. J. SONNIER
ASSOCIATE MEMBER AIEE

H. N. SILER
NONMEMBER AIEE

HIS PAPER discusses generally the electric power distribution systems, trol schemes, supervisory control, metering, and communication means loyed on a crude-oil pipe line con- cted by The Shell Pipe Line Corpora-

he Four Corners pipe line runs from San Juan and Paradox basins in the r Corners area to the refinery area in ear Los Angeles. The line is owned by tinental Pipe Line Company (10%), f Oil Company (20%), Richfield Oil poration (10%), Shell Oil Company %), Standard Oil Company of Cali- ia (25%), and The Superior Oil Com- y (10%). It was designed and con- cted and is being operated by Shell e Line Corporation, as agent. The e of the pipe line and station locations shown in Fig. 1. Initial throughput of line called for the construction of e main-line pump stations and two sure-reducing stations. The first delivery of crude oil to the Los Angeles area was made in April 1958.

Electric Power Distribution

Commercial electric power supply was available at all of the locations. The power distribution system for the main-line motors is 3-phase 4,160-volt 60 cycle. The two pressure-reducing stations are supplied with 3-phase 480-volt 60-cycle service. At two of the main-line stations the power companies furnished and owned the substations, while at the third location the customer had to furnish, own, and maintain the required substation. All power from the substation is distributed through an underground conduit network. Fig. 2 shows a typical single-line diagram of power distribution system employed at a main-line station. Fig. 3 shows a typical underground conduit network for distribution of power.

For auxiliary equipment having electric motor drivers, the 4,160-volt service voltage is transformed to 480 volts by customer. Lighting and unit motor-operated valves are supplied by 208/120-volt 4-wire service from a transformer, also furnished by the customer.

Main-Line Pump Motors

All of the main-line centrifugal pump units are driven, through limited end-play spacer couplings, by 900-horsepower 3,600-rpm synchronous-speed squirrel-cage induction motors which have normal starting torque and running characteristics. Each motor is equipped with embedded temperature detector coils and space heaters. At two of the stations the motors are installed on a concrete pad outdoors and have weather-protected enclosures with built-in air filters. At the third station the motors are installed indoors and are of the totally enclosed forced-base ventilated type.

Paper **58-1057,** recommended by the AIEE Petroleum Industry Committee and approved by the AIEE Technical Operations Department for presentation at the AIEE Petroleum Industry Conference, Dallas, Texas, September 15–17, 1958. Manuscript submitted July 7, 1958; made available for printing December 30, 1958.

J. J. Sonnier and H. N. Siler are with the Shell Pipe Line Corporation, Houston, Tex.

The authors wish to acknowledge the information presented in references 1 through 6 as valuable sources of design features incorporated into this pipe line system.

Local Central Control Cabinets

All locations are provided with a local central control panel. The panels are upright and they incorporate all the necessary pilot lights, push-button stations, and miniature indicating instruments. The pilot lights and push-button stations are grouped by units, and provide control and visual indications of the status of the equipment as follows:

Control

1. Start and stop all units.
2. Discharge pressure set point.
3. Emergency stop.
4. Alarm reset.

Visual Indications

1. On-off main pump units.
2. Opened and Closed unit suction and discharge valves.
3. High station case pressure.
4. High station discharge pressure.
5. Low instrument air pressure.
6. High sump level.
7. Low station battery.

Indicating Instruments

1. Station flow.
2. Station suction pressure.
3. Station case pressure.
4. Station discharge pressure.
5. Gravity.

Device Designations

The device designations are based on the proposed AIEE Standard No. 68.[7] The device numbers used in the schematic drawings are detailed in the Appendix. The schematic drawings illustrated are extracts from construction drawings.

Incoming Line Main Circuit-Breaker Control

The main breaker is located adjacent to the substation. It is an outdoor oil type, rated at 7.5 kv, 1,200 amperes, with 250-megavolt-ampere interrupting capacity. The breaker is equipped with motor-wound spring closing mechanism and 48-volt d-c shunt trip. The breaker is arranged to close automatically unless locked out by device number 51 (overcurrent) or emergency stop, when voltage and phase sequence are normal.

Fig. 4 shows the control schematic used for the control of the main circuit breaker. The breaker is equipped with the following protective relays and devices:

Device No.	Function
47	phase reversal and undervoltage
51	overcurrent
52 UV	d-c undervoltage

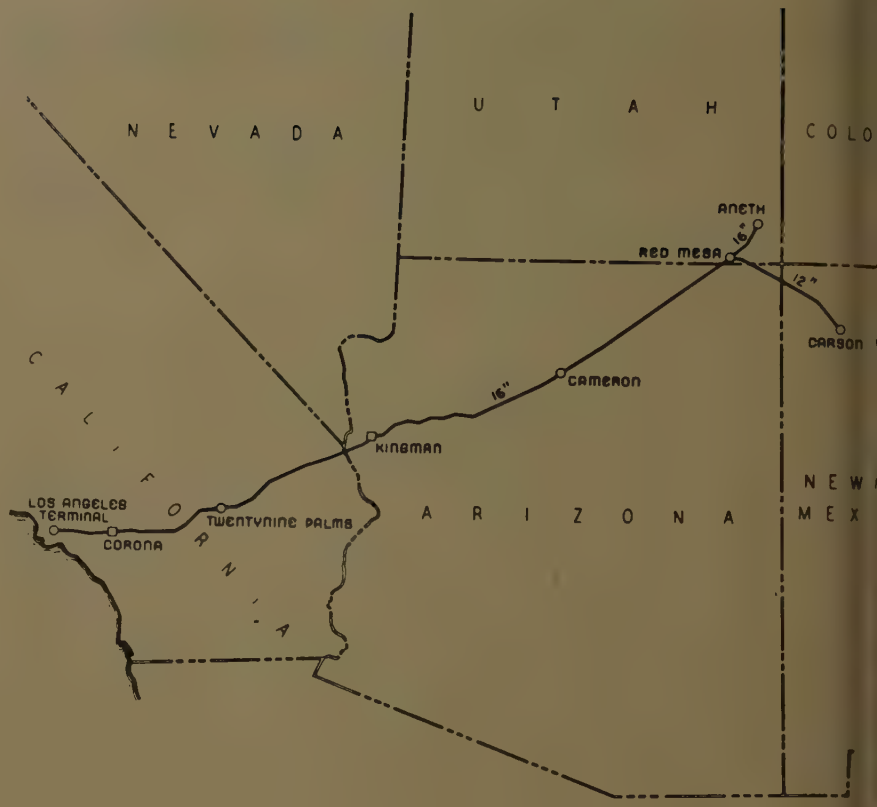

Fig. 1. Pipe line route

The main breaker is locally controlled from three locations: 1. control switch mounted on cubicle 1 of the indoor switchgear assembly, 2. push-button station installed outside the fence enclosure of the breaker, and 3. conventional control switch furnished in the control cabinet of the breaker. Also, the controlling point on the western end of the line by means of supervisory control (to be discussed later) has supervision of each station main breaker.

Main-Line Motor Control and Protective Devices

The power companies' transmission systems dictated the use of reduced voltage starting at all locations for the main pump motor drivers. The reactor method of limiting starting current inrush was satisfactory on all power transmission systems. The motor starters consist of three standard indoor metal-clad switchgear cubicles. Two cubicles house the starting and running circuit breakers. A third cubicle houses the motor-starting reactor. The circuit breakers are of the draw-out, air-break type, rated 5 kv, 1,200 amperes continuous, with interrupting capacity of 150 megavolt-amperes, rectified a-c closing, and 48-volt d-c shunt trip.

Adjacent to each pump unit is a cabinet housing the mechanical protective devices, which are all of the mechan mercury switch type. The cabinet ha push button installed as an integral pa

The unit protective functions are s regated into four categories: 1. electr nonlockout, 2. electrical lockout, mechanical nonlockout, and 4. mechan lockout; see Table I.

Unit Starting and Stopping Sequer

Fig. 5 shows the unit control sche Suction and discharge valves must closed to start the unit. Pressing "start" push button energizes start sequence relay 204 and over-all seque check timer 248. The starting re closes the control circuit to the suct valve "open" contactor, and energizes solenoid valve supplying air to the pu vent pneumatic bleeder valve. When suction valve is 50% opened, the pu vent solenoid valve is de-energized. fully opened position of the suction va actuates the control circuit of the start circuit breaker, causing it to close, connecting the motor through the rea to the switchgear busses. The start breaker closing energizes start-tim relay 219. After preset starting time, "run" breaker is closed and the s breaker is tripped. The discharge va "open" contactor is energized by c ing the run circuit breaker.

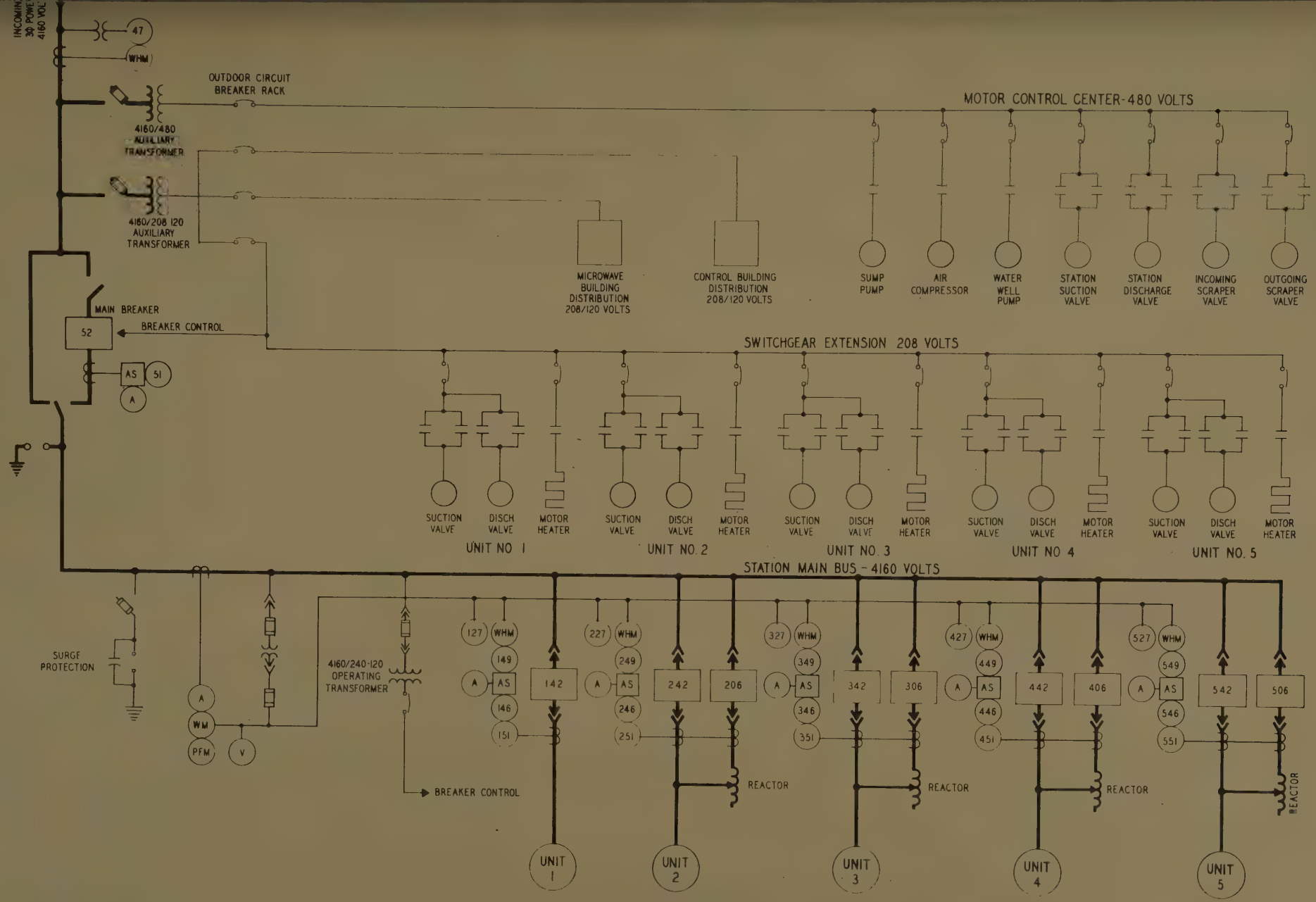

Fig. 2. Single-line diagram

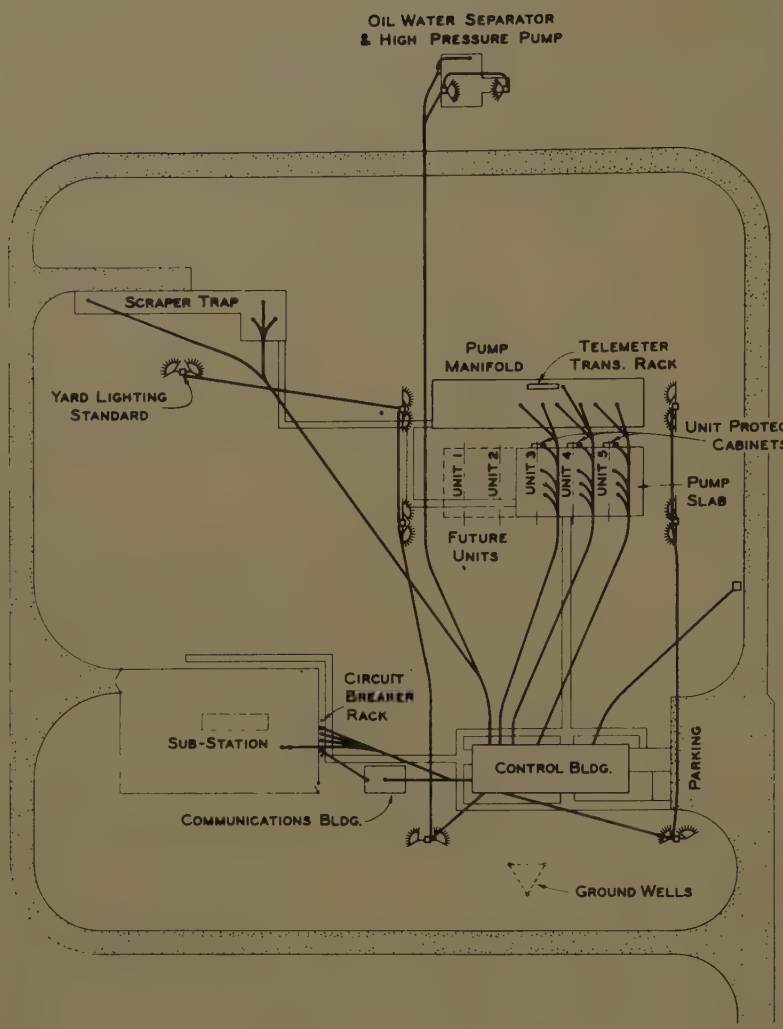

Fig. 3. Underground conduit layout

Over-all sequence check timing relay 248 will trip the run breaker in the event that the unit valves are not fully opened before the preset time. Also, this relay will trip the run breaker in the event that the unit valves leave the fully opened position while a unit is in operation.

All unit-sequencing relays and unit valve-reversing starters are installed in or on switchgear cubicle extensions associated with their respective motor starters. This arrangement makes for unitized motor starters, thereby reducing the number of interconnecting conduits and associated wiring.

In the event of high outgoing line pressure, all of the pump units are tripped. High station case pressure will trip units 1 and 2 simultaneously.

Station Auxiliary Equipment Control Schemes

Motor starters for the auxiliary equipment motor drivers are in a central motor control center. Fig. 6 illustrates the control schemes used for the following auxiliaries:

Auxiliary	Type of Automatic Control	Device No.
Air compressor	pressure switch	63 AIM
Sump pump	float switch	71 SUM
Yard lights	astronomical time switch	42 YL
Battery charger	regulated	
Scraper trap valves	manual	

Pressure-Reducing Station Electric Control

Due to the great differences in groun elevation traversed by the pipe line, tw pressure-reducing stations were con structed. Pressure is reduced by diver ing the line stream through four paralle friction tubes. Each friction tube con sists of a section of 2-inch or $2^1/_2$-inc pipe, 65 feet in length, with three section of 3/4-inch or 1-inch tubing welded insid the larger pipe. Four additional pip sections less friction tubing are arrange in parallel with the friction tubes. pneumatic control valve is installed series with each friction tube and pip section. All valves are controlled ele trically by means of solenoid-operate pilot air valves. The four valves in serie with the pipe sections and one of th valves in series with a friction tube can b opened or closed only electrically. Th other three can be closed electrically placed in "automatic" for automatic an sequential operation responsive to th pneumatic controls.

For the five nonautomatic valves, th solenoid-operated pilot valve admits a to the control valve diaphragm to ope and dumps the air to close. For the thr automatic valves, the solenoid valv dumps the air from the diaphragm to clo and admits instrument-controlled air f partial and full opening. The number nonautomatic flow control valves that a to be placed into operation is determin for any given throughput and those valv are manually put into operation. Th three flow control valves that are con nected to the pneumatic automatic con trol system will sequentially operate maintain constantly the preset values the incoming and outgoing pressure Fig. 7 shows the electrical control schem for this type of station. The followi are electrically controlled locally and r motely from the central control poi

(*Continued on page 218.*)

Table I. Unit Protective Functions

Device No.	Function	Electrical Nonlockout	Electrical Lockout	Mechanical Nonlockout	Mechanic Lockout
226M	motor-winding temperature	X			
227	undervoltage	X			
246	phase balance		X		
249	thermal overload, long time		X		
249	thermal overload, instantaneous		X		
251	overcurrent		X		
226PC	pump case temperature			X	
238M1	motor inboard bearing				X
238M2	motor outboard bearing				X
238P1	pump inboard bearing				X
238P2	pump outboard bearing				X
239PVB	vibration detector				X
239SF	pump seal leak				X
263PC	pump case pressure			X	
263S	pump suction pressure			X	

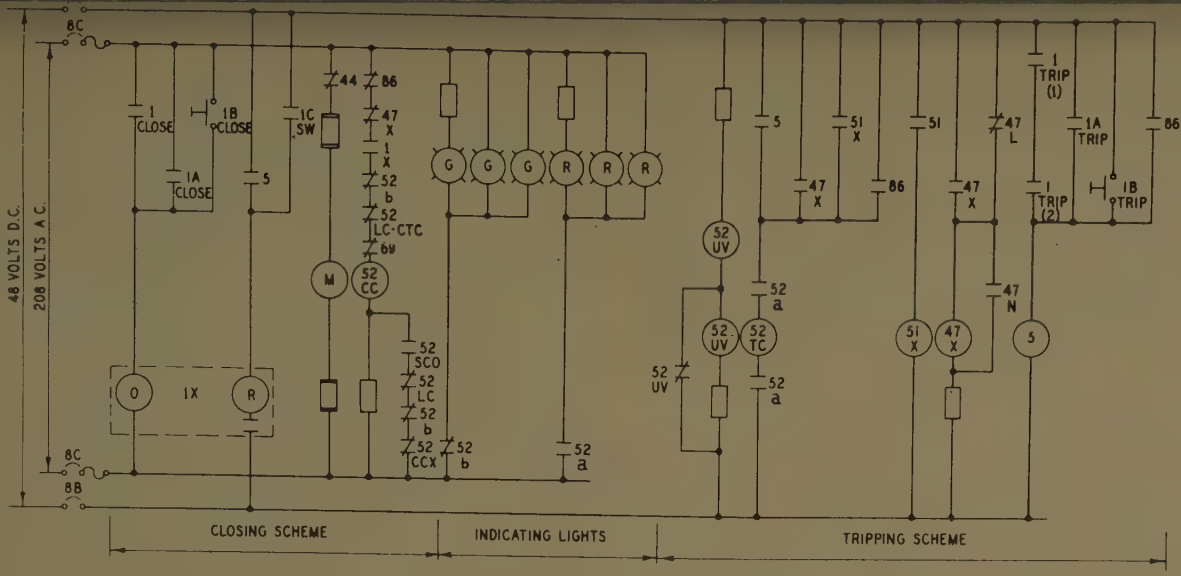

OUTDOOR BREAKER CONTROL

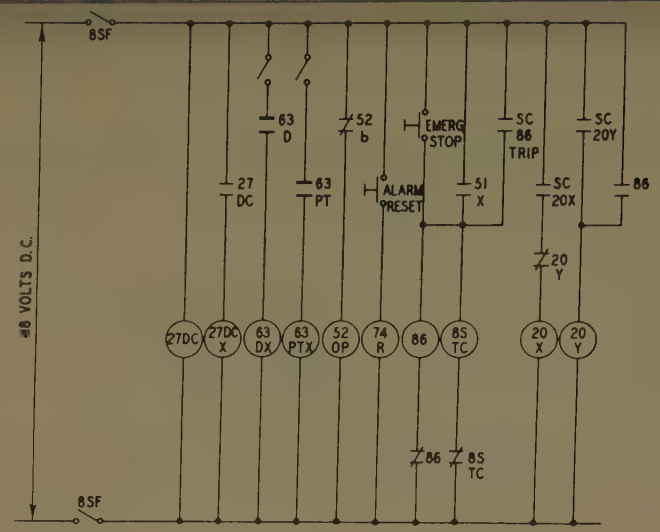

STATION FUNCTION RELAYS

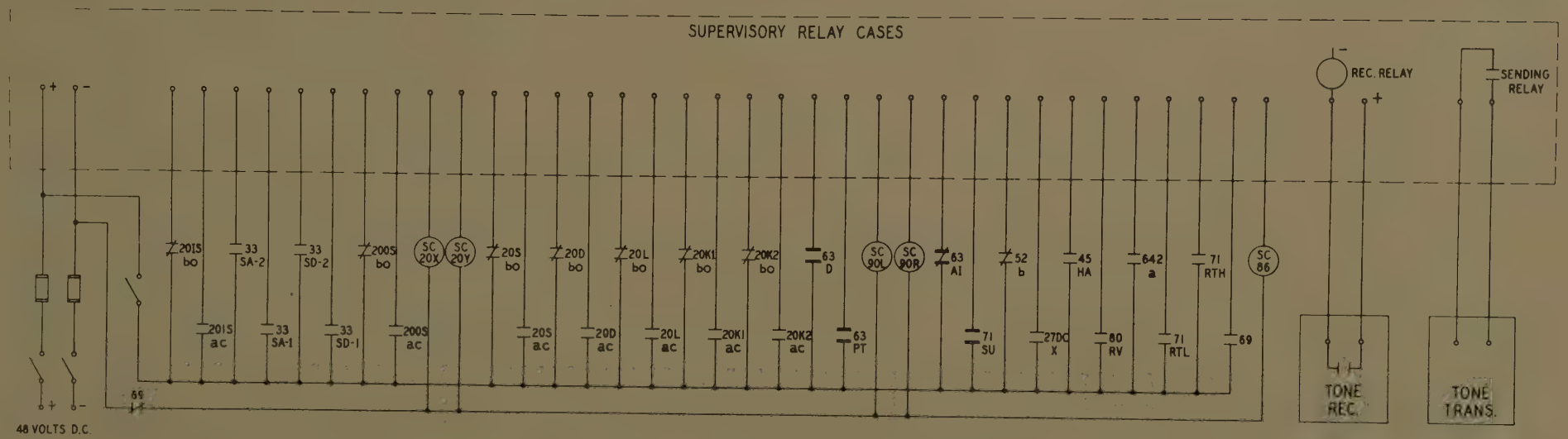

SUPERVISORY CONTROL SCHEME

Fig. 4. Outdoor breaker control and station functions schemes

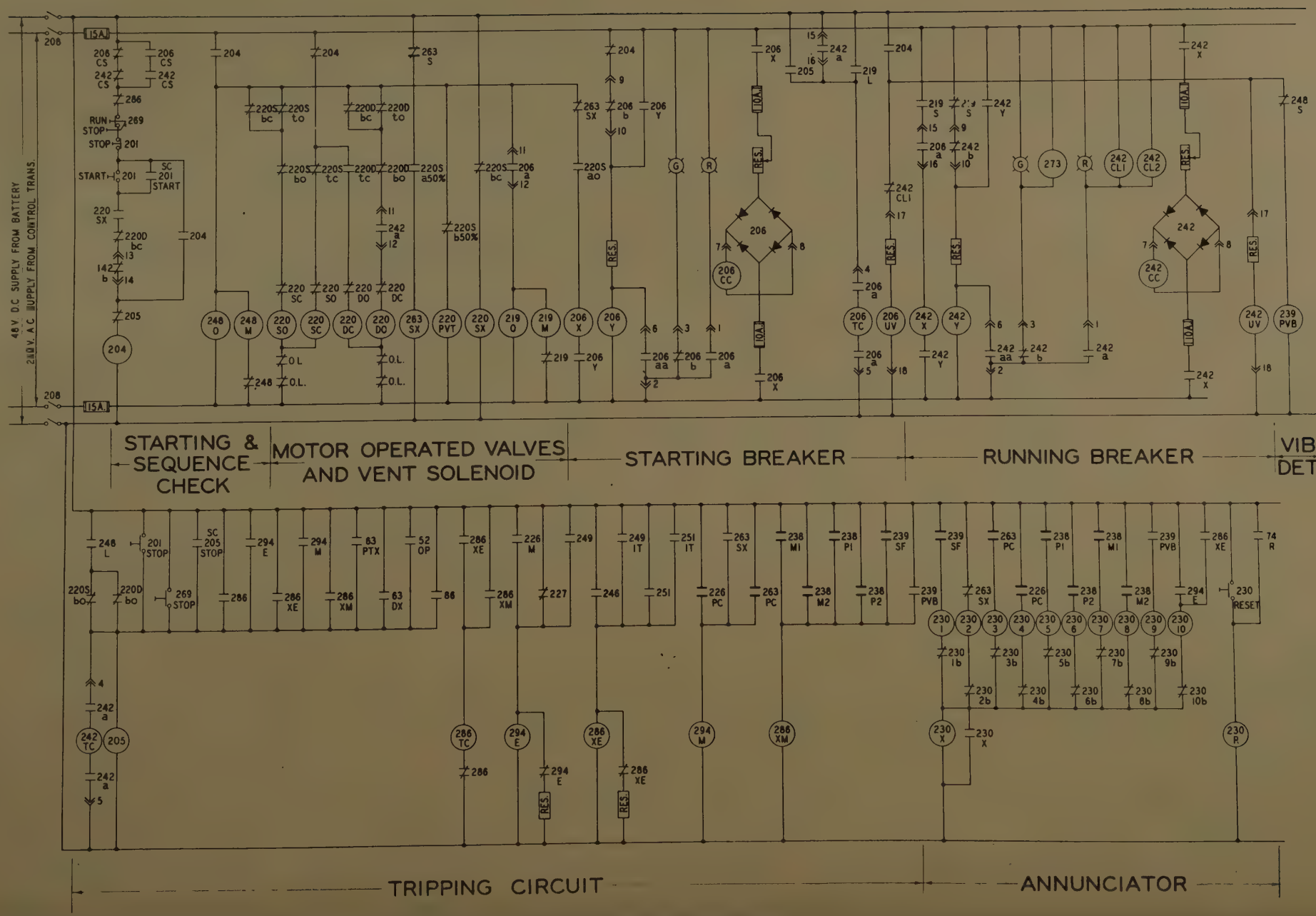

Fig. 5. Pump unit control scheme

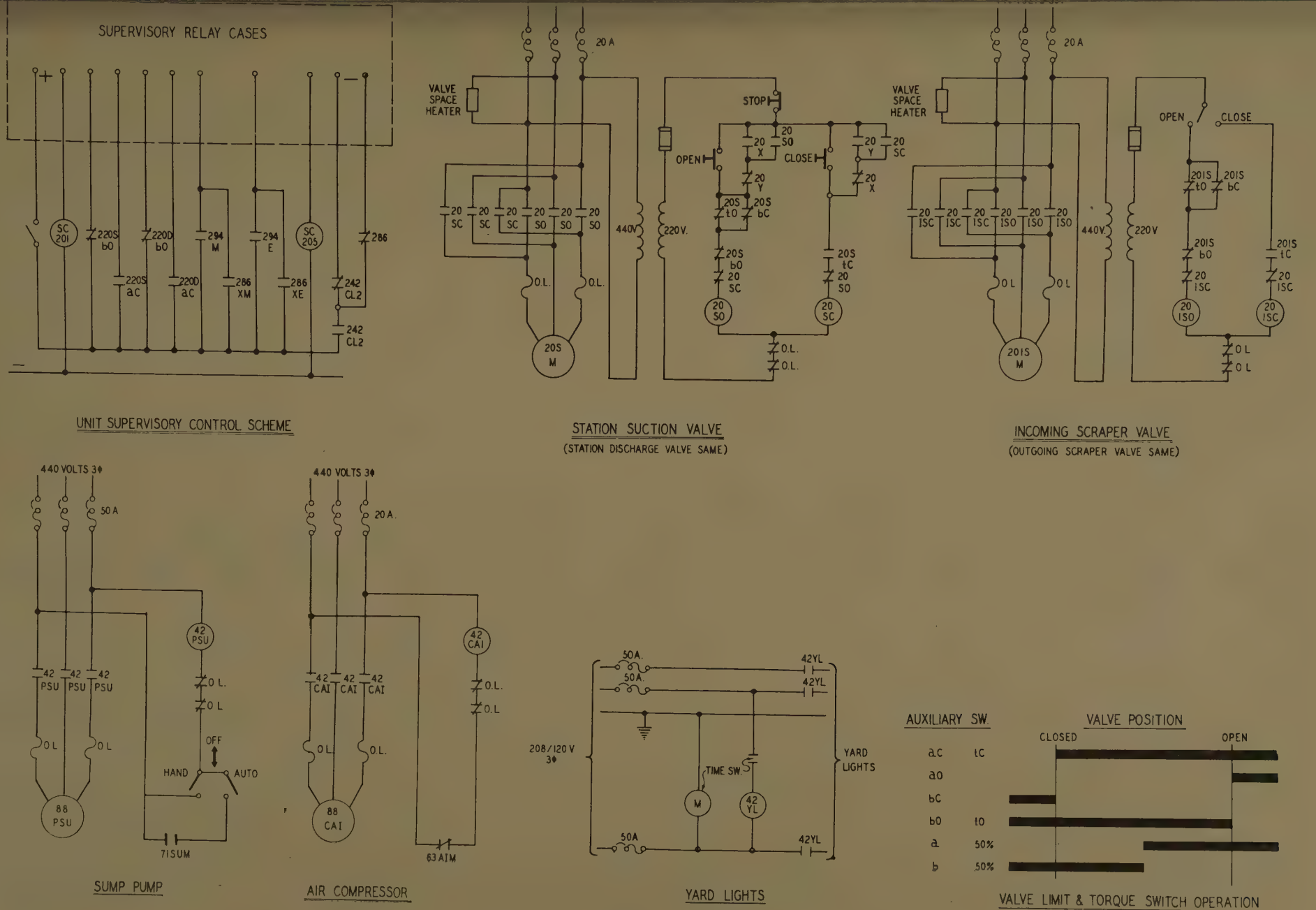

Fig. 6. Auxiliaries control schemes

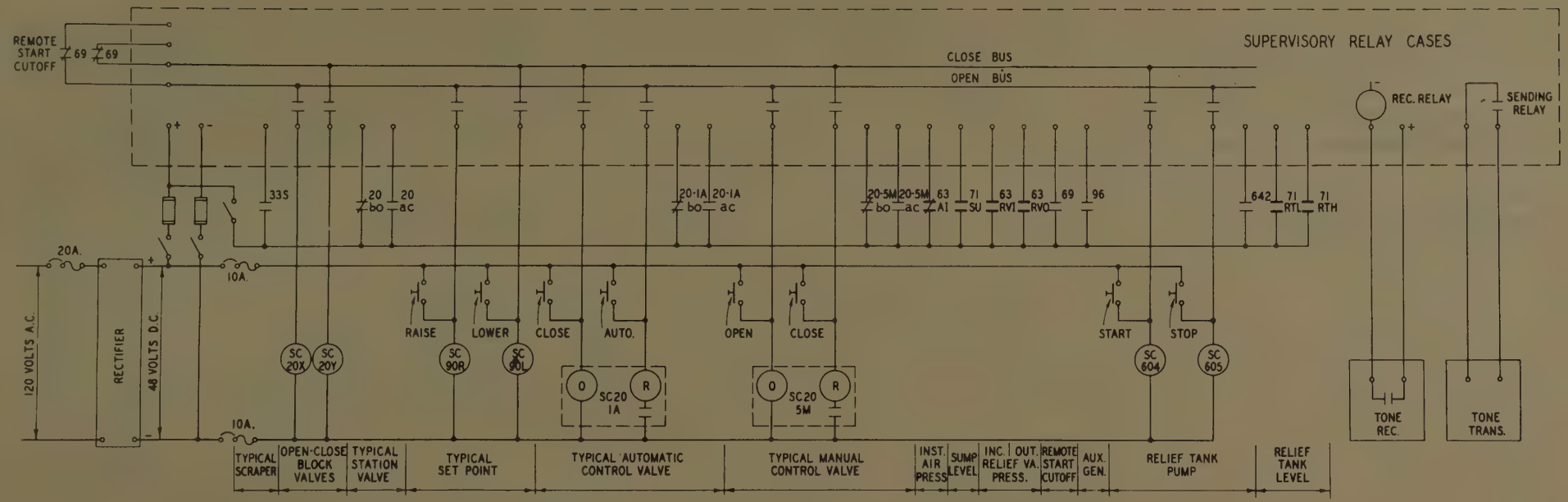

SUPERVISORY & LOCAL CONTROL SCHEME

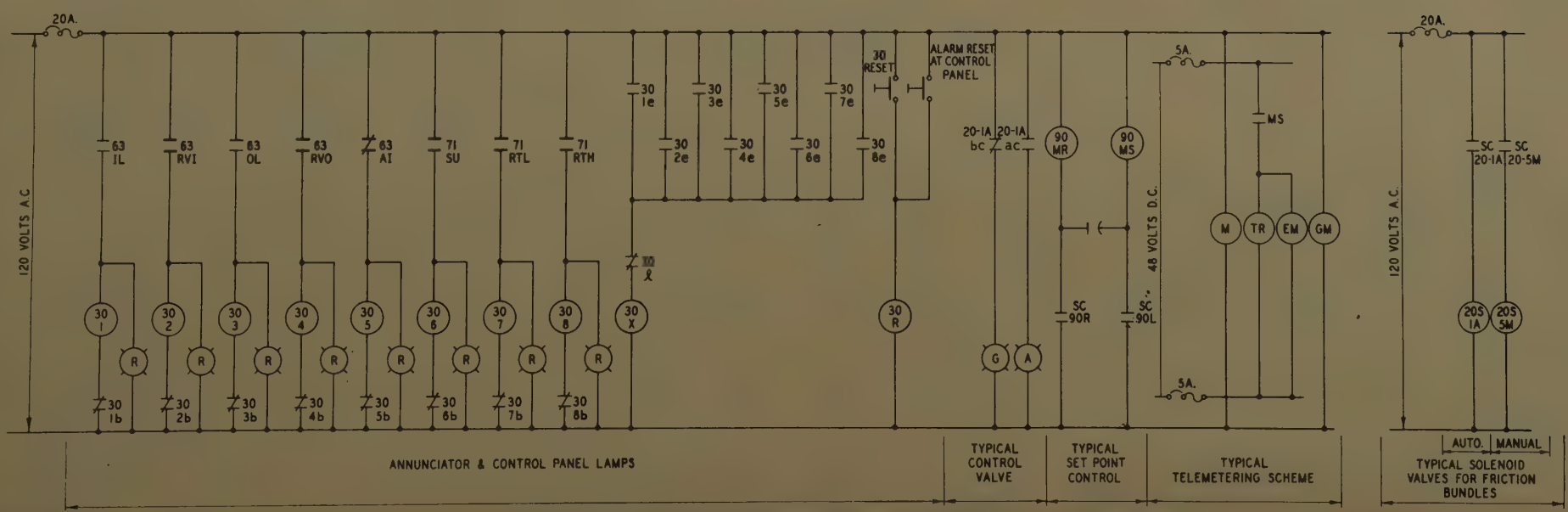

ANNUNCIATOR & MISCELLANEOUS SCHEMES

Fig. 7. Pressure-reducing station control scheme

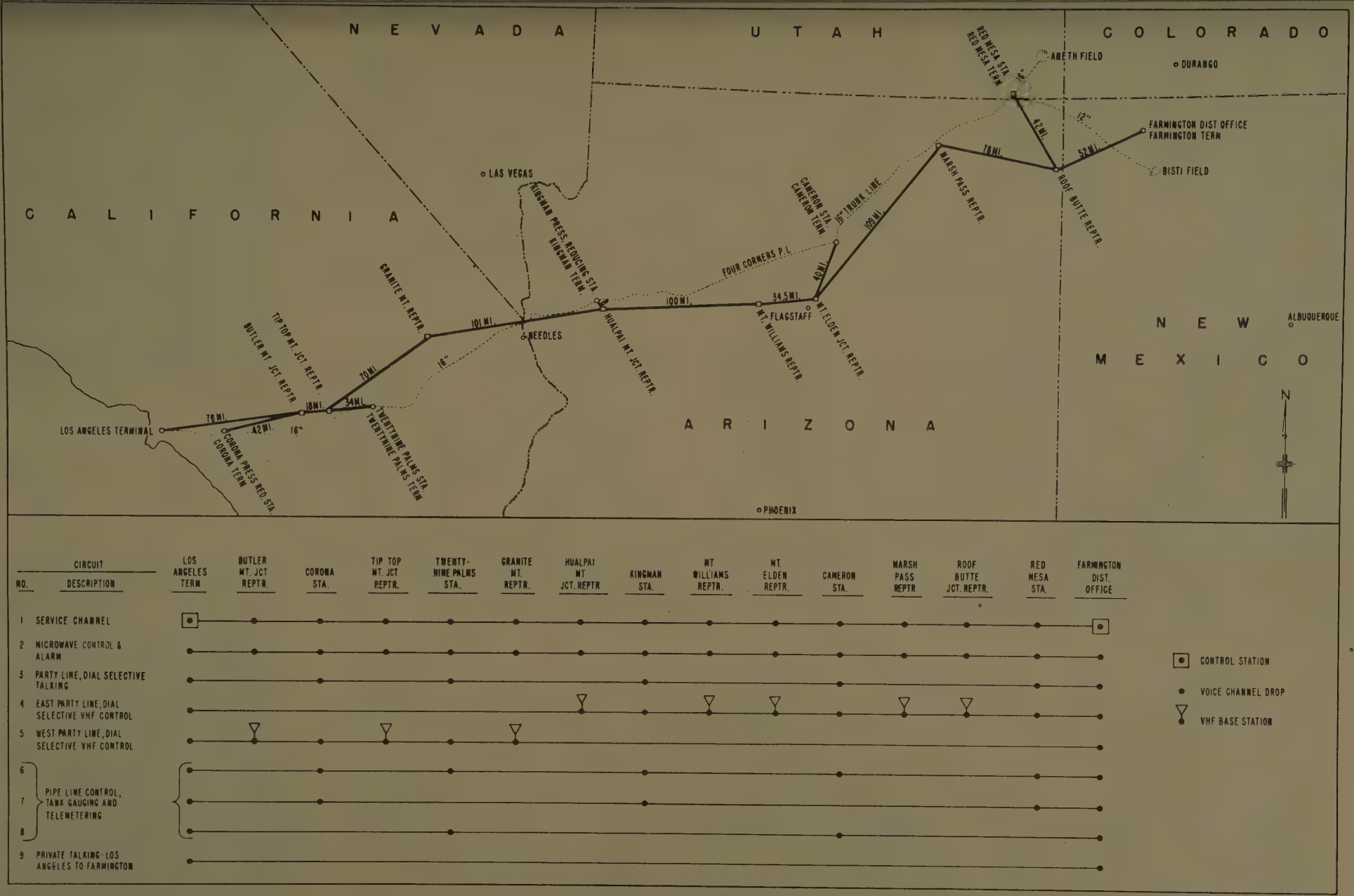

Fig. 8. Microwave communication system route

1. Five open-close flow valves.
2. Three close-automatic flow valves.
3. Incoming line block valve.
4. Outgoing line block valve.
5. Set-point incoming pressure.
6. Set-point outgoing pressure.

These stations are provided with 35-kw stand-by generator units with automatic transfer panels. The importance of the pressure-reducing stations in the system makes it imperative that adequate air supply be available at all times. The stand-by generator capacity is sufficient to carry all the necessary loads for an indefinite period.

Microwave Communication System

The absence of available commercial communication facilities for a greater part of the line dictated the construction of a privately owned microwave system. This system is constructed along the mountain tops, creating a "backbone" system with laterals to connect the intermediate pump stations. The system has 15 installations, as shown in Fig. 8, and consists of seven terminals, five junction stations, and three repeater stations. By routing the backbone system so that the terrain may be used advantageously, it was possible to increase path lengths, thereby reducing the number of installations. The average backbone path is 70 miles long with several paths in excess of 100 miles. The five lateral paths vary from 8 to 42 miles in length. The total system mileage is 795 miles.

The system operates in the 1,850- to 1,990 megacycle operation fixed band. The transmitter is crystal-controlled, using a 90-megacycle crystal oscillator with stability and accuracy of 0.01% of the carrier frequency. Conservatively rated stages provide the necessary frequency multiplication and drive to operate a lighthouse amplifier in the output stage, which delivers a peak power output of 20 watts under pulse carrier modulation. The high power output provides high system gain which is used to provide better fading margins and lower cost installation through the use of lower gain antennas, and a transmission line of higher loss. In using crystal-controlled transmitting equipment, a statement of frequency measurement need be made only once every 6 months in order to comply with Federal Communications Commission requirements. Also, transfer to stand-by equipment is accomplished in minimum time since no "drift-on" time is required for the stand-by unit to become stabilized.

The microwave multiplexing system performs its function of applying 1 to 25 audio channels to the r-f (radio-frequency) system by the time-division (TD) method more specifically described as pulse position modulation (PPM). In a TD multiplexing system, each channel is allocated a small portion of the time in which to accept or reject intelligence to or from the main carrier. The failure of the multiplex equipment on a leg circuit does not affect through transmission of that channel on the backbone circuit.

Full r-f stand-by and stand-by for common multiplexing equipment, together with the necessary fault-detecting equipment, is provided at all microwave installations. The radio-frequency receiver, transmitter, and associated power supply stand-by units automatically transfer as individual items and not as a complete radio-frequency stand-by bay.

Initially, the system utilizes 9 of a possible 25 channels in supplying circuits necessary to the operation of both microwave system and pipe line. The channels are shown diagramatically in Fig. 8. An unusual feature in this system is the incorporation of a microwave supervisory on the alarm channel, to facilitate remote control of the following functions at indicated installations.

All-Microwave Installations

1. Voltage drop test (all power reduced 10% for predetermined times).
2. Exercise of stand-by common multiplex.
3. Lock-up of stand-by common multiplex.
4. Release of locked-up stand-by common multiplex.
5. Release of locked-up normal common multiplex.
6. Exercise of east stand-by r-f.
7. Lock-up of east stand-by r-f.
8. Release of locked-up east stand-by r-f.
9. Release of locked-up east normal r-f.

All Microwave Repeater Installations

1. Exercise of pulse restore east.
2. Lock-up of pulse restore east.
3. Lock-out of pulse restore east.
4. Exercise of west stand-by r-f.
5. Lock-up of west stand-by r-f.
6. Release of locked-up west stand-by r-f.
7. Release of locked-up west normal r-f.
8. Exercise of pulse restore west.
9. Lock-up of pulse restore west.
10. Lock-out of pulse restore west.
11. Exercise of north stand-by r-f.
12. Lock up of north stand-by r-f.
13. Release of locked-up north stand-by r-f.
14. Release of locked-up north normal r-f.
15. Exercise of north stand-by common multiplex.
16. Lock-up of north stand-by common multiplex.
17. Release of locked-up north stand-by common multiplex.
18. Release of locked-up north normal common multiplex.
19. Exercise of stand-by power audible monitor.
20. Exercise of stand-by generator.
21. Lock-up of stand-by generator.
22. Telemeter generator 1 (voltage and frequency).
23. Telemeter generator 2 (voltage and frequency).
24. Energize of stand-by tower beacon (Marsh Pass only.)

All of these functions can be accomplished from any point in the microwave system by dialing a 2-digit code for the desired location followed by a 2-digit code for the particular function desired.

Microwave alarm functions are recorded at the Los Angeles terminal by means of codes printed on tape. The code identifies the particular station followed by coded signal reporting the particular type of fault. The fault-locating unit is capable of handling six coded groups.

For telephone communications, one circuit is utilized for duplex private-line operation between the Los Angeles terminal and the Farmington district office. The Los Angeles end of this circuit is terminated on leased private automatic branch exchange facilities, and it operates as though it were another station within the terminal for outgoing calls, while all incoming calls are handled by the terminal private branch exchange operator. An additional circuit is used to connect the terminal and the Farmington office with all pump stations, selective dialing being used to signal the desired location and instrument. At the terminal this circuit appears at the dispatcher's turret for his use; at the private branch exchange switchboard, for connection to telephones within the terminal.

Two voice channels are used to control very-high-frequency base stations located at all microwave repeater installations. The additional voice channels are used in party line arrangements to provide for the pipe line supervisory control, telemetering, and remote tank-gaging signals. A maximum of 35 narrow-band frequency-shift voice-frequency carriers are transmitted over a single voice channel between 300 and 3,000 cycles per second. Each audio-frequency carrier transmitted

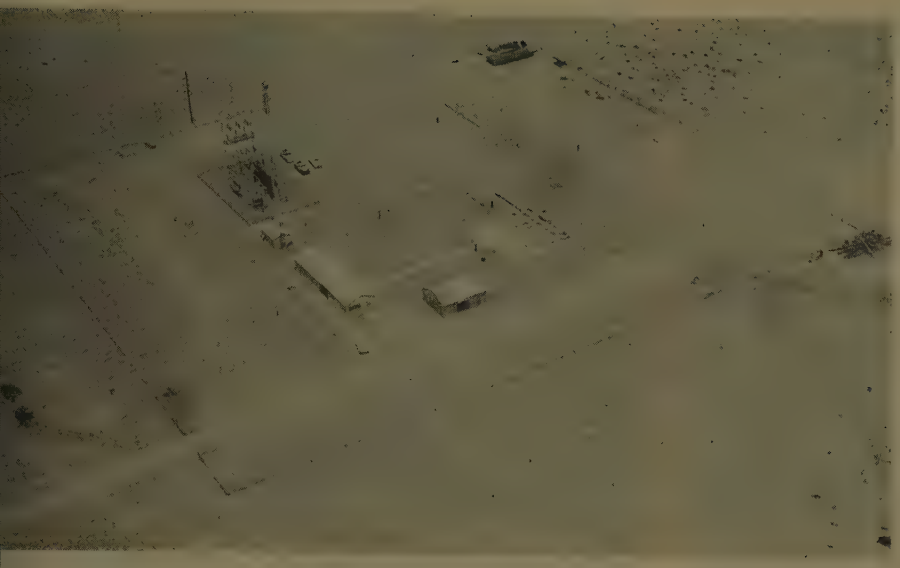

Fig. 9. Outdoor station layout

an be shifted in frequency to either a ark or space frequency. The mark equency is 12.5 cycles above and the ace frequency 12.5 cycles below the annel frequency of 300 cycles per sec-nd, while at the 3,000-channel fre-uency the mark and space frequencies re 25 cycles above and below the channel equency.

For supervisory control and telemeter gnaling, each audio-frequency trans-itter is arranged to be in space frequency ndition during no-signal input and in ark frequency condition when keyed. he associated receiver reflects simulta-eously the condition of its transmitter; ie complete absence of an input signal ill cause the receiver to remain in mark equency condition, thereby providing an arm function where required.

Voice-frequency carriers for supervisory ntrol and telemeter signals between the os Angeles terminal and the various pipe ne distribution points are transmitted ver voice channels leased from the tele-none company. Business telephones are stalled at each of the distribution points to permit maintenance personnel to call the Los Angeles terminal.

Three of the eight mountain-top repeaters are served by commercial power. A propane-fueled stand-by engine with automatic transfer panel is installed at each of these three locations.

With no power available at five of the mountain top repeaters, the operation of privately owned engine-generator sets to provide a source of power was the only alternative. Four of these locations are usually inaccessible during the winter months. The power plants and respective accessories are engineered to operate without attention for 3-month periods. Identical primary and stand-by liquid-cooled diesel engine-generator units are provided at these locations in combination with an automatic transfer panel. Each unit has its own engine-starting panel, starting battery, lube oil regulator, lube supply, and dual primary and secondary filters. A common fuel system with 4 months' capacity is provided.

Microwave equipment at each pump station is housed in a steel-frame asbestos-clad insulated building. At the Farmington district office sheathing and brick were used to conform to the local building code. The repeater-station equipment is housed in standard steel-frame metal-clad insulated buildings, except the Tip Top Mountain repeater equipment, which is housed in a concrete block building having a prefabricated concrete roof to comply with United States Forestry Service requirements. The Los Angeles microwave equipment is housed within the Terminal Building adjacent to the supervisory equipment.

Supervisory Control Equipment

The entire pipe line system, except for the feeder stations, which are automatic, is remotely operated from the terminal office building in Los Angeles County, Calif. Remote operation is effected by means of supervisory control and telemetering equipment installed in the terminal building and at each station. A separate supervisory control system operating over a duplex audio tone channel is provided for each pump station, pressure-reducing station, and valve station. The required channel space for the pump and pressure-reducing stations is provided by the microwave system previously discussed. Leased voice circuits provide channel space for the valve stations in the Los Angeles area.

The supervisory control equipment employed is of the all-relay pulse count type. The equipment in the terminal building consists essentially of groups of telephone-type relays and associated control panels mounted in and on upright cabinets. The cabinets will, with ultimate expansion of the pipe line system, comprise three walls of the dispatcher's office. Generally one cabinet is required for each station, although all the valve stations require only one cabinet and the initial station with its booster pumps and tank manifold requires three cabinets.

Fig. 10 (left). Outdoor motor installation

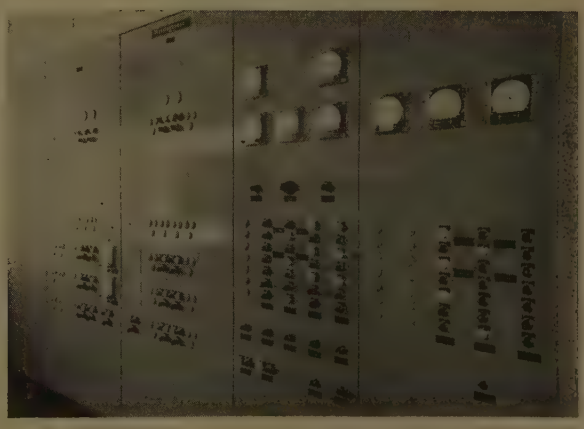

Fig. 11 (right). Local control panels

Fig. 12 (left). Switchgear assembly

Fig. 13 (above). Pressure-reducing station

The cabinets are arranged in order, according to the physical layout of the pipe line. The control panels with push buttons, indicating lamps, and mimic piping layouts are mounted on the front of the cabinets. The telemeter receivers are mounted directly above the control panels.

The sealed supervisory relay cases are mounted on the rear of the cabinets on hinged panels. Access space is provided at the rear of the cabinets for testing and maintenance of the equipment.

The supervisory control equipment at a station consists of a set of telephone-type relays and associated-power-type interposing relays to transfer the signals to the power equipment being controlled. The equipment at the pump stations is installed in a switchgear auxiliary cubicle at one end of the switchgear line-up; at the pressure-reducing stations it is installed on the rear panel of the local control cabinets and at the seven valve stations in outdoor weatherproof cabinets.

Each supervisory control system is divided into "points" of supervision and/or control. A separate point is required for each device under supervision or control. A point will usually have three lights on the control panel. One of these is a white light which indicates that the point has been selected, either by the dispatcher or automatically, when an alarm or change is reported. The other two indicate the position of the supervised device; in the case of an alarm function these are green (normal) and red (alarm). For a valve the lights are green (valve closed); amber (valve open); and green and amber (valve in intermediate position). For a motor the lights are green (off) and amber (on).

The points with control as well as supervision are also provided with push buttons or selector push buttons, as required.

The supervisory signals consist of combinations of pulses called codes. To reduce the number of pulses required to identify a particular point, the supervisory control systems with more than ten points are divided into groups with ten points comprising a group. Each group and each point within a group has a particular code consisting of one to ten pulses. The operation and supervision codes consist of three to five pulses and are common for all points.

Typical Control Operation

Typical control operates in the following steps:

1. The dispatcher pushes the individual control push button of the desired function to be performed.

2. The control station transmits the group selection code.

3. The remote station selects the proper group and transmits a group check cod identical to the group selection code.

4. Upon receipt of the group check cod the control station compares it with th original code sent out and, if identical, trans mits the point selection code.

5. The remote station selects the prope point and transmits a point check code.

6. The control station receives the poin check code and, if this is identical to th point selection code sent out, it lights th associated white light on the control pan indicating that the point has been selecte it then transmits the operation code.

7. Upon receipt of the operation code th remote station energizes the appropriat power-type interposing relay performing th directed function.

8. When the controlled device change position, the remote station transmits supervision code.

9. Upon receipt of the supervision cod the control station changes the indicatin lights on the control panel and transmits reset pulse which resets the equipment a both locations.

If for any reason the selection codes an check codes do not agree, the equipmen will automatically reset, and the operato must again depress the push button of th function desired to be performed.

Since the pulses are transmitted at th rate of 13 per second, the entire operatio just described takes from 2 to 5 second depending on the particular point se lected.

Uncalled for changes in position supervised devices are automatically re

Fig. 14. Local control cabinet pressure-reducing stations

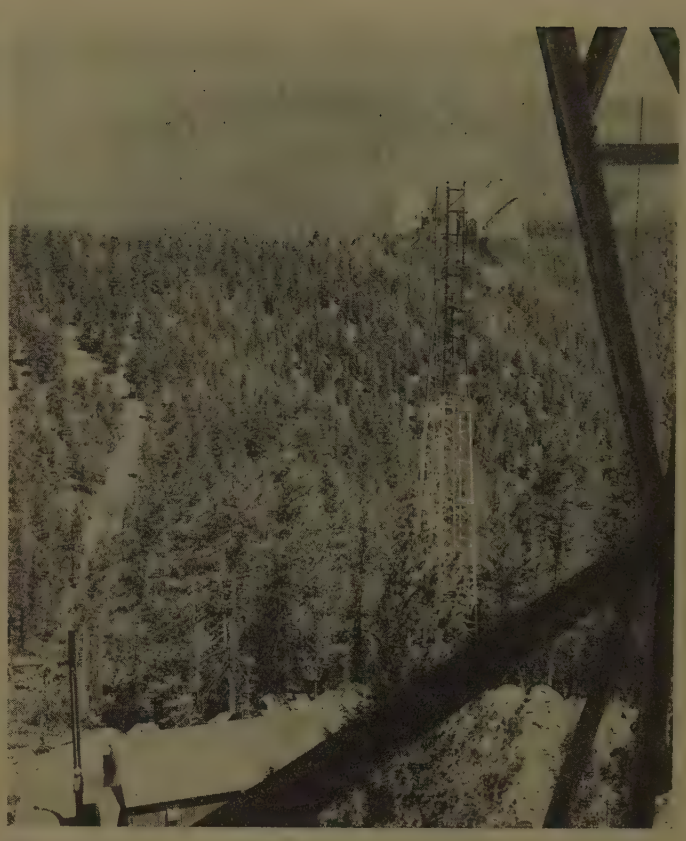

Fig. 15. Mountain-top microwave installation

ted. The operation for this type of ction is similar to a control operation, ept that the selection codes are origi- ed by the remote station; the check es are originated by the control sta- ; and the operation code is omitted. n the case of an alarm-type function omatically reported, the light changes he control panel are accompanied by sounding of an alarm. The audible m is silenced by depressing the alarm t button. A change in position of a ice of a nonalarm type or a change iated by the dispatcher is not ac- panied by an audible alarm.

master check button is provided for h system. Operation of a master check ton will cause the supervisory control tem to check each point in sequence. h point when checked will momen- ly light its corresponding white lamp. n case of communication failure, each ervisory control system affected re- ts a communication failure alarm and ds its indications of station-operating ditions. After communications are ored, the supervisory equipment auto- tically corrects any indications in error ring the outage, the stations continue perate unless shut down by local pro- tive devices.

The supervisory control systems pro- e the following control and supervi- :

All Main Line Units

1. "Start" control and supervision of suction valve.
2. Supervision of discharge valve.
3. Supervision of mechanical trouble.
4. Supervision of electrical trouble.
5. "Stop" control and supervision of unit breaker position and unit lockout.

All Pump Stations

1. Supervision of incoming and outgoing scrapers.
2. Supervision of station valves with control of station block valves.
3. Supervision of station case and discharge pressures.
4. Supervision of station alarms: instrument air pressure, sump level, power failure, and station battery.
5. Control of emergency stop.
6. Raise-lower control of discharge pressure set point.
7. Supervision of remote start cutoff.

Initial Pump Station Only

1. Control and supervision of booster pumps.
2. Control and supervision of tank manifold valves.
3. Control and supervision of tank mixers.

Pressure Reducing Stations

1. Automatic-close control and supervision of three automatic control valves.
2. Open-close control and supervision of five manual control valves.
3. Raise-lower control of incoming and outgoing pressure set points.
4. Control and supervision of relief tank pump.
5. Supervision of incoming and outgoing scrapers.
6. Supervision of station valves with control of station block valves.
7. Supervision of auxiliary generator.
8. Supervision of station alarms: instrument air pressure, sump level, incoming line pressure, outgoing line pressure, and relief tank level.
9. Supervision of remote start cutoff.

Delivery Valve Stations

1. Control and supervision of delivery valves.
2. Supervision of pressure and flow alarms.

An unusual feature is the remote set point control. The set point changer installed at a station consists of a 2-winding reversible motor positioning a precision regulator. The output of the regulator (3 to 15 pounds per square inch air) is fed to a set point bellows located in the discharge pressure controller. The air signal is also fed to a telemeter transmitter.

The gearing is arranged to produce a 1% adjustment for each 1-second operation of the motor. To adjust the set

Fig. 16 (left). Communication equipment racks

Fig. 18 (right). Supervisory relay cabinet assembly

point, the dispatcher turns the set point selector push button to the desired position (raise or lower) and pushes it. Operation of the supervisory control equipment results in the motor being energized for a period of 2 seconds, resulting in a 2% change of the set point. Any amount of adjustment desired can be obtained by repeated operation of the raise-lower push button. The set point control scheme is shown in Fig. 7.

Telemetering and Tank Gaging

The telemetering equipment is of the impulse duration type with a 5-second period. Each telemetered quantity is transmitted on a continuous basis over a simplex audio tone channel.

The telemeter transmitters are of explosion-proof design and are grouped outdoors on a common rack. Local telemeter receivers working directly off the transmitters are provided at each station for use when local control is required.

The telemetering receivers at the terminal building are of the miniature type and are installed above the control panels in the supervisory control cabinets. The majority of the receivers are recording, and some are equipped with high and low alarm lights.

The telemetering equipment is self-synchronizing and will automatically correct its readings upon restoration of communications after an outage. During an outage, all receivers affected will read full-scale indicating to the dispatcher their in-operation.

The following quantities are telemetered from an intermediate pump station: station suction pressure, station case pressure, station discharge pressure, flow, gravity, and discharge pressure set point. The initial pump station has, in addition to the foregoing, the flows of the two incoming feeder lines and pressures relat to the booster pumps.

Telemetered quantities received fr a pressure-reducing station include i coming and outgoing flow, incoming a outgoing pressure, incoming and outgoi pressure set point, and gravity. A telemetered is the position of the aut matic friction tube control valve operation. Since only one of the thr automatic valves is in an intermedia position at any one time, a single tele etering system with automatic selecti serves all three. Telemetered quantiti from the delivery valve stations inclu pressure, gravity, and flow from requir locations.

A remote reading tank-gaging syste is provided for the storage tanks at t initial station and the relief tanks at t two pressure-reducing stations. Ea tank is equipped with liquid level gag and averaging thermometers. Two

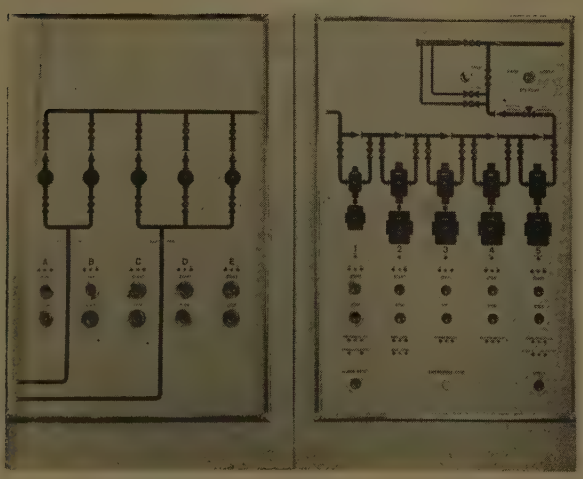

Fig. 17 (left). Supervisory control panels

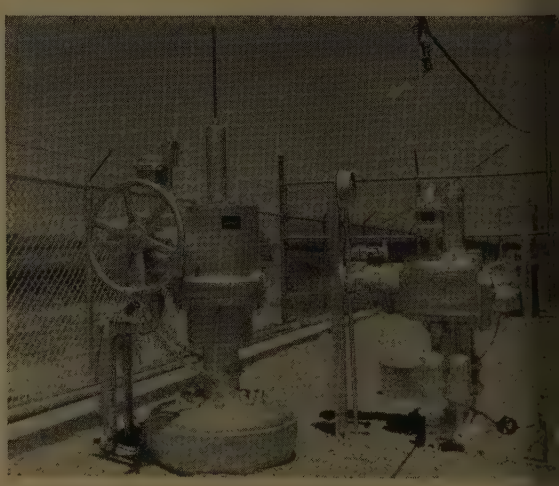

Fig. 19 (right). Delivery valve station

ers are installed, one at the initial on and one at the Los Angeles Termi- Building. The entire system works on rty line basis, and readings from all s can be taken at either receiver.

he system employed is of the pulse type. Transmitted information is al rather than analog, thus eliminat- the possibility of errors being intro- d by the transmission system. To a reading, the dispatcher dials the tion and tank desired, by means of a rentional telephone-type dial. After t 5 seconds, a reading appears on a al read-out panel giving the tank ber and liquid level or temperature. id level high and low alarms are matically reported.

igs. 9 through 19 show various indoor outdoor views of the system.

mary

he Four Corners pipe line is designed completely unattended operation. main line pump stations, pressure- cing stations, delivery valve stations, ter pumps, and tank-filling and suc- valves are designed for remote opera-

Most of the feeder stations are pped for automatic custody transfer ation.

he design of the communications and rol features incorporated into the em provides for safe and reliable ation of the pipe line from the dis- her's office in the terminal building ted at the western terminus of the

The design provides the controlling t with all the necessary telemetered ntities, pressures, flows, gravity, and points necessary for the remote opera- of the facilities. All necessary local ective devices are provided at all tions to permit safe operation during munications or supervisory control pment failures.

pendix. Device Designations

esignations are based on the proposed E Standard No. 68.[7]

ion Functions

ation functions are given in the follow- with the device numbers.

ain breaker control
-control switch at breaker
A—indoor control switch
B—outdoor control switch
CSW—automatic operation cutoff switch
ain breaker tripping relay
-main breaker tripping power disconnect switch
8C—main breaker closing power circuit breaker
8SF—station functions disconnect switch
8STC—shunt trip coil unit valve feeder breaker
20-1A—friction tube automatic control valve No. 1-A
20-5M—friction tube manual control valve No. 5M
20D—station discharge valve
20IS—incoming scraper valve
20ISC—incoming scraper valve closing contactor
20ISM—incoming scraper valve motor
20ISO—incoming scraper valve opening contactor
20KI—outgoing scraper No. 1 kicker valve
20K2—outgoing scraper No. 2 kicker valve
20L—incoming scraper lead-in valve
20OS—outgoing scraper valve
20S—station suction valve
20S-1A—solenoid valve control valve No. 1A
20S-5M—solenoid valve control valve No. 5M
27DC—battery undervoltage relay
30—Annunciator drop
33SA-1—arriving scraper detector switch No. 1
33SA-2—arriving scraper detector switch No. 2
33SD-1—departing scraper detector switch No. 1
33SD-2—departing scraper detector switch No. 2
42CAI—air compressor starter
42PSV—sump pump starter
42YL—yard light contactor
45HA—combustible gas alarm switch
47—undervoltage or reverse phase voltage relay
51—overcurrent relay
52—main circuit breaker
63AI—instrument air pressure switch
63AIM—air compressor control pressure switch
63D—station discharge pressure switch
63IL—incoming line pressure
63OL—outgoing line pressure
63RVI—incoming relief valve pressure switch
63RVO—outgoing relief valve pressure switch
69—remote control cutoff switch
71RTL—low-level relief tank switch
71RTH—high-level relief tank switch
71SU—sump level switch
71SUM—sump pump control level switch
74R—alarm reset relay
80RV—flow to relief tank switch
86—station lockout relay
88CAI—air compressor motor
88PSU—sump pump motor
90MR—set point control motor-running winding
90MS—set point control motor-starting winding
96—auxiliary generator-running contact
EM—telemeter receiver electromagnet
GM—telemeter receiver gear motor
M—telemeter transmitter cam motor
MS—telemeter transmitter keying switch

Unit Functions

The following device numbers are for unit 2. Device numbers for the other units are the same except that the prefix number is the same as the unit number.

201—start-stop control push button
204—sequence-starting relay
205—sequence-stopping relay
206—starting circuit breaker
208—control power disconnect switch
219—start period timing relay
220D—discharge valve
220PVT—pump vent valve
220S—suction valve
226M—motor-winding temperature relay
226PC—pump case temperature switch
227—a-c undervoltage relay
230—annunciator drop
238MI—motor inboard bearing temperature switch
238M2—motor outboard bearing temperature switch
238P1—pump inboard bearing temperature switch
238P2—pump outboard bearing temperature switch
239PVB—pump vibration detector switch
239SF—pump seal leak switch
242—running breaker
246—phase balance relay
248—over-all sequence check timing relay
249—thermal overload relay
249IT—thermal overload relay instantaneous trip contact
251—overcurrent relay
251IT—overcurrent relay instantaneous trip contact
263PC—pump case pressure switch
263S—pump suction pressure switch
269—permissive switch
273—motor space heater relay
286—lockout relay
286XE—electrical trouble relay, lockout
286XM—mechanical trouble relay, lockout
294E—electrical trouble relay, nonlockout
294M—mechanical trouble relay, nonlockout

Supervisory control interposing relay device numbers are the same as the numbers of devices they control except when prefixed with SC.

References

1. Four Unattended Pipeline Pumping Stations, **R. S. Cannon, T. V. Bockman.** *The Oil and Gas Journal*, Tulsa, Okla., Dec. 7, 1953, pp. 178–79.

2. Electricity's Contribution to Modern Pipelining, **M. A. Hyde.** *The Westinghouse Engineer*, Pittsburgh, Pa., Sept. 1953, pp. 154–61.

3. Remote Operation of Pipe-Line Pumping Stations, **W. A. Derr, M. A. Hyde.** *AIEE Transactions*, pt. II (*Applications and Industry*), vol. 73, Sept. 1954, pp. 190–98.

4. Microwaves for Pipeliners, Part VIII, Supervisory Control and Telemetering, **C. B. Lester.** *The Pipe Line News*, Bayonne, N. J., July 1953, pp. A1–A8.

5. Basic Circuitry for Electrically Powered Pipe-Line Pump Stations Under Automatic or Remote Control, **M. A. Hyde, W. A. Derr.** *AIEE Transactions*, pt. II, vol. 74, Mar. 1955, pp. 4–14.

6. Remote Controlled Unattended Pump Stations Utilized by Great Lakes Pipe Line Company, **P. R. Madden, A. P. Riehl.** *PEPA Paper*, Petroleum Electric Power Association, Dallas, Tex., May 16, 1956, pp. 51–59.

7. Proposed Device Numbers and Functions for Pipeline Pump Stations Under Automatic or Remote Control. *AIEE Standard No. 68*, Feb. 1958.

The Life Expectancy of Class A Random-Wound Motor Insulation As Determined by AIEE Standard No. 510 Test Procedure

AIEE COMMITTEE REPORT

TEST PROCEDURES for determining the relative life expectancies of different insulation systems for random-wound machines, using either complete motors or models, called motorettes, are provided for by AIEE no. *510*.[1] The procedure calls for subjecting the motorettes to successive periods of high temperature in ovens, followed by vibration and exposure to moisture, and an overvoltage check. The cycle is repeated until the test unit fails under voltage. The tests are conducted at three or more temperatures, and are made on a sufficient number of samples to obtain the desired statistical accuracy. The tests on motors are similar, but the heating, vibration, and voltage exposures are all obtained at the same time by operating the motors on a frequent starting or reversing cycle. The results of the tests are given in the form of a life-temperature chart, as in Fig. 1.

To make this procedure fully useful, and a basis for standards, it is necessary to establish the life expectancy that AIEE no. *510* determines for widely used insulation system that has proved satisfactory in extended service use. Then those who are responsible for standards, after they have decided what the relative insulation life required for the standards should be as compared with the familiar system, will be able to set a numerical value for the hours of life under the no. *510* procedure that an insulation system should have to satisfy the requirements.

With this purpose in view, the committee responsible for the development of AIEE no. *510* undertook to carry out a series of tests to establish by this procedure the life expectancy of the present-day widely used class *A* random-wound motor insulation system, that is giving highly satisfactory service in motors built under American Standards. This present system has evolved as the result of many years of experience. Formerly cotton-covered wires and paper slot liners were used. About 1937, film-covered wires began to replace the cotton. Another marked change occurred about 1952 when the polyester Mylar* came into use for slot liners. The slot liners used in the present-day systems contain a layer of polyester sheet (synthetic) material, which has markedly superior life under extreme moisture conditions, as compared with the cellulosic materials (paper or varnished-cloth) in the slot liners of the class *A* insulation system employed up to about 5 years ago. In Europe, where the motor insulation systems are similar to ours, this superior life of the synthetic materials under extreme conditions very recently has been recognized by designating the all-synthetic system as class *E* for which the limiting temperature has been set at 115 C (degrees centigrade). In the United States, this superior system is still designated as class *A*, with a limiting temperature of 105 C. Thus, present-day motors built under the American Standards are more conservatively rated than European motors. This means that, other things being equal, the life expectancy of standard American motors at their rated temperature rise, corresponding to the usual 1.15 service factor (50 C), should be about twice as long as that of the comparable European motors at their rated-load temperature rises (60 or 65 C).

There are a good many variations in the details of the present-day materials and processes used by different manufacturers. However, the differences are minor, and probably they do not cause variations any greater than those resulting from other causes inherent in the test procedure.

Test Program

Nine laboratories participated in the program, which was conducted in the following manner.

The insulating materials to be used in the tests were supplied to all the laboratories from a common stock, made up of the following items:

Copper Wire. 0.040-inch no. 18 AWG (American Wire Gauge) heavy Formvar covered wire, with a total build of 3 mils. Using this material, coils of 14 turns of two wires wound in hand were used in the motorettes.

Slot Liners. 0.005-inch Mylar laminated to 0.005-inch rag paper. The Mylar was on the inside of the liners. The length of overhang at each end of the slot, while not specified, was approximately 1/4 inch.

Varnish. Oil-modified phenolic, 2 dips and bakes. The viscosity, and the time and temperature of bake were not specified, but typical values are 400 cycles per second at 25 C, with a bake of 3 hours at 150 C.

Wedges. Vulcanized curved fiber 1/32 inch thick.

Tying Cord. No. 12 cotton cord was treated.

Sleeving. Oil-varnished-glass sleeving.

Phase Separators. 0.015-inch rag insulating paper.

Motor Leads. Silicone rubber was used to facilitate handling. The leads do not form a part of the system under test.

All these items are typical of those regularly used in American general-purpose class *A* insulated motors, but they are not identical with those used by any one manufacturer, so far as known. The one material that varies most widely between different manufacturers probably is the insulating varnish.

Each laboratory assembled these materials into motorettes, or into motors, in accordance with their own practices, following the general rules specified in AIEE no. *510*. All parts of the motors and motorettes not listed were obtained independently.

Each laboratory performed the sequence of tests prescribed in AIEE no.

Paper 58-1334, recommended by the AIEE Rotating Machinery Committee and approved by the AIEE Technical Operations Department for presentation at the AIEE Winter General Meeting, New York, N. Y., February 1–6, 1959. Manuscript submitted October 27, 1958; made available for printing December 8, 1958.

Members of the AIEE Working Group on Insulation for the Rotating Machinery Committee are: P. L. Alger, *chairman*; R. L. Balke, D. R. Blake, H. P. Boettcher, E. L. Brancato, J. F. Dexter, T. J. Gair, G. P. Gibson, W. T. Gordon, L. Greer, J. L. Kuehlthau, L. P. Mahon, G. L. Moses, G. A. Mullen, W. W. Pendleton, W. B. Penn. Messrs. Blake, Boettcher, Brancato, Dexter, Gair, Gibson, Mahon, Mullen, and Pendleton participated in the program.

The committee wishes to express appreciation for the great amount of time and effort put into this test program by the nine committee members and their laboratory associates who participated in the test program. Also, special acknowledgment is due to Mr. L. P. Mahon and his associates in the Canadian General Electric Company, who prepared a program for the International Business Machines Corporation *650* computer, and used this to make all the statistical calculations required in evaluating the test results. This report of the committee's work was prepared by the chairman and secretary, but it includes many suggestions made by committee members after seeing a preliminary draft.

* Registered trade-mark E. I. Du Pont de Nemours & Company, Inc.

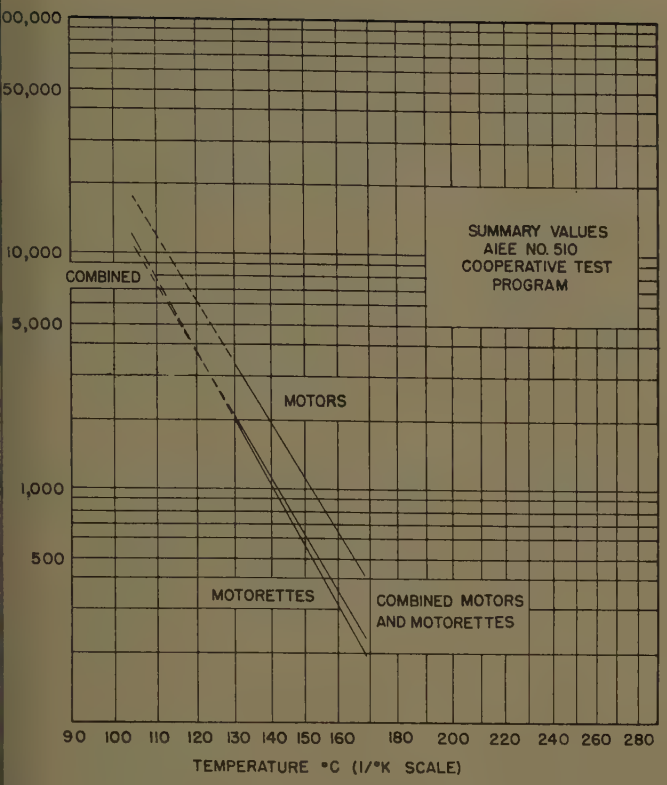

g. 1. Combined life-temperature curves as determined by AIEE no. 510 co-operative test program

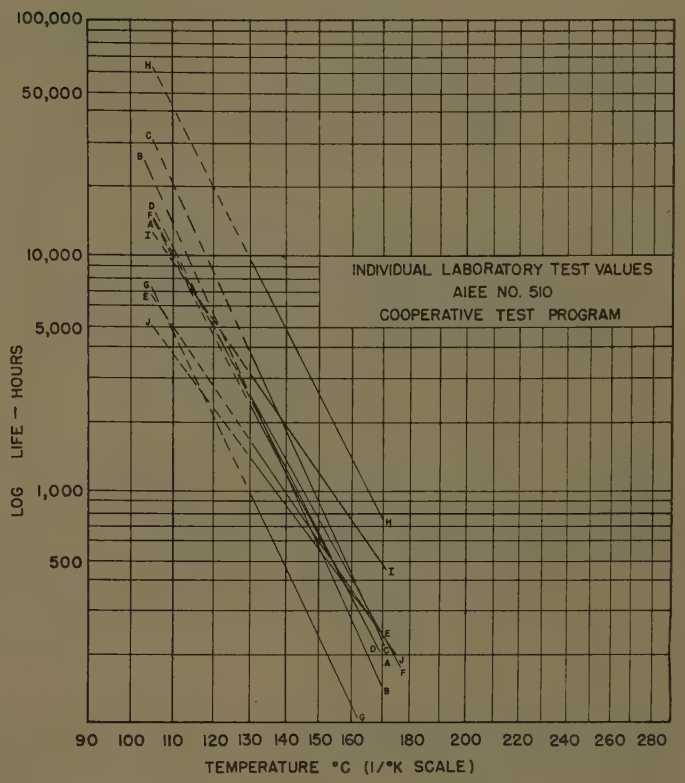

Fig. 2. Individual life-temperature curves as determined by AIEE no. 510 co-operative test program

0 at three or four different temperares (approximately 130, 150, and 170), and used 10 motorettes or 5 motors to termine each point. Six of the laboraries tested motorettes only, two tested otors only, and one tested both motors d motorettes, making ten sets of data in . Another laboratory, *I*, planned to ake both kinds of tests but unforeseen rcumstances prevented the motorette sts from being completed, so the limited ta obtained are not included here.

Table I. Motorette Tests

bo-ory	Life, Hours 105 C	170 C	Type of Failure	Amp Fuse Size	Test Voltage Between Wires
A*	13,742	191	Wire	Neon	60
B†	21,016	140	Wire	Neon	120
C	30,715	220	Wire	Neon	120
D	15,188	187	Wire	1/8	50
E‡	6,606	235	Wire and ground	1	120
G	7,730	61	Wire and ground	5	120
F	14,122	235	Wire and ground	Neon	120

Laboratory A used a low oil-modified phenolic rnish that was not the same as those used by the ier laboratories.

All the laboratories except B used phase separars in the form of grids cut from sheet, whereas used separate strips in each slot.

Laboratory E used 17 instead of 14 turns in the ils, giving a materially tighter fit in the slots and newhat greater length of wire. Also, the varnish ed by this laboratory, obtained from another urce, had a lower viscosity than normal (about 0 cycles per second at 23 C).

Test Results

The over-all results of the program are summarized in Table I, and in Fig. 2. The principal conclusions reached are:

1. The average life of usual class *A* random-wound motor insulation systems, when tested in accordance with the existing AIEE no. *510* procedure, and extrapolated to 105 C, is roughly 12,000 hours, including both motors and motorettes, but values found by different laboratories varied from about 5,000–60,000 hours.

2. The average life expectancy is halved for each 11 C increase in temperature, approximately, over the range between 105 C and 170 C.

3. The motors gave nearly the same average life as the motorettes at 105 C and about 200% at 170 C, with about 12 C for half-life of the motors, and about 10 C for half-life of the motorettes.

Discussion of the Results

Table II gives the results obtained in the ten independent sets of tests, and Fig. 2 shows these in chart form. Inspection of the data reveals a rather wide variation in the results obtained by the different laboratories. This is not surprising when it is considered that a change of only 5 C in the temperature corresponds to about 40% change in the life. After reviewing all the information, the committee decided that plausible reasons can be assigned for the major variations in results, as indicated in the following summary of the differences in the procedural details followed by the various laboratories.

As noted in Table I, two of the laboratories used a lower test voltage between wires than the 120 volts used by the other five laboratories. This came about because the committee decided to change the requirement of 50 volts in the present version of AIEE no. *510* to 120 volts, in order to obtain more definite end points, particularly for fiber-covered wires. This change was made too late for all the laboratories to follow.

In the next edition of AIEE no. *510*, 120 volts will be called for in this test.

It appears from Tables I and III that differences in the fuse size were a major cause for the differences in life obtained by the different laboratories. There is a considerable voltage drop in a neon lamp when only a small leakage current flows, so that the applied voltage falls, and the unit has time to dry out before the initially small leakage current that flows during a voltage check test can reach a destructive value. Also, when a small fuse is employed, the circuit is opened before any damage occurs, and a later test shows no indication of failure, so that the unit could be continued on the test program in the belief that the indication of failure was false.

When a larger fuse is used, the leakage current has a high enough value, and con-

Table II. AIEE No. 510 Summary Table

Laboratory	105 C Extrapolation, Hours			130 C Extrapolation, Hours			150 C Extrapolation, Hours			170 C Extrapolation, Hours		
	Life	UCL	LCL	Life	UCL	LCL	Life	UCL	LCL	Life	UCL	LCL
Motorettes Only												
A	13,742	19,225	9,807	2,253	2,669	1,901	619	650	588	191	202	180
B	21,016	33,564	13,159	2,535	3,042	2,112	556	559	553	140	167	117
C	30,715	41,985	22,470	3,805	4,426	3,271	855	886	825	220	235	205
D	15,188	18,944	12,177	2,365	2,588	2,160	626	627	624	187	204	171
E	6,606	8,021	5,441	1,614	1,775	1,467	589	604	575	235	245	226
F	14,122	17,650	11,299	2,501	2,790	2,243	726	746	706	235	247	225
G	7,730	10,153	5,884	997	1,088	912	230	241	220	61	72	52
Combined Motorettes												
	11,543	13,707	9,721	2,014	2,178	1,863	578	584	572	186	195	177
Motors Only												
H	12,446	22,575	6,862	3,162	4,077	2,453	1,187	1,200	1,176	487	602	394
I	63,886	109,998	37,104	9,559	12,589	7,258	2,458	2,673	2,261	715	782	653
J	5,007	8,656	2,896	1,359	1,839	1,004	535	608	471	229	236	222
Combined Motors												
	17,114	30,520	9,597	3,474	4,656	2,592	1,111	1,214	1,016	394	434	357
Combined Motors and Motorettes												
	11,485	13,891	9,495	2,150	2,349	1,968	649	659	639	218	230	207

tinues long enough, to cause positive damage, thereby giving definite proof of failure. Also, failures are more likely to occur because of creepage over the ends of the slot tubes when very small fuses are used. It appears from the test data that the average life may be only one half or one third as great when the 5 ampere fuses are used, as compared with that when Neon lamps are employed. Consideration of all factors leads to the belief that no material change in life will occur in motorette testing, if the size of fuse is increased above 5 amperes. From the data in this paper alone, it is known that a smaller fuse than 5 amperes may be adequate, but it appears that when fiber-covered wires are tested, as in higher temperature systems, a somewhat larger fuse will be needed than is required for enameled-wire systems. It is expected that further evidence on this subject will be brought out in AIEE papers now being planned to cover additional test data.

On this basis, it was decided to include in the next revision of AIEE no. *510* the specific requirement that 1-ampere fuses be used in motorette testing for film-covered wires, and that 5-ampere fuses be used when the wire is fiber-covered.

Variations in the degree of humidity and the ways in which the samples were exposed are important also. In laboratory *B*, the motorettes were placed vertically in the humidity chamber, while in the other laboratories they were horizontal. In laboratory *E*, they were upside down, so that they were protected from drip. In laboratories *D* and *F* all metal parts of the humidity chamber and motorettes were either made of stainless steel or thoroughly plated, so that water dripping on the units was pure. In the other laboratories, the dripping water may have carried with it a certain amount of rust. Laboratory *E* mounted ten motorettes on 2 plates of Mycalex and placed them in the humidity chamber in a horizontal position, unit side down. This mounting technique permitted more abundant condensation on the units, and its localization in drops, then the procedure followed by other laboratories. Laboratory *E* removed the motorettes from the humidity chamber and placed them in plastic containers to limit evaporation, before applying the electrical tests. The test voltage was applied to all ten motorettes at the same time. In Laboratory *C*, electrical tests were made on the motorettes in air, after they were brought out from the humidity chamber, whereas in the other laboratories except *E* the voltage was applied with the unit still in the humidity chamber.

In all cases, there was water in the bottom of the humidity chamber that was vaporized by immersion heaters, so that extensive condensation occurred in drops on the test units, but there was no way to be sure that the amount of condensation was the same in all laboratories. It appears that the differences in life caused by variations of this kind are reduced when larger fuses are used. Earlier tests have shown that the test life of motorettes is roughly doubled when they are exposed to 100% humidity without condensation, and may be of the order of five times as long when tested dry. Despite the variations inherent in the humidity exposure, the committee decided that the procedures given in AIEE no. *510* should be retained with some changes in the wording to define them more precisely. It is especially important to maintain the water temperature above that of the units in the humidity chamber, so that condensation will actually occur on the units, and not merely on the walls of the chamber.

Other variations in the test life were undoubtedly caused by differences in the methods of assembly, varnish dipping, and baking of the samples and still others by inaccuracies in the temperature control. A difference of 2 or 3 C may easily occur in different parts of an oven, and in different parts of a motor winding, and these alone would account for differences of 15-25% in insulation life. Errors of this type should be averaged out by testing a sufficient number of samples, however. Measurements showed that the amplitude of motion of units differently placed in the vibration test varied between 4 and 12 mils more or less, as compared with the 8 mils that are specified. Here again the errors should be averaged out in testing a considerable number of units.

On the whole, it appears that the degree of variation can be reduced appreciably in the future by more accurately defining the procedures of AIEE no. *510*, especially the fuse size as mentioned previously. It also appears that the variations that occurred in the present test program were generally on the high side, so that tests made in the future in accordance with the proposed revision of AIEE no. *510* should give somewhat shorter life on motorettes.

In the motor tests, the windings are subjected to transient overvoltages, when the motor is switched on and off, and these

Table III. Motor Tests

Laboratory	Life, Hours 105 C	Life, Hours 170 C	Type of Failures	Amp Fuse Size	Slot Liners	Type of Motor Phase	Hp	Poles	Volts
I	63,886	715	Between phases	6½	5/32-inch cuff	1	1/6	4	110
H	12,446	487	Wire	35	3/8-inch straight	3	10	6	440
J	5,007	229	Wire and between phases	40	5/16-inch cuff	3	5	4	440

Laboratory I used no phase separators. Laboratory H used separate strips in each slot, and Laboratory J used phase separators in the form of grids.

vervoltages are concentrated on the rminal coils. The motorettes do not xperience any similar transient voltage, ut they are subjected to 120 volts be- veen turns throughout the entire wind- g. These differences, together with the fferences between the stresses caused by arting and reversing the motors, as com- ared with those produced by vibration of ie motorettes, give ample cause to ex- ect a somewhat different life to be ob- ined for motors than for motorettes. urther differences are caused by the fferent procedures for the single-phase id 3-phase motors, and by the choice of ie size, number of poles, and voltage ting of the motors tested. A smaller umber of motors are used to check each oint than is the case for motorettes.

These factors help to explain why there a wider dispersion in the results of the otor tests than for the motorettes. aboratory *H*, in making some of their sts on single-phase motors, applied a peated surge impulse voltage of 600 olts, as a periodic check on one group of otors, in addition to the normal tests. his procedure did not change the ob- rved life appreciably. For this and her reasons, the committee decided not make repeated surge impulse tests a rt of the normal procedure in AIEE no. 0. It is thought that, with the normal pe of industrial contactor used in itching, the transient voltages that cur in a random manner during switch- g are adequate, and give fairly compa- ble stresses to those produced by the rn to turn test on the motorettes.

However, it is recognized that, when sts are made on higher temperature and gher voltage insulation systems, the e of moisture as a means of searching t insulation defects caused by aging ay not be as effective as in the low volt- e class *A* tests just described. For is reason, the use of repeated surge im- lse tests on an optional basis is per- tted by AIEE no. *510*.

It is expected that additional tests will made as time goes on to evaluate higher ltage and higher temperature random- ound motor insulation systems, follow- g the procedures of AIEE no. *510*, and at experience so obtained may indicate ther desirable changes in the procedure. is believed that AIEE no. *510* after the visions indicated in the foregoing and plained more completely in the appendix this paper have been made, will be ite satisfactory as a means of evaluating merits of different random wound tor insulation systems. In general, it believed that the use of motorettes is rticularly desirable as a means of eval- uating new materials and complete sys- tems for general-purpose use, while tests on motors will be desirable to check and extend the motorette results, and also to evaluate insulation systems for par- ticular kinds of service and environ- ments.

It should be noted that the twisted pair aging test specified in AIEE no. *57*[2] gives a typical life of about 30,000 hours at 105 C for the same wire used in this series of motor and motorette tests. Such a difference is natural, and to be expected, because in AIEE no. *57* failure is obtained by applying a relatively high voltage, in air, in the absence of condensation, instead of by a low voltage with condensation on the units as in AIEE no. *510*. It is desirable to prescribe the system test conditions in such a way as to make the life expectancy less for the complete insulation system than it is for the component materials when tested separately, because the system tests are inherently more expensive, and also sub- jected to many more causes of variation, so that they often need to be repeated. It is the opinion of the committee that on the broad grounds of economy and prac- ticality it is desirable to adjust the re- quirements of AIEE no. *510* to give a usual life expectancy under test condi- tions of about 10,000 hours, more or less, when extrapolated to the limiting tem- perature of normal operation.

Conclusions

The committee believes that the over- all results of tests, as given in Table I and Fig. 2, show that it is entirely fea- sible to base the requirements for ran- dom-wound motor insulations in future American motor standards on test results obtained by following the procedures of AIEE no. *510*. So far as the test pro- gram reported in this paper goes, it ap- pears that the present-day insulation sys- tems for general-purpose random-wound motors built in accordance with American Standards, have an extrapolated life of somewhere between 5,000 and 15,000 hours at 105 C, when tested in accord- ance with the procedures of AIEE no. *510* as they now are. However, the com- mittee does not consider the data reported here sufficiently consistent to warrant standards being based upon these figures. Accordingly, the committee has decided to undertake a new test program using motorettes, to be carried out with exactly the same materials as in the present pro- gram, but following the modified pro- cedures prescribed in the proposed re- vision of AIEE no. *510*. The appendix of this paper gives the text of the revisions that are proposed in AIEE no. *510*.

It is hoped that the data from this new program will be available in about one year from the present time.

Appendix. Proposed Changes in AIEE No. 510

Methods of Evaluation

Pages

6 Paragraph 3, line 10 should read: *A*, *B*, *F*, and *H* for each type of specimen.

6 Paragraph 3, line 17 should read: in which any new insulation, (omitting, material or).

6 The second sentence of the paragraph with the asterisk preceding it should be deleted.

Part I. Motorettes

6 In section 1–2 Motorettes, the second paragraph should be changed to read:
Specifically it is recommended that for the purpose of testing random wound motor insulation, two standard sizes of motorettes are available. Experience indicates that comparable results are obtained whichever size is used. Since the smaller one is economical, it is suggested that it be used when new test programs are undertaken.

8 Add the following sentence to the last paragraph:
It is suggested that the slot liners be made 1/4 inch longer than the slots in order to prevent failure by creepage over the ends.

Temperature and Exposure Time

11 In section 2–4 Moisture Exposure, in the first paragraph insert these two new sentences after the first sentence:
The condensation should consist of fine drops over the entire surface of the unit. To secure this, it is desirable to mount the units in a horizontal position.

11 Under note, delete the words room temperature and add to the sentence the following: temperature of the units themselves, so that condensation will occur on them and not merely on the walls of the chamber.

Voltage Checks

11 In section 3–1 the voltage between conductors should be changed from 50 to 120.

12 Add the following sentences to the second paragraph, face up.
To obtain definite and uniform indication of failure, a fuse shall be placed in series with each unit. The size of the fuse shall be 1 ampere if the wires being tested are film covered, and 5 amperes if the wires are fiber covered. The use of neon lamps in place of fuses is not permissible.

Part II. Motors

15 Section 2–5 Voltage Checks is to be completely deleted and this new 2.5 inserted in its place.

2.5 Voltage Checks. The test motors are to be run during the heat exposure periods at their highest rated nameplate voltage. The end point of the motor life in these tests is fixed by its electrical failure under the applied voltage, as indicated by the melting of a fuse that is connected in series with each motor. The current rating of the fuse should be 5 amperes, or at any rate not less than 1 ampere and not more than 10 amperes. The use of neon lamps or similar indicating devices in series with the motor, in place of or in addition to fuses, is not permissible, because even a small current through such a device creates a considerable voltage drop, thereby lowering the voltage that is impressed on the motor, and prolonging the time before failure occurs.

It is important that the motors should be restarted on the heat exposure phase of each cycle immediately after humidification, and the voltage check tests, described in the following paragraph, be made with a minimum of elapsed time.

Since the insulation of the individual wires in a random winding is not adequately checked by the application of normal line frequency voltage, it is desirable that some type of surge voltage be applied to the windings also. Normally, this is provided by the transient overvoltage surge that occurs each time voltage is applied to the motor by closing the line contactor. The magnitude of the surge will be greater when the contactor is reclosed immediately after being opened, as in the operation of motor reversal. Also, the magnitude will vary materially, depending on the type of contactor, the circuit capacitance as measured at the motor terminals, and the time phase angle of the voltage at the instant the contactor is closed. Therefore, the amount of overvoltage applied will vary in a random manner, on repeated starts or reversals.

It is recommended that the magnitude of switching voltage surge be measured, and steps be taken, if necessary, to adjust the value to approximately 600 volts crest to ground for motors of 110 voltage rating or less, and to 2,000 volts for motors rated 440 volts. It is not important, nor is it practical, to control this overvoltage accurately. It is expected that proper values will always be obtained if normal industrial type magnetic contactors are used, with a time delay in reclosing of 2–5 cycles.

As an alternative to reliance on the overvoltage due to switching—or in addition thereto—a repeated surge impulse voltage may be applied to each motor, immediately following each period of humidity exposure with visible condensation on the winding.

For this purpose, the surge voltage should be applied for a period of one minute to each phase of the motor winding in turn. The magnitude of the voltage surge should be 600 volts crest to ground for motors rated 110 volts, and 2,000 volts crest to ground for motors rated 440 volts, with intermediate values varying linearly in accordance with the equation:

$$\text{Crest voltage} = 150 + 4\ (\text{Rated Voltage})$$

approximately

If the motor does not fail under this check test, it should be immediately returned to the operating and heat-aging cycle, as indicated in the foregoing.

References

1. Test Procedure for Evaluation of Systems of Insulating Materials for Random-Wound Electric Machinery. *AIEE Standard no. 510* Nov. 1956.

2. Test Procedure for Evaluation of the Thermal Stability of Enamelled Wire in Air. *Ibid.*, Jan. 1959.

A Relay-Type Feedback Control System Design for Random Inputs

A. M. HOPKIN
MEMBER AIEE

P. K. C. WANG
NONMEMBER AIEE

EARLIER literature has suggested the design of the so-called optimum relay control system, where the term "optimum" is based on the system having the fastest possible response in terms of reducing the error to minimum following a step or ramp input.[1–4] It has been pointed out that these systems are optimum only in this special sense, and that their response to other types of input may be undesirable.[5]

Attempts have been made to combine predicting devices with the concept of the optimum relay control system to produce systems which possess good response for a large class of inputs.[6–10] The limitation on these schemes is that they become difficult to realize in their given form for systems of an order higher than second, with the result that the concepts have not been carefully explored.

This paper is the report of an attempt to accomplish some further exploration of the possibilities of optimum predictor relay control systems by exploiting a slightly different viewpoint, and to set up a simple model of the system on an analog computer so as to obtain some idea of the behavior of a system in the presence of random inputs.

Basic Assumptions

A relay-type control system can be designed to operate with random input signals if the following assumptions are satisfied:

1. The structure of the input signal and associated noise is such that the input signal can be predicted for a moderate distance into future time in terms of a power series whose term coefficients are functions of the present value of the total input and a finite number of its time derivatives. For the simple noise-free case the prediction function might be in the form of a truncated Taylor's series whose variable would be distance from the present into future time, and whose term coefficients would be present values of the input signal and a finite number of its derivatives.

2. For relay forcing the controlled process response and its $(n-1)$ order derivatives can be adequately described by power series approximations in the time domain.

3. The criterion for satisfactory system behavior is as follows: The system shall operate to reduce predicted error and its $(n-1)$ order derivatives to some small nominal value in a minimum time. The symbol n is the order of the differential equation describing the controlled process behavior.

4. For certain types of controlled processes with oscillatory modes, the magnitudes of error and its various order derivatives are so bounded that only one mode of relay logic is necessary for control. This restriction is placed in this paper only to simplify discussion; it can be removed at the expense of complicating the decision logic required.

The Form of the System

The general form of system operation is shown in Fig. 1, and is as follows. The command signal $v(t)$ is assumed to be made up of two components, a desired signal $r(t)$ and an undesirable noise signal $n(t)$. The total signal $v(t)$ is fed into a composite filter F, which produces signals representing the coefficients of

Paper 59-218, recommended by the AIEE Feedback Control Systems Committee and approved by the AIEE Technical Operations Department for presentation at the AIEE Winter General Meeting, New York, N. Y., February 1–6, 1959. Manuscript submitted November 3, 1958; made available for printing December 8, 1958.

A. M. Hopkin and P. K. C. Wang are with the University of California, Berkeley, Calif.

This report is based on work done as a result of financial support supplied by National Science Foundation Grant *G-1707*.

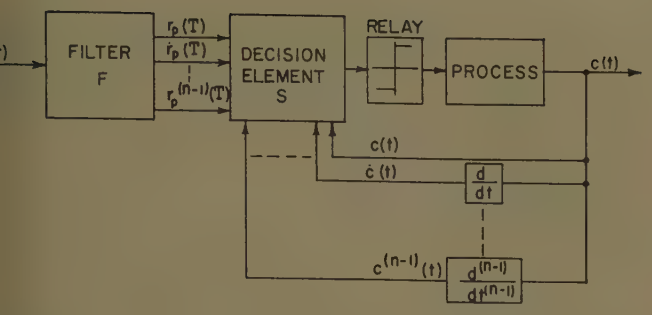

Fig. 1 (left). Simplified control system block diagram

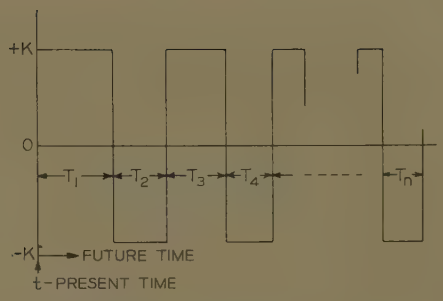

Fig. 2 (right). Relay-forcing function

predicted desired input power series

$$, \tau)=A(t)+B(t)\,\tau+C(t)\,\tau^2+\ldots \quad (1)$$

ere $r_p(t, \tau)$ represents a prediction de at the present time t of the value of t some future time $(t+\tau)$, with τ resenting the prediction time.

With the use of the series form of the dicted values for the desired system onse to maximum forcing in either ction, the predicted switching inter- s $\tau_1, \tau_2, \tau_3 \ldots$ of a relay forcing func- n of the form shown in Fig. 2 can be nputed continuously. Again, the ref- nce for $\tau_1, \tau_2, \tau_3 \ldots$ is always present e t. The system response for future e $c_p(t, \tau)$, may be formulated as a ylor's series, using $c(t)$, $\dot{c}(t)$, $\ddot{c}(t)$, etc., he initial condition values determining series coefficients. The criterion for ermining the switching times is based the fact that at the end of the nth tching interval, the predicted error , $\tau_1+\tau_2+\ldots\tau_n)$, and its $(n-1)$ order ivatives should equal zero. For the es where the resulting equations lead multiple choices of τ_1, τ_2, τ_n, the selec- n must be made to make all of the tching intervals real and positive, and bring the error to zero in minimum e.

he error conditions result in a family quations of the form:

$$+\tau_1+\tau_2+\ldots+\tau_n)$$
$$=r_p(t+\tau_1+\tau_2+\ldots\tau_n)-$$
$$c(t+\tau_1+\tau_2+\ldots\tau_n)=0$$

$$+\tau_1+\tau_2+\ldots+\tau_n)$$
$$=\dot{r}_p(t+\tau_1+\tau_2+\ldots\tau_n)-$$
$$\dot{c}(t+\tau_1+\tau_2+\ldots\tau_n)=0$$

$$^{-1)}(t+\tau_1+\tau_2+\ldots+\tau_n)$$
$$=r_p{}^{(n-1)}(t+\tau_1+\tau_2+\ldots\tau_n)-$$
$$c^{(n-1)}(t+\tau_1+\tau_2+\ldots\tau_n)=0 \quad (2)$$

f assumption 4 is valid there will be witchings and n equations required to cribe a system whose equations of ion are of nth order.

he time τ_1, which represents the time he next relay reversal, is of primary rest. When τ_1 has a value greater n zero, the present switching mode is ect for the moment. When τ_1 als zero, reversal of the relay is called and if τ_1 has only values less than zero, the system is in error, and reversal of the relay is called for. The case where τ_1 has no real solution represents a momentary form of input which the system cannot follow because of its inherent limits. A careful study is necessary to determine the proper switching mode to make the best of this bad situation.

In general a computer can be set up with a decision logic element S to operate on present input and output information in such a way as to strive to bring the predicted future error to some nominal small value in minimum time.

Discussion of a Particular System

A better idea of the considerations involved in designing and operating this type of system may be obtained by considering the particular system shown in Fig. 3, consisting of a linear process such as a simple motor with the Laplace domain transfer function

$$G(s)=\frac{1}{s(Ts+1)}$$

The future time response of the process for a fixed amplitude step forcing of $\pm K$ applied at the present time t is

$$c_p(t, \tau)=c(t)\pm K\tau+ T(\mp K+\dot{c}(t))(1-\epsilon^{-\tau/T}) \quad (3)$$

The predicted response at time $t+\tau_1+\tau_2$ of the same system to a fixed amplitude step-forcing function of $\pm K$ applied at the present time t followed by a step reversal of forcing function to $\mp K$ at time $t+\tau_1$ is given by

$$c_p(t_1, \tau_1, \tau_2)=c(t)+T\dot{c}(t)\pm [K(\tau_1-\tau_2)+KT-2KT\epsilon^{-\tau_2/T}]+ [\pm KT-T\dot{c}(t)]\epsilon^{-(\tau_1+\tau_2)/T} \quad (4)$$

The predicted input for time $t+\tau_1+\tau_2$ is given by

$$r_p(t, \tau, \tau_2)=r(t)+\dot{r}(t)[\tau_1+\tau_2]+ \frac{\ddot{r}(t)}{2}(\tau_1{}^2+2\tau_1\tau_2+\tau_2{}^2) \quad (5)$$

So the predicted error at $t+\tau_1+\tau_2$ is given by

$$e_p(t, \tau_1, \tau_2)=e(t)+\dot{r}(t)(\tau_1+\tau_2)+ \frac{\ddot{r}(t)}{2}[\tau_1{}^2+2\tau_1\tau_2+\tau_2{}^2]-T\dot{c}(t)\mp [K(\tau_1-\tau_2)+KT-2KT\epsilon^{-\tau_2/T}]+ [\mp KT+T\dot{c}(t)]\epsilon^{-(\tau_1+\tau_2)/T} \quad (6)$$

To find the initial values of $e(t)$, $\dot{c}(t)$, $\dot{r}(t)$, and $\ddot{r}(t)$ which must exist to bring the error and error rate to zero simultaneously in time τ_2 after switching, expressions are written for the predicted error and error rate at the switching time $(\tau_1=0)$ and set equal to zero.

$$e_p(t, 0, \tau_2)=e(t)+[\dot{r}(t)\pm K]\tau_2- [\pm TK+T\dot{c}(t)][1-\epsilon^{-\tau_2/T}]+ \frac{\ddot{r}(t)}{2}\tau_2{}^2=0 \quad (7)$$

$$\dot{e}(t, 0, \tau_2)=\frac{\partial e_p(t, 0, \tau_2)}{\partial \tau_2} =\dot{r}(t)\pm K-[\pm K+\dot{c}(t)]\epsilon^{-\tau_2/T}+ \ddot{r}(t)\tau_2=0 \quad (8)$$

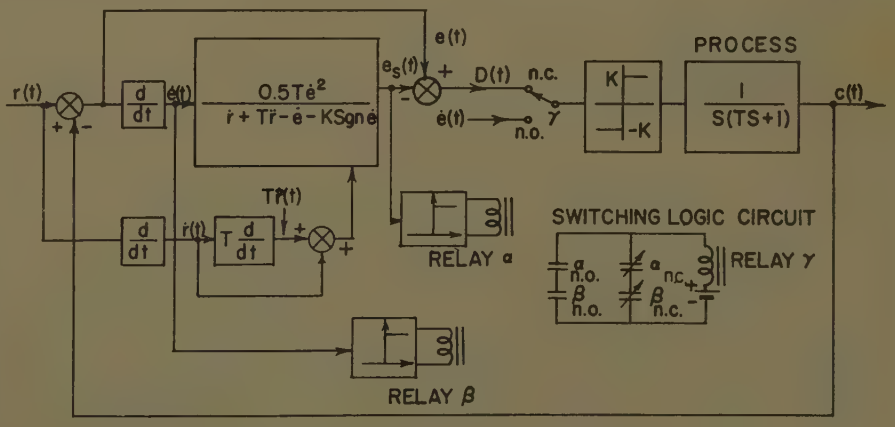

Fig. 3. Block diagram for a particular system

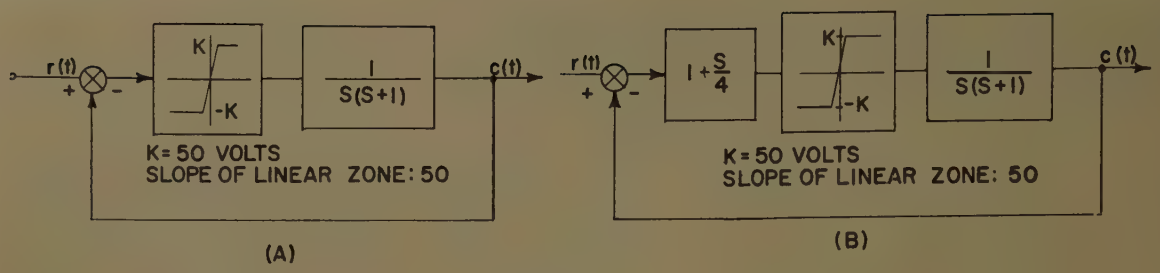

Fig. 4. Motor-p sitioning syste A—System B. B System C

Equations 7 and 8 should then be solved simultaneously to give the desired relationship between $e(t)$, $\dot{r}(t)$, $\ddot{r}(t)$, and $\dot{c}(t)$.

However, because the equations are transcendental, their solution is difficult. This difficulty is removed by making use of assumption 2, and replacing the exponential terms in equations 7 and 8 by the first few terms of their equivalent power series to obtain

$$e_p(t, 0, \tau_2)=e(t)+\dot{e}(t)\tau_2-\left[\frac{\pm K-\dot{c}(t)}{2T}\right]\tau_2^2+\frac{\ddot{r}(t)}{2}\tau_2^2=0 \quad (9)$$

$$\dot{e}_p(t, 0, \tau_2)=\dot{e}(t)-\left[\frac{\pm K-\dot{c}(t)}{T}\right]\tau_2+\ddot{r}(t)\tau_2=0 \quad (10)$$

Equations 9 and 10 can be solved simultaneously to give the switching boundary relationship

$$e_s(t)=\frac{0.5T\dot{e}^2(t)}{[\mp K+\dot{c}(t)+T\ddot{r}(t)]} \quad (11)$$

Equation 11 sets up the boundary relation between the present values of $e(t)$, $\dot{e}(t)$, $\dot{c}(t)$ and $\ddot{r}(t)$ at which reversal of the forcing function should occur. To reduce the number of quantities involved, $\dot{c}$ can be replaced by $\dot{r}(t)-\dot{e}(t)$ to give expression

$$e_s(t)=\frac{0.5\dot{e}^2(t)}{[\dot{r}(t)+T\ddot{r}(t)-\dot{e}(t)\mp K]} \quad (12)$$

Since the sign of the forcing term $\pm K$ is determined by the additional requirements that τ_2 be positive and of minimum duration, it is shown in the Appendix that the sign of $\pm K$ should be chosen to be the negative of the sign of the error rate. Assigning $(-\text{signum } \dot{e})$ as the sign of K, yields

$$e_s(t)=\frac{0.5T\dot{e}^2(t)}{\dot{r}(t)+T\ddot{r}(t)-\dot{e}(t)-K \text{ Signum } \dot{e}(t)} \quad (13)$$

Note that $e_s(t)$ is negative if $([\dot{r}(t)+T\ddot{r}(t)])$ is zero and $\dot{e}$ is positive. However, in general the value of $e_s(t)$ for a given value of $e(t)$ will vary as $[\dot{r}(t)+T\ddot{r}(t)]$ varies.

As shown in the Appendix by use of phase-plane concepts, if $\dot{e}(t)$ and $e(t)$ have the opposite sign and $e(t)$ is greater than $e_s(t)$, then the sign of the forcing $\mp K$, should be positive, and if $e(t)$ is less than $e_s(t)$, then the sign of the forcing should be negative. This suggests the rule: *Apply the forcing function having the sign of* $D(t)=e(t)-e_s(t)$.

The phase plane plots shown in the Appendix demonstrate that tangential intersections of $r(t)$ and $c(t)$ without error overshoot cannot occur for initial conditions $e(t)$ and $\dot{e}(t)$ have the same sign. For these initial conditions the sign of the forcing should be the same si as the error rate. The switching lo can be formalized as follows:

Condition 1: If $e_s(t)$ and $\dot{e}(t)$ have the sa signs, give the system forcing function t sign of $\dot{e}(t)$.

Condition 2: If $e_s(t)$ and $\dot{e}(t)$ have oppos signs, give the system-forcing function t sign of $D(t)$, where

$$D(t)=e(t)-e_s(t) \quad (1$$

Experimental Results

A motor-positioning system of the ty described was set up on the anal computer in order to obtain experiment data concerning its response to vario inputs. This system was called syste A, and is shown in the block diagram Fig. 3.

Two other systems were set up f comparison with system A. One, d ignated as system B, consisted of motor positioning system driven by high-gain amplifier saturating at t levels $\pm K$; see Fig. 4(A). The secon

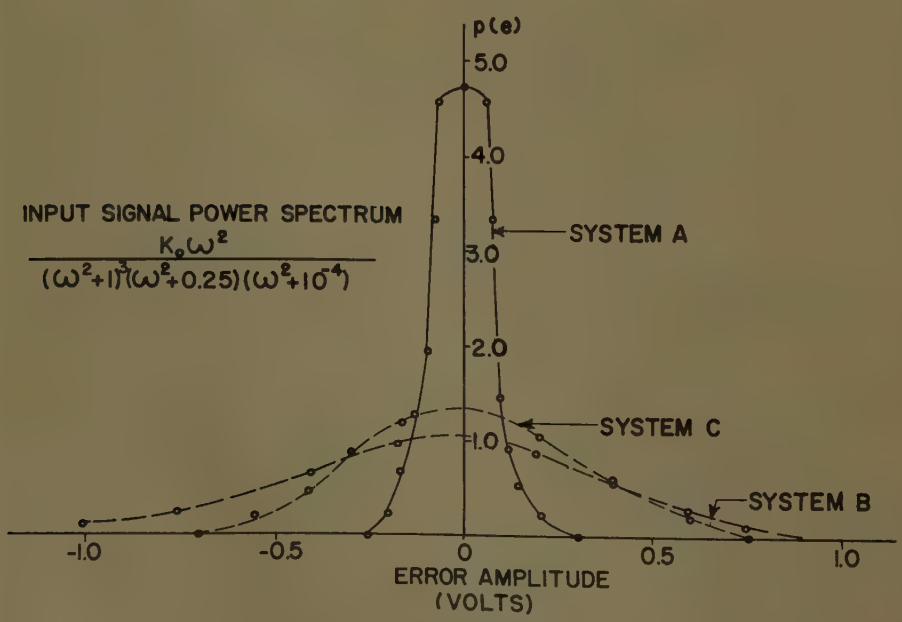

Fig. 5. Comparison of error amplitude probability density curves for systems A, B, and C

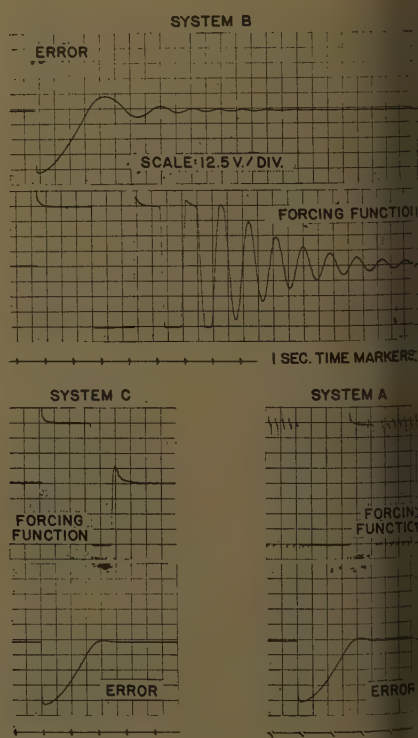

Fig. 6. Step responses of systems A, and C

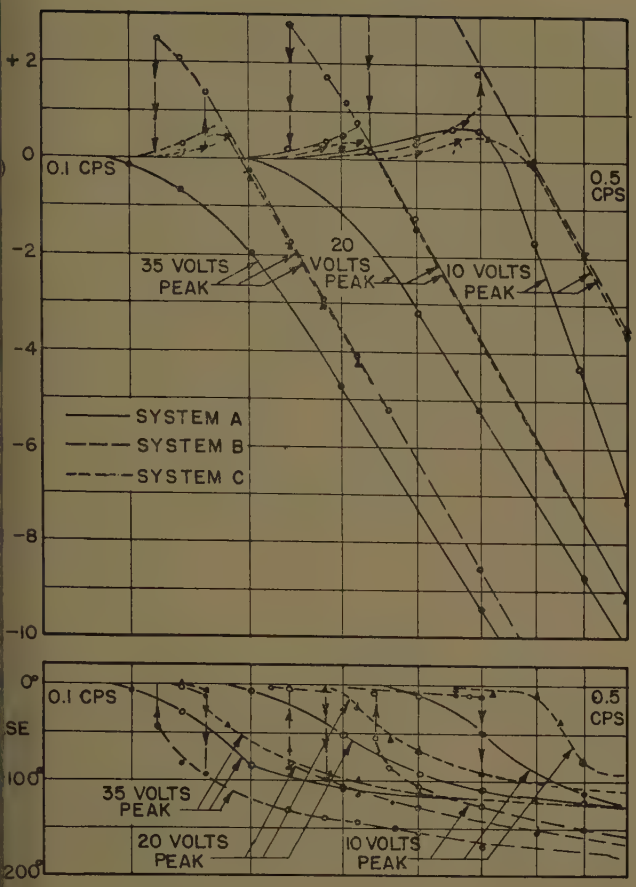

Fig. 7. Frequency response of systems A, B, and C

em *C*, was the same as system *B* pt that the sharply saturating ampli- was preceded by a derivative-com- ating element so adjusted as to give itially the same step response as em *A;* see Fig. 4(B).

ach system was tested by supplying put with a signal generated by pass- he output of a Gaussian random sig- generator through a low-pass filter. type of random test signal was ted because it was considered fairly esentative, and because it was con- ently generated.

ne resulting input and output data recorded and the error amplitude ability density functions were com- d from these data; they are plotted g. 5.

interpreting the error amplitude probability density function curves as a measure of the "goodness" of the system response it must be recognized that the ideal error probability density function would be a unit impulse at the error amplitude of zero, and that, in general, assuming a symmetrical distribution of error about the origin, the control system which produces the narrowest error amplitude probability density function curve for a given random input has the best response. Comparison of the error amplitude density functions of the three systems shows that for the random test inputs the predictor-controlled relay system has a far better measure of behavior than the other two systems.

It is interesting to compare the amplitude density functions of the three systems as given in Fig. 5 with the step responses of these systems as plotted in Fig. 6. This comparison would lead one to suspect that the step response is not necessarily a good measure of the behavior of a nonlinear systems response to a random input.

Frequency response tests were also run for the three systems; the results are shown in Fig. 7. The predictor system behavior was degraded by the response of the prediction coefficient filter at frequencies above those expected in the random input signal.

In general it was felt that test results on the predictor system were good when the predictor was able to predict with reasonable accuracy for a length of time representing the maximum expected value of time τ_2 required to bring the error to zero. This maximum expected time depends upon the nature of the statistical structure of the input signal. When the nature of the input was changed so as to render the predictor less effective, the degradation of system performance was immediately noticed. Fig. 8 shows predicted responses to give some idea of the effectiveness of the prediction scheme used for different Gaussian inputs. For Fig. 8(A)

$$\frac{K\omega^2}{(\omega^2+1)^3(\omega^2+10^{-4})(\omega^2+0.25)}$$

and for Fig. 8(B)

$$\frac{K_0\omega^2}{(\omega+1)^4(\omega^2+10^{-4})}$$

Other Types of Systems

A similar procedure may be used to derive the switching criterion for the case of a relay-driven two-time-constant system with a linear Laplace transfer function of the form

$$G(s)=\frac{1}{(T_1s+1)(T_2s+1)} \qquad (15)$$

The general solution for the system output at time $(t+\tau)$ resulting from a step input of $\pm K$ applied at time t is given by

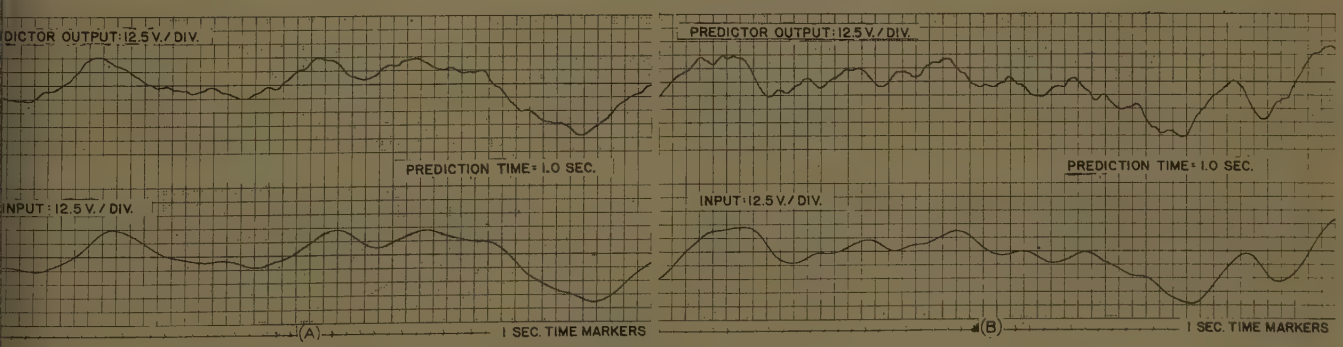

Fig. 8. Response of Taylor series predictor to Gaussian input signal with power spectral density

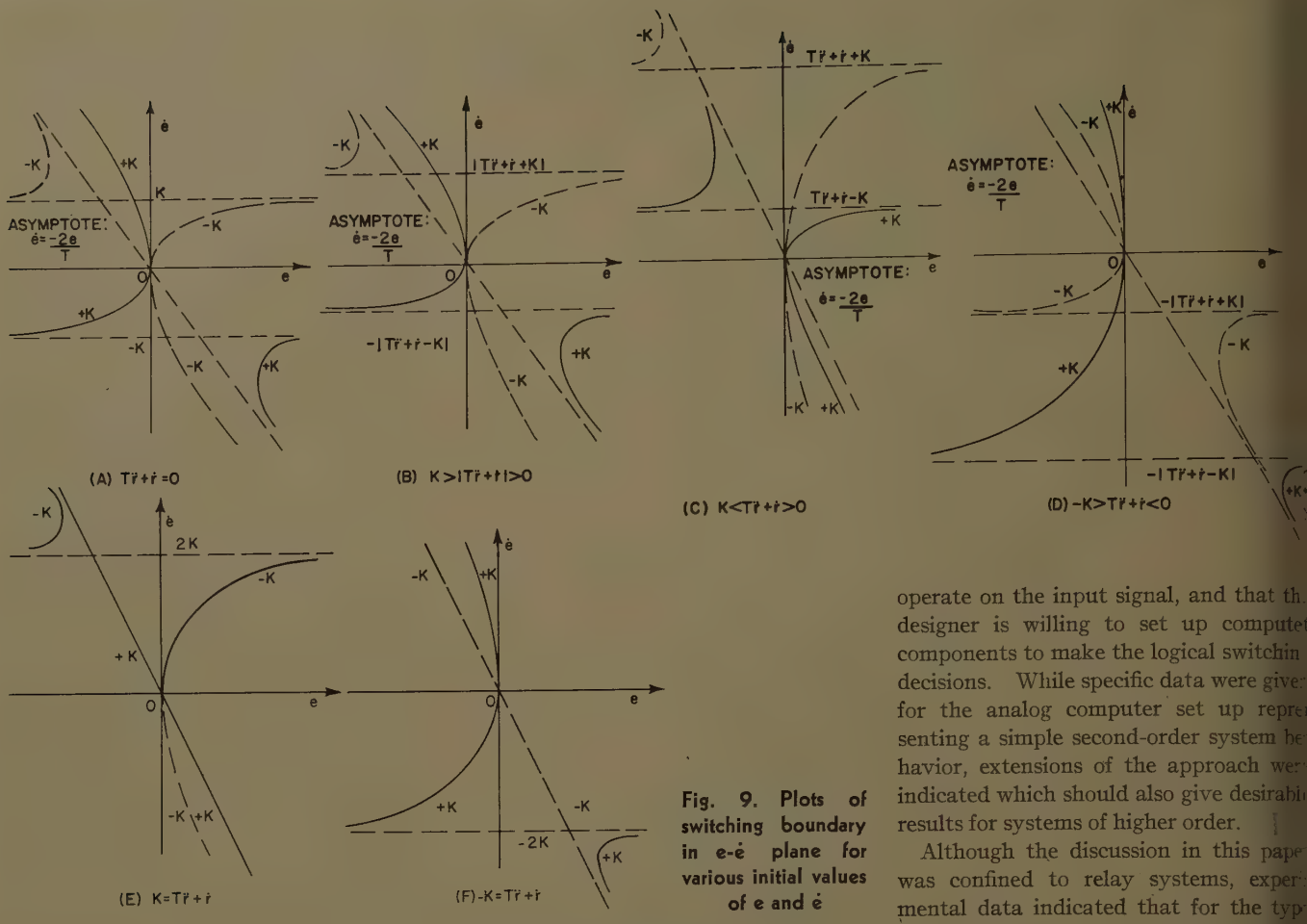

Fig. 9. Plots of switching boundary in e-ė plane for various initial values of e and ė

$$c(t,\tau)=\frac{T_1T_2}{T_1-T_2}\left[\left(\frac{c(t)}{T_2}+\dot{c}(t)\right)\epsilon^{-\tau/T_1}-\left(\frac{c(t)}{T_1}+\dot{c}(t)\right)\epsilon^{-\tau/T_2}\right]\pm K\left[1+\frac{1}{T_2-T_1}\left(T_1\epsilon^{-\tau/T_1}-T_2\epsilon^{-\tau/T_2}\right)\right] \quad (16)$$

The procedure used in the preceding case can then be followed with appropriate choice of ± sign specification to produce positive, real values for τ_2 to give the following switching boundary expression:

$$e_s(t)=-\frac{K\,\text{signum}\,\dot{e}(t)+[T_1+T_2]\dot{e}(t)-I(t)}{2}+1/2\,\text{signum}\,\dot{e}(t)\times\sqrt{[K\,\text{signum}\,\dot{e}(t)+(T_1+T_2)\dot{e}(t)-I(t)^2-2T_1T_2\dot{e}^2(t)} \quad (17)$$

where

$$I(t)=T_1T_2r(t)+(T_1+T_2)\dot{r}(t)+\ddot{r}(t) \quad (18)$$

From this point the switching criterion can be established in a fashion similar to that given in the preceding example.

The general procedure holds also for oscillatory second-order systems. However, the power series expansion is not so accurate, particularly for systems with appreciable damping. The considerations discussed in assumption 4 apply here.

The procedure can be extended to third-order systems and higher. In general the criterion must require that the error and its $(n-1)$ order derivatives be zeroed simultaneously for an nth order system. This usually leads to the assumption of $(n-1)$ reversals of the forcing relay. Writing the n equations implied by this statement, setting the time to the first switching τ_1 to zero in each, and eliminating the remaining $\tau_2, \tau_3 \ldots \tau_n$ variables, will give an expression for the switching criteria.

The procedure is straightforward but it leads to complicated algebra. Only the simplest types of third order system have criteria which can be set up on a small analog computer. However, this approach may have promise when the use of a digital computer is justified.

Conclusions

It was felt that the general experimental results show the possibility of making the relay or saturating type of control systems which are quite effective in following random inputs, providing that an adequate predicter can be set up to operate on the input signal, and that th designer is willing to set up computer components to make the logical switchin decisions. While specific data were give for the analog computer set up repre senting a simple second-order system be havior, extensions of the approach wer indicated which should also give desirabl results for systems of higher order.

Although the discussion in this pape was confined to relay systems, exper mental data indicated that for the typ of random inputs used, systems wit narrow-proportional-band saturating am plifiers operated with the amplifiers i the saturated mode most of the time, an so the mode of operation would be es sentially the same if the amplifier wer replaced by an ideal relay. The philos ophy of control system design outlined i this paper should be of particular interes when other considerations dictate th necessity of using a digital computer i conjunction with the system.

Appendix. Phase Plane Description of Switching Criteria

Since equation 13 represents the cond tion where instantaneous reversal of th forcing function will ultimately bring th system error and error rate to zero simu taneously, it is the expression for th critical switching boundary in the erro error-rate plane; see Fig. 9. It shoul be noted that changing the > sign to a sign in the conditions given in Figs. 9(B and (D) turns the plane over with respe to the e-axis.

Trajectories and boundaries in this plan are sometimes confusing because the syste is not autonomous, i.e., the system has time-varying forcing component in the for of $r(\tau)$. There is also some difficulty i that the mathematical solution allows th physically impossible case where the tim

less than zero. The problem is to select ysically realistic criterion for switching d on equation 13.

he plot of this boundary expression as vn in Fig. 9 is labeled with signs of K, esenting the direction of the forcing tion after switching, i.e., during the od τ_2. In all cases the solution boun- es in the first and third quadrants (where e equals sign $\dot{e}$) represent solutions for itive values of τ_2, so there is no realizable mum switching mode in these quadrants. best mode of operation under these litions is to make the sign of the forcing tion K the same as the sign of e and $\dot{e}$, s to reduce error and error-rate as rapidly possible. In the second and fourth drants there are, in general, two solu- s for the Taylor's series approximation. one which leads to simultaneous zero r and error rate in the minimum time is curve with the maximum magnitude of mponent for a given value of e. Thus, he upper half-plane, only solutions for K) are meaningful, and in the lower half- e only solutions for $(-K)$ are meaning-

nce in the upper half-plane all system ectories move from left to right, with easing time, a $(+K)$ switching boundary des the upper half-plane into two regions τ_1 and $(-K)$ to the left, and τ_2 and K) to the right. Similarly, since all se trajectories in the lower half-plane go right to left, the $(-K)$ switching ndary divides it into two regions with nd $(-K)$ to the left and τ_1 and $+K$ to right. Thus, in all cases the region to right of the appropriate boundary for $(+K)$, and the region to the left for $(-K)$.

he switching criteria just given are d on the truncated series form of expressions for $r_p(t+\tau_1+\tau_2)$, and $c_p(t+\tau_1+\tau_2)$ and are valid only when $(\tau_1+\tau_2)$ is small compared to the time constant. This means that for cases where e_p and $\dot{e}_p$ are large, the switching logic may not be effective.

One may select the appropriate value of $\pm K$ for computing the e_s boundaries by the rule: *Make the sign of K in equation 13 the negative of the sign of $\dot{e}$.* The sign of the actual applied forcing function can be determined by the following rules:

1. If sign $e_s(t)$ = sign $\dot{e}(t)$, make the sign of the forcing function the same as the sign of $\dot{e}(t)$.

2. If sign $e_s(t) \neq$ sign $\dot{e}(t)$, make the sign of the forcing function the sign of $D(t)$, where $D(t)=e(t)-e_s(t)$.

Nomenclature

$r(t)$, $\dot{r}(t)\ldots$ = desired component of input signal and its time derivatives
$n(t)$ = undesirable noise component of input signal
$v(t)$ = actual input signal $v(t)=r(t)+n(t)$
t = present time
τ, τ_1, τ_2 = future time
$r_p(t, \tau)$ = predicted future desired signal at $(t+\tau)$, predicted at time t
$A(t)$, $B(t)$, $C(t)$ = time-varying coefficients
$c_p(t, \tau)$ = predicted future system response at $(t+\tau)$ predicted at time t
$c(t)$, $\dot{c}(t)$, $\ddot{c}(t)$ = present system response and its time derivatives
$e_p(t, \tau)$, $\dot{e}_p(t, \tau)$ = predicted system error $r_p(t, \tau)-c_p(t, \tau)$, and its time derivative
S = decision logic element
T, T_1, T_2 = system time constant
$e_s(t)$ = time-varying switching boundary value of $e(t)$
signum (x) = sign of x
$D(t)$ = time-varying switching function $D(t)=e(t)-e_s(t)$

References

1. A Phase-Plane Approach to the Compensation of Saturating Servomechanism, **Arthur M. Hopkin.** *AIEE Transactions*, vol. 70, pt. I, 1951, pp. 631–39.

2. Nonlinear Techniques for Improving Servo Performance, **D. McDonald.** *Proceedings*, National Electronics Conference, Chicago, Ill., vol. 6, 1950, pp. 400–21.

3. An Investigation of the Switching Criteria for Higher Order Contactor Servomechanisms, **J. Bogner, L. F. Kazda.** *AIEE Transactions*, vol. 73, pt. II, July 1954, pp. 118–27.

4. Differential Equations with a Discontinuous Forcing Term, **D. W. Bushaw.** *Report no. 469*, "Experimental Towing Tank," Stevens Institute of Technology, Hoboken, N. J., Jan. 1953.

5. A Differential-Analyzer Study of Certain Nonlinearly Damped Servomechanisms, **R. R. Caldwell, V. C. Rideout.** *AIEE Transactions*, vol. 72, pt. II, July 1953, pp. 165–70.

6. A Predictor Servomechanism, **N. C. Walker.** *M. S. Thesis*, University of California, Berkeley, Calif., 1953.

7. A Taylor's Series Approach to the Design of a Predictor Servomechanism, **G. F. Aroyan.** *M. S. Thesis*, University of California, Jan. 1957.

8. Feedback Control Systems (book), **O. J. M. Smith.** McGraw-Hill Book Company, Inc., New York, N. Y., 1958, pp. 505–603.

9. Optimum Design of Final Value Control Systems, **R. G. Booton.** *Proceedings*, Symposium on Nonlinear Circuit Analysis, Microwave Research Institute, Polytechnic Institute of Brooklyn, New York, N. Y., vol. XI, 1956.

10. Final Value Controller Synthesis, **M. V. Mathews, C. W. Steeg.** *Transactions*, Professional Group on Automatic Control, Institute of Radio Engineers, New York, N. Y., vol. PGAC-2, Feb. 1957, pp. 6–16.

Detector Car History and New Developments

H. W. KEEVIL
NONMEMBER AIEE

HE rail detector car is an assemblage of specialized test equipment mounted elf-propelled railroad cars and is used the detection of all types of defects develop in railroad rails. The y of detector cars should start w years before there were any such . Before 1926, the railroads were d with a serious and fast-growing ace to their very life: the breaking of . The source of this menace was the sverse fissure, a very thin crack h would start within the rail and lop outwardly until it caused the to break.

areful rail failure records showed that if a rail developed one transverse fissure the probabilities were that there would be one or more additional fissures in the same rail. Thus if one fissure broke it would create additional strain on the rest of the rail which would then cause the rail to break at the other fissures. This, of course, caused a very dangerous condition because parts of the rail might fall completely out of track. These fissures starting within the rail and developing outward gave no sign of their presence until the rail actually broke.

It is interesting to note that through joint research by the AAR (Association of American Railroads) and the rail manufacturers the cause of the transverse fissure was determined. It was found to be a shatter crack which is formed in the steel as it cools after rolling. By a new controlled cooling process put into service in 1938, these shatter cracks have been eliminated and rail since that date has been practically free of transverse fissures.

Fig. 1 shows large, well-developed transverse fissures. This is the type of defect that was instrumental in the development of detector cars. There are other types of defects that develop in rail which can be detected and removed from track before the rails fail.

Fig. 2(A) shows various sized vertical split heads. This defect is a longitudinal crack that may be a few inches to a full

Paper **59-267,** recommended by the AIEE Land Transportation Committee and approved by the AIEE Technical Operations Department for presentation at the AIEE–American Society of Mechanical Engineers Railroad Conference, Chicago, Ill., April 7–9, 1959. Manuscript submitted June 5, 1958; made available for printing February 9, 1959.

H. W. Keevil is with the Association of American Railroads, Chicago, Ill.

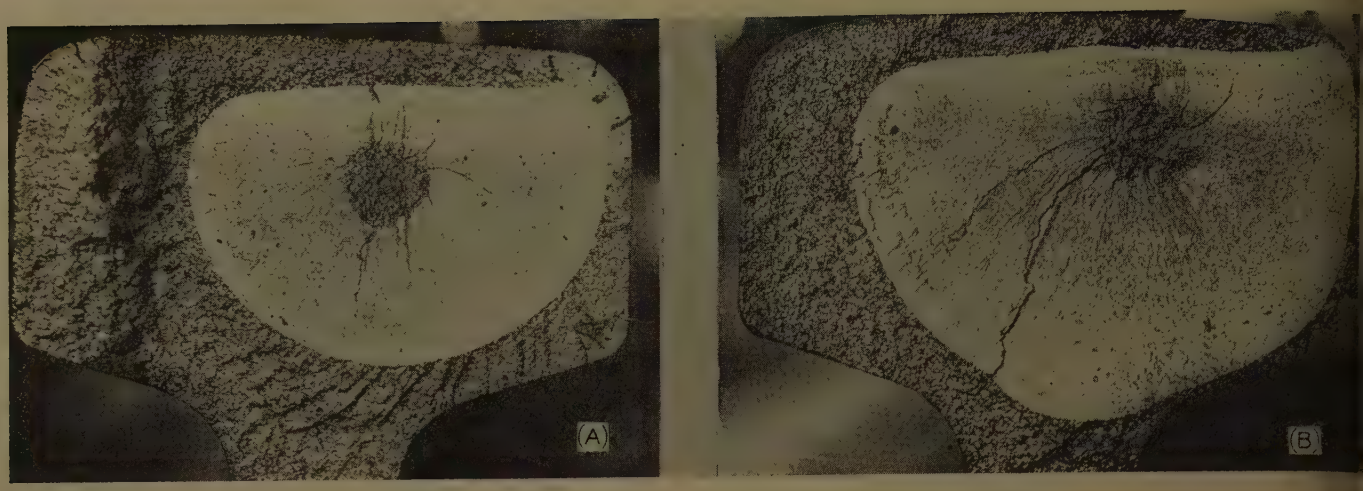

Fig. 1. Large, well-developed transverse fissures

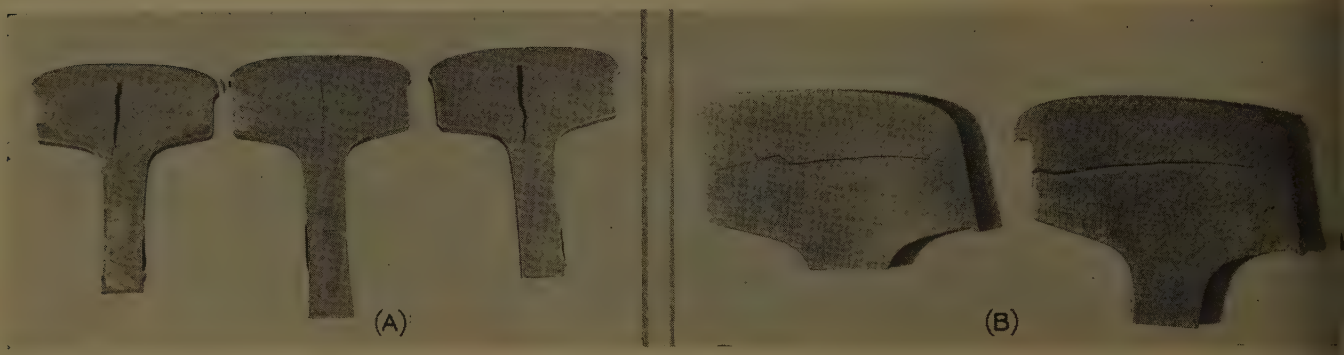

Fig. 2. A—Vertical split heads. B—Horizontal split heads

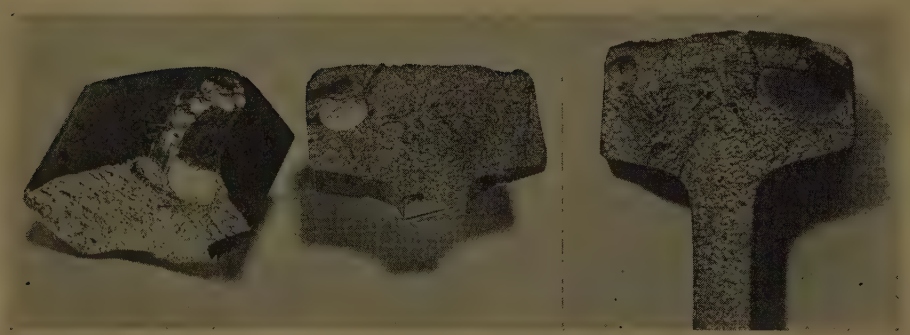

Fig. 3. Example of shell fractures, which usually start at edge of rail

Fig. 5. Butt weld failure developing in g
pressure butt weld: this progressive fractu
caused by small inclusion

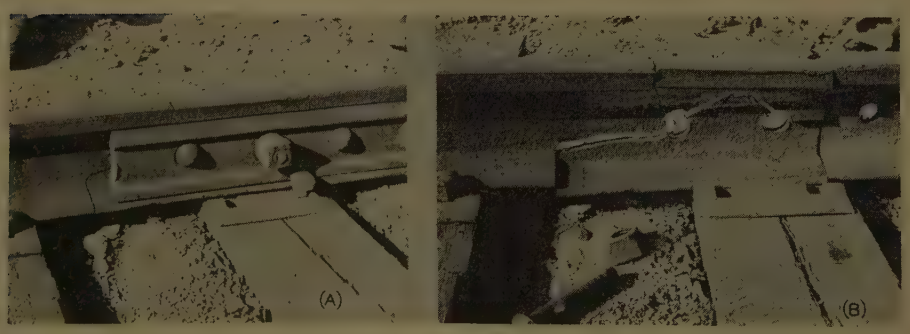

Fig. 4. A—Bolt-hole breaks, which can progress in all directions. B—Same joint, angle bars removed

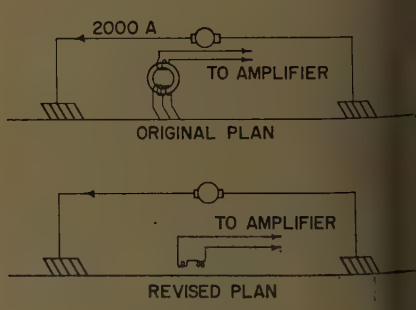

Fig. 6. Electro-inductive system: origin
plan for drop-of-potential detection

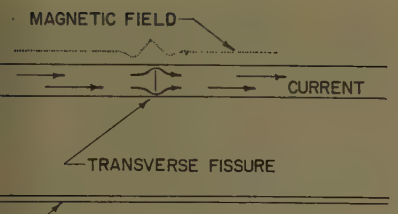

7. Magnetic field produced by rail current

in length. The crack causes the of the head to break off.

g. 2(B) shows a similar defect known horizontal split head because the k is a horizontal plane. This de- may also progress along the rail any length. The great danger here at the defect may turn either upward ownward and progress until it breaks rail.

ig. 3 shows progressive fractures ch usually start in a little shelling he edge of the rail. This type of ct is on the increase and has re- ed the transverse fissure as the most us type of defect.

ig. 4(A) is another serious defect ch is usually found in older rail. This k starts in a bolt hole and can pro- s in all directions. Fig. 4(B) shows same joint after the angle bars were oved. The danger here is that a ing train may kick the top piece ly out of the joint, thereby causing tural derail.

g. 5 shows the latest type of defect ch develops in a gas pressure butt . The small inclusion was the e of this progressive fracture.

s may be seen, there was real need for a flaw detector. In 1926, W. C. Barnes, neer of tests on the Rail Committee e AAR, was delegated to investigate and all possible means of detecting e defects before the rails failed.

A promising means of detecting internal rail fissures was suggested by Dr. Elmer A. Sperry, of gyroscope fame. He proposed passing a current through the rail longitudinally and measuring the drop of potential between two fixed points. This system was tried in the laboratory and proved successful. For use on a car he proposed using three contacts on the rail which would thus give two equal voltages as long as the contacts were on good rail. These two voltages were opposed so as to produce a balanced input to an amplifier. This automatically balanced out the effect of any fluctuation of the current in the rail but if a set of the contacts bridged a fissure the two current-resistance drops were unbalanced, and thus there was an impulse fed to the amplifier and recorded.

Mr. Barnes recommended that the AAR finance the development and the building of the first detector car by Dr. Sperry. The recommendation was approved and the car was scheduled to be completed by December 1927. The car construction was proceeding well by November 1927, and it was moved to a New York Central Railroad shop for completion and testing.

When car operation was attempted, it was found that there were many difficulties to overcome. One of the major difficulties was the inability to obtain and maintain perfect contact on the top of the rail. It had been thought that the top surface of the rail would be bright, clean, and easy to contact. This proved to be just the opposite of what actually existed. The rail surface, while it may look bright and clean, actually has, in most cases, a hard film of dirt and oxide rolled on it.

Many months were spent trying to devise some means of maintaining good contact on the rail. All of this work was

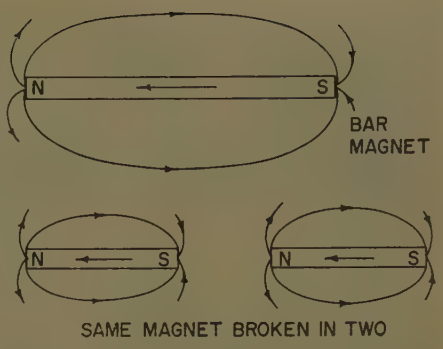

Fig. 9. Basic magnetic principle: magnetized rail showing defect sets up local poles, detectable above rail

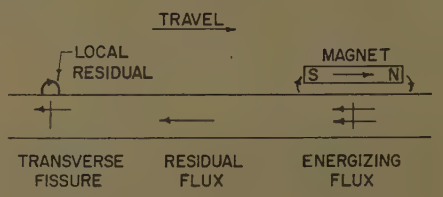

Fig. 10. Principle of residual magnetic detection: progressively magnetized rail produces detectable local fields at points of defect

Fig. 11. First residual magnetic detector car, 1936

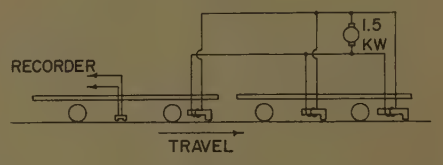

Fig. 12. Principle of first successful residual magnetic detector car

Fig. 8. First electro-inductive detector car

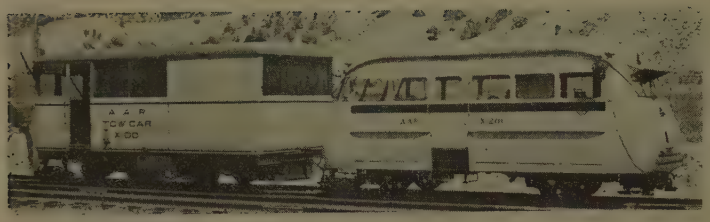

Fig. 13. One of 14 successful residual magnetic detector cars; all still in use

of no avail because as soon as pressures were made great enough to cut through this film, thermal voltages were produced that far exceeded the potentials that were to be picked off the rail. Finally the drop-of-potential method was given up and it was decided to try a pair of balanced induction coils as pickup. A pair of these were built in the summer of 1928 and tried out on the car. This experimental test showed that fissures could be detected by a pair of coils working above the rail in the field created by the heavy current in the rail.

Fig. 6 shows the original plan for the drop-of-potential detection, and the induction system that finally proved successful. This change of pickups changed the whole method of detection. Instead of picking a drop of potential off the rail, the pickup coils generated voltages when they passed through any distortion in the magnetic field that surrounded the rail.

Fig. 7 is a crude representation of the magnetic field strength above the rail containing a transverse fissure. This distortion of the magnetic field is due to the change in the direction of the heavy current as it passes around the defect.

It took several months to build the new induction pickup, and revise the amplifiers and associated equipmen In November 1928, one year late, th Association car was ready for roa testing.

Fig. 8(A) shows the AAR car approx mately a year after it had originall started working. Many changes an improvements had to be added to mak it operate successfully. Fig. 8(B) show the main brush carriage, set betwee wheels, which contacted the rail and als carried the induction pickups.

This car, while successful, operate under many difficulties, so Mr. Barne and the writer were engaged by the AA to develop an improved flaw-detecto car that did not conflict with patents i the art owned by others. During ex perimentation, it was discovered that transverse fissure could be magnetize with a small permanent magnet, and residual field left after the magnet wa removed.

It has been demonstrated in physic that a bar magnet, when broken i two, produces two magnets. In th case of the rail, it was magnetized and there was a defect present, local pol

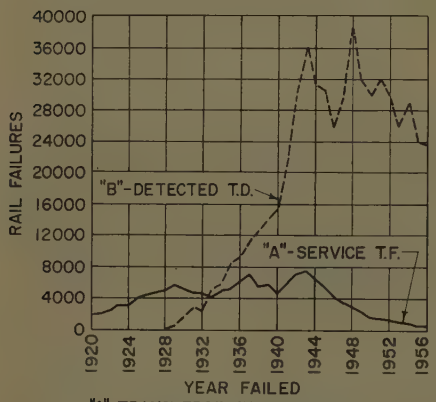

Fig. 14. Results of rail testing in U.S.: Annual service rail failures due to transverse fissures and detected transverse defects as reported by all railroads

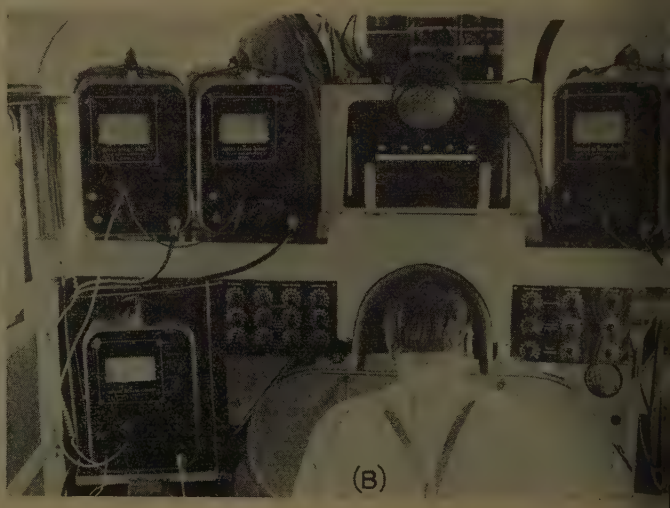

Fig. 15. A—German ultrasonic detector car. B—Cabin and monitors. C—Crystal carriage and housings

. 16. A—ATSF ultrasonic detector car, operable on track or on highway. B—Detail: one vertical probe used for in-joint detection

Fig. 17. AAR residual magnetic detector car, recently rebuilt with modern test equipment

re set up which were detectable above rail; see Fig. 9.

Fig. 10 illustrates the principle of idual magnetic detection. The rail progressively magnetized and a strong idual flux is left within it. At points defect small local fields are produced tside the rail. The local field can be tected and recorded. This discovery s checked and demonstrated to various lroads. The building of the first idual magnetic detector car was then thorized.

Fig. 11 shows the first residual mag-ic detector car, which was put on road in 1936, and promptly failed to tect transverse fissures. It was de-mined that a single U-shaped magnet, en though very strong, would not ve a fissure magnetized. It was also termined that a single magnet of any ape would not magnetize a small nsverse fissure. From these experi-nts it was learned that three magnets re needed and that they should be haped with a high rear pole. This was obviate any strong vertical flux the leaving end of the magnet. To get three magnets over each rail, it was necessary to go to two cars instead of the original one. This was done by borrowing the tow car from the induction-type car. With two cars it was possible to put three L-shaped magnets over each rail. This combination was the first successful magnetic detector car.

Fig. 12 shows the principle of the first successful residual magnetic detector car; and Fig. 13, the actual cars used for this development. This car was so successful that a number of railroads requested the AAR to build cars for them. A total of 14 cars was built: 12 for the railroads and 2 for leasing service, all of which are still in regular testing service.

After these residual magnetic detector cars had been in service for some years, the Telewald Company developed another type of magnetic car, using what was termed "sustained-field" detection. On this car the pickups were carried behind the last magnet but close enough so that some of the leakage flux passed through the pickups. The test results and operating problems were very similar to those of the AAR's residual magnetic system. Two of these cars were built and are now owned by a western railroad.

The basic job of the AAR Detector Car Service is the development and construction of improved test equipment. This includes the installation of such equipment on railroad-owned cars and the Association's help in the operation and maintenance of this equipment. The construction and installation of new, much more powerful magnetizing equipment has recently been completed on all except one of the road cars.

Fig. 14 shows the results of all rail testing in the U. S. An all-time high record of both detected and service failures was recorded in 1943, after which there has been a very rapid decline of both. With the extensive testing program and the use of controlled cooled rail since 1938, the transverse fissure service failure has been practically eliminated. Most defects are now detected; these are various forms of progressive fractures such as shell fractures, engine burn fractures, detail fractures from gage check, etc.

For the future, another new system of detection is indicated: this is the ultrasonic method which is quite well developed in Germany. Fig. 15(A) shows the German Federal Railway ultrasonic detector car; (B), the ultrasonic recording camera and monitors; and (C), the ultrasonic crystal carriage and housings.

This car was built by the German Federal Railways and uses one vertical, two 30-degree and two 70-degree crystals to detect all types of rail defects. The car records photographically on a 35-millimeter paper tape. With this type of recording they are not limited to slow-speed testing but can operate up to 40 miles per hour very successfully. The one drawback with this type of recording is that the tape must be developed, dried, and then analyzed. After the tape is analyzed, word must be sent out to the road men advising them where the defects are located. This means a delay of about 5 days between the time the car runs over the track and when the defective rails are actually removed. The procedure is quite different from the testing procedure in this country. Here the railroads want to know immediately if the rail is defective because, if it is, they want to replace it before another train goes over it.

Fig. 16(A) illustrates an ultrasonic type of rail-flaw detector car developed by an engineer of the Atchison Topeka & Sante Fe (ATSF) railway system. Fig. 16(B) shows a detail of the Sante Fe car, which uses only one vertical probe on each rail, thus detecting horizontal-split heads, vertical-split heads and bolt-hole breaks in joints. This in-joint detection is its strong point because the ultrasonic method can test in the joint areas with no difficulty. The Sante Fe car is built in a "hi-rail" truck, i.e., it can operate on the track or on highways. By taking to the highway considerable time can be saved running to and from tests.

The Southern Pacific Railroad now has a similar car The Sperry Company is also working on an ultrasonic car and is now operating, as an experimental car one of their regular induction type cars on which is installed a vertical probe ultrasonic unit. This again is principally for the detection of cracks within the joint areas.

The AAR is now in the process of developing a miniaturized embodiment of the residual magnetism type of rail-flaw detector car. It will have flanged wheels for operation on the railway track, and also pneumatic tires by means of which the vehicle can be moved on highways. It is estimated that substantial economies can be effected by operation of a car of this type.

Fig. 17 shows the AAR *X201-X203* which has recently been rebuilt and on which is installed all of the latest type of test equipment. The improved magnetizing and test equipment has greatly improved both the speed of operation and the efficiency of the testing.

Discussion

Robert H. Webb (Sperry Rail Service, Danbury, Conn.): I should like to compliment Mr. Keevil on his description of the rail defect detector car. The purpose of this discussion is to elaborate on the developments made in the field of railway quality control by explaining some of the results of Sperry Rail Service research in this area. We believe that this research over the last 30 years has resulted in significant technical progress in the safety of American railroads.

As a point of departure from Mr. Keevil's historical discussion, the voltage drop method of rail defect detection should not be overlooked. While, indeed, the potential drop technique proved unsuccessful for dynamic testing due to the rail surface condition described, this technique has been employed by Sperry as well as other known induction and magnetic test cars over the past 30 years for the confirmation and classification of defects located by any of the dynamic systems. The size of transverse defects can be determined quite accurately by this measurement.

From the conception of a successful means for rail defect detection by Dr. Elmer A. Sperry in 1927 and 1928, our company has continuously invested in research and development toward the refinement of equipment and techniques for this vital service. H. C. Drake, Sperry research consultant, was recognized by the Franklin Institute award for his contributions to these developments. As the name implies, Sperry Rail Service provides on a contract basis a

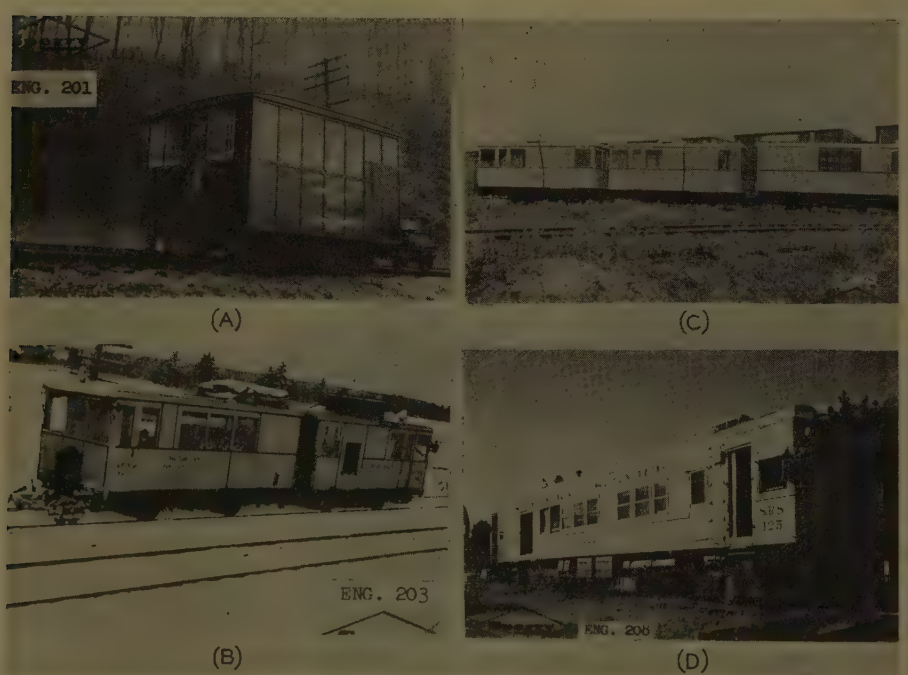

Fig. 18. Early designs of Sperry detector car. A—Single unit. B—Double unit. C—Triple unit. D—Current diesel electric-propelled car

Fig. 19. Current design of commercial test service

Fig. 20. Ultrasonic rail joint inspection ca

g. 21. Special unit designed to negotiate severe subway grades

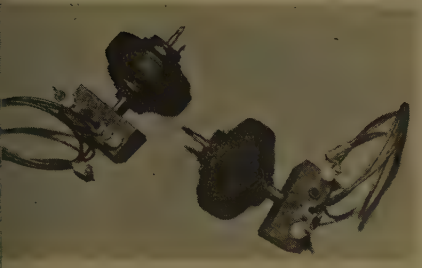

g. 22. Small, flexible tires housing various angle transducers, as sensing devices

ality control inspection; it covers cur-ntly over 15),000 miles of North American ilways per year.

In briefly reviewing our progress toward il safety I should like to show that the mplexion of the Sperry detector car has anged significantly since 1928. Fig. 18 ows the development of early designs of uipment transported in small vehicles of gle, double, and triple units; see Fig. (A), (B), and (C), respectively. The esent diesel electric-propelled car, shown (D), represents our increasing require-ment for improved service has yielded more complex equipment to pace the expansion of the railroad industry and its attendant increased tonnage hauls through the years.

Providing the industry with a reliable commercial test service calls for rugged dependability which has been embodied in current design; see Fig. 19. Unitized construction, with transistor circuitry where practical, lends itself to optimum performance, ease of crew training and operation, and reduction of nonproductive time through quick change-out of the various equipment modules.

Industrial ultrasonic inspection equipment has been one of our standard product lines since 1944. In 1947 and 1948, experiments were conducted to determine the applicability of ultrasonic techniques to rail inspection. Particular areas of interest were the structurally joined rail ends. Cracks issuing from bolt holes as well as rail head and web separations eluded effective detection by the induction method because of the confused magnetic pattern set up in the joint area by the induction equipment. Research led to the development of the ultrasonic rail joint inspection car (Fig. 20) capable of detecting and evaluating bolt-hole cracks and head-web separations with uncanny accuracy. This service was made available in early 1950 and our present fleet stands at 13 cars, including three special units designed to negotiate the severe grades in subways; see Fig. 21.

We are at present installing ultrasonic rail detection equipment in our fleet of 15 induction cars for service; the first car was completed in July of this year. Resulting from 5 years' research and development, one element of this apparatus detects transverse defects occurring in the rail head, while another element detects bolt-hole cracks and head-web defects comparable to the service provided by the small ultrasonic car previously described. Small, flexible tires housing the various angle transducers are the

Fig. 23. New York transit system car, 1959

sensing devices for this system; see Fig. 22. These combination induction-ultrasonic cars will provide complete end-to-end rail testing with attendant rail safety not heretofore enjoyed.

As an adjunct to this newly developed equipment, a small portable ultrasonic hand test unit has been designed for defect confirmation and classification. This advance over the potential-drop method permits evaluation of defects under severe surface conditions caused by engine drive wheel burns, slivers, and what is known as shelly rail. The device has important implications, not only in the improved quality of test, but in increased production rates for the fleet.

It should be pointed out that, in 1954, Sperry made cross-licensing agreements with the Krautkramer Company in Germany, the company responsible for the advances in ultrasonic rail defect detection mentioned by the author. One of the principal purposes of this was a mutual exchange of technical information, a major concern being that of rail defect detection. In late 1957, Sperry representatives informed the American Railroad Engineers Association Rail Committee that we intended to bring such a car into the United States for demonstration to American railroads. At this writing, this car was expected to be delivered in August of 1959, to be placed into operation in the New York transit system; see Fig. 23.

luminum Bus for Shipboard Application

G. J. THOMPSON
MEMBER AIEE

S. H. BEHR
ASSOCIATE MEMBER AIEE

HERE is special interest in aluminum for shipboard use because of the ings realized in weight and because of rtages in copper that occur especially times of national emergency when pbuilding is at its peak. Although minum has been considered for cable nductors for shipboard use it is gener-y without over-all advantage because larger conductor size results in a ater volume and weight of insulating d sheathing materials. These factors olving insulation are not imposed in lying aluminum to electrical bus. In lizing aluminum bus for switchgear plication problems arise that are mostly but not entirely confined to the making of satisfactory electric connections. The literature on the subject contains a large body of information. Much effort is devoted to coping with a particular environmental stress or material property considered to predominate in the reliability of a specific system. Some of the work stresses the advantage of a proprietary material or a particular method. Instances of controversy are attributed largely to differences of conditions of evaluation and as such appear best capable of resolution by re-evaluation on the same basis. The rather extreme conditions and their wide variety in shipboard service justify additional evaluation. A comprehensive experimental investigation was therefore carried out to determine the optimum means of utilizing aluminum bus in switchgear with the primary objective of long-term service reliability. Measurements taken on large numbers of specimens determine the extent to which different types of aluminum joined by various bolting methods, and with joint surfaces prepared with various joint compounds, are affected by prolonged load cycling, overload, weather-

Paper 59-654, recommended by the AIEE Marine Transportation Committee and approved by the AIEE Technical Operations Department for presentation at the AIEE Middle Eastern District Meeting, Baltimore, Md., May 19–21, 1959. Manuscript submitted January 19, 1959; made available for printing March 19, 1959.

G. J. THOMPSON and S. H. BEHR are with the New York Naval Shipyard, Brooklyn, N. Y.

The opinions or assertions contained in this paper are the private ones of the authors and are not to be construed as official or reflecting the views of the Naval Service at large.

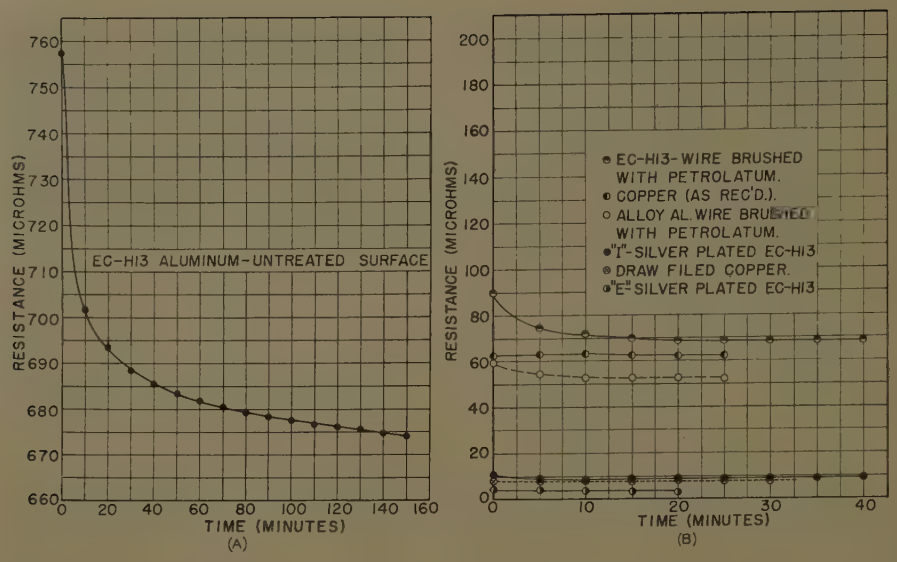

Fig. 1. A—Joint resistance at 3,000 psi. B—For copper and prepared aluminum bars

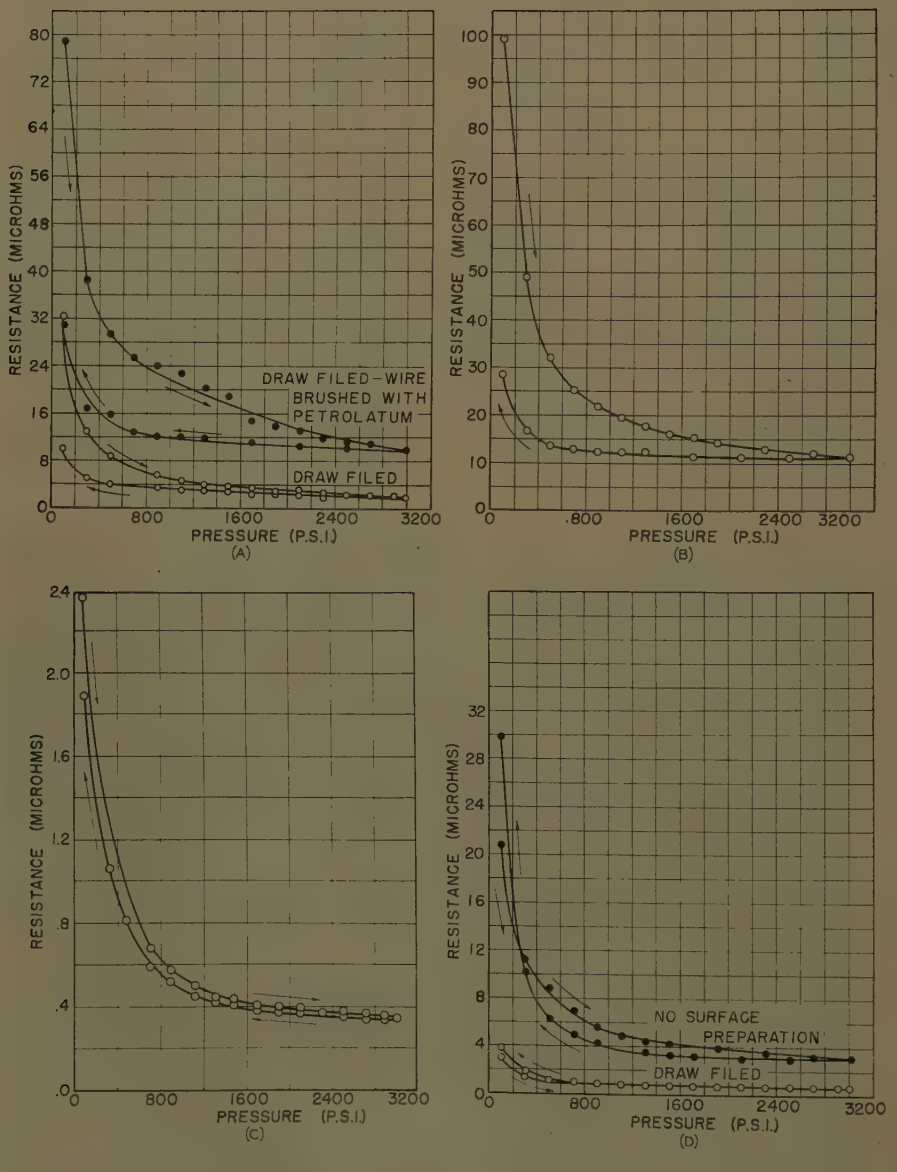

Fig. 2. A—Joint resistance versus pressure: EC-H13 aluminum. B—EC-H13 aluminum wire-brushed with joint compound. C—EC-H13 aluminum silver-plated surface. D—Copper bars

ing, vibration, and high impact shock similarly tested is the extent to which silver platings are affected. Measurements on an actual marine installation after 20 years of service are correlated with the results of experimental laboratory work. In addition, information is provided which is useful in the design of bus supports needed to withstand fault currents.

Measurements on Stacked Bars

Measurements on specimens of typical joints were preceded by studies of the variation of joint resistance under carefully controlled mating pressures. This was done on stacks of bar material by the method previously employed by Denault[1] and others.[2] Electrical aluminum bus of two grades of hardness was used. The softer grade is commercially known as EC-H13 aluminum bus conductor. The harder grade is an aluminum magnesium silicide alloy bus conductor[3] which is hereinafter termed "alloy bus." The stacked bar technique consists essentially of measuring the series resistance of a number of flat specimens held together at various steps of constant pressure. Each setup consisted of eleven $1^1/_2$- by 1- by 1/4-inch specimens of electrical aluminum of the same grade with the blocks arranged to cross each other at right angles so as to form ten mating surfaces of one square inch area each. Pressure on the stacked specimens was maintained by a well-sealed hydraulic press and the resistance was measured by a Kelvin double bridge using a current of 10 amperes to minimize heating effects. The value measured included the resistance of the aluminum material as well as the joint resistance. The resistance of the body of aluminum in the stack is between 2.7 and 3 microhms. Figs. 1 and 2 accordingly show the average resistance of one joint and the material in one block.

An indication of the extent of heating effect of current on resistance measurement was gained from measurements of joint resistance on stacks of uncleaned aluminum bars while the current was increased from 10 to 50 amperes. Joint pressures used varied from 2,000 to 8,000 psi (pounds per square inch) in 1,000-psi increments. Below 4,000 psi there was a progressive increase in resistance with current. The rate at which resistance increased with current was greater at lower than at higher pressures. At 4,000 psi the resistance rose less than 1.0% as the current was increased from 10 to 50 amperes; at 2,000 psi the rise was about 4%. Although

urements were made rapidly to nize temperature rise, the increased ance is nevertheless attributed to an tected temperature rise of the actual ct points which are of very small and which exist in smaller numbers wer joint pressures than at higher. result of this exploratory work equent measurements were made at mperes, which was also a convenient nt for the Kelvin bridge employed.

easurements made on stacked blocks ntreated EC-H13 aluminum under tant pressure show a change of tance with time. Joint resistance ped 7% of initial value 10 minutes applying 3,000-psi joint pressure continued to diminish, tapering off to 1% drop in 2½ hours, as shown in 1(A). Additional evidence shows tantial stabilization in 3 or 4 hours. is attributed to creep of the alumi- The deformation results in the uction of an increase in the number size of actual contact areas within mating surface, as the oxide layer is en through, thus progressively low- the joint resistance until further of the metal has ceased.[4] This onstrates the necessity of stipulating time interval between application of pressure and the making of resistance surements. Subsequent measure- s indicated that resistance stabiliza- could be achieved earlier with less ee of change and at lower values when er pressures were employed. Meas- ents of this nature, as shown in Fig. on draw-filed copper bars and on r-plated[5] aluminum bars indicate little change of resistance with time. inum bars, that had been brushed and coated with petrolatum, ex- ed a lowering of resistance with time, ming substantially stabilized after 10 tes. Where applicable thereafter, resistances reported are those meas- 10 minutes after application of pres- During the making of measure- s at 1,000 psi it was observed, cularly for low resistance, that joint tance varied as much as four to one een different adjacent blocks within stack. The variability existed to a er extent at lower pressures. In her experiment the blocks were re- ged within the stack and the resist- of the stack varied about 20% in ials. Such variability is due princi- to joint-mating surface condition o a much lesser extent by instrument ation. At stack resistances of over icrohms the variability is almost ely due to joint surface variation. figures reported herein are for an average of ten joints, which tends to minimize the effect of this variability.

The effect of relaxation of pressure on joint resistance is shown in Fig. 2(A), which is the result of measurements on stacked bars of draw-filed EC-H13 aluminum. Joints made on petrolatum-coated aluminum bars are shown in this figure to exhibit only about a 25% rise in resistance when joint pressure is relaxed by as much as 75%. It is further observed that the slope of the resistance versus pressure curve is significantly greater when the pressure is being increased than when it is being decreased. This was found to be generally characteristic of joints made with unplated EC-H13, the relatively softer grade of aluminum. This is demonstrated by Fig. 2(B). Virtually no difference was found between slopes for ascending and descending pressures for compound brushed joints of the harder alloy aluminum, copper, or silver-plated aluminum of either of the two grades of hardness. Fig. 2(C) illustrates this effect. Fig. 2(A) shows the insulating effect of petrolatum on joints made on EC-H13 aluminum. The film insulating effect was found so much more serious with silicone grease as to preclude its consideration as an inhibitor. Further measurements showed no significant differences in joint resistances between silver-plated EC-H13 surfaces whether they were coated or not coated with petrolatum. Repeating this type of test on unplated EC-H13 showed an increase in joint resistance of about five times when the surfaces of the same blocks were coated with petrolatum. Electrodeposited silver has a Vickers hardness pyramid number of 100 as compared to 38 for a specimen of EC-H13. This suggests that the "high points" on the harder silver mating surface may be more effective in shearing through the petrolatum film than the high points of the softer EC-H13 aluminum. Figs. 2(C) and (D) both show relatively low resistance and, in addition, show a narrow spread between curves for increasing and decreasing pressure. Figs. 2(B) and (C) indicate that the resistance of silver-plated joints in the region of 100 to 500 psi is between one tenth and one fiftieth that of compounded joints, and that at these low pressures the silvered joint resistance is less than is generally exhibited by compounded joints at 1,800 psi. This means that a joint of acceptably low resistance can be made with silver-plated bars at a fraction of the bolting torque required for compounded joints. While this does not furnish a basis for condoning the use of a loose or mechanically inferior joint, it does suggest the extra margin of electrical integrity offered by the silver-plated joint. Mechanical disturbance of a joint, incidentally, may be considered to produce no deleterious effect unless it progressively loosens the joint as motion between mating surfaces introduces a wiping action which tends to reduce resistance as described by Xenis.[6] The measurements of resistance change with decrease of joint pressure tend to show that retightening connections on aluminum bus does not decrease joint resistance to the extent that measurement of mechanical relaxation of joint pressure may seem to indicate.

A comparison of the resistance of various types of joints may be made from the results of measurements on stacked bars. Table I is an excerpt of resistance of the various joints at 1,800 psi, a joint pressure approximating that exerted by a single

Table I. Joint Resistance at 1,800 PSI, Microhms PSI

Bus Material	Contact Surface Preparation	Manufacturer Designation	Resistance
EC-H13	silver-plated	*E*	0.4
		F	0.4
		G	0.4
		H	0.7
		I	1 3
		J	0.6
		*	0 6
Alloy bus	silver-plated	*K*	0.6
Copper	no preparation		3.0
Copper	draw-filed		0.6
EC-H13	wire-brushed with compound	*L*	11.0
		M	1.0
		N	6.1
		O	3.0
		P	12.5
	wire-brushed with no compound		3.0
	wire-brushed with petrolatum		25.0
	wire-brushed with silicone grease		400
Alloy bus	wire-brushed with petrolatum		10.0
EC-H13	no preparation		310
Alloy bus	no preparation		110

* Matlab Navshipydnyk.

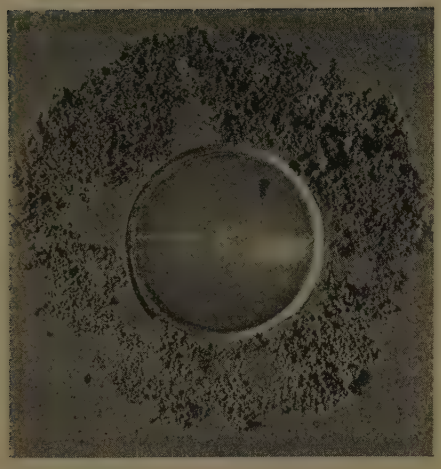

Fig. 3. Pitted contact area

1/2-inch steel bolt torqued to 50 pound-feet on a 2-inch lapped, 2-inch wide bus. Table I shows that there is very little variability of resistance of joints silver-plated by different plating processors. The resistance of silver-plated joints was several times lower than was general for compound treated joints. Silver-plated aluminum produced about the same joint resistance as draw-filed copper. The figures shown in this table may also be compared to the resistances of bus joints in an old installation made by the technique of abraiding the joint surfaces under an inhibiting compound. The installation had been in service aboard ship for about 20 years when the measurements were made. Resistances of 20-year old joints chosen at random were found to be between 0.5 and 300 microhms per square inch. By comparison with the figures in Table I these old connections obviously ranged in resistance from that of the lowest practicably attainable to that resulting from total lack of contact surface preparation.

Cycling Tests

When the effects on joint resistance of the creep of the material and the type of surface preparation had been observed, an operational evaluation in the form of load cycling was undertaken. The load cycle[7] consisted of sufficient current to obtain a 35 C (degrees centigrade) bus temperature rise above a 50 C ambient for 2 hours followed by a shutdown period of cooling at about 25 C for 1 hour. All specimens were subjected to 1,000 such cycles followed by 10 cycles at 125%, 150%, 175%, and 200% of the previous load current. Each specimen consisted of a 3-foot section of 2- by 1/4-inch aluminum bus. Each group of specimens consisted of four 3-foot sections connected in series with three identical single-bolt joints. All groups were connected in series to a low-voltage power source. These were mounted in the same plane in a controlled ambient chamber, each group being isolated from the radiant heat of the adjacent group by baffle plates of thermal insulation. Materials constituting the specimens were as follows:

EC-H13 aluminum bus: 61% International Annealed Copper Standard, tensile strength 17,000 psi.

Alloy bus, aluminum magnesium silicide: 55% (copper standard), tensile strength 29,000 psi, represented by three different manufacturers.

Silver-plated aluminum bus: zincate plating process as produced by six different manufacturers.

Copper bus, electrical grade.

Joint compounds, five different manufacturers.

Aluminum alloy bolts and nuts coated with waxy lubricant: 5/8 inch, 11 threads per inch with $1^{3}/_{4}$-inch-outside-diameter aluminum washers.

Galvanized steel bolts and nuts: 1/2-inch, 13 threads per inch with galvanized steel washers, Belleville type spring washers rated at 6,600 pounds flattening force.

Steel spring lock washers; for 1/2-inch bolt, medium size.

Types of joint mating surfaces included the following:

As received (no preparation).
Draw-filed.
Wire-brushed.
Wire-brush through joint compound.
Silver-plated.

Bolting methods at 50-pound-foot tightening torque included the following:

Galvanized steel bolt and nut with flat steel washers.

Galvanized steel bolt and nut with flat steel and split spring lock washer.

Galvanized steel bolt and nut with flat steel and Belleville-type spring washer.

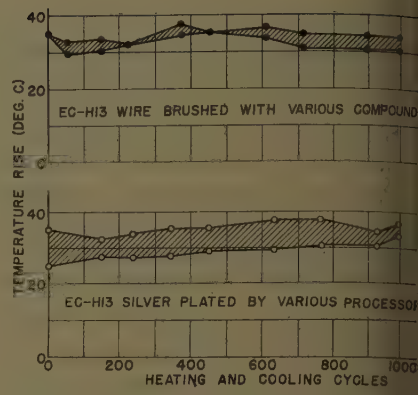

Fig. 4. Full-load temperature rise of joi

Aluminum bolt and nut with two flat al minum washers.

All joints were made with a 2-in overlap and held with a single bolt. Tw thermocouples were cemented on each b connection for temperature measur ments. Millivolt drops were measur between points 4 inches apart across ea connection. Load cycling, together wi ambient temperature cycling of the cha ber was automatically controlled, and te peratures were automatically recorde D-c loading was substituted for a-c loa ing at intervals to facilitate measureme of millivolt drops of the connections.

To study the behavior of poorly ma connections, the effect of load cycling w observed on joints made without surfa treatment. In a few instances the joints exhibited small temperature ri and low resistance, showing that it m be occasionally possible to secure an a parently satisfactory joint without prop preparation. This circumstance is a tributed to a favorable, although ha hazard, degree of abrasion of the oxi film during the assembly of the conne tion. Most of each of the other join made without surface preparation e hibited wide reversals in trends of resis

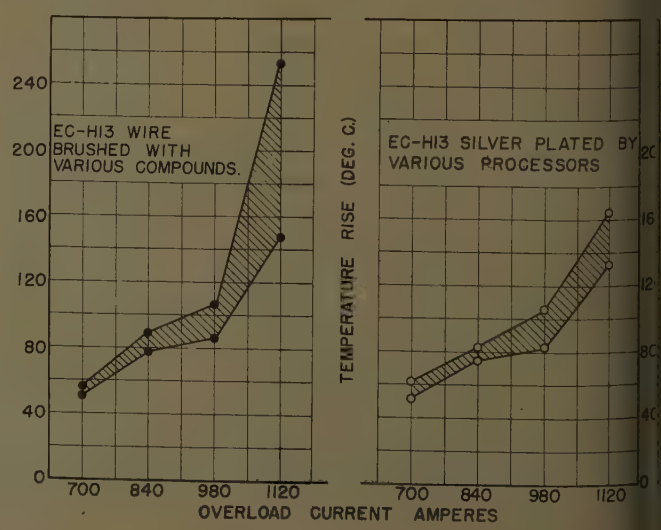

Fig. 5. Overload temperature rise of joints

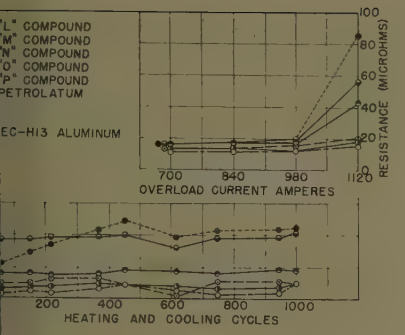

6. Resistance of wire-brushed compounded joints

and temperature changes during ng, which may indicate mechanical rbance caused by load cycling. After) cycles of loading as described, erature rises ranged from 40 to 175 C joint resistances ranged from 20 to microhms. Load cycling of these y made joints synthesized the so- d "runaway" condition caused by nteraction of resistance and tempera- which progressively deteriorates the , culminating in destructive tempera- rise. One mating surface of such a is shown in Fig. 3. Joints like this consistently found to produce higher erature on a-c than on d-c loading. ng, particularly at the start of the cycle, led to the disclosure that the s which were being formed at the face were less substantial if they had formed by alternating current than irect current. This resulted in a r resistance during the passage of nating current.

e extent to which temperature rise resistance is reduced by the various ods of preventing the formation of film is shown by the results of load- ng well-prepared joints. Tempera- rise ranged from 25 to 38 C and resist-

Fig. 7. Resistance of silver-plated joints

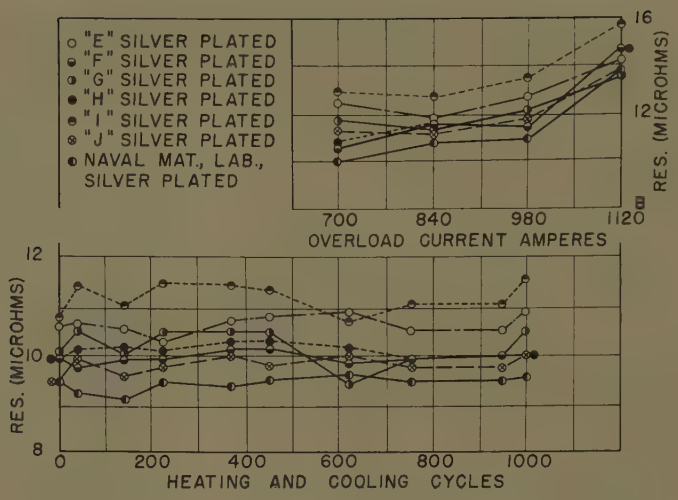

ance ranged from 9 to 15 microhms. Fig. 4 shows that temperature rises of silver-plated and compound-prepared joints fastened with a steel bolt, flat washer, and dished spring washer are of the same order. Overload cycling shown in Fig. 5 shows that the silver-plated joint runs only slightly cooler at the most extreme overload employed. Figs. 6 and 7 were drawn with an expanded ordinate scale for the purpose of maintaining the identity of the results for each type of joint. This has the effect of exaggerating the swings in resistance. It is observed that the compounded joints under cycling are generally about 15% higher in resistance than the silver-plated joints and that this difference tends to widen as overload cycling is applied. Furthermore, both the load cycling and the overload cycling show that compound-prepared and silver-plated joints are stable. Cycling tests were made on a wide variety of combinations of bolting methods applied to both EC-H13 and alloy aluminum bus. The results of only a few of these combinations are shown in Figs. 8 and 9. All joints appear stable and differences between joint temperatures and resistance are not wide enough to rule out any material or method. The simplest form of connection, that of the steel bolt and nut with flat washers, when used on alloy aluminum bus, maintained a relatively low resistance and temperature rise throughout load and overload cycling. The cycling results indicate no significant advantage attributable to any of the various forms of springs used on alloy aluminum bus.

Joint Pressure Relaxation

Neither joint temperature nor resistance change during the load cycling employed is a completely reliable measure of the extent of the joint pressure relaxation which can be expected with aluminum bus. Earlier it was demonstrated with stacked aluminum bars that joint resistance change is not a direct measure of joint pressure change. Therefore, to find joint pressure relaxation, torque measurements were made on connection bolts

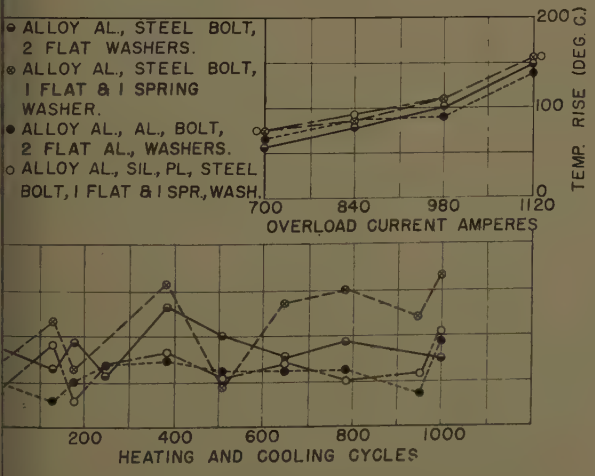

. 8. Temperature rise of joints: various bolting methods

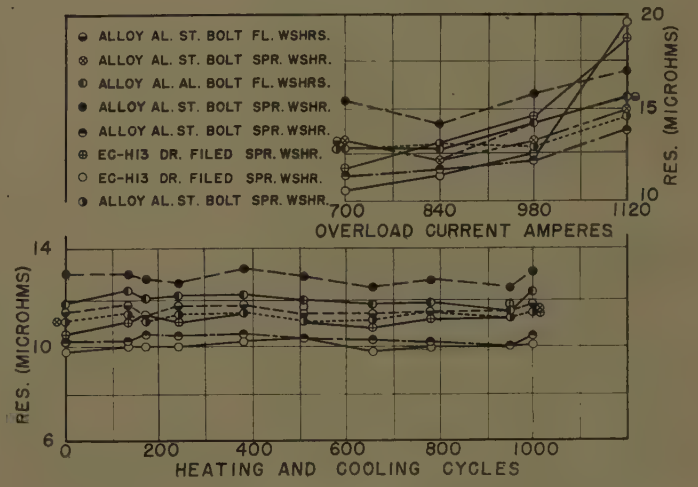

Fig. 9. Joint resistance: various bolting methods

Table II. Bolting Method: Original Torque 50 Pound-Feet

Type of Aluminum	Joint Fasteners: Type of Bolt	Joint Fasteners: Components	Torque, Pound-Feet: After 1,000 Heating Cycles	Torque, Pound-Feet: After 1,000 Heating Cycles and Overload
EC-H13	1/2-inch steel	spring, 1 flat washer	29	16
		spring, 2 flat washers	26	4
		1 flat washer	45	10
		2 flat washers	27	2
		split lock and flat washers	20	3
	5/8-inch aluminum	2 flat aluminum washers	50	32
Alloy	1/2-inch steel	spring and 1 flat washer		77
		2 flat steel washers		51
	5/8-inch aluminum	2 flat aluminum washers		102

before and after load cycling. It is recognized that torque measurement includes friction as well as pressure components which are related and not readily separable. It is assumed, however, that friction will not decrease unless pressure decreases, so that diminished torque can be attributed to diminished pressure under the bolt head. As shown in Table II, there are instances of increases in torque above the originally applied torque. These inconsistencies, which are due to the nature and the material of thread surfaces, to the lubricant, and to the nature of the nut face, have been investigated and described by Pickel.[8] Despite such limitations, torque measurements were found to coincide with other indications of pressure relaxation. Table II shows that the cycling used to effect changes in joint resistance and temperature rise caused reductions in torque whenever EC-H13, the softer grade aluminum, was used with steel bolts; this was true regardless of attempts to compensate for unequal coefficients of thermal expansion. Neither the Belleville type of spring washers nor split-lock washers showed any superiority over flat washers in preventing loss of joint pressure as measured by torque after heat cycling. Spreading the bolting pressure over a wider area by using two large, flat washers with Belleville-type spring washers was equally ineffective in this respect. With the single exception noted, the torque after 1,000 heating cycles relaxed to approximately half the original values. It is likely that, even with such reduction in contact pressure, satisfactory joint resistance could be maintained, because joint resistance increases at a very low rate while the joint is undergoing considerable reduction in pressure, as has been previously shown in studies on stacked bars. After overload cycling, the torque on all steel bolts joining EC-H13 grade aluminum relaxed to 10% or 20% of the original. The corresponding contact pressure produces a joint which is likely to have excessive resistance and to be considered unreliable. The use of the aluminum alloy bolt (the next size larger than steel, according to current commercial practice), with an aluminum nut and flat aluminum washers, produced no torque relaxation after 1,000 heat cycles and a reduction of about 30% of the original after overload cycling. Where the alloy bus (which is the harder grade of aluminum) was used, there w no relaxation of torque after overl cycling, regardless of bolting method. determine whether maintaining joints elevated temperature produced the sa effect on connection bolt torque as peated cycling, joints made with b grades of aluminum and with steel a aluminum bolts were oven-heated to C for 16 hours and torque was remeasu afterward at room temperature. Ta III gives the results of the average of specimens for each connection. Th results show that connection bolt tor responds to a single temperature cha between room temperature and 150 C a similar manner to repeated heat cycli Where the harder grade aluminum (al bus) is used no relaxation of torque indicated, even without spring washe as contrasted with the results wh EC-H13, the softer grade aluminum, used. Torque measurements, taken an indication of contact pressure, sh that the choice of the type of alumin bus as well as the bolting method depe on the temperature and the temperatu range of operation. Joints made w the harder grade aluminum appear ca ble of withstanding a wider temperatu variation than those of the softer gra Fig. 10 shows the effect of temperature relative hardness of EC-H13 and al bus aluminum. This figure is based short time exposure to elevated tempe tures. Longer periods of time at lo

Table III. Effect of Heat on Connection Bolt Torque: Original Torque 50 Pound-Feet

Bolting Method: Type of Aluminum	Bolting Method: Type of Bolt	Bolting Method: Type of Washer	After Heating Cycles, Pound-Feet
EC-H13	Steel	Flat	25
Alloy	Steel	Flat	55
EC-H13	Aluminum	Flat	62.5
Alloy	Aluminum	Flat	93.0

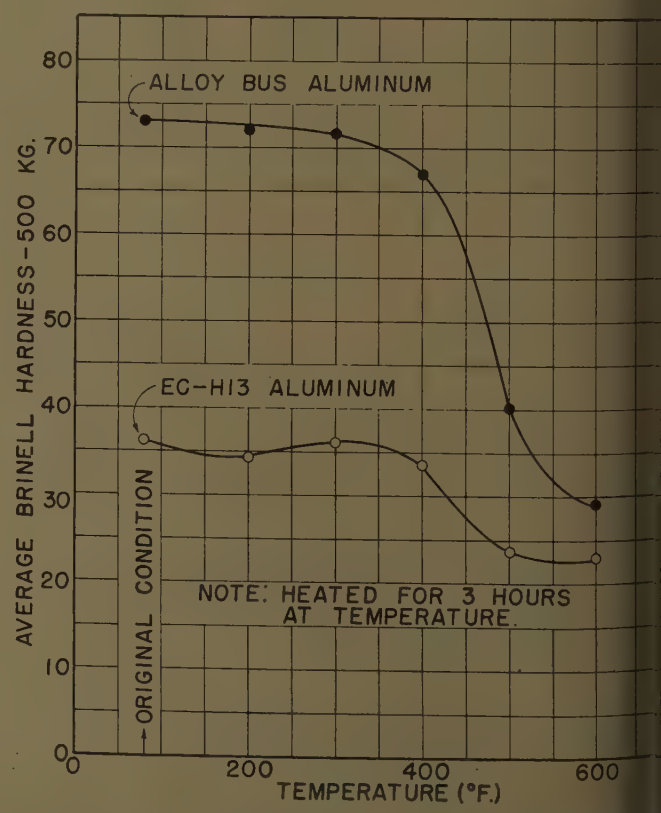

Fig. 10. Change of hardness in alumi-

Fig. 11. Corrosion test specimens

peratures may be expected to produce milar effect.

rosion Effects

hort specimens of aluminum bus with ped joint connections representing the des of aluminum, bolting methods, and es of contact surface preparation em- ved in the load cycling tests, were mbled and mounted on a weathering facing due South and also facing the an. The rack is at a seaside location ond the immediate New York City an area which provides wide tempera- variation with time of day and sea- salt-laden air and wind-driven sand rain. This is an extreme condition xposure. Fig. 11 shows the severity corrosion displayed by typical joint imens exposed to this weathering for ut $1\frac{1}{2}$ years. Periodic measurements oint resistance were made over the osure period. Table IV shows median ues of the results of several of the joints ed. Examination of the detailed re- s shows that the joint resistance does change uniformly with exposure time. ts exhibiting resistance increases at end of $1\frac{1}{2}$ years in the order of ten es original show a higher rate of in- se in resistance after 1 year than dur- the first 12 months. Cleaned dry ts held with aluminum bolts show less tance change than those held with l bolts. Dry joints of all types in- se in resistance to a much greater nt than joints protected by a coating oint compound. The greater joint rioration observed when steel bolts and washers were used is partly attributed to the physical weakening of the joint by the partial disintegration of the steel. The wax-coated aluminum bolts and washers suffered no appreciable deterioration even when fastened to silver-plated bus. These results generally confirmed those of Connor and Wilson,[9] indicating the superior stability of silver-plated aluminum joints.

Short-Circuit Tests

The difference in mechanical properties between present electrical grade aluminum alloys and copper suggests the need of bus supports and spacers especially suitable for aluminum bus work. Space conservation aboard ship generally requires closer spacing between phases than is customary in industrial practice. This in turn produces greater electromagnetic forces for the same short-circuit currents than those occurring with wider spaced bus. To determine the extent of bus deformation, bus structures of EC-H13 and alloy bus were set up and subjected to 3-phase short circuits corresponding to the short-circuit capability of the installation contemplated. Each phase consisted of two 3- by 1/4-inch aluminum bars 1/4 inch apart. Center-to-center spacing between phases was 3 inches and 7/8-inch glass melamine supports were spaced at various intervals of from 6 to 24 inches. Table V shows the maximum permanent deformation for each spacing produced by a 3-phase 60-cycle 100,000-ampere short-circuit current of 5 cycles duration. Figs. 12 and 13 show the bus structures

Table IV. Effect of Seaside Weathering on Joint Resistance of EC-H13 Aluminum: 1/2-Inch Galvanized Steel Bolt, Belleville, and One Flat Steel Washer

Type of Surface Preparation	Resistance, Microhms					
	Initial	Results, No. of Months Later				
		3	6	9	12	15
No preparation; no protective compound	15	45	65	72	70	88
Silver-plated joints; no protective compound	5	10	10	10	19	60
Compounded joints	7	9	7	7	7	9

before and after imposing the fault current. It is recognized that the measurements of deformation shown in Table V are taken from bus distortions resulting not only from the magnitude of current and bus spacing but depending on the time of current interruption. For this reason the action was observed by means of high-speed motion pictures taken at 2,000 frames per second. These pictures showed actual contact and arcing between sections of bus bars of adjacent phases which later appeared completely separated, following the current interruption. Table V is to be taken only as an approximation of what can be expected as a result of such a short circuit.

Vibration and Shock Tests

Vibration, which is generally more prevalent and severe aboard ship than in industrial plants, is a condition that was considered as having possible effect on the reliability of bolted aluminum bus bar connections. Accordingly, specimens of 2- by 1/4-inch aluminum bar connection were mounted on a vibration machine table with 15 inches between supports, and with the bolted connection mid-way between supports. The specimen was vibrated in the planes of both major and minor axes with an amplitude of 1/16 inch (total excursion of 1/8 inch) for 2 hours. The frequency of vibration was varied

Table V. Maximum Permanent Deformation in Inches of Bus Following 3-Phase 60-Cycle 100,000-Ampere Short Circuit

Type of Aluminum	Support Spacing, Inches, Center to Center						
	6	8	12	15	18	21	24
EC-H13	0		3/4	3/4	3 1/8	1 3/4	support broken
Alloy	0	0	1/4	5/4	2 3/8	5 1/2	

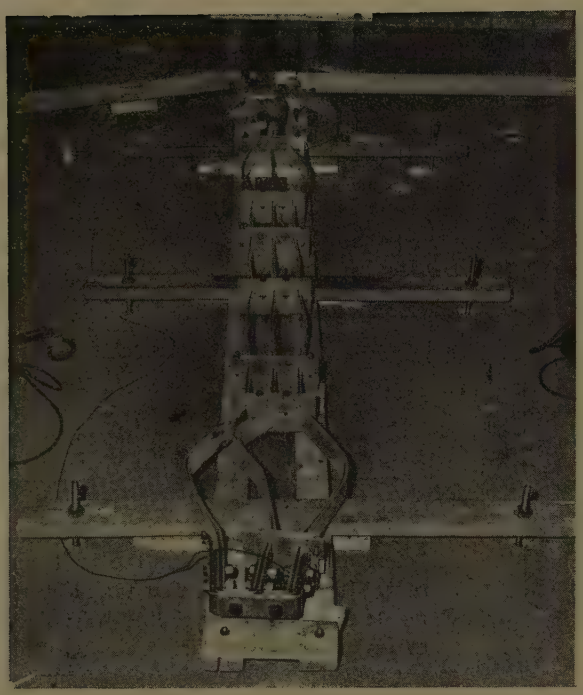

Fig. 12 (left). EC-H13 bus after 3-phase 100,000-ampere short circuit

Fig. 13 (right). Alloy bus after 3-phase 100,000-ampere short circuit

from 10 to 55 cycles per second and back to 10 cycles per second each minute. The electrical resistance of the joint and the bolt torque of each specimen were measured before and after the 2-hour vibration period. Four specimens of each connection were subjected to vibration. Aluminum bolts and steel bolts with and without spring washers were used in connecting both grades of aluminum. There was no evidence of loosening after vibration. Joint resistance decreased in all cases, indicating that vibration may have produced sufficient additional flow to increase the number of joint interface contact points, but with too small a loss of contact pressure to be detected by torque measurements.

There was some concern about aluminum bolts breaking under high-impact shock because of the general practice of tightening to within 80% of the ultimate strength. Two specimens of 2- by 1/4-inch EC-H13 aluminum bus joined with 5/8-inch aluminum bolts were bolted at the ends to the high-impact shock machine specified in reference 10. The specimens were mounted with 15 inches between supports, the joints being positioned mid-way between supports. The 2-inch surface of the bus faced the direction of impact blow. The connections were subjected to five 2,000-foot-pound blows. There was no significant change in connection bolt torque and no permanent deformation of the bus bars.

Conclusions

The choice of aluminum bar material, contact surface preparation, bolting method, and joint protection depends upon the nature and severity of the service for which the installation is intended. It is concluded that an aluminum bus installation in a protected inboard location aboard ship should include the following features:

1. The use of aluminum magnesium silicide alloy, which is preferable to the softer EC-H13 aluminum as bus conductor because bolted joints made with it are more electrically stable and it has greater resistance to deformation under fault currents within a bus structure.

2. Silver plating of the entire bus by the zincate process after forming and punching, which is preferable to compound brushed joint preparation because the joint on silver-plated bus has lower resistance. The resistance is lower than that of a compounded joint, even when the bolting pressure is but a fraction of that required for a compounded joint, thereby ensuring a greater margin of electrical integrity. In addition, the quality of connection is obviously more uniformly controlled, with resulting improvement in reliability.

3. Coating of the silver-plated joint surfaces with a joint compound before assembly, which is an effective measure of insurance against long-time corrosion effects.

4. The use of one or more steel bolts and nuts with flat washers, which is sufficient to maintain effective joint pressures when it is used with aluminum alloy bus. Retightening of bolts is generally unnecessary.

5. Bus support and bracing against fault currents required for alloy aluminum bus, which is substantially the same as required for copper bus of equal current-carrying capacity.

The investigation also furnished information applicable to the operation of the bus at over 85 C. An added measure of connection reliability may be secure for such operation by the use of aluminu bolts and nuts. The substantially equ coefficients of thermal expansion of alum num bolt and bus materials will prever metal flow to which aluminum bus m terial is increasingly susceptible at el vated temperatures. Torque-limitir wrenches should be used on aluminu bolts to prevent overstressing. The lac of absolute imperviousness of silver pla ings and the acceleration of oxidatic rate with increase in temperature pla further reliance on a joint compoun coating with good retention ability. Th investigation shows alloy bus to be cap ble of operation at somewhat high temperature than EC-H13 but its lim as concerns softening with temperatu and time has not been determined in th investigation.

While not primarily intended to furnis information for performance under weat ering, the investigation showed that mo than a year of severe atmospheric weat ering was required to establish significa results. Because of the difficulty maintaining protection for steel connec ing bolts, it is concluded that aluminu bolts applied with a torque-limitir wrench will produce a more reliable join As all dry joints deteriorated when e posed to weathering and as joint com pound coatings inhibited this action, is concluded that the use of a compoun is necessary for such service.

References

1. Electric Contacts of Bus Bar Joints, C. Denault. *Electric Journal*, East Pittsburgh, P vol. 30, 1933, pp. 281–82.

ALCOA ALUMINUM CONDUCTOR HANDBOOK. minum Company of America, Pittsburgh, Pa., , pp. 102–06.

USE AND PROPERTIES OF EXTRUDED HIGH-ENGTH ALUMINUM FOR ELECTRIC BUS CONDUC-s, **W. Switney, C. L. Carlson.** *AIEE Transac-s*, pt. III (*Power Apparatus and Systems*), vol. June 1956, pp. 449–53.

ELECTRIC CONTACTS (book), **Ragnar Holm.** ers, Stockholm, Sweden, 1946, pp. 7–9, p. 86, 59.

ELECTROPLATING OF ALUMINUM ALLOYS. *Bul-no. 7*, Aluminum Company of America, June 4.

FUNDAMENTAL PROBLEMS ENCOUNTERED IN MINUM CONNECTIONS, **C. P. Xenis.** "Sym-um on the Use of Aluminum for Insulated Conductors," *AIEE Special Publication S-56*, Oct. 1953, pp. 29–32.

7. EFFECT OF HEAT CYCLING ON BOLTED ALUMINUM BUS JOINTS, **H. E. House, N. T. Bond.** "Proceedings of the Conference on the Electrical Utilization of Aluminum," *AIEE Special Publication T-72*, Mar. 1955, pp. 94–98.

8. TIGHTENING CHARACTERISTICS OF NUT, **W. F. Pickel.** *Product Engineering*, New York, N. Y., Jan. 1949, pp. 98–102.

9. PERFORMANCE OF ELECTRICAL JOINTS UTILIZING NEW SILVER COATING ON ALUMINUM CONDUCTORS, **T. J. Connor, W. R. Wilson.** *AIEE Transactions*, pt. III, vol. 72, Aug. 1953, pp. 702–12.

10. *Military Specification MIL-S-901B*, U. S. Navy, Washington, D. C., 1954.

11. MECHANICAL PROPERTIES OF ALUMINUM ELECTRIC BUS, **G. W. Stickley, C. O. Smith** *AIEE Transactions*, pt. III-A, vol. 73, Apr. 1954 pp. 100–06.

12. THE EFFECT OF SURFACE PREPARATION ON THE ELECTRICAL RESISTANCE AND TEMPERATURE RISE OF ALUMINUM BUS CONDUCTOR JOINTS. *Report no. 5603-12*, Westinghouse Materials Engineering Department, Pittsburgh, Pa.

13. ALUMINUM IN HEAVY CURRENT CONDUCTORS, **William Deans.** *AIEE Transactions*, pt. III, vol. 74, Dec. 1955, pp. 1192–1200.

14. ALUMINUM FOR MARINE SWITCHGEAR, **H. F. Harvey, Jr., E. J. Dawson.** *Ibid.*, vol. 75, Apr. 1956, pp. 134–42.

15. CONTACT RESISTANCE—THE CONTRIBUTION OF NONUNIFORM CURRENT FLOW, **W. B. Kouwenhoven, W. T. Sackett, Jr.** *Ibid.*, pt. I, vol. 70, 1951, pp. 791–95.

Discussion

T. Bond (Alcoa Research Laboratories, ssena, N. Y.): It is encouraging to se interested in using aluminum bus ductors that investigations as compre-sive as this are being reported. How-r, it is unfortunate that no more distinc-n is made between the several proprietary t compounds than a difference in the er by which they are identified in this estigation.

here are vast differences between joint pounds both in the job they are intended lo and in the manner in which they do Some joint compounds are "grease-" materials which serve primarily as tective sealers. It is for this particular ction that a joint compound is recom-nded, in conclusion 3, for joints in silver-ted conductor. Other joint compounds tain particles which deform the contact faces. Still other joint compounds con-n active chemicals which are effective in nging about low contact resistance. oa no. *2* electrical joint compound is an mple of the last-mentioned type. Each the joint compounds has as one of its ctions that of protecting the joint against ironmental corrosion.

t is pointed out that "Figs. 2(B) and (C) icate that the resistance of silver-plated ts in the region of 100 to 500 psi is be-en one tenth and one fiftieth that of pounded joints..." but the type of t compound used is not indicated. In ition, conclusion 2 states that "The stance [of a silver-plated joint] is lower n that of a compounded joint, even when bolting pressure is but a fraction of that ired for a compounded joint..." Fig.) gives the resistance of a joint which was e-brushed with joint compound as 14.5 rohms at 1,800 psi, whereas Table I gives resistance of a joint wire-brushed with pound *M* as 1.0 microhms at 1,800 psi. fact, the latter resistance is lower than obtained from the joint silver-plated by nufacturer *I*, which was 1.3 microhms; Table I. It would appear that the state-t regarding Figs. 2(B) and (C) and that conclusion 2 should be qualified or re-cted to certain joint compounds. It is ortant that a distinction be made be-en different joint compounds, or at least ween their different types.

n the discussion of corrosion effects it is ted out that "Cleaned dry joints held with aluminum bolts show less resistance change than those held with steel bolts." It is also stated that "The greater joint deterioration observed when steel bolts and washers were used is partly attributed to the physical weakening of the joint by the partial disintegration of the steel." It is worth mentioning that the differential expansion of the steel and aluminum when subjected to normal temperature variations would cause the clamping force to vary and would allow corrosion to destroy some of the contact spots which would not have been destroyed if the clamping force had been constant.

Because the purpose of the investigations was "... to determine the optimum means of utilizing aluminum bus in switchgear with the primary objective of long term service reliability," it would appear that aluminum bolts should be the primary recommendation with the use of steel fasteners subordinated.

G. J. Thompson and **S. H. Behr:** We thank Mr. Bond for his comments. Although we agree that identification of joint compounds rather than the use of code letters would be more informative, the work which furnished the basis for the paper was conducted under authorization of the Navy, and identification of competitive manufacturers was deliberately avoided as a matter of policy. However, in Figs. 4 and 6 it is demonstrated that the temperature rise and the joint resistance for full load current during and after 1,000 heating and cooling cycles are of the same order regardless of the type of proprietary joint compound used.

Concerning Mr. Bond's comment on Figs. 2(B) and (C), the curves shown were obtained by the stacked block method. Although resistance measurements for all joints compounds were made on aluminum blocks, Fig. 2(B) was selected as representative of curve shape and was code *L* compound: Table I shows 11 microhms as release resistance. Compound *M* showed a contact resistance comparable to silver-plated connections but it was slightly higher than all zincate process plated specimens. Manufacturer *I* would not divulge his method of plating which was other than the zincate process. Further to qualify conclusion 2, the authors believe that satisfactory aluminum bus connections can be prepared using joint compounds such as codes *M*, *N*, or *O* providing careful workmanship and sufficient working space is available.

Shipboard bus installations are normally crowded, often making it impractical to prepare reliable wire-brushed joints, especially on multibar connections. An analysis of several shipboard installations substantiated by voltage drop measurements made on a 20-year-old vessel with wire-brushed aluminum connections proved this latter statement. The resistance of many of these bus connections were of the same order as that of well-prepared new joints, yet others in inaccessible locations were of a value that would cause severe overheating had full-load current been applied. For this reason the authors recommend silver-plated connections for shipboard (or similar) installations so that connecting methods similar to those used for copper will be applicable.

With reference to Mr. Bond's question on what joint compound was used on the silver-plated blocks tested, represented by Fig. 2(C), these blocks were uncoated to facilitate comparison of silver platings by various processors. The application of a coating compound for these tests would have introduced a variable that may have affected results.

Mr. Bond's comment concerning the increase of resistance of bus connections fastened with steel bolts when compared to aluminum bolts after weather exposure is well taken. Difference of thermal expansion between the steel bolt and aluminum bolt may have been the major factor. The extreme degree of corrosion of the steel bolts, washers, and nuts (heavy scaling and partial disintegration) lead the authors to believe that part of the loosening may have been caused by loss of fastener material during about $1\frac{1}{2}$ years of weathering. The high rate of disintegration of the steel indicated that, if this was not the major factor in a short period of time, it would be the major factor in a longer period.

Although aluminum bolts are considered satisfactory for bus connection fastening they require the use of a bolt one size larger (1/2-inch steel bolt versus 5/8-inch aluminum bolt) and, to obtain sufficient contact pressure, the aluminum bolt must be tightened to approximately 80% of its ultimate strength. The additional space required for the aluminum fastener and the necessity of controlling tightening torque were the basis for conclusion 4 of the paper.

Predicting the Performance of a Wind Tunnel Regulating System Using an Analog Computer

R. HERBST
ASSOCIATE MEMBER AIEE

J. O. NICHOLS
ASSOCIATE MEMBER AIEE

F. W. KEAY
ASSOCIATE MEMBER AIEE

R. W. MILLER
ASSOCIATE MEMBER AIEE

THE USE of an analog computer, particularly one of the electronic differential analyzer type, in the analysis and design of feedback control systems has been well established in the past few years. Quite often, however, a detailed computer investigation of a control system is not necessary. For example, in some instances the control system may contain only a few components which can be represented by linear transfer functions, in which case the familiar methods of linear servomechanism analysis may be employed. It is also possible in some cases that it is just as economical to optimize a design on the test floor without benefit of a computer study.

In general, wind tunnel drive-regulating systems may not be similar in many respects, e.g., in ratings of the equipment involved and types of regulation required. Because of the large power requirements of a wind tunnel, the stability of the regulating system is of primary importance, and usually rapid response times can be sacrificed for stability improvement. Wind tunnels may have a wide operating range over which stability must be maintained. For example, it has been observed that a system may be stable through an acceleration cycle while under the control of current or power regulators, but may be unstable at operating speed. The control system usually contains components which have nonlinear characteristics such as saturation, clipping, and backlash which cannot be neglected in the analysis. Therefore, linearizing a system and investigating the stability with respect to small excursions about some operation point cannot be regarded as safe procedure. The size of the equipment involved in a wind tunnel installation would, in general, prohibit the assembly of the complete system on the test floor. Also, the high costs of tests and equipment changes at the permanent installation site would not be desirable. For these reasons, a detailed analog computer study of a complex wind tunnel regulating system is extremely useful.

Paper 59-646, recommended by the AIEE Feedback Control Systems Committee and approved by the AIEE Technical Operations Department for presentation at the AIEE Middle Eastern District Meeting, Baltimore, Md., May 19–21, 1959. Manuscript submitted August 18, 1958; made available for printing March 18, 1959.

R. HERBST, J. O. NICHOLS, F. W. KEAY, and R. W. MILLER are with the Westinghouse Electric Corporation, East Pittsburgh, Pa.

Computer Approach

The purpose of this paper is to discuss the analog computer approach in the analysis of a typical wind tunnel drive-regulating system. Before the system is ready for computer simulation, the basic design of the individual components is complete and their transfer characteristics have been determined. In the computer representation, the components are coupled in the designer's proposed arrangement. A typical starting cycle is then initiated and the system behavior is immediately available on time-scaled pen-recorded oscillograms. If a system proves to be unstable, the influence of various stabilizing measures which are suggested by a preliminary analysis employing approximate linear analytical methods (Bode or Nyquist diagrams) may then be studied. Since each component of the actual system has its computer counterpart, the parameters in the analog hav physical identity, and the effect of varia tion of these parameters can readily b observed. It is important to bear i mind that the computer will not auto matically optimize the performance o recommend the types of stabilizatio which may be required. The computer i simply a tool which is an aid to the en gineer. It enhances the designer' intuitive "feel" for his system and refute or confirms his predictions. Althoug this direct system simulation can be pro grammed for a high-speed digital com puter, it is not as economical and con venient as the analog computer approach

Regulating System

The wind tunnel under discussion con sists essentially of a single wound-roto induction motor which drives severa stages of compressors. The total momen of inertia of the rotating machines and th load torque characteristic of the com pressors are specified.

The regulating system will be discusse in a general manner with reference to th schematic diagram; see Fig. 1. The soli lines may be considered as flow lines o intelligence of the basic system, and th dashlines are feedbacks deemed necessar for stabilization.

The tachometer voltage which is pro portional to induction motor speed i compared with a reference and the erro is clipped by a diode circuit which i labeled "Clipper." The output of th clipper is then amplified by a preamplifie and a power amplifier, and this voltage i turn supplies the control windings of shunt-tuned Rototrol. The Rototrol i turn controls the pilot motor which posi tions the liquid rheostat electrodes. Th amount of rheostat resistance determine the total secondary resistance of the in duction motor, and ultimately the torqu and speed. In addition, the clipper signa

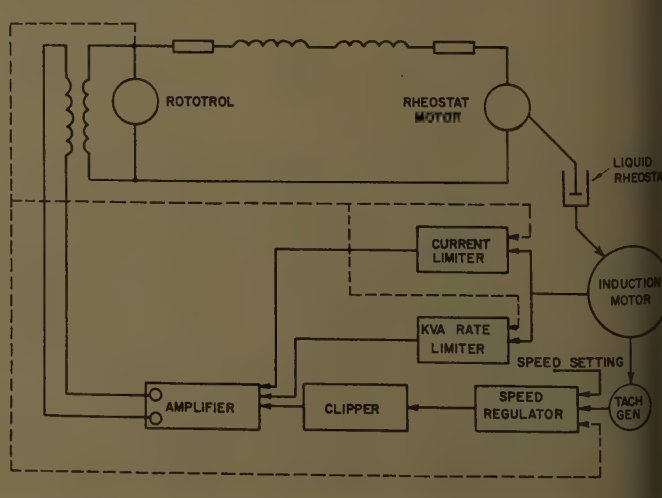

Fig. 1. Schematic of regulating system

be annulled by the current limiter, ich limits the secondary current of the uction motor, or by the kva (kilovolt-pere) rate limiter which limits the rate change of the induction motor primary rent.

Three different types of regulators are ociated with this sample system: ed, induction motor secondary current, l kva rate limiter. Some other types regulators which may be present will mentioned as examples. A dynamic king current regulator could control braking torque during a shutdown op-tion. In the case of a system contain-more than one induction motor, cur-t balance regulators may be required, one induction motor may be con-lled by speed regulation and a second current balance with the first. In some es, a wind tunnel drive may be accelera-d to operating speed by an induction tor, at which time the load is appro-ated by a synchronous motor. If at time the load were to exceed the chronous motor rating, a kilowatt ex-s transfer regulator could be used to re the load with an induction motor. pendix I gives the equations which cribe the various components of the ulating system.

ALYSIS AND RESULTS

ig. 2 is a per-unitized block diagram structed from the equations derived Appendix I. The solid lines indicate nponents of the basic regulator, while hed lines indicate components intro-ed as stabilizing measures. The log representation shown in Fig. 3 ows from the block diagram. The ial gains and time constants of the ious stabilizing feedbacks are selected the basis of a preliminary analysis and vious experience. These parameters then varied to determine their individ-effects, and are then adjusted to ain their optimum values.

ig 4(A) is a pen recording of a typical eleration cycle to rated speed without stabilizing measures present. The tem performs satisfactorily until the que reaches the value of 1.25 per unit. this time, the current limiter becomes ve, the kva rate limiter becomes in-ve, and a nonlinear instability ap-rs simultaneously.

he preliminary linear analysis of the tem revealed that the speed-regulating tended toward instability, and also t the two minor regulating loops in-ving the kva rate limit and the over-rent limit were inherently unstable. s analysis also indicated the types of lback that should be employed for

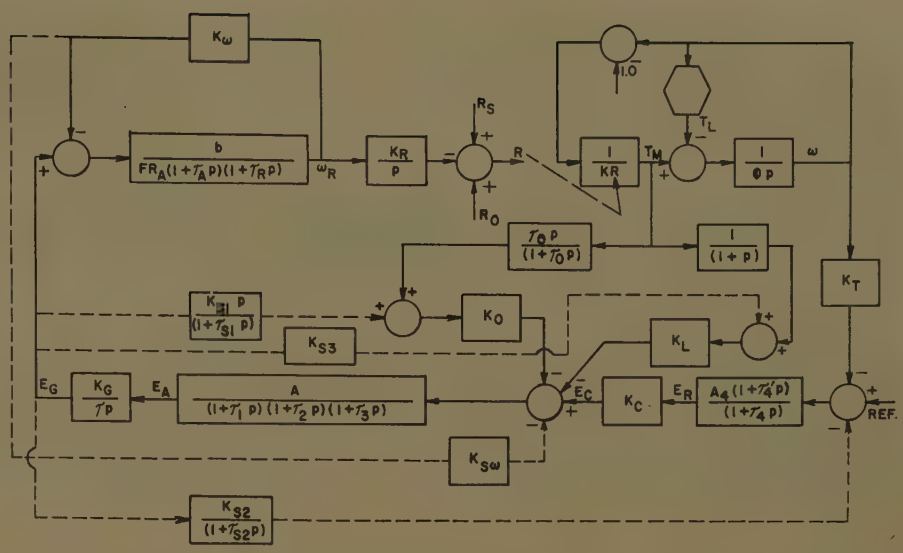

Fig. 2 (above). Block diagram of regulating system

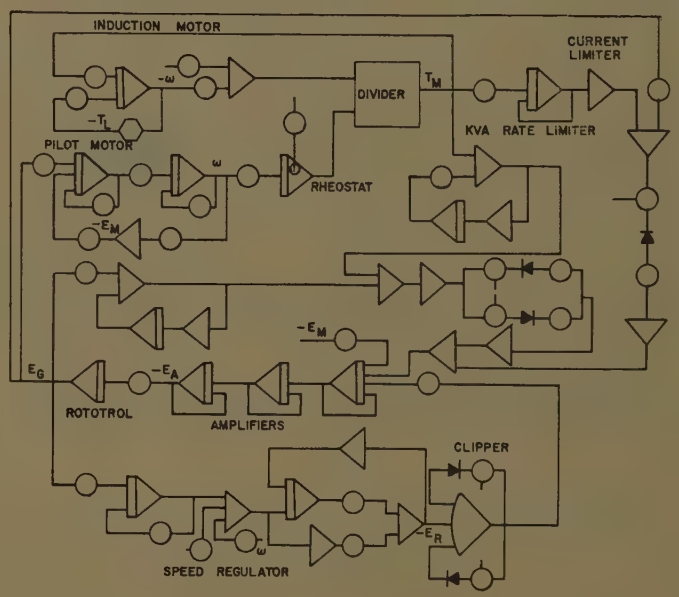

Fig. 3 (right). Computer analog of regulating system

stabilization. The stabilizing measures were introduced individually into the analog and the gains and time constants adjusted to their optimum value. Fig. 4(B) shows the effects of using a derivative feedback from the Rototrol internal voltage to the kva rate limiter. The system still has an unstable response but has improved in that rated speed is attained and the system passes through the "minor" loop instabilities. A direct feedback to the current limiter removed the minor loop instabilities; see Fig. 4(C). Finally a time delay network from the Rototrol internal voltage to the speed regulator proved effective in stabilizing the major loop; see Fig. 4(D).

A method suggested for obtaining the feedback signals from the back emf (electromotive force) of the pilot motor and the internal voltage of the Rototrol is shown in Fig. 5. For further discussion of Fig. 5, see Appendix II.

Conclusions

The use of an analog computer in conjunction with the analytical techniques of linear feedback control offers a powerful method for the investigation of systems of the type exemplified in this paper. The results of a study such as this do not dictate precisely the actual values of the feedback parameters which will appear in the final system. However, the performance curves of the final system, which in the case of a large wind tunnel would be obtained at the permanent installation site, should correspond very closely with the computer results. Because of probable inaccuracies in the physical data available for the computer study, minor "trimming" adjustments of some components will be necessary.

It is important throughout the computer study to bear in mind that only quantities which are physically obtainable

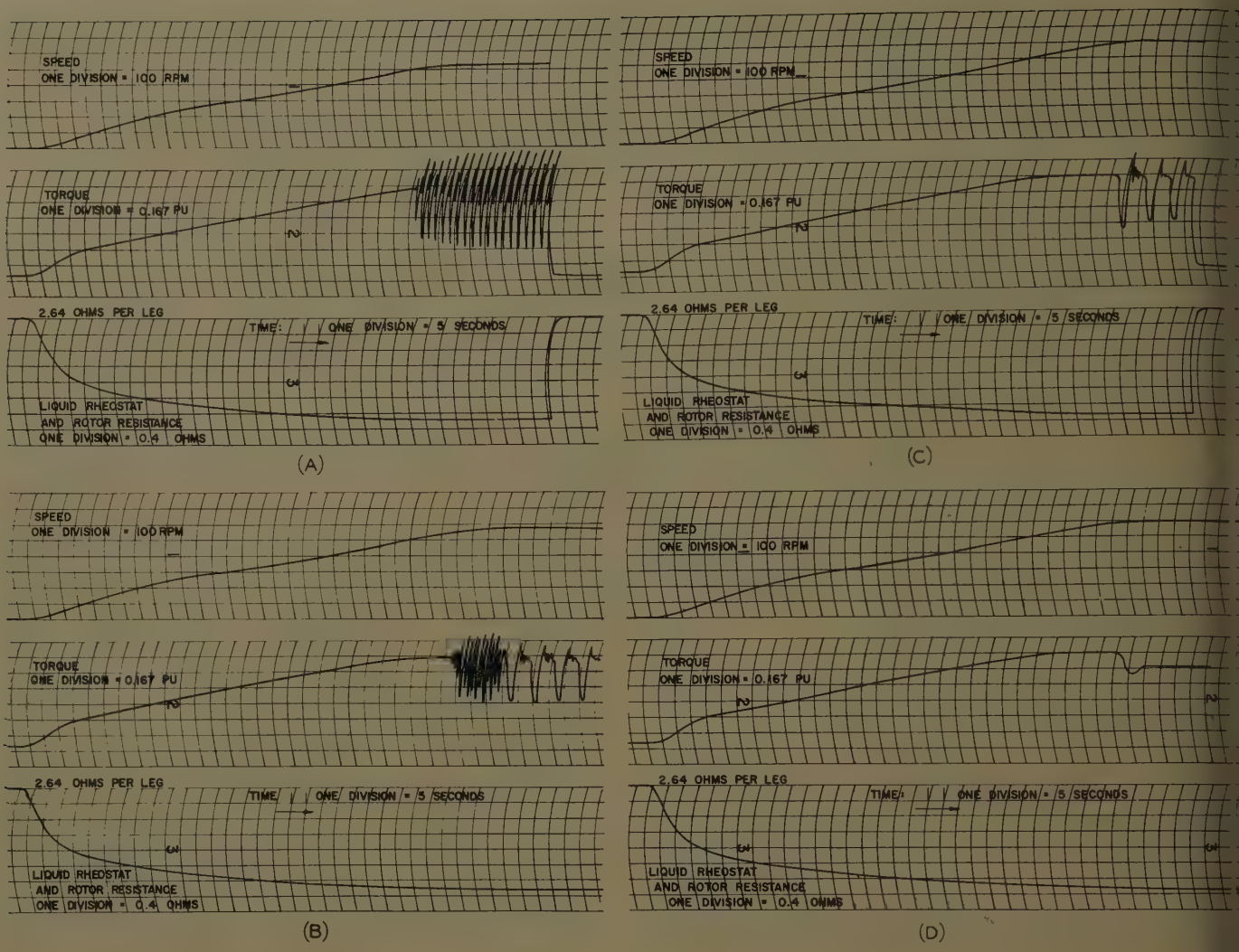

Fig. 4. Simulation of starting cycle

A—Without stabilizing measures
B—With feedback from internal Rototrol voltage to kva rate limiter
C—With feedback from internal Rototrol voltage to kva rate limiter and current limiter
D—With feedbacks from internal Rototrol voltage to kva rate limiter, current limiter, and speed regulator

should be used as feedbacks. Thus, a feedback from the internal voltage of the amplifier to the speed regulator should not be considered in the study even though this results in a favorable response, because the internal voltage of the amplifier is not available in the actual physical system (even though it is available on the computer analog).

Although the use of analytical techniques should be emphasized, the regulator discussed in this paper would be difficult to analyze completely by these methods, due to the nonlinear characteristic of the closed loop transfer function. However, with the aid of an analog computer, highly satisfactory results were obtained with relative ease.

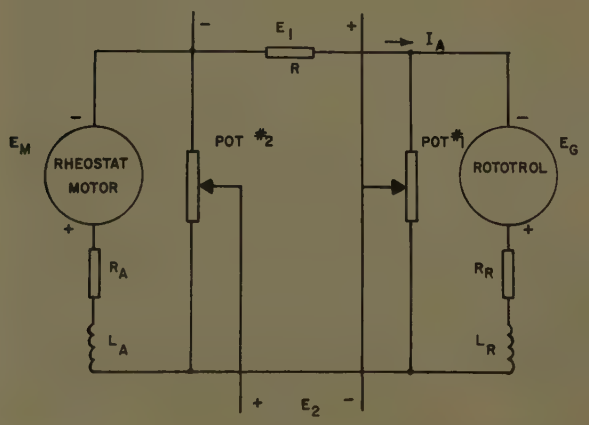

Fig. 5. Circuit for obtaining stabilizing feedbacks

Appendix I. Development of Equations

Induction Motor Equations

On a per unit basis

$$T_M = \frac{I^2 R}{S} \qquad (1$$

The torque of the induction motor is proportional to the secondary current if the secondary resistance is sufficiently large or if the speed of the motor is near synchronous speed; see Fig. 6(A). In this region of operation, equation 1 can be written as

$$S = KT_M R \qquad (1A$$

and

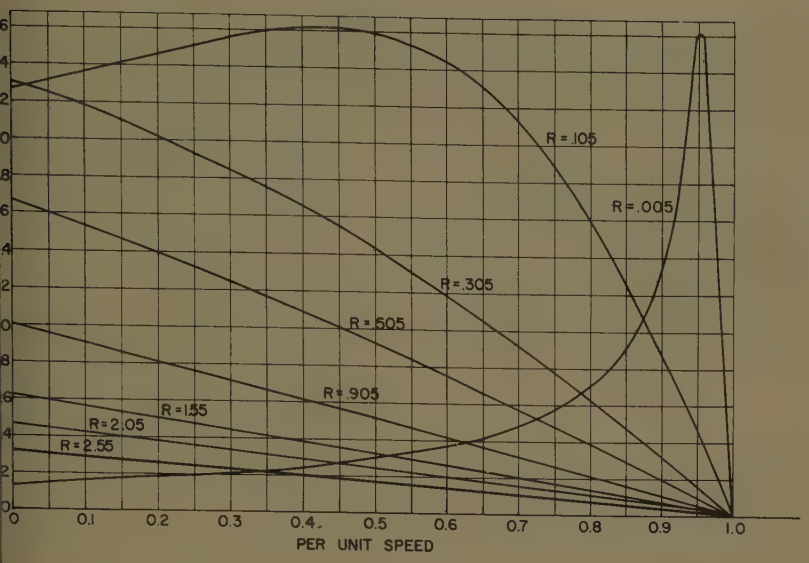

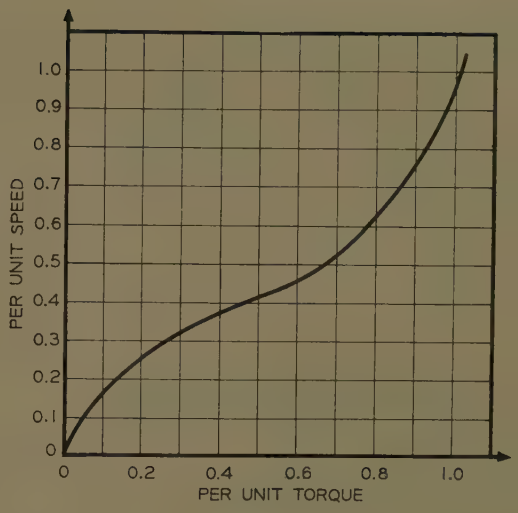

Fig. 6. A—Speed-torque curves of induction motor. B—Speed-load torque curve

$$1-S=1-KT_MR \tag{2}$$

e value of K can be determined from the que-speed curves; see Fig. 6(A).
he induction motor torque-speed curves calculated from the equivalent circuit wn in Fig. 7.
he equation of motion is

$$\frac{\omega}{t}=T_M-T_L \tag{3}$$

eostat Pilot Motor Equations

$$=\frac{E_g-E_M}{1+\tau_A p} \tag{4}$$

$$\frac{\omega_R}{t}=T_e-T_R$$

$$=bI_A$$

$$=F\omega_R$$

$$=\frac{bI_A}{F(1+\tau_R p)} \tag{5}$$

$$=\frac{b(E_g-E_M)}{FR_A(1+\tau_A p)(1+\tau_R p)} \tag{6}$$

$$=K_\omega\omega_R \tag{7}$$

eostat Equations

he relative position of the electrodes of liquid rheostat is proportional to the ular displacement of the pilot motor ft, and the resistance of the rheostat is proportional to the separation of the electrodes. In operational form

$$R=R_R+R_0-\frac{K_R\omega_R}{p} \tag{8}$$

Rototrol Equations

Since the Rototrol has a self-excited shunt field, the internal voltage of the Rototrol is a function of control field current and shunt field current.

$$I_C=\frac{E_A}{R_C(1+\tau p)}$$

$$I_S=\frac{E_g}{R_S(1+\tau p)}$$

$$E_g=N_CK_g'I_C+N_SI_SK_g'$$

$$E_g=\frac{N_CK_g'E_A}{R_C(1+\tau p)}+\frac{N_SK_g'E_g}{R_S(1+\tau p)} \tag{9}$$

If the Rototrol has a shunt-tuned field,

$$N_SK_g'=R_S$$

$$E_g=\frac{N_CK_g'E_A}{R_C\tau p} \tag{10}$$

Amplifier

The amplifier has the following transfer function

$$E_A=\frac{AE_C}{(1+\tau_1 p)} \tag{11}$$

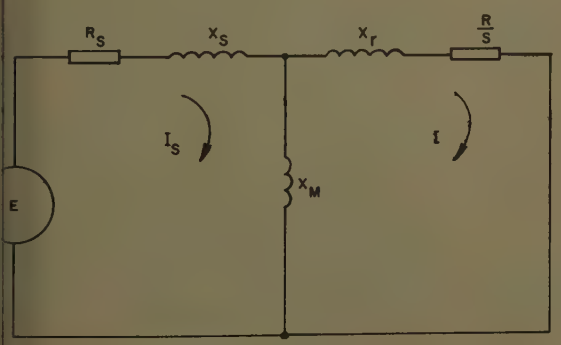

Fig. 7. Equivalent circuit of induction motor

Clipper and Limiter

Both the clipper and the limiter are nonlinear and hence do not lend themselves to a convenient analytical representation. However, their analog representation is quite accurate; see Fig. 3.

Speed Regulator

Incorporated in the speed regulator is an anticipation network; its transfer function is

$$E_R=A_\tau\frac{(1+\tau_4' p)}{(1+\tau_4 p)}\,(\text{reference}+E_T) \tag{12}$$

Tachometer

The tachometer device is linear throughout the region of operation and has the simple transfer function

$$E_T=K_T\omega$$

Appendix II. Stabilizing Feedback Circuit

The circuit shown in Fig. 5 is a modification of one proposed by Tustin.[1] It is intended as a means of obtaining voltages proportional to the back emf of the pilot motor and the internal voltage of the Rototrol. In the circuit of Fig. 5, it is assumed that negligible current will flow through potentiometers 1 and 2.

Applying Kirchoff's voltage law around the loop containing E_1 yields

$$\begin{aligned}E_1&=E_M+I_A(R_A+L_Ap)-\\&\quad\alpha(E_M+I_AR+I_AR_A+I_AL_Ap)\\&=E_M(1-\alpha)+I_A[R_A(1-\alpha)-\alpha R]+\\&\quad I_AL_Ap(1-\alpha)\end{aligned}$$

Assume that $I_AL_Ap(1-\alpha)$ is negligible; then

$$E_1=(1-\alpha)E_M$$

if

$$R=\frac{1-\alpha}{\alpha}R_A$$

Solving for E_2 yields

$$E_2=\alpha[E_g-I_A(R_R+L_Rp)]-\beta(E_q-I_AR_R-I_AR-I_AL_Rp)$$
$$=E_g(\alpha-\beta)+I_A[R_R(\alpha-\beta)+\beta R]+I_AL_Rp(\beta-\alpha)$$

Assume that $I_AL_Rp(\beta-\alpha)$ is negligible; then

$$E_2=E_g(\alpha-\beta)$$

if

$$\frac{\beta}{\alpha-\beta}=\frac{R_R}{R}$$

Appendix III. Nomenclature

Induction Motor

T_M = induction motor torque
R = total resistance of induction motor secondary circuit
I = secondary current of induction motor
S = slip
ω = speed of induction motor
$K^{1/2}$ = constant of proportionality between induction motor current and torque
Φ = total moment of inertia of wind tunnel drive
T_L = load torque of compressors; see Fig. 6(B)

Rheostat Pilot Motor

I_A = armature current
E_g = internal Rototrol voltage
E_M = motor back emf
R_A = total resistance in armature circuit
L_A = total inductance in armature circuit
$\tau_A=L_A/R_A$ = armature circuit time constant
$p=d/dt$ = differential operator
λ = total moment of inertia associated with pilot motor
ω_R = speed of pilot motor
T_e = electrical torque of pilot motor
T_R = load or resisting torque of pilot motor
b = proportionality constant between armature current and torque
F = proportionality constant between pilot motor speed and resisting torque
τ_R = mechanical time constant of pilot motor
$K\omega$ = proportionality constant between pilot motor speed and back emf

Rheostat

K_R = constant of proportionality between rheostat resistance and pilot motor speed
R_0 = maximum resistance of rheostat
R_R = secondary winding resistance of induction motor

Rototrol

E_g = internal voltage of Rototrol
E_A = control field voltage
R_C = control field resistance
τ = total time delay due to all field windings
I_S = shunt field current
I_C = control field current
R_S = shunt field resistance
N_C = number of turns on control field
N_S = number of turns on shunt field
K_g' = volts per ampere-turn gain of Rototrol

Amplifier

E_A = internal voltage of amplifier
E_C = input voltage of amplifier
τ_1 = time delay of amplifier. (If more than one stage is used in amplification network, there will be additional delays associated with each additional stage)

Speed Regulator

E_R = output voltage of regulator
E_T = output voltage of tachometer
ref = reference voltage
τ_4', τ_4 = time constants of anticipation network which may be adjusted

Tachometer

K_T = proportionality constant between induction motor speed and tachometer output voltage

Anti-hunt Circuit

α = setting of potentiometer 1
β = setting of potentiometer 2

References

1. Direct Current Machines for Control Systems (book), A. Tustin. The Macmillan Company, New York, N. Y., 1952, pp. 232–36.

2. Analog Computer Study of Wind Tunnel Drive, K. G. Black, R. J. Noorda. *AIEE Transactions*, pt. I (*Communication and Electronics*), vol. 76, 1957 (Jan. 1958 section), pp. 745–50.

3. Electrical Transmission and Distribution Reference Book (book). Westinghouse Electric Corporation, Pittsburgh, Pa., 1950, pp. 191–92.

A New Chart Relating Open-Loop and Closed-Loop Frequency Responses of Linear Control Systems

C. F. CHEN
NONMEMBER AIEE

D. W. C. SHEN
MEMBER AIEE

CONTROL ENGINEERS generally adhere to the use of frequency response as the fundamental tool for feedback control systems. Through the use of the Nichols chart,[1] the open-loop characteristics can be quickly converted to the closed-loop characteristics. The performance of control systems can be estimated according to the gain and phase margins and the magnitude of peak M. Although actual performance may be quite different from that predicted by a certain value of a particular specification, yet by means of Meerov's method[2] it should not be difficult for engineers to determine the limits of applicability and to evaluate its effectiveness.

This paper attempts to develop a new chart which has several practical advantages over the well-known M-contours or Nichols chart. Some of the advantages are outlined as follows:

1. The graphical construction is easier, because it is based on the rectangular coordinates of both the open-loop frequency response, $G(j\omega)$, and the closed-loop frequency response, $M(j\omega)$. On the M-plane, the contours of constant real and constant imaginary parts of G are two families of orthogonal circles which intersect at a common point.

2. The G-locus when plotted on this chart gives the M-locus directly in terms of the rectangular or polar co-ordinates, whereas if the Nichols chart is used a replot of the M-locus is necessary.

3. To find the transient performance from the closed-loop frequency response, one usually resorts to the method devised by Floyd.[3] Floyd's method requires the determination of the real part of the closed-loop response, and this can be directly read from the new chart.

4. From this chart, the most common performance specifications of closed-loop systems, such as the gain margin, the phase margin, peak M, bandwidth, and rise time, etc., can be readily determined. In some cases, they are actually simpler than the use of conventional charts.

Construction of New Chart

In a unity feedback control system, such as shown in Fig. 1, the following relation obtains:

$$\frac{C}{R}=M\underline{/\alpha}=\frac{|G|\underline{/\phi}}{1+|G|\underline{/\phi}} \quad (1)$$

Paper 59-647, recommended by the AIEE Feedback Control Systems Committee and approved by the AIEE Technical Operations Department for presentation at the AIEE Middle Eastern District Meeting, Baltimore, Md., May 19–21, 1959. Manuscript submitted September 16, 1958; made available for printing March 18, 1959.

C. F. Chen is with Christian Brothers College, Memphis, Tenn., and D. W. C. Shen is with the University of Pennsylvania, Philadelphia, Pa.

The authors express their thanks to Dr. J. G. Brainerd, Dr. Y. H. Ku, and Dr. Lambert Thomas for their constant encouragement. *Note:* Attention has been directed to the possibility that the charts, and uses of them similar to those described in the paper, may have appeared earlier in the literature of the Russian *Automatika i Telemekhanka*. In *Automation and Remote Control*, the available English translation, the authors have not found similar charts.

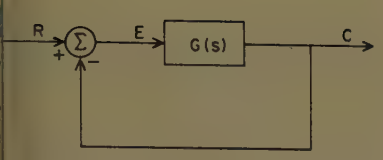

1. Typical configuration of feedback control system

terms of rectangular co-ordinates, $=a+jb, M/\underline{\alpha}=U+jV$, equation 1 can esolved into two equations involving real and the imaginary parts respec-ly, i.e.,

$$\frac{a^2+b^2+a}{(1+a)^2+b^2} \tag{2}$$

$$\frac{b}{(1+a)^2+b^2} \tag{3}$$

nination of b from equations 2 and 3 s

$$\left(U-\frac{2a+1}{2(1+a)}\right)^2+V^2=\left(\frac{1}{2(1+a)}\right)^2 \tag{4}$$

elimination of a gives

$$U)^2+\left(V-\frac{1}{2b}\right)^2=\left(\frac{1}{2b}\right)^2 \tag{5}$$

ation 4 represents a family of con-t-a circles having centers on the xis at $2a+1/[2(1+a)]$ and radii of $2(1+a)]$. Equation 5 is that of stant-b circles having centers on the 1 line at $1/2b$ and radii of $1/2b$. se two families of circles are orthog-l and they intersect at the common t $U=1$, $V=0$.

he chart is shown in Fig. 2. Contours a and b are plotted in solid lines, le the polar co-ordinates of $M/\underline{\alpha}$ drawn in dashed lines. Symmetry ts in the plane containing the a and b tours with respect to the U-axis or 0, a 180-degree line only. The com-n point of intersection is the limit of a b contours when either a or b ap-aches infinity. Physically it means n the open-loop gain G approaches nity, the closed-loop gain M ap-aches unity. The b contour de-erates into a straight-line which is U-axis, when b approaches zero. mentioned previously, this line is the of symmetry for the b contours. sically, if the open-loop response G is ure gain with zero phase angle, so he closed-loop response M. On the er hand, the a contour when a ap-aches zero is a circle having center at $1/2, V=0$, and with a radius of -half unit. All a contours for posi-values of a, i.e., $0 \leqslant a \leqslant \infty$, are fined within the $a=0$ contour. For $<a \leqslant 0$, the a contours expand to the left-hand side until $a=-1$, where it degenerates into a straight line which is $U=1$. For $-\infty<a<-1$, a contours are shrinking circles on the right-hand side of $U=1$. The limit is again the point $U=1$, $V=0$, as a approaches $-\infty$.

It is interesting to note that the region within the contour $a=0$ is a replica of the so-called Smith chart[4,5] well known in high-frequency transmission-line theory.

Stability Considerations

The essential feature of the new chart is that the closed-loop response manifests itself directly in terms of either the rectangular or the polar co-ordinates, once the open-loop response is plotted on the a and b contours.

Leonhard's method[6,7] may be used to determine the stability of control system in the M-plane. For the case of the open-loop transfer function having no poles in the right-hand half-plane, his criterion is as follows: If the M-locus in going from zero frequency toward infinity, sweeps through as many quadrants (in a negative direction) as the highest power of s (the Laplace transform variable) in the denominator of M diminished by the highest power of s in the numerator, the control is stable.

For the majority of control problems that are stable when the control system loop is open, Bode's network theorems[8] provide the basic information necessary to simplify greatly the work of a designer in obtaining a stable system. A new stability criterion is established as follows: When the M-locus crosses the line $U=1/2$, if the value of V is positive, the system is unstable; otherwise, it is stable.

It is evident that when $U=1/2$, equation 2 becomes $a^2+b^2=1$; hence the line $U=1/2$ corresponds to the unit circle in the conventional G-plane. In many systems, the sign of a at crossover is negative; the sign of b follows that of V. Therefore the foregoing criterion is equivalent to the familiar statement that "systems having positive phase margin when their transfer function crosses the unit circle are stable, whereas systems with negative phase margin when their transfer function crosses the unit circle are unstable.[9]

It follows that phase margin is obtained from the new chart by measuring $\tan^{-1} b/a$ at the crossover. The gain margin is given by the reciprocal value of a at the point where the M-locus crosses U-axis, since the U-axis coincides with the $b=0$ contour.

The advantages of the new chart are

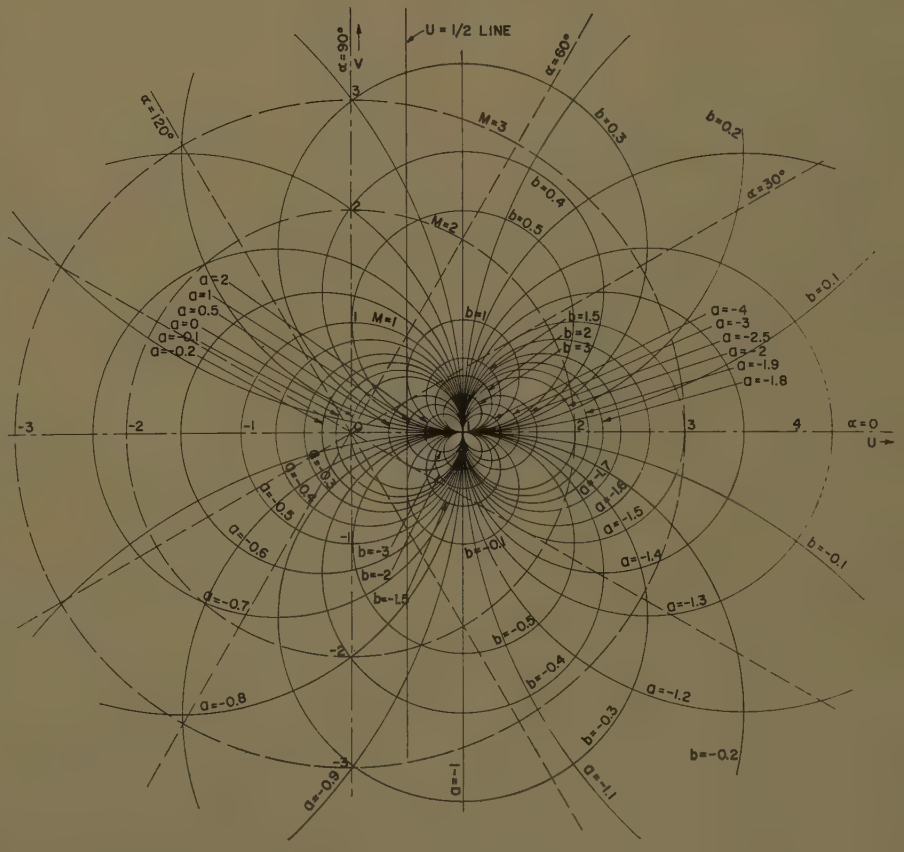

Fig. 2. The new chart

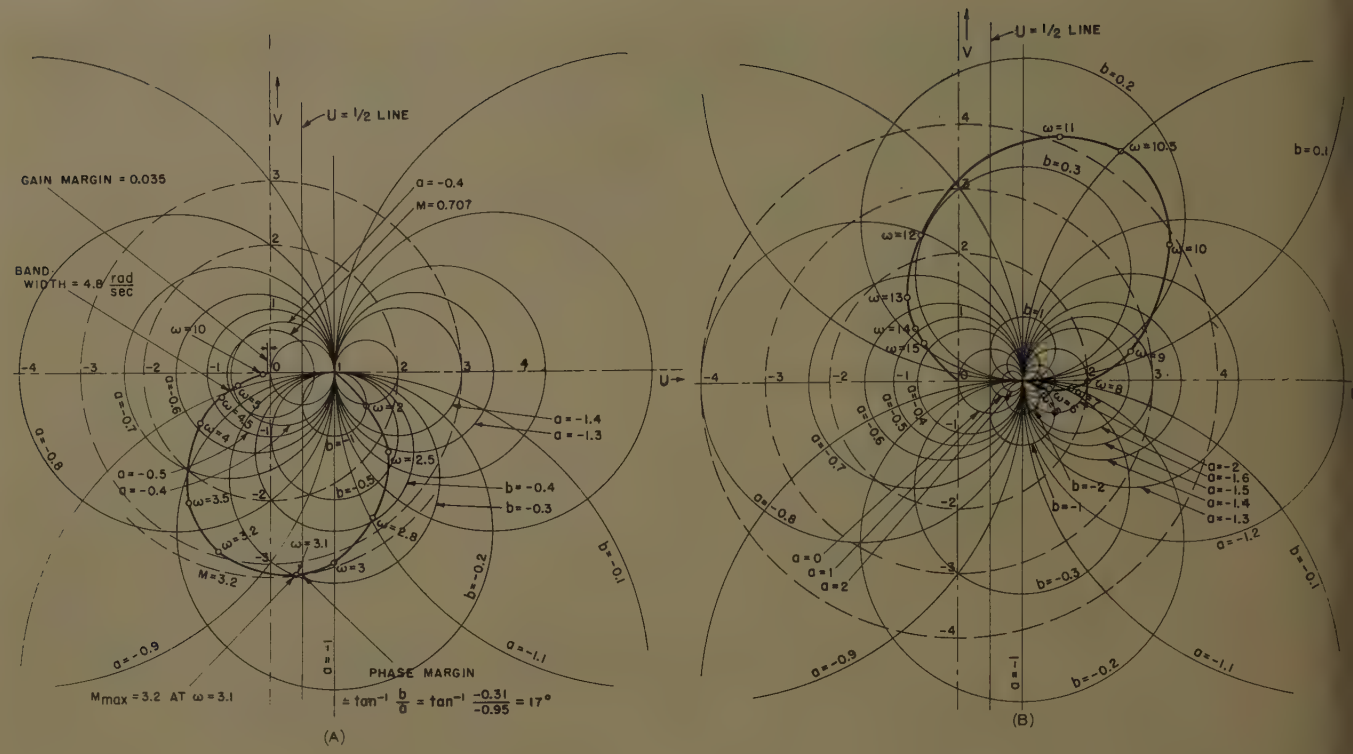

Fig. 3. Frequency response. A—Of stable system. B—Of unstable system

also obvious when the quantity of peak M is to be evaluated. It can be accurately read from the M-locus itself. Likewise, bandwidth can also be determined from the M-locus itself. It is simply the frequency at which $M=0.707$.

Illustrative Examples

The utility of the new chart can be demonstrated by working out two simple examples.

Example 1: Consider an aircraft propeller pitch-control system having a loop transfer function represented by the following relation:

$$G=\frac{k}{s(s+1)(1.2\times10^{-4}s^2+3\times10^{-3}s+1)}$$

Assume $k=10$, the real and the imaginary parts of the foregoing equation as a function of frequency are computed and plotted on the chart as shown in Fig. 3(A). The resultant curve also represents the M-locus.

The gain margin is reciprocal of the value a when the M-locus crosses the line $V=0$ or $b=0$. Thus, $a=0.035$, and $1/a=30$.

The values of a and b at the point where the M-locus crosses $U=1/2$ are $a=-0.95$, $b=-0.31$. Therefore, the phase margin is $\tan^{-1} b/a=17$ degrees.

Since the sign of b is negative, accordin to the criterion just given, the system i stable.

The peak value of M and the band width are directly read from the chart t be 3.2 and 4.8 radians per second re spectively.

To find the transient response, evaluat the following real form of the Fourie integral:

$$h(t)=\frac{2}{\pi}\int_0^\infty R(\omega)\cos\omega t\,d\omega \qquad (6$$

which is the basis of Floyd's graphica method. In equation 6 $R(\omega)$ represent the real part of the closed-loop frequency response $M(\omega)$.

The function $R(\omega)$ is directly read from the chart and is plotted in Fig. 4. The corresponding time response to a uni step input is shown in Fig. 5.

It should be noted that when an M,α chart is used, an auxiliary chart of con

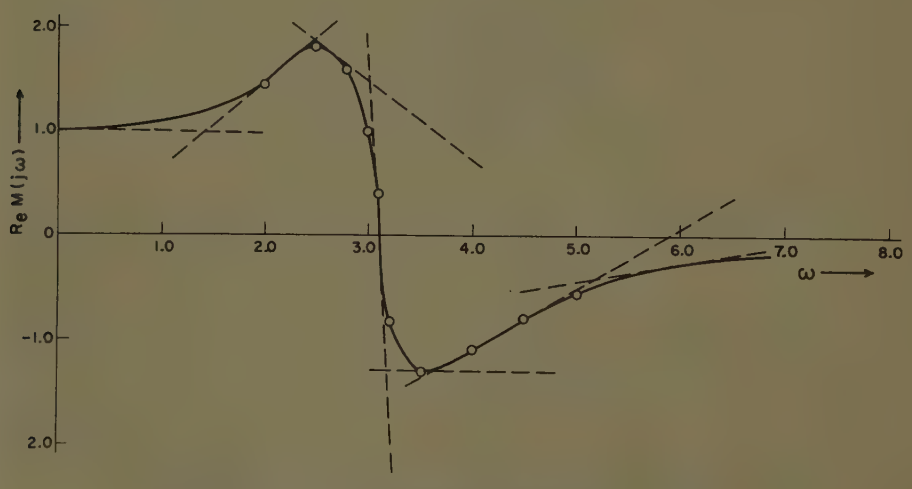

Fig. 4. Real parts of frequency response of example 1

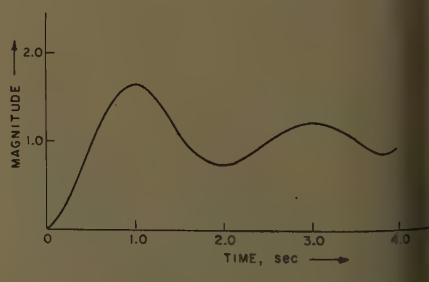

Fig. 5. Transient response of example 1

is necessary, as suggested by Floyd, der to obtain $R(\omega)$.

though this system is stable, the low e margin and low damping ratio ate that the system is rubbery with ssive overshoot and long settling time.

ample 2: A system with

$$\frac{40}{S(25\times10^{-2}S+1)(625\times10^{-3}S+1)}$$

tted on the chart shown in Fig. 3(B). *M*-locus crosses $U=1/2$ with positive e of b, and therefore the system is able.

clusions

new chart is developed which cor- es the open-loop and closed-loop nses of a unity feedback control m.

aphically, M,α contours look like the old ultrahigh-frequency transmission line chart and the new chart looks like the Smith chart if the latter is extended to the region of negative real parts.

Aside from some of the practical advantages of the new chart already mentioned, it is hoped that this paper may broaden the viewpoint of engineers and students alike when they make a study of the conventional M,α contours or the inverse complex plane plot as recommended by Marcy[10] and Whiteley.[11]

References

1. Theory of Servomechanisms (book), **H. M. James, N. B. Nichols, R. S. Phillips.** McGraw-Hill Book Company, Inc., New York, N. Y., 1947, pp. 158–62, 179–86.

2. Estimating the Performance of Control Systems According to Their Stability Margin with Respect to Modulus, Phase and the Quantity M (in English), **M. V. Meerov.** *Avtomatika i Telemekhanika*, Moscow, U.S.S.R., vol. 17, no. 10, 1957, pp. 963–69.

3. Principles of Servomechanisms (book), **G. S. Brown, D. P. Campbell.** John Wiley & Sons, Inc., New York, N. Y., 1948, pp. 339–46.

4. Transmission Line Calculator, **P. H. Smith.** *Electronics*, New York, N. Y., vol. 12, Jan. 1939, pp. 29–31.

5. An Improved Transmission Line Calculator, **P. H. Smith.** *Electronics*, vol. 17, Jan. 1944, pp. 130–33.

6. Die Selbsttätige Regelung (book), **A. Leonhard.** Springer-Verlag, Berlin, Germany, 1957, pp. 233–47.

7. Neues Verfahren zur Stabilitatsuntersuchung, **A. Leonhard.** *Archiv für Electrotechnik*, Springer-Verlag, vol. 38, 1944, pp. 17–28.

8. Network Analysis and Feedback Amplifier Design (book), **H. W. Bode.** D. Van Nostrand Company, Inc., New York, N. Y., 1945, pp. 312–19.

9. Servomechanism and Regulating System Design (book), **H. Chestnut, R. W. Mayer.** John Wiley & Sons, Inc., 1951, pp. 292–97.

10. Parallel Circuits in Servomechanisms, **H. Tyler Marcy.** *AIEE Transactions*, vol. 65, Aug.-Sept. 1946, pp. 521–29.

11. Theory of Servo Systems, with Particular Reference to Stabilization, **A. L. Whiteley.** *Journal*, Institution of Electrical Engineers, London, England, vol. 93, pt. 2, 1946, pp. 353–67.

12. A Quick Method for Estimating Closed-Loop Poles of Control Systems, **K. Çhen.** *AIEE Transactions*, pt. II (*Applications and Industry*), vol. 76, May 1957, pp. 80–87.

Generator Insulation Systems Development for Hypersonic Aircraft

W. B. PENN MEMBER AIEE **R. L. BALKE** MEMBER AIEE **F. M. PRECOPIO** ASSOCIATE MEMBER AIEE

RESENT and future aircraft require- ments for electric power are con- tly increasing, with operational re- ements of speed, altitude, and equip- t imposing greater loads on the elec- generating systems. The need there- exists for generators capable of ating at higher temperatures than e presently available.

arious methods have been considered are being used to extend the opera- al range of present insulations in the tric power generators by techniques extracting heat. However, these im- a weight penalty upon the system in ns of the weight of cooling fluid and circulatory systems needed, or the weight and wind resistance of the heat exchanger employed by their cooling devices.[1,2] It would be desirable and advantageous to have a generator insulation system which in itself is capable of withstanding temperatures in the vicinity of 500 C (degrees centigrade) for continuous operation, so that the excessive weight of any cooling system could be eliminated. This system would be ventilated by the ram air available in flight just as corresponding generators are now cooled for conventional speeds and altitudes, but the new system would be capable of withstanding the elevated temperatures encountered at the higher speeds and altitudes of future aircraft. Though oil cooling was finally adopted for this machine, the original goal of a high-temperature insulation system, as for air cooling, was retained.

For this purpose, a proposal was accepted under a U. S. Air Force contract for the development of a machine which would meet their specification requirements. Since these requirements were presented in terms of performance, i.e., output under defined conditions of altitude, air inlet temperature, and load, it was necessary to tie in the best estimates of design criteria to permit an estimate of the temperatures which the windings would attain under these conditions. These temperature estimates formed the basis of a test cycle which the insulation system would be required to meet. Dielectric requirements of 1,200 volts rms for one minute, to measure ability of insulation to withstand various environmental conditions, were also contained within the specification.

The technical approach in the development of components of such an insulation system was 3-pronged: first, the capabilities of presently commercially available materials would be evaluated to determine whether they could withstand the simulated duty cycle for the required service life; second, presently available materials would be modified or adapted, if necessary, to extend their temperature capabilities to permit them to operate successfully; and third, a completely new system would be developed in terms of new materials not available at present to meet the required operational conditions.

It was recognized early in this program that the successful development of a useful insulation system was dependent on the development of a technique of testing which would screen and evaluate, first, individual materials, then components, and then simulated or actual structures such as would be contained in the ultimate design of the machine. For this reason procedures were considered and used

r 59-864, recommended by the AIEE Air sportation Committee and approved by the E Technical Operations Department for ntation at the AIEE Summer and Pacific ral Meeting and Air Transportation Confer- Seattle, Wash., June 21–26, 1959. Manu- t submitted March 23, 1959; made available rinting April 23, 1959.

. Penn, R. L. Balke, and F. M. Precopio are the General Electric Company, Erie, Pa.

authors wish to acknowledge the technical tance and the benefit of consultation provided H. Terry, J. A. Dimond, F. E. Johnson, P. A. , and J. T. Bateman, all of the General Elec- Company.

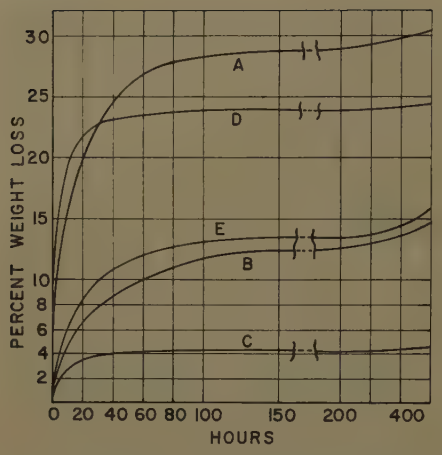

Fig. 1. Weight loss of conventional silicone resins at 300 C as function of time

based on previously successful work in the evaluation of aircraft generator insulation systems[3] as well as procedures developed and incorporated in AIEE Standards 510 and 511.[4,5] The test duty cycles of the contractor's specification were translated into time and temperature co-ordinates from which a test cycle for laboratory evaluation was evolved. To permit closer measurement of the deterioration process, moisture was included in the cycle of time at temperature, vibration, and high-potential testing so that a procedure analogous to AIEE Standard 510 was developed.

So that actual components could be evaluated, a test vehicle was developed which could be assembled by conventional manufacturing techniques and operators, and which permitted a number of measurements to be made. This fixture evaluated factory ease of handling of the components, assembly techniques, and treating procedures, while measuring the ability of the insulation system to withstand the rigorous test cycle established. With this general approach established, the details of the development program proceeded as described in the following.

Development of Materials

The mechanical and electrical properties of organic or metal-organic insulation materials are affected by such environmental conditions as humidity, vibration, thermal shock, corona, etc., but the most important deteriorating factor, either alone or in combination with these, is high temperature. As operating temperatures are raised, the number of materials which can function properly for reasonable periods diminishes rapidly. At 100 C, there are scores of organic polymers which may be used to give long life as electrical insulators under severe mechanical and chemical conditions. Treated natural fibers, polyamides, polyesters, polymers of many vinyl compounds, epoxides and phenolics are representative of these. At 200 C, this list has narrowed to no more than three or four polymer types (phenolics, special epoxides, silicones, polytetrafluoroethylene); and above 300 C, the silicones alone are serviceable but only if properly formulated and if the length of service required is very short. Therefore, as the use temperature exceeds 300 C, it is necessary to turn to inorganic or ceramic materials for electrical insulation. Their mechanical properties leave much to be desired, the electrical properties fall off badly at very high temperatures, and processing presents many difficulties. However, they inherently possess high thermal stability and therefore present a promising approach to the solution of the ultrahigh-temperature insulation problem.

Silicone Insulations

Because of the afore-mentioned disadvantages of ceramics to be overcome, and since more conventional methods and materials were not to be overlooked, two insulation materials programs were carried along in parallel with the ceramic developments.

The first was an evaluation of the top limit to be expected from conventional silicone varnishes. Motorette tests have been conducted for some time in connection with the development of insulation systems for aircraft generators.[3] The most promising high-temperature systems have been based on silicones, mica, and glass. The results of these tests indicated that a possibility existed that a silicone system could meet the requirements of this program if a silicone varnish of truly superior thermal resistance could be found. Five commercially available silicone resins were chosen for evaluation, and weight-loss tests were conducted at 300 and 450 C. Fig. 1 shows the weight-loss results at 300 C and it is evident that silicone resins can differ greatly in thermal stability. An attempt to heat-age the resins at 450 C gave very bad degradation in one hour (see Fig. 2) and the tests were not continued further. The most stable varnish was then used to treat motorettes constructed with glass-served silicone-treated magnet wire and glass-mica-glass ground and phase insulation. After baking 8 hours at 200 C, the motorettes were subjected to 6 hours at 275 C, 6 hours at 350 C, and 24 hours at 500 C. The varnish remained intact through the 350 C run but degraded to a sandy deposit after the 500 C exposure.

Fig. 2. Photograph of conventional silicone resins after 1 hour at 450 C

Leakage-current measurements at 1,20 volts to ground showed that the system were electrically sound after the 350 C aging but high leakage (30 microamperes was observed after the 500 C aging. I was concluded that conventional silicon systems could not be relied upon for us at 500 C but that, for limited exposur times, use up to the vicinity of 400 C might be feasible.

Filled Solventless Silicones

The second approach was based on a evaluation of filled solventless silicone reported to be capable of continuou operation at well over 300 C. Two dif ferent solventless silicones were com pounded with such fillers as alumina silica, barium silicate, zirconium silicate zirconia, mica flakes, glass shorts, an glass beads, to obtain the highest loading which would still be pourable. Air in hibition of cure was observed and it wa necessary to cure the materials in nitro gen. A more serious problem was th tendency of the fillers to settle out durin cure, leaving a layer of clear resin whic cracked extensively due to thermal shock

Table I. Specific Resistivity and Dielectri Strength of Three Ceramic Glazes on Steel as Function of Temperature

Temperature, C	Type of Glaze Designation A	B	C
Specific Resistivity, Ohm-Centimeters			
RT*	2.8×10^{11}	5.6×10^{8}	1.6×10
100	6.6×10^{10}	2.6×10^{8}	1.3×10
200	3.1×10^{8}	5.1×10^{7}	2.8×10
300	7.0×10^{7}	3.4×10^{7}	1.4×10
400	3.8×10^{7}	2.5×10^{7}	5.0×10
500	3.2×10^{7}	5.5×10^{6}	1.2×10
600	2.6×10^{7}	4.2×10^{5}	2.8×10
Dielectric Strength, Volts per Mil			
RT*	570	260	290
300	150	110	120
500	110	60	60
600	90	40	60

* Room temperature.

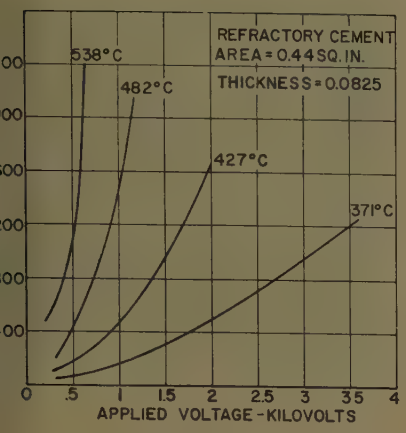

3. Leakage current as function of voltage temperature for typical low-porosity cement

s problem was overcome by the use of ll percentages of a thermally stable pending agent. The materials were t into 2-inch-diameter 1/4-inch-thick s which were then heat-aged at 300, , and 600 C. The resistance of the n-filler combination to thermal deg- ation varied greatly. A few samples ntegrated after a short time at 300 C some showed unexplainable strength r aging at 600 C, where presumably interaction has taken place. Results tatorette testing of some of these ma- als will be discussed later.

RAMIC INSULATIONS

he major effort in this program was ced on the development of ceramic apsulating compounds and glazes. glazes were studied as sealing ma- als for the encapsulating cements, and or structures, and as bonding agents the glass-mica sheet insulations and gnet wire. A large number of vitreous es were screened by resistivity versus perature measurements, dielectric akdown, humidity corrosion tests, salt ay, compatibility with substrate ma- als, thermal shock, and thermal aging. he more than 60 glazes tested, 3 were nd to withstand 100 hours in 100% (relative humidity) at 50 C, 100 rs in salt spray, thermal shock from C to room temperature, and heat ng for 100 hours at 600 C without any s of spalling, pitting, loss of gloss, or r evidence of failure. Specific re- ivity and dielectric strength of these erials as a function of temperature e measured by coating them on steel els and attaching a 2-inch-diameter trode to the glaze over a coat of con- ting paint. The results are shown in le I.

he use of refractory cements for im- gnation of windings to give a solid void-free structure would be very desirable. The cement could be applied in a wet-winding procedure or by vacuum-pressure cycling techniques. Such cements have been limited by high porosity, poor electrical properties, and short pot life.

This work has been directed at the development of low-porosity cements with reasonable pot life and acceptable electrical properties. It was found that combinations of refractories, binders and frits were capable of giving cements of very low porosity. This was accomplished by firing the cement above the melting point of the glass frit. Cements have been formulated that show less than 1% moisture absorption after boiling in water for 2 hours. The pot life of these cements can be varied from minutes to days. Leakage current as a function of voltage and temperature of a typical low-porosity cement is given in Fig. 3.

MICACEOUS AND QUARTZ INSULATIONS

In addition to these materials programs, work is in progress on the fabrication of solt liners made from mica paper saturated with a borate-phosphate complex. Slot liners have been molded successfully and used in making statorettes and test assemblies. Stability and retention of adequate dielectric properties have been demonstrated up to 600 C. Attempts are also being made to develop a mica mat slurry similar in composition to the slot liner material for use as an inorganic treating varnish. Moisture resistance is the main difficulty. A flexible flake mica composite bonded with an inorganic resin has successfully demonstrated its ability to withstand 500 C and retain moisture resistance.

The recent commercial availability of quartz fibers has led to a consideration of its use as serving for magnet wire. The build approximates that obtained with 150 series glass filaments. Test results have not been obtained with this magnet wire at this time.

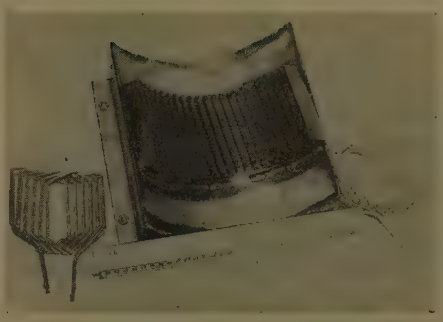

Fig. 4. Photograph of statorette fixture and coils, prior to assembly

Development of Systems and System Tests

The evaluation of materials alone or in simple combinations is useful and important for screening and selecting the components to comprise an insulation system. More often, however, the manner in which materials are combined and the processing necessary to achieve a system will cause materials to perform differently in a system from the way they do as elementary components. Therefore, the need was recognized for a system test that would provide a means to study processes for combining materials and a means to measure system performance.

DEVELOPMENT OF TEST FIXTURE

To facilitate evaluation of the insulation systems developed for this generator, a test fixture was developed embodying the electromagnetic features and configuration of the anticipated generator-stator assembly. This was done primarily to introduce the element of realism in component fabrication and placement, material processing, and finally measuring performance of the combined system under the stringent environmental conditions to be imposed on the generator. For instance, use of a realistic test fixture provides experience in handling some of the more unusual materials selected to meet the generator requirements and

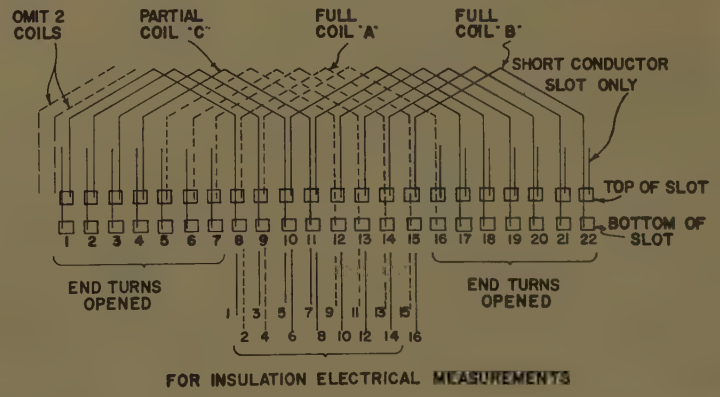

Fig. 5. Schematic diagram of statorette winding

permits study of best processing for coil bonding and environmental protection of the windings. In addition, a fixture closely resembling the generator stator provides a method to study design parameters of insulation thicknesses and spacing considered critical at the specified high altitudes and temperatures. Although test fixtures were also developed for other smaller assemblies of the generator containing insulations, this paper concerns only the stator assembly since it contains the majority of insulations, most of which are common to other assemblies.

A stator section of a production aircraft generator best met these conditions and was selected as the main element of the test device. Therefore, a production stator was selected which was approximately 10 inches in diameter, with a bore of 8.00 inches, stack length of 4.25 inches, and 66 skewed rectangular open slots having dimensions of approximately 0.190 inch wide by 0.406 inch deep. One-third sections of this production stator, simulating the anticipated high performance generator stator design, were mounted on stainless steel racks to facilitate handling and to provide a frame around the stator winding conforming closely to the generator design.

A view of this portion of the test fixture is shown in Fig. 4. It provided 22 stator slots and, by utilizing the same preformed hairpin shape coil for lap-type double layer winding, and the same span and forming fixtures employed in the selected production stator, two full coils with two conductors per slot could be inserted into these slots. A partial winding from a third coil was necessary to complete the winding. However, in so doing, a number of slots contained one conductor and a length of conductor shorter than the stack length was inserted into these slots to achieve compactness. The test fixture was designed to permit a number of electrical measurements by opening the involute ends of all coils on one end of the winding. For example, with the described configuration it is possible to obtain 8 individual measurements of conductor-to-conductor in the slots, 15 measurements of conductor-to-stator iron, and a multitude of crossover measurements in the end-turn windings. Fig. 5 illustrates this condition by schematic diagram. The developed test fixture was called a "statorette"; see Fig. 6.

The study of insulation thicknesses and spacing required can be made with this fixture by varying the conductor cross-section area. At the offset of this program, a 0.145- by 0.145-inch conductor size was selected with a 0.012-inch insulation build. Initial slot tube insulation thicknesses were 0.010 inch nominal. By allowing 0.003 inch for lamination stagger and skew, a reasonably tight slot was obtained. Increase or decrease of insulation thicknesses, which may be required for study purposes, can be achieved by a change in conductor cross section without affecting the desired compactness of slot.

To summarize, the function of the statorette is considered to be related to that of the motorette, now adopted for evaluation of insulation systems by the test procedure in the AIEE Standard.[4] The statorette is intended to satisfy the more specific requirements of this particular aircraft generator stator design.

Test Cycle

A test cycle was established primarily on the basis of the flight profile and endurance time of the high-performance aircraft. Conditions of test were patterned after those imposed on the generator with consideration for winding temperature rise, operating voltages, and conditions to provide best evaluation of the insulations.

Temperature, thermal shock, humidity, vibration, and the combination altitude and temperature were considered the most significant and critical of the many environmental conditions imposed on the generator. It was considered more practical to treat the combination altitude and temperature exposure as an independent test not to be included in the proposed cycle since such an exposure presents major evaluation problems in itself. Therefore, a tentative test cycle for evaluation of insulation systems by statorette test was established as shown in Table II.

Fig. 6. Statorette fixture with coils and insulation inserted and with temporary hold-down slot wedges of Teflon

Steps 2 through 11 of the cycle just described are repeated 10 times. This is representative of the endurance cycle and the test required of the generator. To satisfy a test condition for the overload requirement of the generator, an exposure to 600 C for 30 minutes is included after alternate 500 C exposure conditions. A test has not yet been developed for the altitude-temperature condition.

Preliminary Results

Three statorettes have been built and have completed four of the required ten cycles of heat aging, vibration, and humidity. Leakage current measurements are being made at the various stages of each test cycle to provide a nondestructive test tool for following possible degradation of the systems.

The procedure appears quite capable of differentiating between various systems, as shown by leakage current measurements taken at 1,200 volts in the fourth cycle of test. The room temperature readings were taken after a dry-out period which followed the exposure to moisture of the third cycle. The readings at 500 C

Table II. Tentative Test Cycle

Sequence	Exposure	Time, Hours	Condition
1	temperature	300	200 C oven
2	temperature	8	300 C oven
3	temperature	1	300 C to 500 C
4	temperature	2	500 C oven
5	temperature	1	500 C to 300 C
6	thermal shock		300 C to 25 C
7	vibration	1	60-cycle 30-mil amplitude
8	measurements		*IR** and leakage current
9	humidity	48	95% RH, 95 F
10	dielectric test	1 min†	208 volts, wet
11	dielectric test	1 min	1,200 volts, after drying

* Current resistance.
† Minute.

Table III. D-C Microampere Leakage on Three Statorette Insulation Systems Measured at 1,200 Volts

System	Room Temperature	500 C	95% RH	
A	0	10–25	>2,500	
B	0	5–10	70–90	p-to-g*
			400–450	p-to-p†
C	0	3–5	8–12	p-to-g
			4–10	p-to-p

* Phase-to-ground.
† Phase-to-phase.

wed the fourth exposure of 8 hours at C plus 2 hours at 500 C. The final ings were taken in the humidity net after vibration and exposure for hours to 95% RH at 100 degrees renheit. Leakage is given in micro-eres at 1,200 volts, where this voltage d be attained. On one sample, ex-ive leakage prevented reaching this age. Readings were taken phase to se, and phase to ground; see Table These readings have been main-ed throughout the test thus far.

mary

his presentation is essentially a status progress report. The detailed test results will be reported at the conclusion of the program. To summarize the work to date:

1. A test vehicle has been developed which simulates an actual generator structure to permit evaluation of factory handling properties as well as materials. It permits observation and measurement of the ability of the insulation system to withstand the deteriorating effects of a testing cycle based on specification conditions and requirements of temperature, vibration, humidity, and high-potential test.

2. There are available and in process materials and component structures whose adequacy is now being determined, and whose properties can be modified, if necessary or desirable, in order to produce a satisfactory insulation system, meeting the requirements of the generator specification for supplying electric power to hypersonic aircraft.

References

1. Ram-Air Cooling Systems for Aircraft Generators, **R. M. Moroney.** *AIEE Transactions*, pt. II (*Applications and Industry*), vol. 76, Sept. 1957, pp. 217–21.

2. Thermal Consideration of Generators in High-Speed Aircraft, **A. Kusko.** *Ibid.*, pp. 205–08.

3. The Motorette as a Tool for the Development of Improved Insulation Systems, **W. B. Penn.** *Ibid.*, pt. III-B (*Power Apparatus and Systems*), vol. 73, Dec. 1954, pp. 1505–07.

4. Test Procedure for Evaluation of Systems of Insulating Materials for Random-Wound Electric Machinery. *AIEE Standard No. 510*, Nov. 1956.

5. Test Procedure for Evaluation of Systems of Insulating Materials for Electric Machinery Employing Form-Wound Pre-Insulated Coils. *AIEE Standard No. 511*, Oct. 1956.

Battery Impedance: Farads, Milliohms, Microhenrys

E. WILLIHNGANZ NONMEMBER AIEE

PETER ROHNER NONMEMBER AIEE

HE ELECTRICAL RESISTANCE of storage batteries is important to groups of people. Designers of tele-ne equipment need to know the re-nce to alternating current in order to uate the cross talk between simulta-us telephone conversations which must through the central station battery. y must also be able to evaluate the unt of filtering required to remove , noise, and switching pulses from the ut of the charging and switching pment. In addition, designers of ral power stations need to know the tance of the battery which must sup-short pulses of power to operate elec-switches.

rprisingly little has been published t the electrical resistance of batteries. V. Vinal[1] reviews what has been pub-d. Most of the published material s with methods of test and the cause discrepancies between the various nods. There is, however, practically ata of interest to the engineer dealing commercial types of batteries.

This work, therefore, has been undertaken to supply actual measured resistance values on batteries which are of engineering interest. A series of telephone-type lead-calcium batteries was selected for this test since they appear to be the type of greatest importance today.

Definition of Terms

The battery properties to be discussed are illustrated in Fig. 1. This is an oscillogram of the cell voltage during a 1-second discharge at about the 1-hour rate. When the discharge begins there is a sudden decrease of voltage because of the electrical resistance, and then a gradual decrease in voltage caused by chemical changes occurring at the surface of the active materials. When the discharge is interrupted, the voltage recovers in the same sequence. The electrical resistance can be calculated from either the sudden voltage change at the beginning of the discharge, or the sudden change at the end of discharge.

The rest of the curve represents the result of chemical changes. The chemical changes within the battery produce a counter emf (electromotive force) called polarization. This polarization cannot be precisely duplicated by a combination of the ordinary circuit elements, but it can be approximated by a capacitance shunted by a leakage resistance. The capacitance is responsible for the initial slope of polarization curve, while the leakage resistance is responsible for the curvature of this line.

The battery also possesses a measurable inductance. The initial part of the polarization curve shows a slight irregularity. Where the current is large, or the pulse length short, this irregularity can be clearly identified as the result of battery inductance. When large batteries are being studied, the effect of inductance assumes a major importance.

The equivalent circuit of a battery therefore contains a resistance, an inductance, and a capacitance, as shown in Fig. 2. This capacitance is shunted by a nonlinear resistor. The battery resistance has been divided between the metal resistance R_m and the acid resistance R_a. The resistance of the active material has been ignored, since it is believed to be negligible.

Because of the wide range of battery sizes tested, results were reduced to an amp (ampere)-hour basis. The measured resistance was multiplied by the ampere-hour rating of the battery, and the measured capacitance was divided by the ampere-hour rating of the battery. The inductance measurements, however, are tabulated directly without calculation because they varied only slightly with battery size.

Bridge

The oscillograms were used principally to define the terms used. All batteries were first tested using oscillograms, but this report contains principally Wheat-

59-823, recommended by the AIEE Chemical try Committee and approved by the AIEE ical Operations Department for presentation AIEE Summer and Pacific General Meeting, ir Transportation Conference, Seattle, Wash., 21–26, 1959. Manuscript submitted March 59; made available for printing May 15, 1959.

LLIHNGANZ and Peter Rohner are with C & teries, Inc., Conshohocken, Pa.

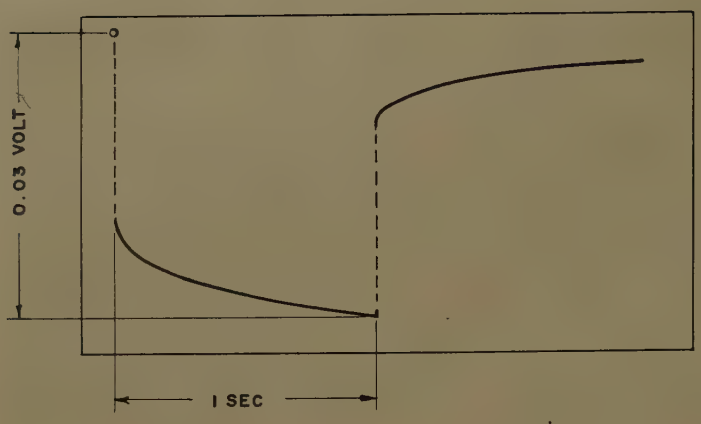

Fig. 1. Battery voltage during square wave pulse

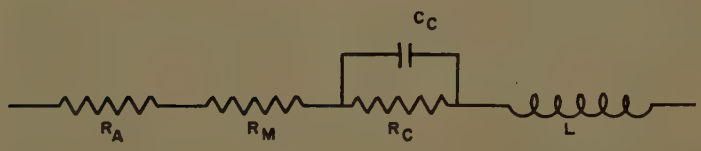

Fig. 2. Equivalent circuit of a battery

stone Bridge measurements, because they are not only more precise, but also considerably easier to obtain.

The bridge is shown in Fig. 3. The test cell was bolted directly to an ammeter shunt which served as a standard resistor R_2. The shunt was then bolted to a straight copper rod of negligible resistance which served as a variable inductor, L_2, by using a travelling contact. The ratio arm, R_4, was a 100,000-ohm fixed resistor. The measuring arm consisted of an adjustable resistor, R_3, zero to 1 megohm, and an adjustable capacitor 0 to 1 microfarad, C_3. The null indicator is a cathode-ray oscillograph with vertical plates across the bridge and horizontal plates across the variable frequency oscillator.

The bridge was used only up to 5,000 cycles because of battery properties. The bridge was checked by comparing ammeter shunts and was found to be within 1% over a frequency range up to at least 50,000 cycles.

For measurements, the bridge was first balanced for resistance and inductance at 5,000 cycles, with the capacitance omitted. The inductance setting was then left unchanged while the bridge was balanced for resistance and capacitance at 1,000 cycles.

Inductance

The inductance of batteries is summarized in Fig. 4 and is about 0.1 microhenry. The 10 to 1,000-amp-hour part of the chart describes batteries having single posts. The 300 to 1,600-amp-hour section describes batteries with double posts. For these larger batteries, a heavy copper bus-bar was firmly bolted to both positive posts, and another similar bar bolted to the negative posts. Bridge connections were made to the mid-point of these copper bars. The chart shows the result of measurements at 5,000 cycles.

The voltage developed across the inductance was measured directly with a calibrated oscillograph and compared with the voltage developed across the ammeter shunt so that the inductive reactance could be calculated. This was then translated into inductance.

Resistance

The resistance measured at 1,000 cycles and multiplied by the amp-hour capacity rating of the battery is shown in Fig. 5. The smaller batteries show 0.14 ohms for the range of 10 to 100 amp-hours. In these batteries the metal parts are relatively large, their size being determined by mechanical need rather than by electrical resistance. Calculation shows that most of this battery resistance is caused by acid between the plates. Therefore, we have considered R_a as 0.14 ohm. This represents the acid path modified by the presence of separators, glass mats, and gas bubbles.

The acid resistance can be reduced, at the expense of other battery properties, by reducing the distance between plates, increasing the porosity of the separators, or reducing the number of layers of insulation.

For the batteries of 180 amp-hours or larger, the resistance per amp-hour is no longer constant, but increases gradually. It is believed that part of this reflects the larger size without a corresponding increase in the area of the grid ribs, and the larger number of plates, which require a longer strap to connect the plates to the post. Finally, the posts contribute significantly to the battery resistance in the larger battery sizes. These effects may amount to as much as 0.1 ohm for the largest battery sizes. This resistance can be reduced by the use of copper insert posts, and by a complete redesign of the battery if such a low resistance becomes essential.

Capacitance

When alternating current is passed through a battery, one component of the voltage lags the current 90 degrees, and can be balanced in the bridge circuit by a capacitor. The calculated battery capacitance is surprisingly large and amounts to 17,000 microfarads per amp-

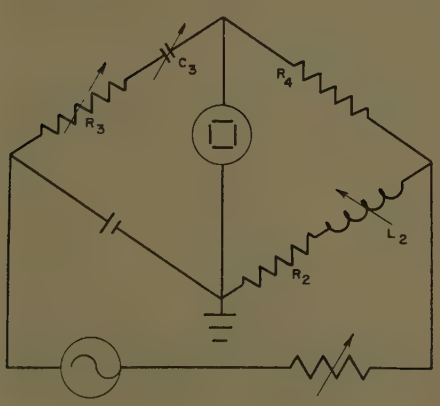

Fig. 3 (left). Wheatstone bridge

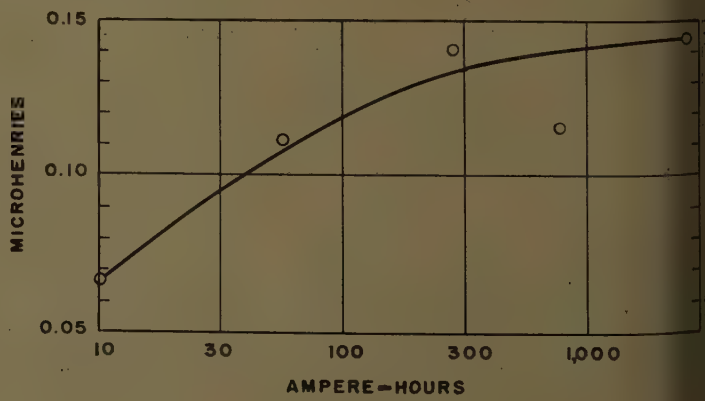

Fig. 4 (right). Inductance and battery size

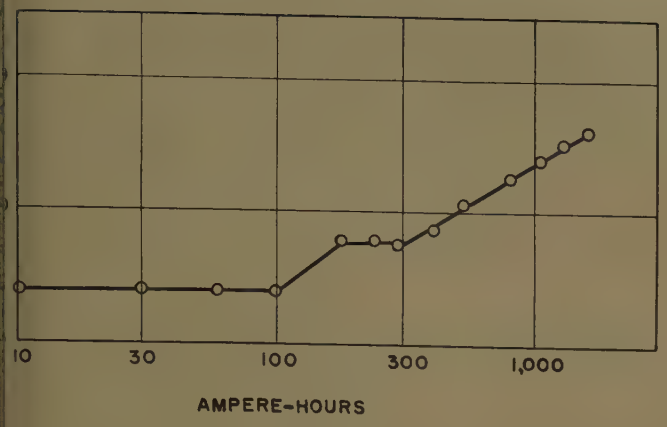

Fig. 5. Resistance and battery size

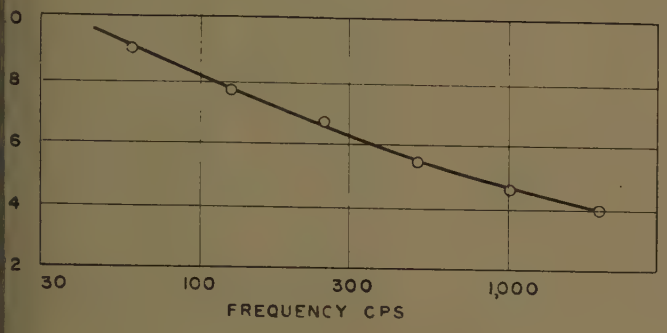

Fig. 6. Apparent resistance and frequency

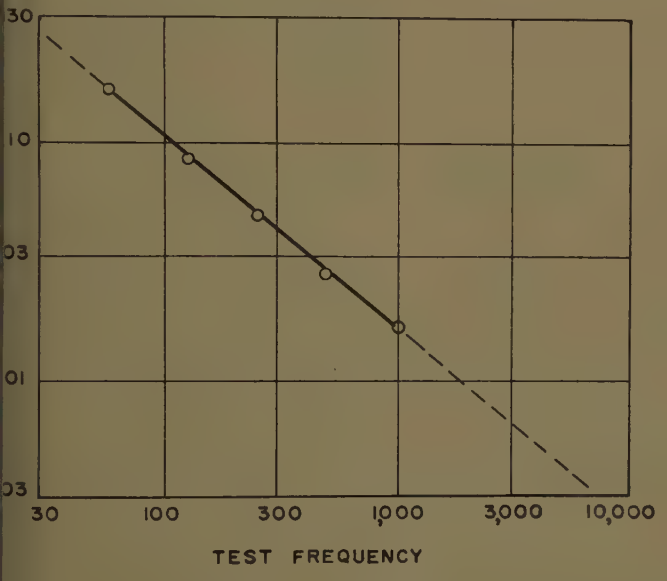

Fig. 7. Apparent capacitance effect of frequency

of capacity. A 1,000-amp-hour cell l, therefore, have a capacitance of arads. This is several orders of itude larger than any other capacitor n, and offers a new circuit element tering or energy storage applications. is capacitance is measured at 1,000 s. In view of the leakage resistance e apparent capacitance becomes conably greater at low frequencies. This e discussed later.

age Resistance

e battery capacitance describes only itial slope of the voltage curve. The subsequent slope can be approximated by using the time constant of the circuit. The time required for 63% of the polarization to disappear amounts to about 3,000 microseconds, and this time constant corresponds to that of a 0.016-farad capacitor discharging through a resistance of approximately 0.20 ohm. Since this is on an amp-hour basis, the leakage resistance is therefore 0.20 ohm per amp-hour.

Where the discharge is at a high rate, and lasts for more than a second, this simplified picture no longer appears to be valid. The shape of the curve becomes more complex, and wide variations of the leakage resistance may be observed. This aspect of battery properties is not yet clear.

Where, instead of using pulse tests, the a-c bridge is used, the capacitance and leakage resistance form a frequency sensitive network which can dissipate energy. The apparent capacitance and resistance therefore, will vary with the frequency and since the equivalent circuit is not quantitatively correct, the variation with frequency must be measured.

Table I. Measured Battery Capacitance

Amp-Hours	Capacitance, Farads	Farads per Amp-Hour
10	0.16	0.016
50	1.05	0.021
300	5.1	0.017
840	13.5	0.016

Resistance and Frequency

The internal resistance of the battery has, up to this point, been the resistance measured at 1,000 cycles, and it has been found that this is identical with the resistance read from the pulse oscillogram of Fig. 2. If the test frequency is varied, part of the a-c energy is dissipated by the chemical reaction and shows up as an apparent increase in resistance as seen by the bridge circuit. This effect of frequency is shown in Fig. 6.

Capacitance and Frequency

The capacitance tabulated previously was the value measured at 1,000 cycles. When the test frequency is varied, the apparent capacitance varies, and the results can be plotted on a straight line up to 1,000 cycles as shown in Fig. 7. At higher frequencies a battery introduces too much inductance, but by using a specially designed test cell Lange has indicated that this line is straight to at least 20,000 cycles, provided data are plotted on logarithmic scales.

Relative Importance of Impedance Components

Up to this point the discussion has been primarily on an amp-hour basis in order to minimize the effect of battery size. The absolute values of the components of the battery impedance are shown in Fig. 8 for a 180-amp-hour cell. The experimental points fall on the solid line. Dotted extensions on these lines shown where we would expect the lines to fall if the areas were accessible to experimental work.

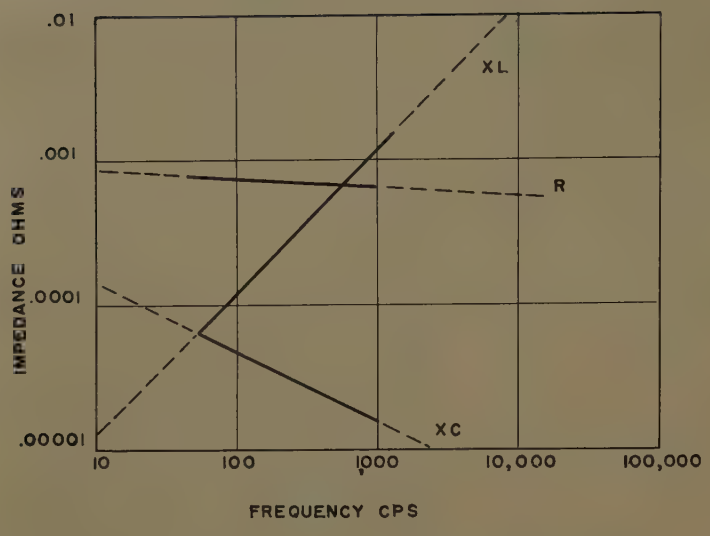

Fig. 8. Impedance components, 180-amp-hour battery

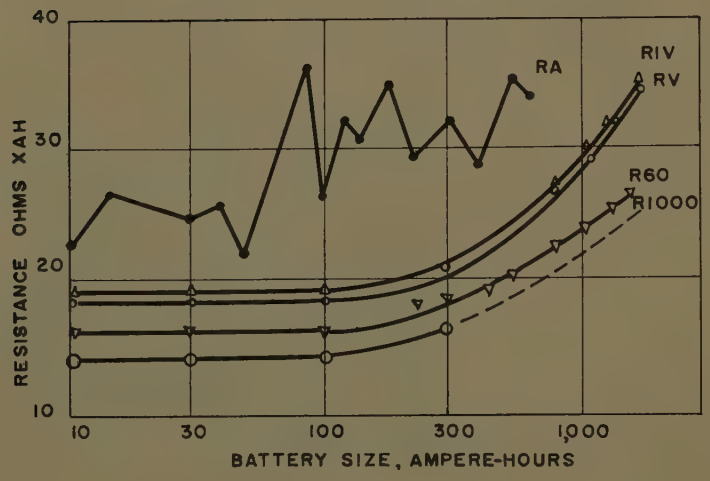

Fig. 9. Practical resistance measurements

It is clearly evident that the inductance of the battery controls its counter emf at high frequencies, and in view of the data in Fig. 4, the position of this line will not shift seriously with battery size. At low frequencies, both resistance and capacitive impedance control the counter emf. These vary inversely with battery size, and for an 18-amp-hour battery the values would be 10 times the quantities shown.

Practical Resistance Measurements

Various numbers associated with the electrical resistance are shown in Fig. 9. The bottom line shows the resistance measured by the a-c bridge at 1,000 cycles. The resistance measured at 60 cycles is shown next. This measurement avoids the need for a 1,000-cycle generator with an output of 100 amp for measuring the resistance of the larger batteries, and also makes inductance troubles less important.

The next curve, R_V, is the "virtual" resistance. If a battery is discharged for 5 seconds at a preselected current and the voltage is read immediately before, and 5 seconds after, the current interruption, the change in voltage divided by the current gives an apparent resistance which we have called the virtual r sistance.

The next curve shows the resistan R_{IV} measured by the initial-voltage lin If the voltage after 5 seconds of discharg is measured at various current levels, an the voltage is plotted against the curren this is described as the initial voltage lin The points fall on a straight line over mos of the range, and the slope of this line ca be regarded as an electrical resistanc

Finally, the top curve shows the a parent resistance R_A calculated from discharge pulse. If a battery is discharge for 5 seconds and the voltage at the en of 5 seconds is subtracted from the ope circuit voltage, and the difference is d vided by the current, the result is anothe apparent resistance.

Of these various methods of measurin resistance, the 1,000-cycle method com closest to giving the actual resistance, an the other methods include variou amounts of polarization. Obviously whenever resistance is mentioned, th method of measurement should be spec fied and we suggest that the word, "r sistance" be limited to the 1,000-cycle r sults, and the term "virtual resistance be reserved for one of the pulse test preferably the current-interruptio method.

Summary

From this discussion it can be seen th the apparent capacitance of a battery w be in the range of 1 farad to sever hundred farads depending on the size an test frequency. The resistance will 0.1 to 10 milliohms depending on th battery size, and the inductance will less than 0.1 microhenry.

These quantities are in the expecte range, except for the capacitance whi is so large that it offers an interesti challenge to the electrical enginee There must be places where a capacit with these characteristics is needed.

Reference

1. Storage Batteries (book), G. W. Vin John Wiley & Sons, Inc., New York, N. Y., 1955

The Effect of Variable High-Altitude Humidity on the Wear of Nondusting Brushes

L. E. MOBERLY
NONMEMBER AIEE

J. L. JOHNSON
ASSOCIATE MEMBER AIEE

HE important effect which water vapor has on the performance of on brushes has been recognized for y years. Prior to 1935,[1] cases of ssively short brush life were found e due to the low humidity of the cold of midwestern United States winters. ly in World War II, when bombers an flying at altitudes above 20,000 this low-humidity problem was e spectacularly demonstrated when it found that the brushes on the dc erators were wearing out completely ng flights as short as one hour. ts in simulated high-altitude atmos- res showed, conclusively, that the emely rapid wear, or "dusting," of on brushes was caused by the in- ity of the brushes to maintain icating films on commutators in the emely low atmospheric humidities ch were found to exist at high alti- es.

became necessary to develop a new e of brush for high-altitude service. se so-called "altitude brushes" con- special constituents which sub- ute for atmospheric water, providing friction running and acceptable brush even at extremely low humidities.

he earliest special-altitude brushes ch were successfully applied were the allic halide containing brushes of Dr. M. Elsey. Theories providing possible anations of the role which water, or ubstitutes, plays in maintaining lubri- ng films between carbon brushes and mutators are discussed by Elsey,[2] age,[3] Sims,[4] and Campbell.[5] This er, however, is concerned not so much the mechanism by which altitude treatments function, but rather with the actual performance of presently available high-altitude brushes under conditions which may be encountered in modern flights.

Throughout the development of high-altitude brushes, it has been necessary to rely to a great extent on evaluation data obtained from laboratory bell jar testers and simulated-altitude chambers. Since the humidity of the atmosphere has been recognized as a most important factor in brush life, this is one of the testing parameters which has been maintained at levels consistent with conditions anticipated at altitudes of actual flight. Information concerning actual humidities at various altitudes has been difficult to obtain but, until fairly recently at least, it seems to have been generally accepted that the humidity represented by a dew point of −50 C (degrees centigrade), or lower, has been acceptable for evaluating altitude brushes.

Fig. 1 shows the relationship between dew point and absolute humidity. The absolute humidity of air whose dew point is −50 C is shown to be 0.02 grain of water per cubic foot. This is a very low water content, particularly when compared with the humidity of 2–4 grains per cubic foot which is normally supplied to brushes operating at the earth's surface. It has frequently been assumed that 0.02 grain per cubic foot represents such a low level of water content that drying to still a lower humidity would produce a negligible change in the performance of carbon brushes.

Along with the development of the jet airplane, with its capabilities of flying higher and faster, the performance requirement for altitude brushes became even more severe. Where the aircraft and its equipment formerly were operated for appreciable periods at sea level, they could now be taken almost immediately to high altitudes. This meant that the brushes must be capable of performing satisfactorily under high-altitude conditions with negligible prefilming of commutators or slip rings. Brushes which meet this requirement are currently available and have become known as "immediate-filming" altitude brushes.

A number of immediate-filming brush grades have been successfully tested during the past few years in the Westinghouse laboratory bell jar tester at an established testing condition simulating air pressures at 60,000 feet altitude and at a dew point of −60 C. Some of these grades have also been operated satisfactorily on electric equipment in altitude chambers in which dew points are reported to be −50 C, or lower. Following the successful evaluation tests, as is the usual practice, these brushes have been applied on aircraft for actual high-altitude service and, in general, have shown excellent performance.

Recent data, however, indicate that altitude brushes might experience occasional erratic and unexplained accelerated brush wear on actual flight tests. Although the wear in these cases was much too low to be considered dusting, it might be several times that expected from testing experience when taking into account the altitude service which has been endured.

A study of available meterological sounding data[6,7] indicates that the absolute humidity of air between 20,000 feet and 65,000 feet probably is quite variable depending to some extent on geographical location and to seasonal fluctuations. In fact, there is good evidence that dew points of the air at 60,000 feet, for example, may vary as much as from −50 C to −80 C.

It occurred to us that although the difference in the total water content of air with −50 C dew point and −80 C dew point is extremely small, altitude brushes

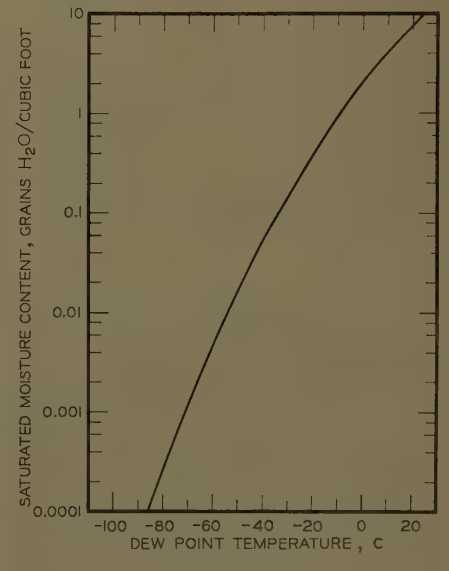

Fig. 1. Grains of moisture per cubic foot (saturated gas) versus dew-point temperature

r 59-565, recommended by the AIEE Air sportation Committee and approved by the E Technical Operations Department for ntation at the AIEE Summer and Pacific ral Meeting and Air Transportation Confer- Seattle, Wash., June 21–26, 1959. Manu- t submitted August 1, 1958; made available rinting February 24, 1959.

. MOBERLY and J. L. JOHNSON are with the inghouse Electric Corporation, Pittsburgh, Pa.

authors wish to acknowledge the advice and sel of Dr. H. M. Elsey, chemical consultant, originally foresaw the possibility of the effects ed out in this paper.

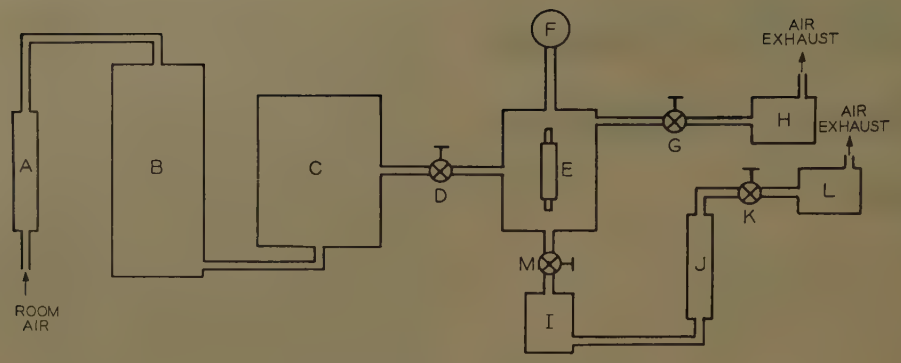

Fig. 2. Schematic of components comprising air-flow system

A—Flow meter
B—Air predryer and purifier
C—Air-humidity control
D—Constriction
E—Test chamber, slip ring, brushes
F—Vacuum gage
G—Valve
H—Vacuum pump
I—Dew-point cell
J—Flow meter
K—Valve
L—Vacuum pump
M—Valve

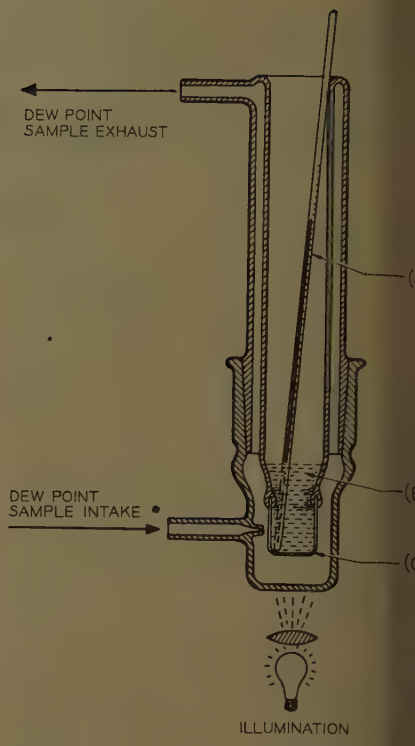

Fig. 3. Cross section of dew-point cell

A—Thermometer
B—Cooling medium
D—Mirror polish cup

still might be sensitive enough to be affected appreciably by this difference. If this were true, the erratic brush wear which has been experienced on actual altitude flights could be explained by variable atmospheric humidity.

Apparatus and Techniques

A laboratory bell jar tester, employing all the usual precautions for preventing contamination from organic materials and other sources, was utilized for this investigation. The tester has been generally described in an earlier paper[8] and only slight modifications in the air-flow system were necessary for the present high-altitude tests. The brushes and brush holders were the same design as are currently applied on the exciters of some aircraft alternators. Two brushes, one of each polarity, were held at 15-degree trailing angles on a helically grooved copper slip ring with a spring pressure of 6 pounds per square inch. The $3^1/_4$-inch-diameter ring was operated at a peripheral speed of 2,930 feet per minute. Electrical load on the brushes was supplied from a 3-phase full-wave rectifier and was automatically controlled at preselected current levels.

A schematic diagram of the air-flow system is shown in Fig. 2. The air-flow rate, measured at atmospheric pressure at *A*, was maintained at 10 cubic feet per hour. The air was predried and purified at *B* by being passed through a tower filled with activated alumina. This purified air was then passed into a humidity control unit *C* which varied to some degree depending upon the humidity level desired for a particular test. A constriction at *D* expanded the air to a pressure equivalent to 60,000 feet altitude inside the test chamber *E*, measured by gage *F*, and maintained by vacuum pump *H* through a control valve *G*. A dew-point measuring apparatus *I* was connected to the test chamber. A measured flow of air, using flow-meter *J*, could be drawn from the test chamber through the dew-point apparatus using vacuum pump *L*. This air constituted a small fraction, 5%, of the total air flowing through the system. Thus, a direct measurement of the humidity existing in the test chamber could be made at any time during the test.

Humidities were measured by the dew-point cup method which has been found by experience to give very reliable measurements, particularly in the range studied.[6,9] The actual apparatus used, shown in Fig. 3, is one of the many modifications of cooled cup devices which can be used for measuring dew points.

An important feature of this particul apparatus is that it can be used at the lo air pressures which exist at high altitude The techniques utilized in obtaining t dew point of the air were those common practiced. A dry-ice–acetone mixtu was used as the coolant and the temper ture was measured with a calibrated, lo temperature thermometer.

The observation of the dew point, frost point, was enhanced through the u of special illumination on the mirror. T amount of moisture present in the air

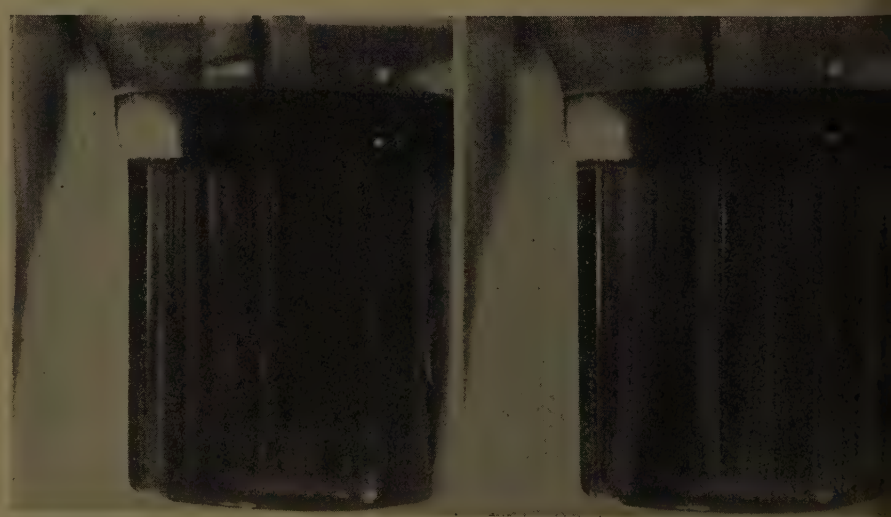

Fig. 4. Appearance of dew-point mirror before (left) and after (right) frost formation

I. Comparison Between Calculated and Measured Humidities with Westinghouse Dew-Point Cell

Condition of Air							
Before Pressure Reduction			After Pressure Reduction				
	Measured Humidity			Calculated Humidity		Measured Humidity	
sure, neters cury	Dew Point, C	Grains per Cubic Foot³	Pressure, Millimeters Mercury	Dew Point, C	Grains per Cubic Foot³	Dew Point, C	Grains per Cubic Foot³
19	+17	6.30	54	−18	0.474	−19	0.430
19	0	2.15	54	−29	0.161	−31	0.135
19	−28	0.18	55	−52	0.0138	−51	0.0155
19	−44	0.034	55	−64	0.0026	−64	0.0026
19	−47	0.024	19.5	−74	0.00065	−74	0.00065

points of −60 C, or below, is quite l and thus very light deposits of frost obtained. It has been found that at e dew points the moisture condenses he mirror as individual minute ice tals which can be observed, readily, through their reflection of light from ial light source. Fig. 4 compares the arance of a dew-point mirror before forms and at a dew point of −74 C. e data in Table I were taken to show reliability of the dew-point readings n with our apparatus. In this case, was passed through a completely d glass system and its humidity sured, first at room pressure and again expansion to a low pressure. By suring the pressure of the air at both itions, it was possible to calculate the humidity should be at the expanded pressure from the easily measured and controlled value obtained at room pressure. The table shows quite good agreement between measured and calculated dew points indicating very good reliability for our measuring apparatus and techniques in the range of humidities investigated.

For this investigation on brushes, it was desirable to test at several humidity levels while maintaining the air pressure, or "altitude," at a fixed 60,000 feet. This was accomplished by making variations in the air humidity control unit referred to previously. For example, to provide a humidity of −20 C at 60,000 feet altitude, air was saturated with water at +17 C at room pressure in the air-humidity control unit. The ultimate expansion of this air to the 60,000 feet altitude pressure resulted in an atmosphere whose dew point was −20 C. Similarly, air saturated at 0 C at room pressure, when expanded, gave dew points in the order of −30 C to −35 C. For humidities in the range of −55 C dew point, the air was saturated at −30 C before expansion. For the lowest humidities tested, the air was passed through a dry-ice-cooled tower prior to expansion to 60,000 feet altitude. Resulting dew points in the range of −65 C to −80 C were measured.

It should be pointed out that the calculated humidity of air which is saturated at dry-ice temperature and then expanded to a 60,000-foot altitude is considerably lower than the −65 C to −80 C which was obtained. The difference can be easily explained by the occurrence of extremely small and variable leakage of room air into the low-pressure system. This leakage is one of the problems universally associated with simulated altitude testing and is the reason why humidity must be measured in the test chamber itself. We have had the opportunity of measuring humidities in several altitude chambers in which it was customary to calculate "chamber humidity" from the values measured on the ventilating air prior to expansion. In every case, considerably higher humidity values were found than had been assumed. Calculated air humidities can be reliable

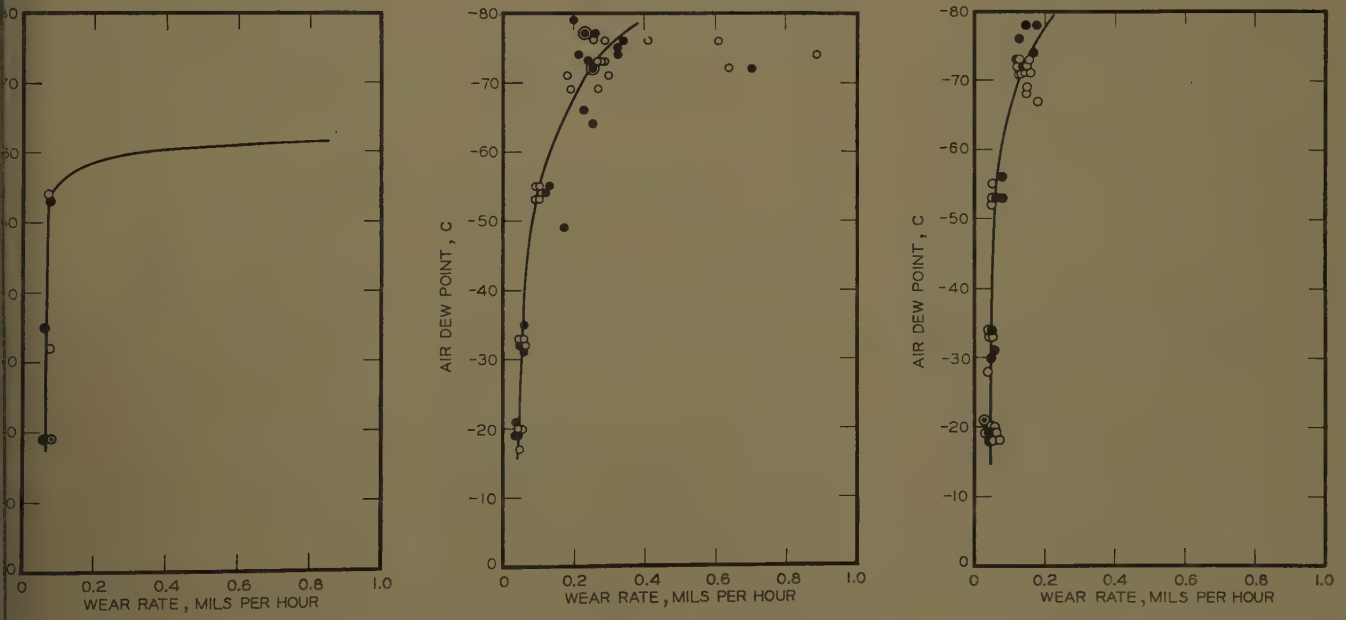

Fig. 5. Wear rate of brushes as a function of air humidity

A—Type A brushes
B—Type B brushes
C—Type C brushes
Operating conditions: 60,000 feet altitude, 6 pounds per square inch, 2,930 feet per minute
● 107 amperes per square inch
○ 60 amperes per square inch

only if the system is absolutely tight since even a small leakage of moist room air into the extremely dry test chamber will produce a major change in the ultimate humidity level.

For example, a normal value for room air humidity is 50% relative humidity at 25 C. This corresponds to an absolute humidity of 5 grains per cubic foot. The absolute humidity of air whose dew point is −80 C is 0.00026 grain per cubic foot. Thus, when these two are mixed, as occurs in a leaking "altitude" system, the humidity ratio involved is 20,000 to 1, i.e., one volume of room air leaking into 20,000 volumes of dry chamber air would double its water content.

Experimental Results

The brushes tested were commercially available grades of the immediate-filming type. The principal filming agent in all the brushes was molybdenum disulfide (MoS_2), which has become established as the most generally applied material for obtaining high-altitude protection without prefilming. The brushes studied were conveniently separated into three types based essentially on the manner in which the MoS_2 was applied. All three types contained the same weight ratio of MoS_2 to carbon in the working section of the brush. In brush type *A*, the MoS_2 existed as extremely fine particles which were uniformly distributed throughout the brush structure. The MoS_2 in the type *B* brushes, while being present in the same weight ratio, was concentrated in small localized areas in the brush structure. Type *C* brushes were similar to type *B* with the exception that a small amount of barium fluoride was also added to the brushes.

In all tests, the brushes were operated with electrical load at earth's surface conditions for one-half hour on a freshly cleaned ring prior to being measured and taken to 60,000 feet altitude pressure. They were operated at this altitude for 24 hours. The humidity was maintained at a steady value for each test and several humidity levels were investigated for each brush grade. Brush wear rates were calculated from the change in length of the brushes occurring during the high-altitude testing period.

Since the electrical load on brushes may vary considerably in actual flight service, it was interesting to determine what effect load conditions might show on brush wear. Two loads, 60 amperes per square inch and 107 amperes per square inch were compared as representing typical load variations. It can be seen from Fig. 5

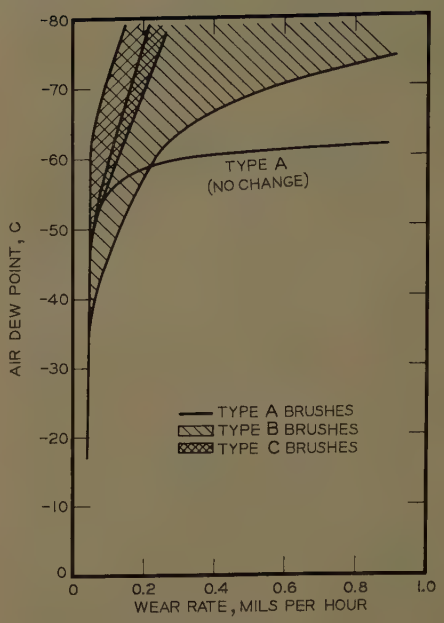

Fig. 6. Brush-wear rate range as a function of air humidity

60,000 feet altitude, 6 pounds per square inch, 60–170 amperes per square inch, 2,930 feet per minute

that no detectable difference in wear occurs within this load range.

Fig. 5(A) is a curve showing the relationship between brush wear rate and humidity for brushes of type *A*. These brushes appear to operate uniformly well at humidities represented by dew points down to −50 C. The brushes become very sensitive to humidity below this level, wear rates actually approaching dusting below the critical dew point of −55 C.

Fig. 5(B) shows the data obtained with type *B* brushes. As observed for the type *A* brushes, these also show a sensitivity to humidity level. A very gradual increase in wear rate occurs as the humidity drops from −20 C dew point to −55 C dew point. As the humidity is decreased still further to dew-point values between −70 C and −80 C, the wear rate increases several fold. In addition, the wear rates obtained from duplicate tests under the lowest humidity conditions are quite variable whereas those at dew points of −55 C, or above, are quite uniform.

The effect of humidity on the wear rate of a third type of immediate-filming brush, type *C*, is shown in Fig. 5(C). Here again, the increasing wear rate occurs at humidities lower than −55 C dew point. In this case, however, the wear rates are still reasonably low even under the lowest humidity conditions which were studied.

Fig. 6 shows the combined test results from all three brush types. Here the range of wear rates obtained for a la number of tests on each brush type shown as a shaded area. A comparis between the different types shows th in respect to wear rate, an improvement brush life is gained in going from type through type *B* to type *C*. Wear rates type *C* brushes are lower and much m consistent than was found for the ot two types. No area is shown for the ty *A* brushes since very little range w observed in their wear performan Down to −50 C dew point, the valu were quite uniform from test to test, wh at lower dew points the wear rate w extremely rapid. Thus, the humid level near −55 C dew point appears to quite critical for brushes of this type a they are expected to be unsatisfactory extended periods at humidities at or bel this level. Type *B* brushes fall somewh between the others, becoming somewh erratic in wear at humidities lower th −70 C dew point.

Since the geometry of the added M is the major difference between type and type *B* brushes, it is apparent th this is important in providing the diff ences in wear characteristics noted tween the two types. No positive c clusion has been developed to explain w this is so but it is interesting to conjectu

MoS_2 is a good dry lubricant in v uum[10] in the absence of moisture. It presumed that the low-humidity prot tion of carbon brushes by MoS_2 is due this dry lubricating effect rather than a chemical reaction with the meta commutator or slip ring to produce lubricating film. Since the friction graphite is increased as the humidity lowered a condition is reached un which a given proportion and arran ment of MoS_2 in a carbon brush becon unable to provide sufficient lubrication maintain a low wear rate. In the case type *A* brushes, for example, a criti point is reached at −55 C dew point a high brush wear results. This effect shown to some extent in all three br types with the critical humidity occurr at a different level for each.

Since type *A* brushes contain the sa proportion of MoS_2 as type *B* brushes is evident that the latter utilizes its lu cant more efficiently. This might explained by the fact that the M which exists in type *A* brushes in a p ticle size of the same order as brush w particles, is uniformly distributed in carbon network in the brush. This fectively dilutes the MoS_2 over the contact area of the brush. As brush w occurs, a relatively high percentage these MoS_2 particles become thrown

the wear dust and thus cannot be sferred to the brush track to help ntain a low-friction film.

contrast, in the type *B* brushes, the e MoS_2 particles are held firmly in the on structure. As each particle be- es exposed at the brush face through nal brush wear, it is rubbed directly the ring surface and thus a heavily ed area is developed on the brush k. With the random distribution of S_2 particles, practically all areas of the sh track receive the benefit of the ing action. Since the mechanical load rimarily supported by these heavily ed areas, the net result is lower wear better altitude protection for the e *B* brushes.

he improvement exhibited by type *C* shes can be explained by the extra ning" obtained from the barium fluo- whose properties as a high-altitude sh treatment are well known. The cts of MoS_2 and BaF_2 appear to be itive.

lthough this study has been extremely ul in the evaluation of brushes for stinghouse aircraft equipment, it is gnized that there are many character- s of brushes, in addition to wear rate, ch must be considered when making selections for individual machines. Therefore, it should be emphasized that brushes of types *A*, *B*, or *C* are not being ranked here for any specific application on the basis of the foregoing data. The chief purpose of this particular study has been to show that all altitude brushes are affected by variable atmospheric humidity and that the level at which this becomes critical varies from one type of brush to another. Even the best brushes show wear rates at −80 C dew point which are four times those at −55 C dew point.

Summary

It is well known that untreated carbon brushes show dusting wear at high altitudes due to the existence of extremely low air humidity. Even though modern, specially prepared, altitude brushes may not experience this disastrous dusting wear, evidence is presented in this paper which indicates that their wear rates are a function of the absolute humidity of the high-altitude air. Previously unexplained cases of erratic brush wear on actual flights can now be explained by the range of fluctuations which may occur in the humidity of the atmosphere at present flight altitudes.

References

1. The Effect of Humidity on Brush Operation, **J. V. Dobson.** *Electrical Journal*, East Pittsburgh, Pa., vol. 32, Dec. 1935, pp. 527–28.

2. Treatment of High-Altitude Brushes by Application of Metallic Halides, **Howard M. Elsey.** *AIEE Transactions* (*Electrical Engineering*), vol. 64, Aug. 1945, pp. 576–79.

3. Graphite Lubrication, **R. H. Savage.** *Journal of Applied Physics*, New York, N. Y., vol. 19, Jan. 1948, pp. 1–10.

4. The Wear of Carbon Brushes at High Altitudes, **R. F. Sims.** *Proceedings*, Institution of Electrical Engineers, London, England, vol. 100, pt. I, July 1953, pp. 183–88.

5. Wear of Carbon Brushes in Dry Atmosphere, **W. E. Campbell, R. Kozak.** *Transactions*, American Society of Mechanical Engineers, New York, N. Y., vol. 70, July 1948, pp. 491–98.

6. Meteorology of the Lower Atmosphere, **G. M. B. Dobson, A. W. Brewer, B. M. Cwilong.** *Proceedings*, Royal Society of London, London, England, series A, vol. 185, Jan.–Apr. 1946, pp. 144–75.

7. Some Measurements of the Distribution of Water Vapor in the Stratosphere, **Earl W. Barrett, Lee R. Herndon, Jr., Howard J. Carter.** *Tellus*, Stockholm, Sweden, vol. 2, 1950, pp. 302–11.

8. Air Humidity and Brush Contact Drop, **Howard M. Elsey, Lawrence E. Moberly, John L. Johnson.** *AIEE Transactions*, pt. III (*Power Apparatus and Systems*), vol. 73, Dec. 1954, pp. 1383–89.

9. The Measurement of Water Vapor in Air and Other Gases, **Elmer R. Queer, E. R. McLaughlin.** *Bulletin no. 224*, Pittsburgh Lectrodryer Corporation, Pittsburgh, Pa.

10. Investigation of MoS_2 Lubrication in Vacuum, **Virgil R. Johnson, George W. Vaughn.** *Journal of Applied Physics*, vol. 27, no. 10, Oct. 1956, pp. 1173–79.

evelopment of Fuses and Terminals for High-Temperature Applications

W. F. BONWITT MEMBER AIEE

H. BUTTNER MEMBER AIEE

OMPONENTS TO BE developed under the Hotelec program include s, terminals, and splices. The most ificant new requirement of this pro- n as it affects these components is the nsion of the temperature level to 850 degrees Fahrenheit) for terminals and ces, and to 600 F for fuses; these are ient temperatures with conductor peratures reaching 1,000 F. Other ificant requirements are for the de- s to withstand vibration to 20 *g* vitational acceleration) at a frequency of 80 to 2,500 cps (cycles per second); acoustic noise of 150 decibels, as well as shock of 50 *g* for 11 milliseconds. The altitude of 80,000 feet demands resistance to ozone, and requires consideration of the effects of corona. Similarly, the significant increase of temperature makes it necessary to limit thermal voltages at junctions to 0.1 millivolt.

It was felt that the increased temperature was very likely to be the most rigorous new requirement. Therefore, the materials used in present designs were analyzed. In the case of terminals and splices, which are preferred in the preinsulated, compression type, it soon became obvious that new materials or techniques would have to be developed. In the case of fuses, the new temperature requirement made it necessary to replace plastics with ceramics. New methods and materials to join them to the metal components of the fuse also became necessary.

Hotelec developments are carried out under a general scheme of five phases:

Phase I: analysis of requirements, the state of the art, and preliminary material selection. Planning of Phase II.

Phase II: selection of materials based on screening tests. The determination of suitable design concepts and planning of Phase III.

Phase III: construction of breadboard models and tests to prove out their feasibility. Specification for prototypes and planning of Phase IV.

Phase IV: construction of prototypes. Qualification tests following the applicable specifications.

Phase V: preparation of design manuals.

At this time both developments are at various stages of Phase III. The problems encountered and the progress made to date are described separately for fuses, and for terminals and splices.

Terminals and Splices

The most direct approach to the achievement of high-temperature terminals and splices would be the substitution of high-temperature materials for those

r 59-771, recommended by the AIEE Air sportation Committee and approved by the E Technical Operations Department for ntation at the AIEE Summer and Pacific ral Meeting and Air Transportation Confer- Seattle, Wash., June 21–26, 1959. Manut submitted March 13, 1959; made available rinting April 8, 1959.

F. Bonwitt and H. Buttner are with the dy Corporation, Norwalk, Conn.

Fig. 1. Preinsulated terminal

used in existing designs which are generally limited to temperatures below 400 F. Present terminals consist of a conducting body made of copper or copper alloy suitably plated and an insulating sleeve made of a thermoplastic material such as vinyl, nylon, or Kel-F. While there is little doubt that materials and finishes suitable for the conducting body exist and require only evaluation and selection, the same can hardly be said for the insulating sleeve. Materials which will withstand the plastic deformation under load incident to crimping and which will provide wet dielectric strength throughout the temperature range −65 F to 1,000 F do not exist and are not readily discernible on the technological horizon. Thus, the problem of preinsulating constitutes the main challenge to the designer of high-temperature terminals and splices.

Over 30 means of attaining preinsulated terminals have been considered. Most of them have been discarded in the conceptual stage when measured against the practical yardsticks of size, weight, reliability, and the requirement for field maintenance installation tools. Following are some which have been considered extensively:

Fig. 1 shows a conventional terminal body with a fiberglass insulating sleeve. Crimping imposes a severe stress on the sleeve. Single, double, and triple layer sleeves, each layer 0.015 inch thick, were employed and the resultant assemblies subjected to a dry dielectric test. Marginal results were obtained with single and double sleeves but triple layer sleeves provided dielectric values of 2,400 volts, well in excess of the 1,200 volts considered

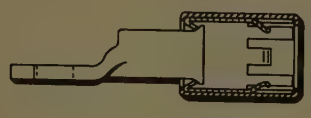

UN-INSTALLED

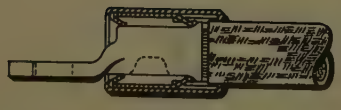

INSTALLED

Fig. 2. Post-insulated terminal

a minimum test value. Of course, it is highly desirable to provide wet dielectric strength in terminals and splices since they will be subject to humidity and may be in contact with each other or grounded material in any practical application. This leads to the search for a material to impregnate the fiberglass and make it water repellent. Such material must have enough tenacity or affinity for the fiberglass to remain in sufficient quantity under the crimp to carry out its assigned function. It must not carbonize or otherwise act as a conductor at any temperature up to 1,000 F and must retain its water-repellent quality up to this temperature.

A second approach to the insulating sleeve problem is the use of a heavily anodized aluminum sleeve. Anodized aluminum wires have reputedly been used successfully in high-temperature transformer and motor windings. The voltage between adjacent turns or layers is of course much lower than that which is required for terminals and splices. There is considerable doubt as to the ability of such coatings to withstand the crimping forces and the dielectric strength required. Anodized coatings are porous and wet dielectric strength is questionable of attainment. This is therefore not considered a very promising approach.

Flexible ceramics have been suggested. These materials are flexible to a limited degree and then only in the "green" state in which they are also highly water absorbent. Thus their use would require curing after crimping, hardly feasible for field maintenance.

While the prospects for a preinsulated terminal having wet dielectric strength are not too promising, there are several alternate courses to be pursued.

Fig. 2 shows what might be termed an almost preinsulated terminal. Crimping is done directly on the terminal barrel itself. The captive insulating sleeve is then pushed forward until it locks in place. This approaches the convenience of a preinsulated terminal. The terminal size can be kept within reasonable limits if a ceramic-clad metal sleeve is used and if crimping is such as to keep the terminal barrel within its original outline. Such crimping is attained without undue complexity in tools. This design is suitable for splices as welll as terminals. A limitation is that insulation grips are not readily incorporated without adding extra length. The sleeve retainer would have to be approximately 1/8 inch away from the end of the grip-closing die during installation.

Sometimes a difficult problem can be met by eliminating it. Fig. 3 shows termination which is so compact as eliminate the need for insulation. (viously the tongue thickness becomes cessive for large size conductors. Ho ever it seems quite practical as to size a economy for wire sizes No. 16 and small Such wires constitute at least 90% of a aircraft or missile electrical system. sulation grips also seem feasible in th small sizes. This concept is obviously suited to splices. A possible comprom solution of the over-all problem is the of Fig. 3 for small size terminals and use of Fig. 2 for larger terminals and sizes of splices since insulation grips not essential for satisfactory performan of splices and large size terminals. T solution would entail the use of duplic crimping tools for small size termin and splices. Therefore, the search fo solution which is applicable to both ter nals and splices in a given size, or wh offers a more acceptable compromi continues.

The determination of suitable materi and finishes for the conducting body o terminal or splice is not nearly so f midable. In Phase I the known ch acteristics of various metals were viewed. Nickel, silver, and copper w selected for further investigation.

The type of nickel selected for furt study is known as *A* nickel, electro grade. This nickel has about 27% of conductivity of copper and has a efficient of thermal expansion very cl to that for steel. It is magnetic at te peratures up to 680 F, having a maxim permeability, μ at 20 C (degrees cen grade) of 600 as compared with iron wh has a value of 5,000. From its modu of elasticity and thermal expansion it

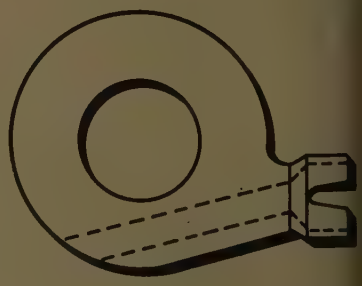

Fig. 3. Washer-type terminal

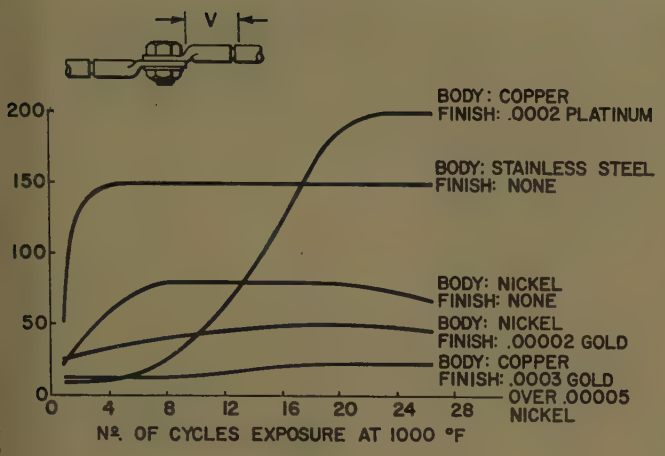

Fig. 4. Effect of high - temperature cycling on various terminal materials and finishes. Each cycle consisted of 7 hours ar 1,000 F with 46 amp, and 17 hours of room temperature and nc load. Conductor was MT-6 as specified in reference 1

edicted that nickel will not creep under mping pressures which would normally encountered. This was borne out in ase II screening tests in that the initial htening torques for stainless steel bolts ed to clamp together terminals made of kel, did not change after repeated posures to temperatures of 1,000 F. lower conductivity relative to copper s reflected in these tests by a higher ltage drop. This can be partially offset plating with gold which has a lower ntact resistance and, being softer, proles more points of contact and therefore eater effective contact area. The magtic properties of nickel do not seem to ult in undue heating or other unsirable effects in the applications inded. Nickel-clad copper conductors described in reference 1 have been ed for some 10 years in aircraft elecal systems without reported difficulty. It was suggested that the high-nperature properties of silver would be proved when alloyed with small pertages of magnesium and nickel. It s found however that the conductivity this material changes markedly after en a few cycles of exposure to high nperatures. The voltage drop at rated rrent increased tenfold after only 6 cles. Thus, this material was dismissed m further consideration.

As regards copper, only the type known OFHC (Oxygen Free High Conducity) was considered. Its surface must protected because of its high oxidation e at elevated temperatures. Its modu- of elasticity and coefficient of thermal pansion are such as to introduce a ques- n of the extent to which it will creep der elevated temperatures. As meas- d by the starting torque required to ighten a stainless steel bolt and nut mping two such terminals together er each exposure to elevated tempera- e, the creep is sufficient to cause a p in torque of approximately 50%. At the same time, retightening such bolted assemblies did not materially alter the voltage drop across the bolted connection. Thus, the type of difficulty encountered in the use of aluminum at substantially lower temperatures is not anticipated here.

The finishes considered were nickel, silver, gold, platinum, and rhodium. Different thicknesses were studied and in some cases nickel was used as an undercoat. The possibility of a stainless steel cladding on copper was also studied.

It had been reported that nickel could develop extremely high contact resistance after exposure to high temperature. This was observed in the case of a thin (0.0001/0.0002-inch) nickel plating on copper. After 4 and 5 cycles of high-temperature exposure it required 18 and 25 volts respectively to pass current across the interface of two such surfaces. This was not observed with nickel plating of approximately 3 times this thickness. In fact, the "starting" currents for all other materials and finishes tested were below 4 microvolts, which was the limit of sensitivity of the instruments used.

Gold appears to be the most satisfactory finish for this application. Fig. 4 shows the effect on voltage drop of repeated exposure to high temperature. Gold alone over copper permits oxidation of the copper, particularly where the plating has been thinned under the crimp. A nickel under-plate provides a degree of protection against this oxidation.

The requirement that the thermal voltage between the terminal and the conductor due to the thermocouple effect shall not exceed 0.1 mv (millivolt) through a conductor temperature range of −65 F to 1,000 F, seems to impose a severe restriction on the choice of material. The thermal voltages generated by several metal combinations at 1,000 F referred to a similar cold junction at 32 F are as follows:

Junction Metals	Thermocouple Voltage, Mv
Copper/Nickel	13.5*
Copper/No. 304 Stainless Steel	3.12†
Nickel/No. 304 Stainless Steel	−9.86†

* From American Institute of Physics Handbook, McGraw-Hill Book Company Inc., New York, N. Y., 1957.
† Data furnished by Lewis Engineering Co., Naugatuck, Conn.

While it is likely that a temperature difference of approximately 1,000 F may exist between the ends of the conductor, the temperature gradient across the terminal itself is very small. Assuming a nickel terminal on copper wire, an unlikely temperature gradient of 35 F across the terminal would be required to produce a thermocouple potential of 0.1 mv. The conductor will very likely consist of a copper core clad with nickel. While this combination would undoubtedly complicate the computation of junction potentials it cannot help but further improve a presently tolerable condition.

Consideration of the generated thermal voltages listed above leads to the suspicion that a problem may exist where the aircraft structure is used for grounding since this structure will be at various temperatures at any given moment. Such considerations are however outside the scope of the development of high-temperature terminals and splices.

High-Temperature Fuse

The fuse is to be self-indicating, with one size (configuration) accommodating several current ratings from 1 to 60 amperes. The fuse should also be as small and light as possible, and shall be distinct from present low-temperature fuses so that any chance of accidental mix-up is eliminated. As specified now and shown in the time-current relation Fig. 5, the primary application will be for system protection. However, wire protection may become a requirement later on, making a change of the time-current characteristic curve necessary. The fuses

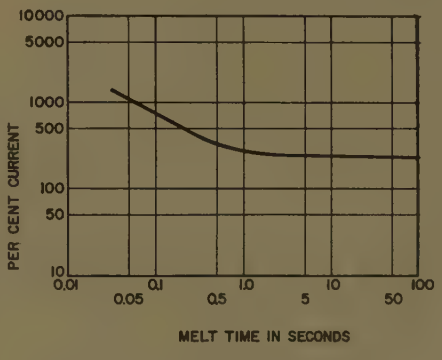

Fig. 5. Time-current characteristic

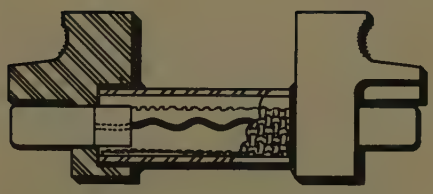

Fig. 6. Visually indicating fuse

are to be used in 3-phase 115/208-volt 400-cps electrical distribution systems so that the various electrical properties of presently available low-temperature fuses will generally remain unchanged.

The test requirements for the fuses are listed in reference 2. Some of the significant tests follow.

A Life Test requires the fuses to carry rated current at an ambient temperature of 100 F for 300 hours at sea level. This is followed by a 100-hour test, divided into 10 cycles of 8 hours at 100 F and 50,000-foot pressure altitude, and 2 hours at 600 F at 80,000-foot pressure altitude. Finally the fuses are exposed for 100 hours at 100 F at sea level. No change of characteristic may result from this test.

A Temperature Shock Test requires the fuses to pass the temperature range from −65 F to 600 F at a rate of 150 F per minute, carrying rated current.

The fuses have to interrupt a maximum current of 4,000 amp (amperes) line-to-ground at 115 volts, 400 cps; a maximum current of 2,500 amp line-to-line at 200 volts, and 4,000 amp at 28 volts direct current. These interruptions have to be accomplished at a pressure altitude of 80,000 feet and at an ambient temperature of 600 F. The arcing time may not exceed 0.002 second.

A Wet Dielectric Test requires immersion of the holder and the fuse separately for 10 seconds in tap water, followed by unagitated drainage for 1 minute. After the fuse is inserted into the holder a potential of 1,200 volts has to be maintained between fuse and ground for 1 minute. The test is performed with the assembly in three mutually perpendicular planes.

When tested after being loaded with rated current for 1/2 hour, the time-current characteristic may not deviate by more than 10%, nor is an overload of 5 times the rated current for 0.1 second, repeated 10 times, to affect the melting characteristic of the fuse. It is of interest that during all tests that may affect the fuse by the high ambient temperature, the fuse and holder must be mounted on a titanium panel 0.05-inch thick.

Two types of self-indicating fuses for temperatures to 250 F are available today: mechanically indicating fuses, and fuses where the interrupted fuse wire itself, or a separate indicator wire in parallel with the fuse wire, acts as a visual indicator. Since visually indicating fuses are much simpler, having no moving parts, it seemed desirable to select this type for high-temperature application.

Visually indicating fuses consist of a tubular translucent housing made usually from a Pyrex glass as shown in Fig. 6. Cemented to the ends of this housing are two molded heat-resistant plastic end caps. These caps act as supports for the blade contacts that terminate the fuse wire. The blades connect to corresponding contact clips in the separate fuse holder or base. The caps also provide convenient finger grips to insert and remove the fuse from its base without the use of tools. A spent fuse is recognized by the break in the fuse wire visible through the glass housing. In larger fuse ratings the considerable arc energy released under certain operating conditions makes it necessary to fill the housing with an arc-quenching filler as shown in Fig. 7. This makes the fuse element invisible, and in such ratings an indicating element in

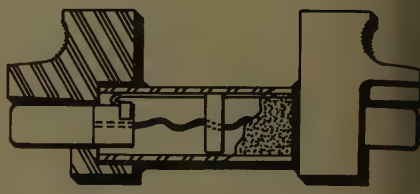

Fig. 7. Visually indicating fuse with separat indicator

parallel with the fuse wire is placed ad jacent to the inside wall of the glass tubin making it readily visible from the outside

The fuse holder is usually a molde block accommodating fuses of the sam physical size, but not necessarily of identi cal ratings. Open contact clips engag the blade contacts of the fuse, and termi nate in contact pads with conventiona hardware for attaching wire terminals

The heart of the fuse is a properl selected fuse wire assembly. Two fus wire metals are used today: silver for th larger ratings, and nickel for ratings belo 5 amp. The reason for using nickel in th small current ratings is one of mechanica strength; silver wire of the required cross section would be so slender that it woul be difficult to handle, quite sensitive t damage, and not readily visible. Nicke has a higher resistivity and a time-curren characteristic similar to that of silver Its cross section and its strength are there fore greater than that of silver for th same fuse rating. Whatever the metal o the fuse wire, it is silver soldered to silve plated copper contact blades.

Considering first the fuse wire, th melting temperature of silver is 1,760 F and that of nickel 2,642 F. Both are con sidered sufficiently above the 1,000 conductor temperature to make them

Table I. Properties of Metals for High-Temperature Fuses

	Gold 99.99+[3]	Copper OFHC[4]	Silver 99.97% Pure[3]	Nickel Inco Grade A[5]	Easy-Flo 45[6]	Rhodium Pure[3]	Inconel X #1 Temper[7]	Stainless Steel Alloy 416 Heat-Treated[8]	Beryllium Copper Berylco Alloy 10 1/2 Hard Heat-Treated
Electrical resistivity microhm-cm (circular mils)	2.35	1.71	1.59	10.0	6.25	4.5	124.6	57.0	3.8–2.9
Thermal coefficient of expansion per F × 10^{-6}	9.9	9.4–9.8	10.9	8.3	10.0	4.6	6.4–8.3	6.5	9.8
Tensile strength psi × 1,000	32–66	18.2–22.9	60–135				130–165	110	100–110
Specific gravity grams/cm^3	19.32	8.94	10.5	8.9	9.34	12.44	8.25	7.73	8.75
Melting point, F	1945	1981	1761	2642	1125	3570	2700–2790		1885–1955
Modulus of elasticity psi × 10^6	12	17	10.3–11.3			42	30–31	29	19

Table II. Properties of Non Metals for High-Temperature Fuses

	Mycalex 2100[10]	Steatite Alsimag 35 L-3A[11]	Lime Glass Corning Code No. 0281[12]	Glass Fiber Electrical Tape ECCO 7 B[13]	Solder Glass Corning Pyroceram Cement No. 95 #2[14]
ctrical resistivity, ohm-n	1.16×10[15]	1×10[14]–7×10[3]	3.16×10[6] (at 250 C)		
rmal coefficient of expansion per F×10[-6]	8–8.7	4.83–5.13	4.83		5.0–6.1
act strength	0.6 ft-lb (Izod)	4.5 in-lb (Charpy)			
er absorption, per cent	0	0–0.02 (impervious)			
rmal stress resistance, F			32.4		
rmal shock resistance, C			126		
ural strength, psi	13,000	18,000			
pressive strength, psi	29,000	80,000			
sile strength, psi	6,000	8,500			
cific gravity, grams/cm[3]	2.94	2.5	2.48–2.59	2.54	6.5
ening temperature, F, and procedure used	1,000*	2,642 (ASTM† C24)	1100+ (ASTM C338)	1380–1550‡	840+§
ectric strength, volts per il	350	225 (1/4-inch specimen)			

aximum temperature maintained for 1,000 hours without sag on 1/8-inch×1/2-inch×3-inch specimen ported on 2-inch centers with no load.
nerican Society for Testing Materials.
ocedure not specified.
aximum continuous safe temperature.

ble for the fuse wires of the high-perature fuse. However, a fuse wire develop a higher temperature than feeder wire. Tests have shown that er and nickel are suitable materials n in an ambient temperature of 650 F connected to feeder wires at 850 F. would appear that an ambient tempera-e of 650 F will result in a decrease of ut 20% in the nominal melting cur-t. The presently used Pyrex glass sing has sufficient physical character-cs to be used in the new environment. wever, other changes required in the design, and discussed later on, made dvisable to adopt a different glass.

ignificant physical characteristics of erials used in the development of high-perature fuses are listed in Tables I II.

s mentioned previously, larger current ngs require arc-suppressing fillers. ts showed that woven glass fabric, and rtz particles, both of which are used today's low-temperature fuses, are sfactory at the new temperature level. rtz fillers require a separate indicator nent. Since this is not desirable, itional tests established that fiberglass gs at the fuse wire ends in conjunction a glass fiber liner would be equally ctive in quenching the arc as quartz rs.

he copper contact blades, but not r silver plating, were found to be sfactory at higher temperatures. r considerable search for a plating would withstand the new conditions, inum and rhodium were found to be l replacements for the silver that failed through excessive oxidation and blistering. Rhodium was selected because it has better wear resistance and more stable contact resistance than platinum. An undercoat of nickel serves as a corrosion inhibitor.

One of the most serious problems in extending the temperature limit of present day fuses was the joining of the fuse housing to the end pieces that support the contact blades and act as finger grips. To solve this problem the configuration of the fuse had to be changed. It was obvious that the molded plastic caps were unsuitable at temperatures of approximately 900 F which is the temperature determined to be the highest reached in an ambient of 650 F for any part of the enclosure of a fuse connected to 850 F feeder wires. Since no other moldable organic material would do the job ceramic materials had to be substituted. Similarly, cements used for joining and sealing the glass housing to the caps would neither withstand the higher temperatures, nor, for that matter, would they bond glass to ceramics. Cements are also used in the low-temperature fuses to seal the contact blades where they pass through the end caps. This function they could not perform in the new environment.

It thus became necessary to:

1. Use a glass housing to accommodate the silver or nickel fuse wire; thus keeping it visible from the outside.
2. Employ ceramic end caps with finger grips.
3. Devise a means of joining the glass and the rhodium-plated contact blades to the ceramic parts.
4. Provide a seal as well as mechanical support.

After considerable experimentation a fuse design evolved that seemed to solve the problem. This design resulted from finding it quite feasible to join certain metals to ceramics by molding-in bushings, and then silver soldering the contact blades of the fuse wire assembly to these bushings. Also, certain glasses could be joined readily to ceramics by the use of solder glass. Fig. 8 shows the design. The fuse housing now became a ceramic, rectangular, open-top box with integral suitable finger grips and guards at the ends. Molded into this box were the two metal bushings to which the fuse contact blades in turn were silver soldered. The open top was then sealed off with a glass window. This design is simpler and stronger than two end caps joined to a glass housing. The question may be asked, "Why not mold the contact blades

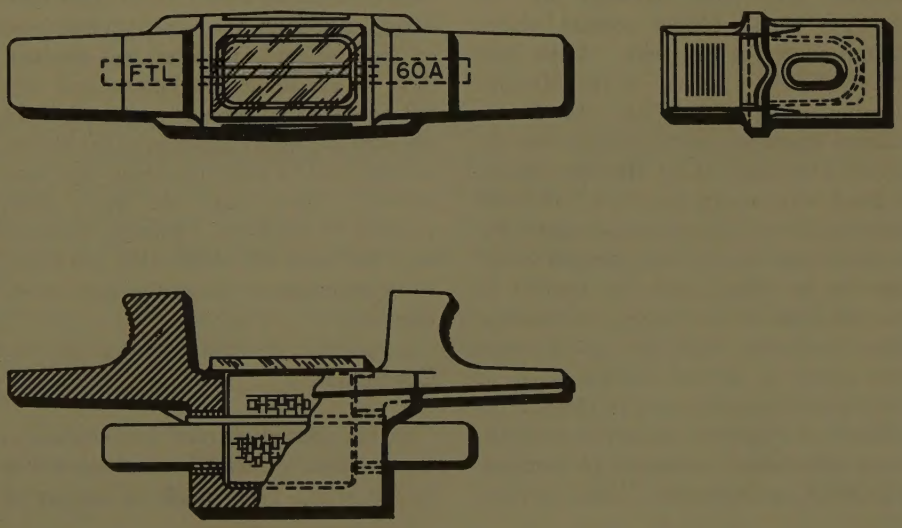

Fig. 8. High temperature, visually indicating fuse

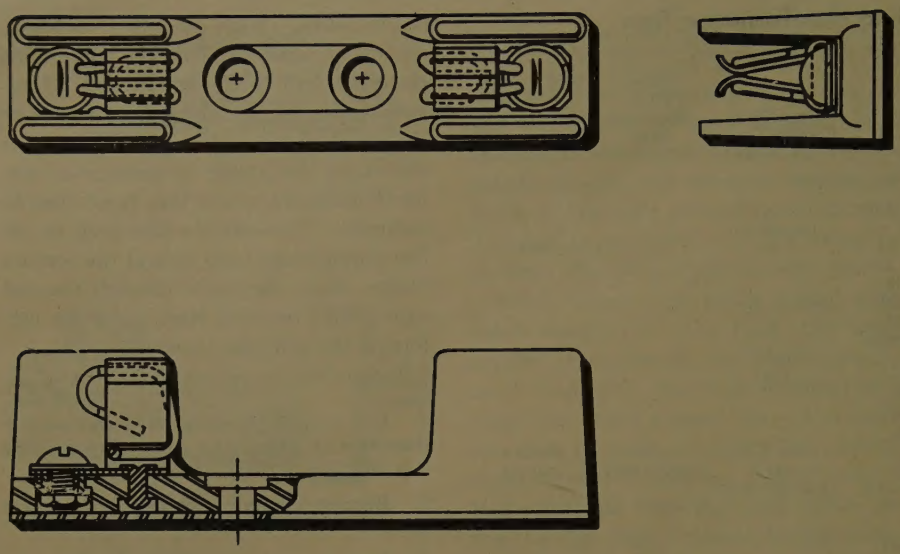

Fig. 9. High-temperature fuse holder

into the ceramic housing, eliminating the bushing?" For the contact blades a good electrical conductor is necessary. Copper and other good conductors have thermal coefficients of expansion incompatible with that of ceramics over so wide a temperature range. Stainless steel and other poor electrical conductors on the other hand have thermal coefficients of expansion that are sufficiently close to that of ceramics. By molding in bushings of the latter metals, and by silver soldering into these bushings the good electrical conductor needed for the contact blades, the difference of thermal expansion is now between metals rather than between metal and ceramic. The metals are sufficiently strong to withstand the resulting stress.

For the molded ceramic housing glass bonded mica in the form of Mycalex 2100 was selected. Molded into this material are stainless steel bushings, and silver soldered into these bushings are the rhodium plated copper contact blades that connect the fuse wire. A flat lime glass window is joined to the Mycalex housing, using solder glass. In the instances where arc-suppressing means are required the inside of the Mycalex housing is lined with woven fiberglass. It could conceivably be filled with quartz particles, in which case an indicating element would have to be added under the window in parallel with the fuse wire. In selecting these particular materials consideration was given to several factors, such as mechanical strength, relative thermal coefficient of expansion, dielectric strength, water absorption, resistance to temperature shock, and economy. Lime glass had to be substituted for Pyrex because so far it alone has been found to be solderable to the Mycalex housing. It withstands the required thermal shock.

Although the fuse holder presented fewer problems than the fuse, some changes had to be made to adapt it to the new environment. Fig. 9 illustrates the high-temperature design. The configuration of the low-temperature molded base was essentially adopted except that the material was changed from plastic to steatite, a ceramic that can be produced economically with the tolerances required, and which has the necessary mechanical and electrical properties. Changes also had to be made in the contact clips presently made from spring-tempered silver-plated beryllium copper, and in the silver-plated brass hardware used with present-day low-temperature fuse holders. The berryllium copper contact clips could only be used at the high temperature when they were plated with a metal other than silver. Rhodium, the same material used on the fuse contact blades, was selected. Also, at the higher temperatures it was felt necessary to provide greater contact pressure exerted by the clips on the blades, and external formed wire spring clips were added. These clips are made from Inconel *X*, unplated. Finally, stainless steel hardware was substituted and found to be satisfactory under the new conditions.

Conclusion

At the present stage of development it appears that terminals and splices will be of the crimp type, made of copper or nickel. Nickel terminals would be gol plated to obtain lower contact resistanc Copper terminals would be clad wit stainless steel or plated with nickel an gold. It is not yet clear whether pre insulated terminals and splices can b achieved by a combination of suitabl crimping technique and material, or if th post insulated approach must be accepted A solution of the problem in one directio or another seems likely.

The high-temperature fuse will in a probability be visually indicating, readil mounted in, and removed from its holde without the use of tools. It will embod the proven fuse wire and arc-suppressin means of present low-temperature fuses However, it will be quite different fro today's fuses in respect to the housing which will be a one-piece, ceramic desig

Thus, the requirements presented b the substantially higher temperature o the environment could only be fulfilled b changing materials and design; mer substitution of materials by others tha would withstand the higher temperature was not sufficient.

References

1. Cable, Electric, Aircraft, High Temperature and Fire Resistant. *Military Specification MIL-C-25038*, Wright Air Development Cente Dayton, Ohio, Apr. 28, 1955.

2. Fuse, Aircraft, High Temperature. *Equipment Specification NA5-7255B*, North America Aviation, Inc., International Airport, Los Angel Calif., July 9, 1957.

3. ASM, Metals Handbook. American Societ for Metals, Cleveland, Ohio, 1948.

4. Copper-Base Alloy Mill Products. *Stand ards Manual*, Copper and Brass Research Associa tion, New York, N. Y., Jan. 1958.

5. Nichrome and Other Nickel Electrica Alloys. *Catalog R56*, Driver-Harris Company Harrison, N. J., 1956.

6. Expansion and Construction in Silve Alloy Brazing. *Technical Bulletin T-7*, Handy Harmon, New York, N. Y., Sept. 1956; also Eas Flo 45, Characteristics and Properties, Ap 1947.

7. Inco Nickel Alloy Helical Spring *Technical Bulletin T-35*, International Nick Company, Inc., New York, N. Y., May 1955.

8. ASME Handbook-Metals Properties, Hoyt, editor. McGraw-Hill Book Company, Inc New York, N. Y., 1954.

9. Wrought Alloys with Unique Properties *Eeryllium Copper Bulletin*, The Berylliu Corporation, Reading, Pa., 1956.

10. Glass Bonded Mica. *Mycalex Bulleti* Haveg Industries, Inc., Taunton Division, Tau ton, Mass. (Formerly General Electric Company)

11. *Alsimag Chart no. 573*, American La Corporation, Chattanooga, Tenn.

12. Properties of Selected Commerci Glasses. *Bulletin B83*, Corning Glass Work Corning, N. Y., 1957.

13. The Inside Story of the New "Hesg Line" of Fiberglas Electrical Tapes. *Bulleti* Horace Linton Division, Hess, Goldsmith Company, Inc., New York, N. Y.

14. Properties-Pyroceram Brand Cement N 95. *Product Information, P. P..I. No. 2*, Corni Glass Works, Apr. 2, 1958 (not available).

Conference Paper Open for Discussion

The conference paper listed below has been accepted for AIEE Transactions and is now open for written discussion until October 29. Duplicate double-spaced typewritten copies of each discussion should be sent to Edward C. Day, Assistant Secretary for Technical Papers, American Institute of Electrical Engineers, 33 West 39th Street, New York 18, N. Y., on or before October 29.

Preprints may be purchased at 40¢ each to members; 80¢ each to nonmembers if accompanied by remittance or coupons. Please order by number and send remittance to:

AIEE Order Department
33 West 39th Street
New York 18, N. Y.

59-492 Multiple-Unit Operation of Diesel and Electric Locomotives on the Milwaukee Road.....Wylie

AIEE PUBLICATIONS

	Member Prices	Nonmember Prices
Electrical Engineering		
Official monthly publication containing articles of broad interest, technical papers, and three news sections: Institute Activities, Current Interest, and Electrical Engineering Education. Automatically sent to all members and enrolled students in consideration of payment of dues.		annually $12* per year
* Subscription price and $1.00 extra for foreign postage both payable in advance in New York exchange.		Single copies $1.50
Bimonthly Publications		
Containing all officially approved technical papers collated with discussion (if any) in three broad fields of subject matter as follows:	annually	annually
Communication and Electronics	$5.00†	$8.00‡
Applications and Industry	$5.00†	$8.00‡
Power Apparatus and Systems	$5.00†	$8.00‡
† Members may receive one subscription to any one of the bimonthlies for $2.50. The balance of the $5.00 subscription price shown above will be paid by application of one's annual dues for the year of the subscription. (Members may not reduce the amount of their dues payment by reason of nonsubscription.) Additional subscriptions will be at the $5.00 rate shown above.		
‡ Subscription price and 50 cents extra for foreign postage both payable in advance in New York exchange.		
Single copies may be obtained when available.	$1.50 each	$1.50 each
AIEE Transactions		
An annual volume in three parts containing all officially approved technical papers with discussions corresponding to six issues of the bimonthly publication of the same name bound in cloth with a stiff cover.	annually	annually
Part I Communication and Electronics	$4.00	$ 8.00**
Part II Applications and Industry	$4.00	$ 8.00**
Part III Power Apparatus and Systems	$4.00	$ 8.00**
Annual combination subscription to all three parts (beginning with vol. 77 for 1958).	$10.00	$15.00***
Annual combination subscription to any two parts.		$12.00***
** Subscription price and 75 cents for foreign postage both payable in advance in New York exchange.		
*** Subscription price and $1.00 extra for foreign postage both payable in advance in New York exchange.		
Electrical Engineering and Transactions		
An annual combination subscription to both publications (effective August 1, 1958).		$24.00§
§ Subscription price and $2.00 extra for foreign postage both payable in advance in New York exchange.		
AIEE Standards		
Listing of Standards, test codes, and reports with prices furnished on request.		
Special Publications		
Committee reports on special subjects, bibliographies, surveys, and papers and discussions of some specialized technical conferences, as announced in ELECTRICAL ENGINEERING.		

Discount 25% of above nonmember prices to college and public libraries. Publishers and subscription agencies 15% of above nonmember prices. For available discounts on Standards and special publications, obtain price lists from Order Department at Headquarters. Send all orders to:

Order Department
American Institute of Electrical Engineers
33 West 39th Street, New York 18, N. Y.